NEUTROPHIL EXTRACELLULAR TRAP-ASSOCIATED CELL DEATH - ROLE IN GOUT AND RELATIONSHIP TO ALTERNATE FORMS OF CELL DEATH

By

Simon Murray Chatfield

MBBS, FRACP

ORCID number - 0000-0001-6111-3461

This thesis is being submitted in fulfilment of the requirements for the degree of

Doctor of Philosophy

The Department of Medical Biology

University of Melbourne

April 2017

ABSTRACT

Cell death has emerged as a critical process in many facets of human disease, ranging from cancer to inflammation and cardiovascular disease. One such modality, Neutrophil Extracellular Trap (NET)-related cell death, or NETosis, is a form of cell death with potential implications in a wide range of human conditions but, at present, understanding of the mechanisms of NETosis and its physiologic and pathological consequences is limited. Finding the key mechanisms underlying NETosis will illuminate roles for NETosis in human diseases and animal models of these conditions, and provide targets for intervention. This thesis examines NETosis in the context of the human inflammatory disease, gout, and explores the relationship between NETosis and the other main types of cell death - necroptosis and apoptosis.

First, I developed a novel time-lapse imaging-based quantitative analysis of NETosis. The assay combines multi-well format live-cell microscopy technique with computerized analysis to obtain detailed kinetic information about the two key components of NETosis - cell death and chromatin decondensation. The technique allowed me to demonstrate that different NETosis stimuli, namely phorbol myristate acetate and monosodium urate crystals, exhibit different kinetics of cell death. Exploring the differences further, I found that crystals induce NETosis through a nicotinamide adenine dinucleotide phosphate oxidase-independent pathway that is distinct from PMA-induced NETosis. I also observed that both forms of NETosis depend on neutrophil elastase activity to cause chromatin decondensation, but not cell death.

I observed NET-like structures in samples taken from gout patients both during the acute inflammation of a gout attack and from the uninflamed crystal-rich tophus tissue, a feature of chronic gout. The NETs released during MSU-induced NETosis were resistant to serum nucleases relative to PMA-induced NETs, suggesting that these DNA structures may persist within tissues, as seen in the patient samples. This nuclease resistance was at least partially attributable to the presence of increased actin in MSU-induced NETs relative to PMA-induced NETs, as identified using proteomic techniques. Given the presence of NETs in both inflammatory and uninflamed contexts, I demonstrated that the presence of NETs dampens the IL-1β

responses of macrophage-like cells and reduces crystal-induced macrophage cell death.

I further demonstrated that NETosis is distinct from both apoptosis and necroptosis. Unexpectedly, two MLKL inhibitors did inhibit NETosis, but this is an indirect effect, dependent on accelerating apoptosis. This finding highlighted that over time in culture, neutrophils lose the ability to release NETs when stimulated with PMA and this loss of "NET competence" is mediated by caspase activation.

Using the power of a live cell imaging approach to simultaneously quantify cell death and NET release, my studies have advanced our fundamental understanding of the mechanistic differences underlying NETosis induced by different stimuli. Further, by applying this assay, I was able to establish that proteins within the apoptosis and necroptosis pathways that had been previously attributed roles in the NETosis pathway, were in fact dispensable. Consequently, I anticipate this assay and the mechanistic insights it provides will play an important part in advancing our understanding of the NETosis pathway.

DECLARATION

I declare that:

1. Thesis is my own original work towards the Doctorate of Philosophy;

2. Due acknowledgement has been given to all other information used;

3. This thesis is fewer than 100,000 words exclusive of tables, figures and references

4. I assess my contribution to the results described in each chapter to be

Chapter 2: 100%

Chapter 3: 90%

Kathrin Grebe contributed to the development of the NET assay, Tom Nebl performed Mass spectrometry and Sarah Ellis prepared samples for electron microscopy as indicated in the Methods chapter

Chapter 4: 100%

Simon Chatfield

Inflammation Division

Walter and Eliza Hall Institute of Medical Research

ACKNOWLEDGEMENTS

I would firstly like to thank my supervisors, Ian Wicks and James Murphy for giving me the opportunity to immerse myself in experimental biology, providing guidance along an interesting path. Their patience has been much appreciated as I balanced the research with clinical work and family commitments. Ian is a great facilitator of research and it has been an honour to be part of the laboratory's expansion into human-focussed research. Working with James and his team more broadly has been a great experience, opening my eyes to the beauty of structural and chemical biology. Dr Brent McKenzie was also a supervisor in the early phases of the PhD and he provided me with a useful different perspective on the research process. I also thank Professor Andrew Roberts for his involvement on my PhD committee.

It has been a privilege to work at the Walter and Eliza Hall Institute of Medical Research. The intellectual and physical resources I was able to access made the work possible. In particular, I am grateful to past and present members of the Wicks Laboratory and more broadly the inflammation and Cell Signalling and Cell Death divisions for guidance and support throughout my time. In no particular order, Annemarie Van Nieuwenhuijze, Kate Lawlor, Alex Dakic, Bartijn Pieters, Jane Murphy, Gabby Goldberg, Tommy Liu, Willy-John Martin, Joanne Keeble, Man-Lyang Kim, Angus Stock, Jacinta Grayden, Ben Croker, Kate MacArthur, Joanne O'Donnell, Tania Kolesnik, Ed Linossi, Akshay D'Cruz, Seth Masters, James Vince, Guillaume Lessene, Paul Baker, Hazel Tye, Cynthia Louis, Joanne Hildebrand, John Silke, and Shereen Oon have helped in multiple ways. Special thanks to Rhiannon Jones, Emma Stuart and Rebecca Stewart for providing outstanding administrative and moral support through the PhD. Tom Nebl performed the mass spectrometry and has been a consistent source of enthusiasm about my project. Kathrin Grebe's input was invaluable in her help in optimising and validating the MPO-DNA NET assay. Thank you to Sarah Ellis and the microscopy staff at the Victorian Comprehensive Cancer Centre for assistance with electron microscopy and Damian D'Silva for assistance with macrophage experiments.

At the Royal Melbourne Hospital, the assistance of Clare O'Neill and Susan Tadros has been invaluable. I also thank the Rheumatology unit as a whole and the registrars in particular for supporting my work. Thank you to Gary Unglik, Department of

Immunology for useful discussions. I acknowledge the generosity of patients and healthy donors from the Royal Melbourne Hospital and the Walter and Eliza Hall volunteer blood donor registry who have contributed the samples to the study that made it possible. Thank you to Jenni Harris, Lina Laskos, Naomi Sprigg and Kimvan Le for the administration of the volunteer blood donor registry that is a critical resource for human research.

The Imaging Centre has born the brunt of most of my experiments and I acknowledge the advice and practical assistance of Kelly Rogers, Lachlan Whitehead for analysis in particular, Cameron Whitehead and Mark Scott.

I would like to thank Yarra trams for many trips to and from the lab during which time I did a lot of my reading and preparation for experiments. I thank Adam Rudegair and John Bailey for their weekly radio shows that have sustained me through the writing period.

I acknowledge the financial support of the Royal Australasian College of Physicians, the Victorian branch of the Australian Rheumatology Association, the John T Reid Charitable Trust, the Woodend Foundation, the Jane Ariandne McLaurin Thompson and Barclay Thomson trust and the May Stewart trust.

I would like to thank my endlessly patient family for supporting me through this long journey. My parents, Graeme and Merilyn, my brother Tim and his family, my “in-laws” Kaye and Jim, housemates Jenny and Richard and James, Chris, Ruth, Elisa and Joe for helpful chats along the way. And finally my partner Samantha and my daughters, Saskia and Lila who have had to put up with me through this process but have always supported me, showed interest and made the rest of my life fun.

TABLE OF CONTENTS

Abstract ii

Declaration iv

Acknowledgements v

Table of Contents vii

Table of figures xii

Table index xvi

Abbreviations xvii

1 Chapter 1 – Literature Review – Gout, Monosodium Urate Crystals and Neutrophil cell death 1

1.1 Gout 2

1.1.1 Neutrophils and gout – clinical observations 3

1.1.2 Gouty Tophi and neutrophils 3

1.2 Murine studies in gout 3

1.3 Neutrophil responses to crystals 4

1.3.1 Neutrophil MSU crystal interaction 4

1.3.2 Lipid Sorting as receptor-independent activator 5

1.3.3 Role of Crystal coating 5

1.3.4 Neutrophil activation – cell signalling 6

1.3.5 MSU crystals and the Inflammasome 6

1.3.6 Neutrophils and the inflammasome 8

1.3.7 Neutrophils and lysosome function 8

1.3.8 Inflammasome-independent pathways 9

1.4 Neutrophil effector mechanisms 9

1.5 Therapeutics for gout and effects on neutrophils 10

1.5.1 Colchicine 10

1.5.2 Non-steroidal anti-inflammatory drugs 11

1.5.3 Glucocorticoids 11

1.6 NETosis 12

1.6.1 NETosis - Basic biology 12

1.6.2 NET-Releasing Stimuli 13
1.7 Mechanistic pathways in NETosis 14
1.7.1 Role of Reactive Oxygen species in NETosis 14
1.7.2 Histone citrullination 15
1.7.3 Neutrophil elastase and myeloperoxidase 16
1.7.4 Autophagy 18
1.7.5 Cell-signalling pathways involved in NETosis 19
1.7.6 Neutrophil Development and NETs 20
1.7.7 Mouse NETs versus Human NETs 21
1.8 NET Proteins 21
1.9 Degradation of NETs 22
1.10 Impact of NETs on the inflammatory response 23
1.10.1 NETs and inflammation in autoimmune diseases 24
1.10.2 NETs and inflammation in crystal diseases 24
1.10.3 NETosis and other particles 26
1.11 Neutrophil cell death and relevance to inflammatory conditions 26
1.11.1 Neutrophil turnover 27
1.11.2 Neutrophil lifespan *in vitro* 27
1.11.3 Neutrophil lifespan *in vivo* 27
1.12 Mechanisms of spontaneous neutrophil apoptosis 28
1.12.1 Intrinsic pathway 28
1.12.2 Pro- and anti-apoptotic Bcl-2-family proteins 29
1.12.3 Extrinsic pathway 31
1.12.4 Morrbid – a novel long non-coding RNA modifying myeloid cell survival 32
1.12.5 Caspase dependency 32
1.12.6 Calpains 34
1.12.7 Reactive Oxygen species 34
1.13 Pro and anti-apoptotic factors 35
1.13.1 Anti-apoptotic factors 35
1.13.2 Pro-apoptotic factors 37
1.13.3 Novel mediators of neutrophil apoptosis 38
1.13.4 Pathogens and neutrophil cell death 41
1.14 Impact of apoptosis on neutrophil functionality 41
1.15 Induction of apoptosis as an anti-inflammatory strategy 42
1.16 Non-apoptotic cell death in neutrophils 43

1.16.1 Staurosporine-induced cell death 43
1.16.2 Autophagic cell death 43
1.16.3 Pyroptosis 44
1.16.4 Necroptosis 44
1.16.5 NETosis and alternate forms of cell death 47
1.16.6 Other Caspase-independent forms of cell death 48
1.17 Conclusion 48

2 Development of Novel Quantitative Imaging approaches to measurE Neutrophil Extracellular Traps 49

2.1 Introduction 49
2.2 NETosis assays 49
2.2.1 Neutrophil isolation and culture 49
2.2.2 Fixed cell imaging quantification 53
2.2.3 DNA release assays 55
2.2.4 Other NETosis assays 57
2.3 Cell death quantified with live cell imaging – rationale for live cell imaging of NETosis 57
2.3.1 Live cell imaging and Quantitative Image Analysis 58
2.4 Further methods 62
2.4.1 Human samples and cell isolation and culture 62
2.4.2 Preparation of stimuli 64
2.4.3 Imaging 64
2.4.4 MPO-DNA measurement 68
2.4.5 Luminol-enhanced chemiluminescence 69
2.4.6 NET protein studies 69
2.4.7 NET degradation assays 72
2.4.8 Inflammasome and IL-1β studies 72
2.4.9 Inhibitors 73
2.4.10 Other Reagents 75
2.4.11 Antibodies 76
2.4.12 Statistical analysis 77

3 NEUTROPHILS SEQUESTER PRO-INFLAMMATORY CRYSTALS USING DNASE-RESISTANT “SAFETY NETS” 78

3.1 Introduction 78

3.2 RESULTS 79
3.2.1 DNA associated with neutrophil granule enzymes is present in acute gout synovial fluid and non-inflamed tophi from patients with chronic gout 79
3.2.2 Live cell imaging of human neutrophils demonstrates stimulus-dependent kinetics of NETosis 85
3.2.3 Crystal-induced NETosis is NADPH-oxidase independent 91
3.2.4 Neutrophil Elastase mediates nuclear decondensation, but not cell death, in response to crystal and non-crystal stimuli 99
3.2.5 Myeloperoxidase 108
3.2.6 Lysosomal detergent LLOme induces NETosis, but crystal-induced NETosis is not mediated by inflammasome activation 110
3.2.7 MSU-containing phagosomes have irregular surrounding membranes ... 116
3.2.8 MSU-induced NETosis and relationship to other forms of cell death 120
3.2.9 MSU crystal-induced NETs are less susceptible to Deoxyribonuclease 1 and serum degradation than PMA NETs 122
3.2.10 MSU NETs are enriched with actin and actin-binding proteins. 128
3.2.11 NETosis reduces the pro-inflammatory potential of MSU-crystals 133
3.3 DISCUSSION 135
4 The Relationship between NETosis, necroptosis and apoptosis 139
4.1 Introduction 139
4.2 Results 141
4.2.1 Chemical inhibition of the cell death pathways and NETosis 141
4.2.2 Ability to undergo NETosis, or “NET competence” diminishes with time . 146
4.2.3 Analysis of MLKL distribution 154
4.2.4 Immunofluorescence analysis 155
4.2.5 Conclusions - Imaging studies of MLKL distribution of human neutrophils 160
4.2.6 Western blotting demonstrates neutrophil MLKL expression 161
4.2.7 Induction of cell death with FasL but not WEHI781 or Hit #14 may cause release of IL-1β 171
4.3 Discussion 173
4.3.1 NETosis does not require activation of the necroptosis pathway 173
4.3.2 Apoptosis and NETosis 174
4.3.3 Caspase-mediated loss of neutrophil functionality 174
4.3.4 MLKL inhibitors and Apoptosis 175

4.3.5 MLKL – involvement in apoptosis 176

5 Discussion 179

5.1 Measurement facilitates understanding of NETosis 179

5.2 Crystal-induced NETosis – another pathway to cell death and chromatin decondensation and relevance to gout 181

5.3 Different stimuli, different NETs 183

5.4 NETs in gout – pro- or anti-inflammatory? 184

5.5 NETosis, apoptosis and necroptosis 184

5.6 Conclusions 185

Appendix 186

Supplementary movies 193

Bibliography ..... Error! Bookmark not defined.

TABLE OF FIGURES

Figure 1.1 Schema of PMA-induced NETosis 17
Figure 1.2 - Summary of NETosis stimuli and pathways 20
Figure 1.3 Neutrophil apoptotic pathways 39
Figure 2.1 - Fixed versus Unfixed images of NETs 55
Figure 2.2 - Suramin exhibits fluorescent interference in the Sytox Green assay 57
Figure 2.3 - Examples of cell appearances from live cell imaging 59
Figure 2.4 - Example of CTG labelled neutrophils counted using MetaMorph 60
Figure 2.5 Cytospin of PolymorphPrep isolated neutrophils 63
Figure 2.6 - Neutrophil shape analysis examples 68
Figure 3.1 Synovial fluid from gout patients contains aggregates of crystals and extracellular DNA 80
Figure 3.2 Synovial fluid from gout patients contains more MPO-DNA complexes than from OA patients 81
Figure 3.3 Crystals from tophi of gout patients are coated in DNA 82
Figure 3.4 Immunofluorescence staining of tophus reveals the presence of neutrophil granule proteins and DNA 84
Figure 3.5 Immunohistochemistry staining for MPO in surgically removed tophi 85
Figure 3.6 Montage of time-lapse live cell imaging of NETosis 86
Figure 3.7 Computerized quantification of live cell imaging assay of NETosis 87
Figure 3.8 MSU crystals induce NETs more rapidly than PMA 88
Figure 3.9 Individual curves from NETosis time-lapse experiments 89
Figure 3.10 PMA and MSU NETosis are dose-dependent 90
Figure 3.11 Time-lapse demonstrates the timing of nuclear decondensation relative to cell death 91
Figure 3.12 NADPH oxidase function is required for PMA- and *Candida*-induced NETosis but not Required for Crystal-induced NETosis 92
Figure 3.13 Fixed cell immunofluorescence imaging of neutrophils treated with different stimuli 93
Figure 3.14 DPI treatment reduces NETosis through reducing cell death 94
Figure 3.15 DPI does not increase cell death over 8 hours 95
Figure 3.16 The ROS scavenger, Pyrocatechol, inhibits PMA- but not MSU-induced NETosis 95
Figure 3.17 MitoTEMPO, mitochondrial ROS scavenger does not effect NETosis induced by either PMA or MSU 96
Figure 3.18 Autologous serum inhibits PMA- but not MSU- induced NETosis 96
Figure 3.19 Latex beads do not induce NETosis 97

Figure 3.20 Western blotting for histones in lysates of PMA and MSU-treated neutrophils with and without DPI 98
Figure 3.21 Neutrophil Elastase inhibitor reduces NETosis but does not change the kinetics of cell death 99
Figure 3.22 PI staining reveals NE inhibitor prevents nuclear decondensation during NETosis 100
Figure 3.23 NE inhibitor prevents degradation of histones during NETosis 101
Figure 3.24 Immunofluorescence staining of neutrophils and relationship to cell permeability 102
Figure 3.25 Neutrophil elastase translocates to the nucleus prior to cell permeability during PMA NETosis 103
Figure 3.26 NET translocates to the nucleus either shortly before or after cell permeabilization during MSU NETosis 104
Figure 3.27 MSU-containing phagosomes undergo maturation 105
Figure 3.28 Bafilomycin A and Nocodazole do not inhibit MSU induced NETosis 106
Figure 3.29 Bafilomycin and Nocodazole do not inhibit phagosome maturation 107
Figure 3.30 Live cell imaging with DQ ovalbumin 108
Figure 3.31 Inhibition of MPO with ABAH partially inhibits PMA NETosis but not MSU NETosis 109
Figure 3.32 NE and MPO nuclear translocation with MSU and PMA stimulation 110
Figure 3.33 Leu-Leu-OMe induces NETosis in a dose dependent fashion 111
Figure 3.34 Leu-Leu-OMe induces NE nuclear translocation 112
Figure 3.35 Inhibitors of inflammasome activation apart from Cytochalasin D do not inhibit MSU NETosis 113
Figure 3.36 Chemical inhibitors of MSU-induced NETosis 114
Figure 3.37 Cytochalasin D reduces neutrophil shape change induced by MSU crystals 115
Figure 3.38 NETosis inhibitors and effects of neutrophil circularity induced by MSU crystals 116
Figure 3.39 CD63 immunofluorescence staining of bead and MSU containing phagosomes 117
Figure 3.40 Transmission electron microscopy of a neutrophil that has phagocytosed latex beads 118
Figure 3.41 Transmission electron microscopy of neutrophils stimulated with MSU crystal 119
Figure 3.42 Inhibitors of alternative forms of regulated cell death and clinical inhibitors of gouty inflammation do not inhibit NETosis 120
Figure 3.43 Annexin V binding occurs before cell death in apoptosis and after in MSU NETosis 121

Figure 3.44 Histone citrullination occurs during PMA and MSU-induced NETosis but is not required 122
Figure 3.45 DNA provides the structural component of NET crystal aggregates 123
Figure 3.46 Serum degrades PMA NETs more effectively than it degrades MSU NETs .. 124
Figure 3.47 MNase degrades PMA and MSU NETs equally, but DNase degrades PMA NETs more efficiently than MSU NETs 125
Figure 3.48 DNA from PMA NETs is more rapidly degraded by DNase than that from MSU NETs 126
Figure 3.49 DNA from PMA NETs is more rapidly degraded by serum than that from MSU NETs 127
Figure 3.50 EDTA inhibits serum nuclease and uricase treatment does not affect DNase degradation of MSU NET 128
Figure 3.51 NET proteomics demonstrated both shared and differential protein expression between PMA and MSU NETs 129
Figure 3.52 MSU-NETs are enriched for β-actin 131
Figure 3.53 F-actin colocalizes with DNA in MSU-NETs 132
Figure 3.54 Gelsolin increases the susceptibility of MSU-NETs to DNase degradation . 133
Figure 3.55 Neutrophils reduce THP-1 IL-1 in response to MSU crystals in a DNA-dependent manner 134
Figure 3.56 Neutrophils reduce MSU-crystal induced THP-1 cell death 135
Figure 4.1 Inhibitors of the necroptosis pathway do not inhibit PMA-induced NETosis 142
Figure 4.2 Hit #14, an inhibitor of necroptosis, inhibits PMA-induced NETosis in a time- and dose-dependent fashion 143
Figure 4.3 Prolonged incubation with inhibitors of RIPK1, MLKL and RIPK3 does not inhibit NETosis 144
Figure 4.4 Prolonged incubation with a MLKL inhibitor does not inhibit NETosis 145
Figure 4.5 Prolonged incubation with a more potent MLKL inhibitor inhibits NETosis .. 145
Figure 4.6 The ability of neutrophils to undergo PMA-induced NETosis diminishes with time in culture 146
Figure 4.7 Neutrophils fail to spread in response to PMA when pre-treated with Hit #14 147
Figure 4.8 Neutrophils demonstrate reduced reactive oxygen species generation in response to PMA over time, further reduced when pre-treated with Hit #14 147
Figure 4.9 Hit #14 and WEHI781 accelerate neutrophil apoptosis 148
Figure 4.10 Caspase inhibition prevents the time-dependent loss of NET competence. 149
Figure 4.11 G-CSF delays the time-dependent loss of NET competence 149
Figure 4.12 Hit #14 and WEHI781-induced loss of NET competence is caspase-dependent 150

Figure 4.13 QVD-OPh but not ZVAD-fmk prevents time-dependent loss of NET competence 151
Figure 4.14 Hit #14 and WEHI781 may subtly reduce NETosis in G-CSF-primed neutrophils 151
Figure 4.15 QVD-OPh and a caspase-3 inhibitor prevent loss of NET competence 152
Figure 4.16 Fas ligand prevents NETosis in a caspase-dependent manner 153
Figure 4.17 A panel of kinase inhibitors does not reduce NET competence 153
Figure 4.18 Effect of Roscovitine on NET competence 154
Figure 4.19 Immunofluorescence imaging of MLKL 155
Figure 4.20 PMA does not induce major microscopic changes in MLKL distribution 156
Figure 4.21 Hit #14-treated cells develop pyknotic nuclei 156
Figure 4.22 Fluorescent imaging analysis of Hit #14 and MLKL 157
Figure 4.23 Fluorescent imaging of anti-MLKL-labelled neutrophils with Hit #14 fluorescence 158
Figure 4.24 Fluorescent imaging of MLKL in WEHI781 and untreated neutrophils 159
Figure 4.25 Fluorescent analysis of MLKL in Hit #14 and QVD-OPh-treated neutrophils 160
Figure 4.26 MLKL Western blots of fractionated neutrophil proteins 162
Figure 4.27 Caspase-8 Western of fractionated neutrophil proteins 163
Figure 4.28 MLKL Western blots of neutrophil protein under reducing and non-reducing conditions 165
Figure 4.29 MLKL Western blots of fractionated neutrophil proteins under reducing and non-reducing condition 167
Figure 4.30 BN-PAGE MLKL Western blot 169
Figure 4.31 Cleaved Caspase-3 Western blots of fractionated neutrophil proteins 169
Figure 4.32 Actin Western blot of fractionated neutrophil proteins 170
Figure 4.33 Actin immunofluorescence staining moves from a cortical to cytoplasmic distribution with WEHI781 treatment 171
Figure 4.34 IL-1β release from neutrophils treated with inducers of apoptosis 172
Figure 5.1 Schema for PMA and MSU-induced NETosis 182

TABLE INDEX

Table 1.1 - NET-releasing Stimuli **13**
Table 2.1 Stimuli and Inhibitors **73**
Table 2.2 Other reagents **75**
Table 2.3 Antibodies **76**

ABBREVIATIONS

Akt	Akt/Protein Kinase B
ANCA	Anti-neutrophil cytoplasmic antibody
APAF1	Apoptotic peptidase activating factor 1
Bak	Bcl-2 homologous antagonist killer
Bax	Bcl-2-associated X
Bcl-2	B-cell lymphoma 2
Bcl-w	Bcl-2-like protein 2
Bim	Bcl-2-like protein 11
BN	Blue native
BN-PAGE	Blue native PAGE
CDK	Cyclin-dependent kinase
CGD	Chronic Granulomatous Disease
CpA	Compound A
COX	Cyclooxygenase
CPPD	Calcium pyrophosphate dehydrate
CTG	Cell Tracker Green
CTSG	Cathepsin G
DAMPs	Danger-associated molecular patterns
DAP12	DNAX activation protein of 12kDa
DFP	Di-isopropylfluorophosphate
DISC	Death-inducing signalling complex
DMSO	Dimethyl sulfoxide
DNA	Deoxyribonucleic acid
DNase	Deoxyribonuclease

DPI	Diphenylene iodonium
DTT	Dithiothreitol
EDTA	Ethylenediaminetetraacetic acid
EGTA	Ethylene glycol-bis(β-aminoethyl ether)-N,N,N',N'-tetraacetic acid
ERK	Extracellular signal–regulated kinases
FasL	Fas ligand
FDR	False discovery rate
fMLP	*N*-formylmethionine-leucyl-phenylalanine
G-CSF	Granulocyte colony stimulating factor
GC	Glucocorticoids
GM-CSF	Granulocyte macrophage colony stimulating factor
HBSS	Hanks' balanced salt solution
HT-RPMI	Human tonicity Roswell Park Memorial Institute media
IAP	Inhibitor of apoptosis
IDO	Indoleamine 2,3-dioxygenase
IFN-α	Interferon alpha
IFNg	Interferon gamma
IL-1ra	Interleukin 1 receptor antagonist
IL-1β	Interleukin-1β
IL-6	Interleukin-6
JAK	Janus activated kinase
kDa	kiloDalton
LC	Liquid chromatography
LDGs	Low density granulocytes
LLOMe	L-leucyl-L-leucine methyl ester
LPS	Lipopolysaccharide

Lyn	Lck/Yes novel tyrosine kinase
Mcl-1	Myeloid leukaemia cell differentiation protein
MEK	Mitogen-activated protein kinase kinase
MLKL	mixed-lineage kinase domain-like
MNase	Micrococcal nuclease
MNDA	Myeloid nuclear differentiation antigen
MPO	Myeloperoxidase
MS	Mass spectrometry
MSU	Monosodium Urate (crystals)
NAC	N-acetyl cysteine
NADPH oxidase	Nicotinamide adenine dinucleotide phosphate-oxidase
NE	Neutrophil elastase
NETosis	Neutrophil extracellular trap-associated cell death
NETs	Neutrophil extracellular traps
Noxa	Phorbol-12-myristate-13-acetate-induced protein 1 (Noxa)
NSA	Necrosulfonamide
PADI	Peptidylarginine deiminase
PAGE	Polyacrylamide gel electrophoresis
PAMP	Pathogen-associated molecular pattern
PBMCs	Peripheral blood mononuclear cells
PBS	Phosphate buffered saline
PCNA	Proliferating cell nuclear antigen
PI	Propidium iodide
PI3K	Phosphatidylinositol-4,5-bisphosphate 3-kinase
PKC	Protein Kinase C
PLS	Papillon-Lefevre Syndrome

PMA	Phorbol myristate acetate
PR3	Proteinase 3
RA	Rheumatoid Arthritis
RIPK	Receptor-interacting serine/threonine-protein kinases
ROS	Reactive oxygen species
RPMI	Roswell Park Memorial Institute media
SDS	Sodium dodecyl sulfate
Smac	Second mitochondria-derived activator of caspases
Src	Cellular-sarcoma kinase
SRR	Sypro Ruby Red
STAT	Signal transducer and activator of transcription
Syk	Spleen tyrosine kinase
TGFb1	Transforming growth factor beta-1
TLR2	Toll-like receptor 2
TLR4	Toll-like receptor 4
TNFa	Tumour necrosis factor α
TUNEL	Terminal deoxynucleotidyl transferase (TdT) dUTP Nick-End Labeling
XIAP	X-linked inhibitor of apoptosis

1 CHAPTER 1 – LITERATURE REVIEW – GOUT, MONOSODIUM URATE CRYSTALS AND NEUTROPHIL CELL DEATH

Neutrophils are the most abundant immune cells in human peripheral blood and provide rapidly responsive innate immune defence against pathogens. The importance of maintaining appropriate levels of neutrophil numbers and activity is evidenced by human diseases. Neutrophil deficiency, termed neutropenia, underlies susceptibility to infection, while neutrophil hyperactivity can contribute to host tissue damage in non-infective inflammatory conditions (Wright et al., 2014). Patients suffering from inflammatory arthritis, including Rheumatoid Arthritis (RA) and gout, have large numbers of activated neutrophils in their synovial fluid. Numerous animal models of arthritis have demonstrated a non-redundant role for these cells in driving inflammation and tissue damage. The fate of neutrophils in inflamed tissues is critical to the outcome of these disorders. Cell death is the ultimate fate of all cells, but the timing and mode of neutrophil death are likely to be important to the persistence or resolution of inflammation.

Until recently, the primary form of neutrophil cell death was thought to be apoptosis, an orderly and largely non-inflammatory cell death triggered and executed by a family of cysteine proteases termed caspases. Apoptosis also flags cells for non-inflammatory disposal prior to the spillage of intracellular contents (Poon et al., 2014). It has become apparent that apoptosis is not the only form of cell death, with caspase-1 or -11 driven pyroptosis and caspase-independent necroptosis subsequently implicated. These forms of cell death appear to be regulated, but result in membrane compromise with release of cellular contents, including danger-associated molecular patterns (DAMPs) that can amplify inflammation.

Neutrophils can also undergo a non-apoptotic, caspase-independent form of cell death termed NETosis, so called because the cells release neutrophil extracellular traps, or NETs, during the death process (Brinkmann et al., 2004). NETs are composed of decondensed chromatin strands non-covalently linked to neutrophil granule proteins. NETosis appears to be an anti-pathogen strategy. It may serve as a back-up mechanism to better-characterised neutrophil functions, such as phagocytosis, reactive oxygen species generation and anti-pathogen mediator release. Evidence is emerging arthritis, gout, vasculitis and systemic lupus erythematosus. This literature review

outlines current knowledge regarding neutrophil cell death and will provide the context for the questions addressed by the thesis:

1. What is the mechanism of monosodium urate (MSU)-induced NETosis? What are the consequences of neutrophil death and DNA release in the context of gout?

2. The relationship between NETosis and other forms of cell death including apoptosis and necroptosis is not clear. Is NETosis distinct from these forms of cell death and how do different forms of cell death interact with one another?

1.1 Gout

Gout is an ancient human disease caused by the accumulation of monosodium urate crystals (MSU) in people with high uric acid levels (hyperuricemia) (Choi et al., 2005). A combination of dietary and lifestyle factors and genetic variability in organic acid handling in the kidneys leads to hyperuricemia and a proportionally increased risk of gout. Humans and higher primates have undergone genetic loss of the enzyme, uricase that in other species metabolizes the uric acid to allantoin, a water-soluble degradation product easily excreted in the urine (X. W. Wu et al., 1989). At levels above 0.35mg/dl, uric acid approaches supersaturation and under certain physiologic conditions, MSU crystals can form (McGill & Dieppe, 1991). Reduction of uric acid with drugs such as allopurinol, a xanthine oxidase inhibitor, decreases the risk of gout and represents standard management of patients with recurrent gout (Shoji et al., 2004).

Gout is one of several diseases driven by immune responses to crystalline particles that include pseudogout (calcium pyrophosphate dehydrate (CPPD) crystals), silicosis (silica crystals) and atherosclerotic disease (cholesterol crystals) (Franklin et al., 2016). Gout is characterized by stereotyped episodes of profound joint and soft tissue inflammation. A typical attack involves the rapid development of the classic features of acute inflammation - pain, swelling, erythema and loss of function. This response is due to the pro-inflammatory nature of crystals demonstrated both *in vitro* and *in vivo*. An untreated attack of gout typically resolves spontaneously within a week or so. Humans who had MSU crystals injected into their knees developed the classical features of gout that lasted for only 24 to 48 hours (Faires & McCarty, 1962) (Seegmiller et al., 1962). How the florid inflammatory response is dampened in the acute attack of gout is not clear particularly given the crystals do not disappear without urate-lowering therapy (Pascual & Sivera, 2007). Gout provides an important contrast

to other forms of inflammatory arthritis, such as RA, where inflammation typically persists and becomes chronic.

Recurrent attacks of gout may be accompanied by progressive accumulation of MSU crystals in individuals with hyperuricemia. This leads to the development of tophi – dense aggregates of MSU crystals present in the soft tissues and joints. These deposits contribute to disability and cause disfigurement and bony destruction (Chhana & Dalbeth, 2015), but are characteristically uninflamed, despite the high load of MSU crystals. The recent advent of dual-energy computerised tomography scan technology, which can identify tophi deep within tissues, has highlighted a significant tophus burden not previously appreciated in patients with gout (Mallinson et al., 2014).

1.1.1 Neutrophils and gout – clinical observations

The presence of neutrophils in acute gout is well established. These cells are prominent in the joint fluid of patients with acute gout attacks. Neutrophil concentrations may reach up to 10^8/ml, comparable to concentrations seen in septic arthritis (Krey & Bailen, 1979). Therapeutic agents used for gout are thought at least in part to suppress pro-inflammatory aspects of neutrophil biology (Terkeltaub, 2010).

1.1.2 Gouty Tophi and neutrophils

Tophi are dense crystal deposits in a proteinaceous matrix, surrounded by fibrotic tissue populated by macrophages. Neutrophils however, are remarkably absent (Dalbeth et al., 2010). This appearance mimics the response to a foreign body. Although intact neutrophils are scarce in tophi, a proteomic analysis of tophi has highlighted the presence cytoskeletal proteins and immune-related proteins including those derived from neutrophils (Kaneko et al., 2014) and, an early immunohistochemistry study demonstrated staining of the acellular crystal core of the tophus with an anti-granulocyte antibody (Palmer et al., 1987). A recent study has reported that neutrophil-crystal aggregates formed *in vitro* and in a mouse model bear a strong resemblance to tophi, supporting a role for neutrophils in tophus development (Schauer et al., 2014).

1.2 Murine studies in gout

Unlike humans, mice do not naturally develop gout because they express uricase (X. W. Wu et al., 1989). To model human MSU responses in mice, investigators have injected the crystals into the peritoneum (Martinon et al., 2006), air pouches (Gordon et

al., 1986), joints (Joosten et al., 2016) and footpads (Schauer et al., 2014). The use of specific gene knockout mice in these models has facilitated the understanding of the key components of responses to crystals, as outlined below.

1.3 Neutrophil responses to crystals

To explore the mechanism of MSU-induced NETosis, it is important to understand the way crystals interact with and trigger inflammatory responses in neutrophils and reflect on studies in other cell types including macrophages and dendritic cells. Neutrophils respond to monosodium urate (MSU) crystals *in vitro* and the following section will outline those responses and the signalling pathways thought to be involved in eliciting them.

1.3.1 Neutrophil MSU crystal interaction

How MSU crystals stimulate neutrophils and other phagocytic cells, such as macrophages and dendritic cells, remains incompletely understood. The cellular receptor responsible for recognition of crystals has not been definitively identified, although several cell surface molecules are thought to contribute to MSU crystal recognition and uptake. Receptors implicated in crystal recognition include FcγRIIIB (CD16), CD11b (Barabe et al., 1998) and CD14 (Scott et al., 2006). MSU crystals may signal through toll-like receptors (TLRs) that normally sense the presence of pathogen-associated molecular patterns such as bacterial lipopolysaccharide (LPS). TLR2 and TLR4 in the mouse have been identified as potential receptors for MSU crystals in the mouse (Liu-Bryan et al., 2005), but do not appear to stimulate TLRs in humans (C. J. Chen et al., 2006). A recently described specific receptor for MSU crystals is Clec12a (Neumann et al., 2014). During cell death, uric acid is released and acts as a DAMP to activate an inflammatory response in adjacent living cells (Kono et al., 2014) and Clec12 appears to play a role in preventing an exaggerated hyper-inflammatory response.

The role of TLRs in human gout may relate to priming these cells prior to crystal-induced inflammasome activation to induce the release of the key pro-inflammatory cytokine, interleukin 1β (IL-1β) (Martinon et al., 2006). Macrophages require priming to translate pro-IL-1β, which is then processed via activated caspase-1 to mature IL-1β when the cells are stimulated with MSU crystals. Additionally, a study in human peripheral blood mononuclear cells (PBMCs) has implicated free fatty acids as

endogenous TLR4 ligands that can promote IL-1β translation prior to inflammasome activation with MSU (Joosten et al., 2010).

1.3.2 Lipid Sorting as receptor-independent activator

While not yet confirmed in neutrophils, recent studies in dendritic cells (DCs) have demonstrated that perturbations in the lipid membrane induced by MSU crystals results in receptor-independent Spleen tyrosine kinase (Syk) signalling, which is critical to phagocytosis (Ng et al., 2008). Normally Syk mediates intracellular signalling through cell surface receptors including integrins and Fc receptors (Mocsai et al., 2002). This study proposes that the interaction of crystals with cell membranes and the response elicited may be independent of protein membrane receptors. This was demonstrated using a broad spectrum pronase to cleave membrane proteins in DCs. DCs treated in this way still had MSU-induced responses. The intracellular signalling pathway triggered by this interaction involves Syk, cellular-sarcoma kinase (Src), Phosphatidylinositol-4,5-bisphosphate 3-kinase (PI3K) and actin polymerization.

1.3.3 Role of Crystal coating

The coating of MSU crystals appears to be important for the inflammatory responses elicited. IgG coating enhances neutrophil activation via FcγRIIIB (Ortiz-Bravo & Schumacher Jr, 1993). Crystals isolated from inflamed joints are typically coated in IgG. Other proteins identified on crystals from gout patients include complement components (C1q, C1r, C1s) (Terkeltaub et al., 1983), which may potentiate MSU inflammatory responses (An et al., 2014).

During the resolution phase of gout, the coating of the crystals changes and IgG is displaced by apolipoproteins. Apolipoprotein B (Terkeltaub et al., 1984) and Apolipoprotein E (Terkeltaub et al., 1991) are candidate pro-resolving factors in gout. These factors appear to coat the crystals, thus altering their “phlogistic” potential, although the exact mechanism is not known.

An alternative hypothesis to explain down-regulation of the inflammation is a change in the local macrophage population. A study of MSU crystal-induced responses of human monocyte-derived macrophages during a time-course of incubation over 7 day found that early on, there was a pro-inflammatory response with release of IL-1β and tumour necrosis factor-α (TNFα). As the macrophages matured, the pro-inflammatory response was attenuated and transforming growth factor beta-1 (TGFβ1) release

increased consistent with a change to a more tolerogenic phenotype capable of dampening inflammation (Yagnik et al., 2004). The MSU-crystal response of leukocytes taken from experimentally-induced skin blisters at early time-points and later time-points when the blister was resolving showed a similar transition from pro-inflammatory to tolerogenic response.

1.3.4 Neutrophil activation – cell signalling

MSU crystals trigger a number of cell signalling pathways in neutrophils. Studies have demonstrated roles for several tyrosine kinases, including: Syk (Desaulniers et al., 2001); Src family kinases, including Lck/Yes novel tyrosine kinase (Lyn) (Gaudry et al., 1995); Tec (Popa-Nita et al., 2008) and protein kinase C (PKC) (Popa-Nita et al., 2009). The tyrosine phosphorylation pattern of MSU crystal stimulated cells is distinct from that elicited by other stimuli, such as *N*-formylmethionine-leucyl-phenylalanine (fMLP) (Gaudry et al., 1993). Colchicine, a therapeutic agent used in gout, inhibited this phosphorylation response (Roberge et al., 1993).

Syk activation is a crucial activation step for signalling from a number of cell surface receptors, both directly through the Immunoreceptor tyrosine-based activation motif of cell surface receptors (e.g. FcR, Dectin, TREM) and indirectly, utilizing an signalling adapter such as FcRγ or DNAX activation protein of 12kDa (DAP12) (e.g. integrin signalling) (Mocsai et al., 2010). Syk appears to function as an important signalling fulcrum, and as described above, MSU crystals may activate Syk in the absence of membrane protein receptor ligation (1.3.2 Lipid Sorting as receptor-independent activator).

1.3.5 MSU crystals and the Inflammasome

Inflammasomes are multimeric molecular platforms that recognise a range of cellular insults and cause caspase-1 activation, with cleavage of pro-IL-1β leading to release of the active or mature form of IL-1b (Latz et al., 2013). MSU crystals activate the NACHT, LRR and PYD domains-containing protein 3 (the NLRP3 inflammasome, (Martinon et al., 2006)) primarily studied in macrophages. IL-1β is a potent pro-inflammatory cytokine with key roles in triggering immune cell recruitment to sites of inflammation (Dinarello, 2009). IL-1β is strongly implicated in the pathogenesis of gout, both in humans and in murine models (C. J. Chen et al., 2006). Phase 2 trials of anakinra, a recombinant interleukin 1 receptor antagonist (IL-1Ra) with a short *in vivo* half life, reduced the clinical severity of gout in human subjects (So et al., 2007). An

anti-IL-1β antibody, Canakinumab (Schlesinger et al., 2012) and an IL-1ra Fc fusion protein (Rilonacept) (Dinarello, 2011) have also demonstrated clinical efficacy in gout, with superior pharmacokinetics to Anakinra. Of note, IL-1α is a closely related pro-inflammatory cytokine that also signals through the IL-1 receptor and is thus blocked by Anakinra, but not Canakinumab. IL-1α may play a role in inflammatory responses to MSU in its own right (Gross et al., 2012).

1.3.5.1 Lysosome destabilization and inflammasome activation

Crystal-induced inflammasome activation in macrophages may be mediated by lysosomal destabilization (Hornung et al., 2008). Inflammasome-activating particulates - including MSU, silica crystals and aluminium salts - were demonstrated to disrupt lysosomes using lysosome-labelling fluorescent dyes including Lysotracker, acridine orange, fluorescent dextran and DQ ovalbumin (Hornung et al., 2008). An inhibitor of crystal uptake (e.g. Cytochalasin D) also prevented both lysosome disruption and inflammasome activation. An inhibitor of phagolysosomal maturation, Bafilomycin, prevented acidification of macrophage lysosomes and inhibited lysosome protease activity reflected by reduced fluorescence of DQ ovalbumin, a fluorophore-labelled protein that becomes fluorescent when cleaved. Bafilomycin also blocked inflammasome activation. The link between phagosome destabilization and NLRP3 activation was proposed to be the release of Cathepsin B (Hornung et al., 2008) based on inhibition of the inflammasome by CA-074-Me, a cell-permeable inhibitor of Cathepsin B. Subsequent studies have shown that Cathepsin B-deficient murine macrophages are not protected from inflammasome activation (Brojatsch et al., 2014) suggesting that the effect of CA-074-Me is through a non-Cathepsin B pathway.

Hornung et al went on to use a non-particulate, lysosome-targeted membrane detergent, L-leucyl-L-leucine methyl ester (Leu-Leu-OMe), and were able to demonstrate that it caused lysosome destabilization and inflammasome activation. Of note, Leu-Leu-OMe only works in the lysosomes of cells expressing the protease dipeptidyl peptidase I (DPPI) (Thiele & Lipsky, 1992). These cell types include neutrophils, macrophages and natural killer NK cells.

Potassium efflux is a mechanism shared by a number of inflammasome activators and elevated extracellular potassium prevents crystal-induced inflammasome activation (Munoz-Planillo et al., 2013). MSU crystal ingestion by macrophages leads to the release of sodium from the dissolving intracellular crystals. Increasing intracellular

sodium levels leads to passive water influx and a drop in effective intracellular potassium levels to levels that can activate the inflammasome (Schorn et al., 2011).

1.3.6 Neutrophils and the inflammasome

The role of inflammasome activation in neutrophils remains unresolved. *In vitro*, MSU crystal stimulation of neutrophils can induce IL-1β generation (Roberge et al., 1991) and, notably, neutrophil proteases including proteinase 3 also have the capacity to mature pro-IL-1β independently of caspase-1 (i.e. inflammasome-independent) (Guma et al., 2009). Beyond its capacity to mature IL-1β, activation of the inflammasome can also lead to pyroptosis, a Caspase-1/11-mediated form of inflammatory cell death. Pyroptosis and neutrophils will be discussed further (Miao et al., 2010) (see below - 1.16.3. Pyroptosis).

1.3.7 Neutrophils and lysosome function

Whether lysosome destabilization plays a role in neutrophil crystal responses has been less well characterised than in macrophages, and drawing direct inferences from macrophages studies may not be appropriate. Neutrophil lysosome biology differs substantially from the better-studied macrophage lysosome (Nordenfelt & Tapper, 2011). First, it remains unclear which neutrophil structure corresponds to the lysosome of macrophages. The neutrophil contains a series of granules sharing some similarities with lysosomes (Cieutat et al., 1998). Both structures contain anti-bacterial proteins that can be deposited into the phagolysosome of the respective cell type, or exocytosed. Further separating the two cell types, neutrophil phagolysosomes undergo alkalinization rather than acidification during maturation (Jankowski et al., 2002). The acidic nature of macrophage lysosomes facilitates the action of lysosomal acid proteases, critical for breakdown of phagosome contents. This characteristic also allows the use of acidic organelle-targeting fluorophores, such as lysotracker and acridine orange (themselves weak bases that accumulate under acidic conditions) to study phagolysosome maturation. Non-pH dependent lysosome markers include fluorescent dextrans and DQ ovalbumin, which is dependent on protease activity for its localisation and fluorescence (Hornung et al., 2008). Neutrophil azurophil granules are acidic, but the proteases contained in neutrophil granules function optimally at a neutral pH as found in the phagosome (A. P. Levine et al., 2015). This suggests that maintenance in a low pH environment may be part of the mechanism to prevent inappropriate enzyme activation until delivery into the phagosome.

Phagocytosis is evident in neutrophils taken from the joint fluid of patients with acute gout that have phagocytosed crystals (Riddle et al., 1967). Whilst most crystals were surrounded by a continuous membrane consistent with phagosome formation, some neutrophils appeared to have crystals free in the cytoplasm, suggesting that they may destabilize the phagosome.

1.3.8 Inflammasome-independent pathways

Crystals can stimulate cells through pathways other than the inflammasome. Release of prostaglandin E2, another important pro-inflammatory mediator from silica- and alum-treated macrophages occurs in an inflammasome-independent manner involving Syk signalling (Kuroda et al., 2011).

1.4 Neutrophil effector mechanisms

Neutrophils are important innate immune cells that have the capability to release a variety of inflammatory mediators. Neutrophil granules contain a series of enzymes that mediate pathogen clearance and can contribute to tissue damage (Amulic et al., 2012). As bone marrow neutrophils mature, they develop granules that store the enzymes safely until they are exocytosed at sites of inflammation or deposited into pathogen-containing phagosomes. Primary or azurophil granules contain neutrophil elastase (NE) and myeloperoxidase (MPO) and several other granule proteins. NE is a relatively non-specific serine protease capable of damaging both pathogens (Weinrauch et al., 2002) and host tissues (Korkmaz et al., 2010).

MPO is important for the production of reactive oxygen species (ROS), a key neutrophil anti-pathogen strategy. Nicotinamide adenine dinucleotide phosphate-oxidase (NADPH oxidase) is an enzyme complex present in neutrophils that forms with stimulation and generates large amounts of ROS critical to the control of pathogens and whose genetic absence leads to the human immune deficiency, Chronic Granulomatous Disease (CGD). ROS initially transmutate to hydrogen peroxide that then acts as the substrate for MPO that generates further types of ROS including hypochlorous acid, a potent antibacterial (Winterbourn et al., 2016). Secondary neutrophil granules are characterised by the presence of lactoferrin and tertiary granules contain gelatinase (Amulic et al., 2012).

MSU crystals induce several types of neutrophil responses that can contribute to inflammation. *In vitro*, MSU crystals cause neutrophils to release ROS (Abramson et

al., 1982), neutrophil granule proteins, lysosomal enzymes (Ginsberg et al., 1977) and cytokines such as IL-1β (Roberge et al., 1991) and IL-8 (Hachicha et al., 1995). MSU crystals also cause the release of as yet indeterminate chemotactic substances from neutrophils. Crystal-induced chemotactic factor was described first in 1976 (Spilbert et al., 1976), but was not found to be one of the expected chemotactic molecules. Another MSU-induced neutrophil chemoattractant and activating factor has been found (Desaulniers et al., 2006). It is a protein of between 30 and 50 kDa in molecular weight that acts through a pertussis toxin sensitive (G protein coupled) pathway and is released preformed from neutrophils within 15 minutes of MSU crystal stimulation.

1.5 Therapeutics for gout and effects on neutrophils

1.5.1 Colchicine

Colchicine has been used as an anti-inflammatory for over a thousand years. Surprisingly, its mechanism of action remains unclear. The therapeutic effects of colchicine are relatively specific for crystal-induced inflammation (Nuki, 2008). It is effective in high doses for both acute attacks and, at low doses, to prevent attacks. In contrast, colchicine is ineffective against rheumatoid arthritis, which is an autoimmune form of inflammatory arthritis.

The potential cellular targets of colchicine in gout include neutrophils and macrophages. Colchicine inhibits microtubule polymerization (Sackett & Varma, 1993), which is important for several cellular functions. Colchicine also has effects on cell motility (Phelps, 1969), leukotriene release (Serhan et al., 1984), IL-1β (Roberge et al., 1991) and IL-8 (Matsukawa et al., 1998) release. Colchicine inhibits inflammasome activation in macrophages (Martinon et al., 2006), suppressing IL-1β production via disruption of microtubule-mediated mitochondrial arrangement critical for assembly of the NLRP3 inflammasome (Misawa et al., 2013).

Studies suggest that PKC-dependent Syk phosphorylation is also inhibited by colchicine (Popa-Nita et al., 2009). Interestingly, colchicine has a paradoxical augmenting effect on tyrosine phosphorylation induced by the chemotactic agent N-formylmethionine-leucyl-phenylalanine or fMLP and increases ROS production (Roberge et al., 1996). Colchicine inhibits crystal-induced calcium release (Naccache et al., 1991), but does not influence crystal-induced release of prostaglandins (Gilbert et al., 2003).

Oral administration of colchicine to mice at doses and blood concentrations comparable to those used clinically to prevent gout in patients reduced *ex vivo* MSU-induced ROS production in human and murine neutrophils (Chia et al., 2008). PMA-induced ROS was not inhibited by colchicine.

Neutrophils from patients on colchicine appear to have reduced L-selectin expression, but no difference in CD11b/CD18 (Cronstein et al., 1995). The authors proposed this could have effects on cell trafficking that might contribute to the preventative effects of colchicine.

1.5.2 Non-steroidal anti-inflammatory drugs

Non-steroidal anti-inflammatory drugs (NSAIDs) are a standard therapy for acute inflammation in gout (Cronstein & Terkeltaub, 2006). These drugs inhibit cyclooxygenase (COX) to prevent formation of pro-inflammatory prostaglandins, which are released from neutrophils by MSU crystals. Cyclooxygenase occurs in two isoforms: the constitutive COX1 important for gastrointestinal homeostasis and platelet function; and COX2 or inducible COX involved in inflammatory responses (Smith et al., 2000). Neutrophils constitutively express COX2 (Gilbert et al., 2003) and blockade of this enzyme leads to reduced PG release. Indomethacin, a potent, non-specific COX inhibiting NSAID also has a partial effect on crystal-induced motility (Phelps, 1969).

1.5.3 Glucocorticoids

Glucocorticoids (GC) are another standard therapy for gout treatment and are of comparable efficacy to NSAIDs (Janssens et al., 2008). GC act via the glucocorticoid receptor and lead to suppression of pro-inflammatory cytokine expression and release of anti-inflammatory molecules, such as MKP-1 and Annexin-1 (Newton, 2014). GC effects on neutrophils specifically are broad (Goulding et al., 1998) with effects on migration likely accounting for a significant portion of their inflammatory effect *in vivo* (Boumpas et al., 1993). Neutrophils are subject to the genomic effects of glucocorticoids including suppression of LPS-induced proinflammatory gene expression (Hirsch et al., 2012) and high doses *in vitro* can interfere with phagocytosis (Jones et al., 1983) and degranulation (Jiang et al., 2014). Given their overall anti-inflammatory effect, glucocorticoids paradoxically increase neutrophil survival (Saffar et al., 2011).

1.6 NETosis

NETosis is a form of cell death that has potential inflammatory consequences and extends the suite of neutrophil anti-pathogen strategies. Beyond inflammatory disorders, NETosis has been implicated in a number of other diseases and pathological processes including thrombosis (Martinod & Wagner, 2014), consequences of metabolic disease (Wong et al., 2015) and cancer (Demers et al., 2012). NETosis has also been recognised as a neutrophil response to MSU crystals.

1.6.1 NETosis - Basic biology

NETs and the associated form of cell death, NETosis have only been recognised as a novel anti-pathogen strategy over the past 13 years (Brinkmann et al., 2004). Initially characterised in neutrophils, subsequent studies have suggested a similar process occurs in eosinophils (2008), mast cells (von Kockritz-Blickwede et al., 2008), and macrophages (Webster et al., 2010). NETs are complexes of DNA, histones and neutrophil granule proteins formed intracellularly after stimulation and then released extracellularly. NETs are thought to be an important effector mechanism of neutrophils in suppressing and killing extracellular bacteria and fungi (Brinkmann & Zychlinsky, 2012). An inability to make NETs may account in part for the immunodeficiency observed in patients with Chronic Granulomatous disease (Fuchs et al., 2007).

Studies have also highlighted a possible pathogenic role for NETs in autoimmune disease (Hakkim et al., 2010; Kessenbrock et al., 2009), pre-eclampsia (Gupta et al., 2005) and cystic fibrosis (Marcos et al., 2010). NET biology is a rapidly developing field with recent discoveries outlining some of the key molecular mechanisms involved in NETosis. However, key questions remain, in particular the *in vivo* relevance of NETs in various contexts (Nauseef & Kubes, 2016).

1.6.1.1 Lytic versus non-lytic NETosis

One point of contention in the NET literature is whether neutrophils release NETs only in the context of cell death and membrane compromise, or whether DNA release can occur from living cells (Yipp & Kubes, 2013). Evidence for both possibilities has been found, suggesting that there may be at least two different forms of NET release. The most compelling data supporting non-lytic or “vital” NETosis release comes from Kubes and co-workers (Yipp et al., 2012). Using intravital imaging, neutrophils were observed to release DNA, but remained viable and continued to traffic through tissues.

Another potentially distinct form of NETosis relates to the expulsion of mitochondrial DNA (rather than nuclear DNA), in a catapult-like fashion from living neutrophils (Yousefi et al., 2009) and eosinophils (2008). *Staphylococcus aureus* also induces rapid NET release that is not associated with cell death (Pilsczek et al., 2010). This NET release is NADPH oxidase-independent and the NETs released are composed of nuclear DNA.

For the purposes of this review, I will focus on the mechanisms of "Lytic NETosis".

1.6.2 NET-Releasing Stimuli

A number of stimuli cause NET release (see Table 1.1 for a general overview of NET inducing agents). Why these diverse stimuli all cause NET release is not clear and whether there is a common mechanistic pathway remains to be elucidated.

Table 1.1 - NET-releasing Stimuli

Pathogens	Bacteria
	Fungi
	Viruses
	Parasites
Chemical inducers	PMA
	Glucose oxidase
	Calcium Ionophores
DAMPs	MSU crystals
	CPPD crystals
	Alum
Other	Autoantibodies
	Immune complexes
	Platelet-activating Factor

1.6.2.1 Phorbol Myristate Acetate (PMA)

The best-studied and most potent NET releasing compound is phorbol myristate acetate (PMA), a PKC-agonist derived from a plant extract (Repine et al., 1974). PMA activates a number of immune cells, including neutrophils (DeChatelet et al., 1976), and causes ROS release, degranulation and cytokine release. PMA bypasses integrin signalling to directly activate PKC (Walker et al., 2004). The potency and direct

activating effects of PMA suggests that neutrophil responses to PMA may not closely reflect those of physiological stimuli. In NET assays, it causes an initial flattening and vacuolation of neutrophils, with subsequent nuclear delobulation and NET release commencing after approximately 2 hours (Remijsen, Vanden Berghe, et al., 2011).

1.7 Mechanistic pathways in NETosis

1.7.1 Role of Reactive Oxygen species in NETosis

PMA-induced NETosis is dependent on NADPH oxidase function. This has been determined by chemical inhibition of NADPH oxidase (with diphenylene iodonium [DPI]) and genetic strategies using neutrophils from patients with CGD (Fuchs et al., 2007). Fungal-induced NETosis is also NADPH oxidase-dependent. This was powerfully confirmed when an individual with Chronic Granulomatous Disease (CGD) recovered a NETosis response to *Aspergillus* following successful gene therapy with retroviral stem cell transfection of the genetically absent NADPH oxidase component $gp91^{phox}$ (Bianchi et al., 2009). The majority of other stimuli including bacteria and fungi that induce NETosis have been reported to be NADPH oxidase-dependent.

How ROS subsequently trigger NETosis remains unclear. A recent study suggests that ROS trigger the dissociation of neutrophil elastase (NE) from a granule membrane-associated complex into the cytosol (1.7.3 below - Neutrophil elastase and myeloperoxidase)

1.7.1.1 NADPH oxidase-independent NETosis

In contrast to PMA, NETosis induced by calcium ionophore is not dependent on NADPH oxidase (Parker et al., 2012). This form of NETosis is dependent on mitochondrial-derived ROS (Douda et al., 2015), the production of which can be partially inhibited by DPI. Some authors have proposed that calcium ionophore stimulation induces a biochemically distinct form of NETosis (Konig & Andrade, 2016).

Immune complexes comprising nucleic acids and autoantibodies derived from patients suffering from Systemic Lupus Erythematosus (SLE) caused the release of NETs containing oxidised mitochondrial DNA (Lood et al., 2016). This NET release is at least partially dependent on mitochondrial ROS generation. Patients with active SLE are frequently found to have a population of neutrophils referred to as low-density granulocytes (LDGs) because these neutrophils appear in the PBMC fraction of density gradient sedimentation blood preparations. LDGs appear to undergo spontaneous

NETosis (Villanueva et al., 2011). Interestingly, CGD patients were also found to have circulating LDGs that can release NETs (Lood et al., 2016). This is also dependent on mitochondrial ROS, providing genetic evidence of a NADPH-oxidase independent pathway of NET release. The role of these cells in healthy patients and other inflammatory conditions such as gout remains to be defined. They provide a technical challenge when assessing NETosis as they do not represent an easily defined population.

Calcium pyrophosphate dehydrogenate crystals (CPPD) deposit in articular structures and cause the human inflammatory arthritis condition, pseudogout so-called because it had very similar clinical manifestations to gout. CPPD crystals were found to elicit ROS release and NETosis. The NETosis however was not inhibited by DPI, despite suppression of ROS (Pang et al., 2013). This contrasts with other crystalline NET inducers that have been reported to require NADPH oxidase function (Schorn et al., 2012; Warnatsch et al., 2015). The role of NADPH oxidase in NETosis is not universal and may separate NETosis into different subtypes categorised on different mechanistic pathways.

1.7.2 Histone citrullination

Citrullination is the chemical conversion of arginine to citrulline, which is a non-standard amino acid. The enzymes that catalyze the citrullination of proteins are peptidylarginine deiminases or PADI. (Vossenaar et al., 2003). Histone citrullination has been previously studied in the context of transcriptional regulation, where citrullination unwinds chromatin, making it accessible to transcription factors (Y. Wang et al., 2004). Dimethyl sulfoxide (DMSO)-treated HL-60 cells, a leukaemia cell line that has neutrophil-like qualities, undergo cell death and DNA decondensation consistent with NETosis when treated with calcium ionophores. The calcium ionophores were found to activate PADI4 that led to hypercitrullination of histones throughout the nuclear chromatin leading to unwinding of the DNA (Y. Wang et al., 2009). The authors concluded that this unwinding is responsible for the chromatin release during NETosis.

A PAD4 gene deficient (*PAD4-/-*) mouse has been developed and demonstrated significant impairment in NET release and susceptibility to bacterial infection (Li et al., 2010). During polymicrobial sepsis, however, PAD4 deficiency does not seem to affect bacteraemia and can even have a beneficial effect on shock (Martinod et al., 2015). PAD4 does not appear to play a role *in vivo* during influenza infection (Hemmers et al.,

2011). Further, in the K/BxN model of inflammatory arthritis, *PAD4-/-* mice were not protected from disease (Rohrbach et al., 2012).

A broad-spectrum inhibitor of PAD enzymes, Cl-amidine, has been used to explore citrullination *in vitro*, but there are conflicting reports (Chow et al., 2010; Khandpur et al., 2013) on whether or not it inhibits human NETosis (Khandpur et al., 2013). A number of different PAD inhibitors failed to reduce NETosis induced by PMA, Candida, bacteria, nigericin and calcium ionophore despite evidence of reduction in citrullination (Kenny et al., 2017). A second-generation PAD4 inhibitor (GSK484) reduced murine NETosis when stimulated with calcium ionophore (Lewis et al., 2015). *In vivo* experiments in a different model of inflammatory arthritis, collagen-induced arthritis, found that both the general PAD inhibitor and the PAD4 specific inhibitor ameliorated disease (Willis et al., 2017; Willis et al., 2011). Experiments with human neutrophils demonstrated some reduction in *Staphylococcus aureus*-induced NETosis (i.e. lytic NETosis).

It is remains to be seen whether PADI inhibition inhibits NETosis triggered by other stimuli. Citrullination during NETosis is stimulus-dependent. Calcium ionophores potently induce citrullination but PMA demonstrates relatively low amounts of citrullination and may actively suppress it through differential activation of PKC isoforms (Neeli & Radic, 2013).

The presence of citrullinated histones has been used as a surrogate marker of NET release, allowing interrogation of tissues for *in vivo* NET formation. However, whether citrullination only occurs in the context of NETosis is not clear (Romero et al., 2013). One group has proposed that neutrophil hypercitrullination may occur without NETosis and urged caution in attributing citrullinated histones to NETosis (Konig & Andrade, 2016).

1.7.3 Neutrophil elastase and myeloperoxidase

Neutrophil elastase (NE) and myeloperoxidase (MPO) are neutrophil azurophilic granule proteins strongly implicated in PMA and *Candida hyphae*-induced NETosis (Papayannopoulos et al., 2010). During PMA and *Candida* NETosis, ROS generation leads to the dissociation of a complex of neutrophil granule proteins called the “azurosome”. This results in the release of NE into the cytosol where it is initially sequestered by actin. NE subsequently degrades the actin, releasing itself to enter the nucleus (Metzler et al., 2014). NE potently degrades histones, the highly positively

charged proteins that condense the chromatin in unstimulated cells (Papayannopoulos et al., 2010). This results in the decondensation of the chromatin prior to cell death and the DNA mixes with the NE, MPO and other proteins before cell membrane lysis and release (Figure 1.1 Schema of PMA-induced NETosis). A recent study found that NE is not required for calcium ionophore and nigericin induced NETosis (Kenny et al., 2017).

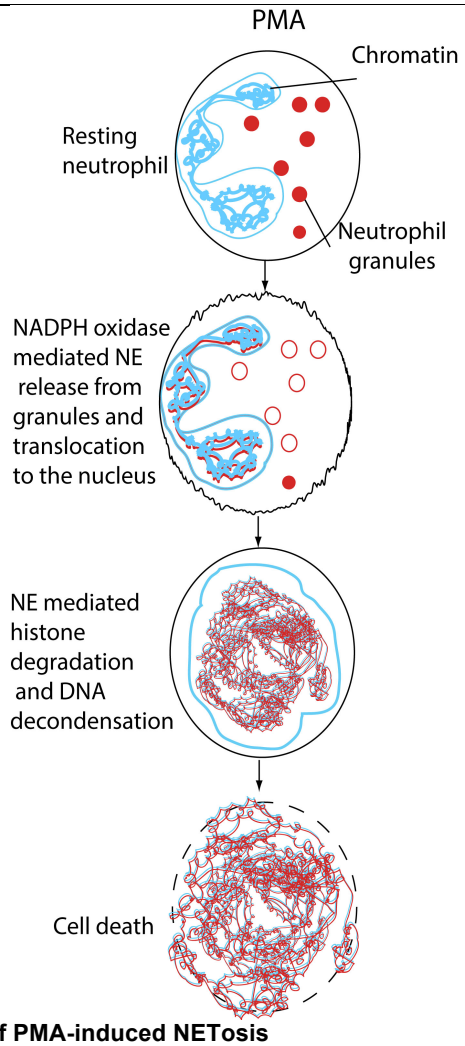


Figure 1.1 Schema of PMA-induced NETosis

This pathway is also triggered during attempted phagocytosis of large hyphae (Branzk et al., 2014). During phagocytosis of smaller particles - such as individual yeast and some bacteria - NE is deposited in the pathogen-containing phagosome. During attempted or frustrated phagocytosis of elongated hyphal forms, a phagosome fails to form and NE is not deposited around the partially ingested organism. Instead, this appears to trigger NE release into the cytosol and NETosis.

Whilst assessment of NETosis in NE-deficient humans has not been described, patients with Papillon-Lefevre syndrome fail to release NETs when stimulated with PMA, or a generator of intracellular ROS, glucose oxidase (Sorensen et al., 2014). These patients are deficient in cathepsin C that is critical for the processing and loading of neutrophil enzymes into granules. Papillon-Lefevre syndrome patients are effectively deficient in NE, cathepsin G (CTSG), proteinase 3 (PR3), and neutrophil serine protease 4. Interestingly, calcium ionophore-induced NETosis was not impaired in a single PL individual (Batinica et al., 2016).

NE gene deficient (*NE-/-)* mice developed fewer NETs in a pneumonia model (Papayannopoulos et al., 2010). This study noted that peritoneal neutrophils responded poorly to NET agonists *in vitro*, limiting the analysis of NETosis. A separate study found the *NE-/-* mice were able to still make NETs using both *in vitro* and *in vivo* models (Martinod et al., 2016). Dual NE and Proteinase 3 gene deficient mice were used in another NETosis study (Warnatsch et al., 2015). NE deficiency alone failed to dampen the effect of the neutrophil proteases in murine neutrophil activation (Kessenbrock et al., 2008).

Myeloperoxidase (MPO) also contributes to DNA decondensation. MPO deficient patients fail to form NETs (Metzler et al., 2011). Extracellular supplementation of MPO did not correct the abnormality, demonstrating that MPO acts in a cell autonomous fashion. As described above, MPO activity appears to facilitate the release of NE from granules. Both MPO and NE demonstrate a characteristic binding pattern on NETs, with uniform coverage of DNA. This compares to other proteins, such as proteinase-3, that are NET-associated but form globular structures along DNA (Urban et al., 2009).

Whether this “canonical” pathway of NE/MPO-mediated NETosis is operative in all forms of NETosis remains to be seen. Further study is required to determine whether the NE pathway and the citrullination pathway operate separately, or can be synergistic.

1.7.4 Autophagy

Autophagy is the cellular process of disassembly and disposal of unnecessary cellular components that occurs through the generation of large vacuoles termed autophagosomes. The mechanism of autophagy has been found to involve dedicated genes and autophagosomes contain LC3 that serves as a immunological marker of autophagy (B. Levine et al., 2011). Several studies have investigated the potential role

of autophagy in NETosis. NETosis induced by PMA is accompanied by a profound vacuolization and LC3 staining suggesting the presence of autophagy. This morphologic change is not evident with apoptosis (Remijsen, Vanden Berghe, et al., 2011). Furthermore, inhibition of autophagy with wortmannin (a potent PI3K inhibitor) reduced vacuolation and NETosis without any effect on ROS generation. Wortmannin did not reduce PMA-induced cell death - cells still died, but did not release DNA. Cell death with Wortmannin treatment bore features more consistent with apoptosis with only slow decondensation of chromatin post-mortem. The formulated schema proposed that both ROS generation and autophagy are required for NETosis.

Autophagy has also been implicated in MSU-induced NETosis (Mitroulis et al., 2011). Once again, autophagy was evident in MSU-stimulated neutrophils assessed with LC3 staining. LY290042 (an alternative PI3K and autophagy inhibitor), 3-methyladenine (3MA – an inhibitor of Class III PI3K) and Bafilomycin A (inhibitor of vacuolar-type H+-ATPase, which is important for phagosome maturation) inhibited NETosis. The inhibitors were added 30 minutes after the crystals to avoid interference with phagocytosis. Wortmannin also partially reduced CPPD crystal-induced NETosis, whilst also suppressing ROS production (Pang et al., 2013), in contrast to the previous reports on PMA-induced NETosis.

Whilst autophagy may play a role in NETosis, it may occur in parallel with apoptotic cell death without playing a direct mechanistic role (Lindqvist et al., 2014). The chemical inhibitors of autophagy used have effects beyond autophagy. PI3K plays roles in phagocytosis that is likely to be of importance in particulate-induced NETosis and the compounds may have other targets as well. Analysis of autophagy gene deficient mice and cell lines may clarify the role in NETosis.

1.7.5 Cell-signalling pathways involved in NETosis

1.7.5.1 Raf-MEK-ERK pathway

A high throughput drug screen found a role for the Raf-MEK-ERK signalling pathway in PMA and *Helicobacter pylori*-induced NETosis (Hakkim et al., 2011). Given the link between myeloid leukaemia cell differentiation protein (Mcl-1) and extracellular signal–regulated kinases (ERK) (Moulding et al., 1998), the authors went on to assess Mcl-1 expression in NET releasing neutrophils. (Moulding et al., 1998). PMA led to significant up-regulation of Mcl-1 (assessed using immunofluorescence) and this up-regulation was decreased in the presence of inhibitors of the Raf-MEK-ERK pathway. Up

regulation of Mcl-1 is usually associated with reduced apoptosis, suggesting PMA activates an anti-apoptotic program that might facilitate NETosis.

1.7.5.2 Protein Kinase B (Akt)

Protein kinase B, also known as Akt s a kinase involved in a number of signalling pathways with multiple signalling partners including PI3K. One particularly relevant pathway that Akt is involved in is neutrophil anti-apoptotic signalling. One study found that PMA activates Akt via NADPH oxidase-dependent ROS. Two Akt inhibitors reduced PMA-induced NETosis (Douda et al., 2014). Inhibition of NETosis was accompanied by evidence of apoptosis including the presence of cleaved caspase-3 on immunofluorescence. The authors proposed that the Akt pathway is a molecular switch between apoptosis and necroptosis.

A summary of the potential pathways involved in NETosis is presented below (Figure 1.2). Whether these signalling pathways and biochemical mechanisms are important for all types of NETosis awaits further study.

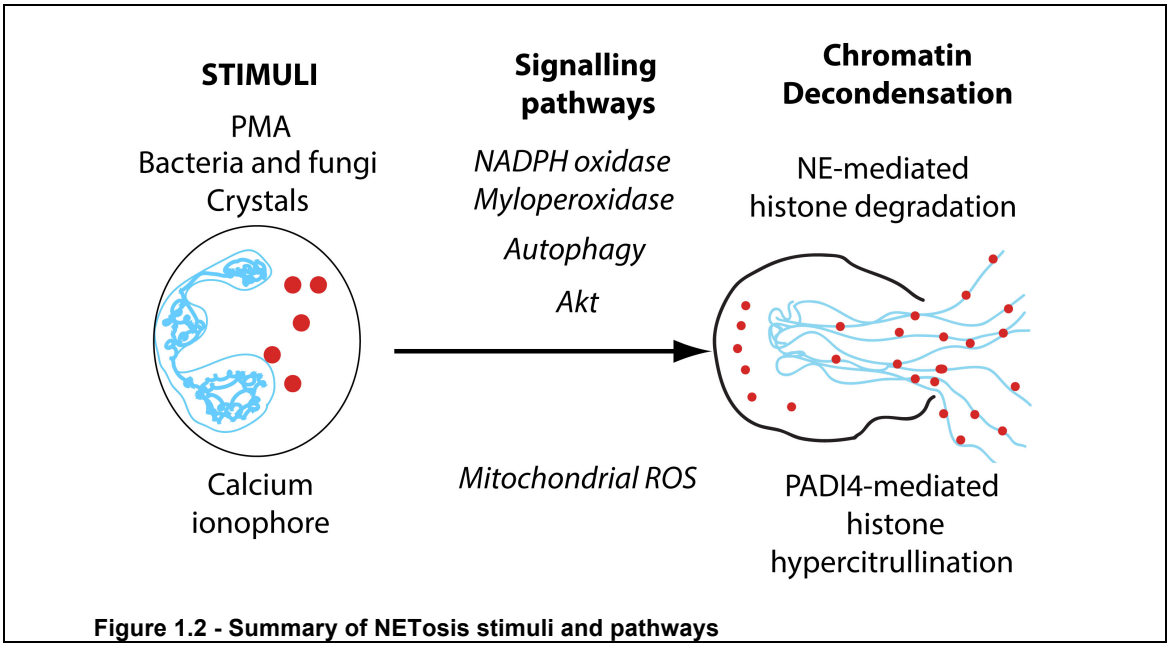


Figure 1.2 - Summary of NETosis stimuli and pathways

1.7.6 Neutrophil Development and NETs

The maturity of neutrophils appears to be an important factor in the ability to release NETs. Immature neutrophils isolated from human bone marrow were unable to produce NETs in response to C5a, following priming with interferon alpha (IFN-α), interferon gamma (IFN-γ) or granulocyte macrophage colony stimulating factor (GM-CSF) (Martinelli et al., 2004). Neutrophils from neonates also showed delayed NET

release compared to those of adults (Marcos et al., 2009). Neonatal serum taken from cord blood contains an uncharacterised factor that has a broad inhibitory effect against NETosis induced by multiple stimuli (Yost et al., 2016).

DMSO treatment of the myeloid cell line, HL-60, leads to partial granulocytic differentiation and the resulting neutrophil-like cells have been used by some authors to study NET release, (Y. Wang et al., 2009). A cell line allows more genetic manipulation compared to freshly isolated, terminally differentiated neutrophils, but it has significant limitations. A recent study has demonstrated that neutrophil-like HL60 cells poorly reproduce the key function of neutrophils including ROS generation, NETosis and overall anti-bacterial activity (Yaseen et al., 2017).

1.7.7 Mouse NETs versus Human NETs

Mice have fewer circulating neutrophils compared to humans, but the difference may reflect the relatively immature immune system of laboratory mice (Beura et al., 2016). How well murine neutrophils reflect human NETosis is not clear but murine neutrophils respond less to PMA, the most commonly used stimulus in human NETosis studies. In one study, only around 30% of mouse neutrophils release NETs after 16 hours, compared to 60-80% of human neutrophils within 4 hours (Ermert et al., 2009). Murine NETs are more compact than human NETs, but are ROS-dependent. Murine neutrophils taken from the inflamed peritoneal cavity do not respond to PMA (Papayannopoulos et al., 2010). Whilst murine models provide genetic power to *in vitro* and *in vivo* investigation of biological processes, these potential species differences need to be borne in mind when interpreting results.

1.8 NET Proteins

The protein content of NETs or the “NET proteome” has been studied in several reports. Urban et al. isolated PMA-induced NETs using a limited nuclease degradation strategy whereby partially digested NETs are obtained after washing away cytoplasmic contents in the supernatant and avoiding proteins associated with the intact cells (Urban et al., 2009). Proteomic analysis revealed a relatively small set of NET-associated proteins, the most abundant of which are the core histones (H2a, H2b, H3 and H4) and neutrophil derived proteins (e.g. NE, S100A8). These findings highlight the relatively specific association of neutrophil granule proteins with NETs. Of note, there was a relative paucity of cytoplasmic proteins, such as actin. Actin is actively

degraded during PMA NETosis (Metzler et al., 2014), perhaps accounting for the absence of actin in these experimentally induced NETs.

An investigation of the role of NETs in RA compared the NET proteome from neutrophils stimulated in vitro with TNFα, immunoglobulins derived from the serum of RA patients or isolated IgM rheumatoid factor (RF). Proteomic analysis demonstrated some heterogeneity of the protein content of NETs, with the majority of proteins shared between different conditions and several proteins more highly expressed or unique to specific stimuli. For example, the RF-treated neutrophils produced NETs containing matrix metalloproteinase 8 and histone 3 that was not found on TNFα-induced NETs (Khandpur et al., 2013).

1.9 Degradation of NETs

The fate of NETs released *in vivo* is uncertain. The DNA backbone of NETs is susceptible to nuclease degradation. Foetal calf serum contains nucleases that readily degrade NETs *in vitro*. Serum also has a direct inhibitory effect on NET release (Fuchs et al., 2007), and so serum is omitted from culture media during NET analysis.

Human serum also contains NET degrading nucleases (Hakkim et al., 2010). Actin, a physiologic inhibitor of Deoxyribonuclease 1 (DNase1) and an antibody against DNase1) both inhibit the NET-degrading effect of serum supporting the hypothesis that DNase1 is the primary nuclease responsible. The same study identified a subset of SLE patients who demonstrated a deficiency of serum nuclease activity. This may be of particular relevance in SLE, where NETs could provide a target of autoimmunity. The lack of nuclease function in SLE was attributed to two types of autoantibodies: one targeting the effect of DNase1 specifically and the other protecting DNA from nuclease attack, including that of micrococcal nuclease (MNase).

NETs generated by neutrophils activated by human saliva have been reported to be relatively resistant to nucleases (Mohanty et al., 2015). The mechanism proposed was an effect of the ionic composition of the saliva promoting actin binding to DNA. Actin is a physiologic inhibitor of DNase I (Lazarides & Lindberg, 1974) but has no effect on MNase (Hakkim et al., 2010). Entrapment of organisms is one of the proposed mechanisms of action of NETs and a number of bacteria express nucleases that facilitate NET breakdown and their escape (Beiter et al., 2006; Buchanan et al., 2006).

1.10 Impact of NETs on the inflammatory response

NETs are composed of a number of components that in other contexts serve as potent danger-associated molecular patterns (DAMPs), including extracellular DNA and protein "alarmins" (e.g. LL-37 and defensins). In the context of infection, these could potentially serve as endogenous adjuvants to facilitate activation of neighbouring immune cells and clearance of the pathogen. These same DAMPs could also serve to drive inflammatory disorders in which NETs have been implicated.

In regard to the response to dead cells, macrophages polarize to an anti-inflammatory phenotype after phagocytosis of apoptotic neutrophils (Fadeel et al., 1998). Different studies have reached different conclusions in regard to the phagocytosis of NETs. Macrophages disposed of PMA-induced NETs in an actin-dependent manner, and in an immunologically silent fashion (Farrera & Fadeel, 2013). The NET DNA was subsequently degraded in lysosomes in a process that was inhibited by chloroquine. Cytokine release was not elicited from the macrophages that had taken up these NETs, even in the presence of chloroquine to delay DNA degradation. In the presence of LPS however, NETs caused an increase in cytokine release including IL-1β, TNFα and IL-6. Another study suggested the response to NETs might depend on the polarization state of the macrophage. Macrophages were either cultured in interleukin-4 to generate a less-inflammatory regulatory macrophage or LPS and type-1 interferon to promote inflammatory macrophage differentiation. A pro-inflammatory response was observed in interleukin-4 polarized THP-1 cells cultured with NETs but the inflammatory macrophages underwent cell death when stimulated with NETs (Nakazawa et al., 2016). A separate study found that micrococcal nuclease-liberated NETs (LPS-induced after one hour) could activate the inflammasome in monocyte-derived macrophages (Kahlenberg et al., 2013) assessed by the presence of cleaved IL-1β and caspase activation measured with a fluorescent probe. The ability to activate the inflammasome was attributed to the LL-37 content of the NETs.

In monocyte-derived dendritic cells, NETs down-regulated lipopolysaccharide (LPS)-induced activation (Barrientos et al., 2014), suggesting the phagocytic response to NETs may be cell type specific. The inconsistency in the inflammatory responses of phagocytosis to NET stimulation may reflect cellular differences and differences in the preparation of the NETs.

1.10.1 NETs and inflammation in autoimmune diseases

In autoimmune conditions, antibodies targeting NET components may alter the inflammatory potential of NETs. NETs may therefore promote or perpetuate autoimmune diseases, such as systemic lupus erythematosus (Garcia-Romo et al., 2011; Lande et al., 2011) and rheumatoid arthritis (Khandpur et al., 2013). In these diseases, autoantibodies appear to facilitate NET uptake and inflammatory potential or interfere with appropriate NET degradation (Hakkim et al., 2010). This likely represents a perturbation of the physiologic role of NETs and by itself, does not confirm a physiologic pro-inflammatory role. NETs generated from SLE neutrophils contain higher levels of LL-37 and HMGB1, potentially enhancing inflammatory potency (Garcia-Romo et al., 2011; Lande et al., 2011). The ability of NETs to drive type-1 interferon responses in anti-neutrophil cytoplasmic antibody (ANCA) associated vasculitis is supported by the finding of colocalization of an interferon-inducible protein myxovirus resistance protein 1 (MxA) with NET structures in the biopsy of a kidney with ANCA-associated vasculitis (Kessenbrock et al., 2009). The generation of antibodies against the specific components of NETosis in these different diseases, possibly driven by genetically determined biases in antigen presentation, may play an important role in the differing manifestations.

1.10.2 NETs and inflammation in crystal diseases

It has long been recognized that MSU crystals can cause lysis of target cells, including neutrophils (Weissmann & Rita, 1972). This lysis has been thought to be due to direct disruption of cell membranes as the crystals also caused lysis of non-phagocytic erythrocytes (Wallingford & McCarty, 1971). Other studies have proposed that the crystals can induce “lysis from within” based on the presence of crystals within neutrophils with evidence of loss of phagosome membranes (Weissmann & Rita, 1972). MSU crystal-induced lysis of neutrophils observed in these old studies may be consistent with NETosis as found in several recent studies (Mitroulis et al., 2011; Schauer et al., 2014).

Reports on the potential role of NETs in inflammation in crystal-induced NETosis are mixed, reflecting possible context-dependence. Using a mouse model of MSU crystal-induced peritonitis, an anti-inflammatory, pro-resolving role for NETs was observed (Schauer et al., 2014). In this study, large aggregates of crystals and neutrophils undergoing NETosis formed *in vitro* and *in vivo* bore a strong structural resemblance to tophi. The authors performed immunofluorescence studies on human tophi and

demonstrated DNA and neutrophil granule proteins. The *in vitro*-generated aggregates also degraded inflammatory cytokines through the action of neutrophil serine proteases but this only occurred at a high threshold neutrophil concentration when large cell-crystal aggregates formed. The *in vivo* inflammation suppressing effect was reduced in the presence of DNase, by as yet unexplained mechanisms. Binding of proteases onto DNA has been previously found to inhibit protease activity in the context of cystic fibrosis (Cantin, 1998). This suggests the DNA structure may also play a role in the physical sequestration of the crystals and creating high DNA-dependent local concentration of proteases.

The anti-inflammatory response was also reduced in mice deficient for a component of the NADPH oxidase. NADPH-oxidase inhibition and ROS scavengers *in vitro* reduced the neutrophil crystal aggregation and ROS-deficient mice formed smaller aggregates *in vivo*. Apart from its effect on aggregate formation, ROS generation may also protect neutrophil serine proteases from circulating inhibitors, such as α2-macroglobulin (Abbink et al., 1991) and α1-trypsin (Taggart et al., 2000). Whether the lack of anti-inflammatory effect of neutrophils in the absence of NADPH oxidase is completely attributable to NETs is not clear. NADPH oxidase and ROS play multiple roles in neutrophils and other cell types and whether neutrophils are required for the pro-resolving effect in the murine model of MSU inflammation is still debated (Reber et al., 2016).

A similar anti-inflammatory effect has been demonstrated when stimulating PBMCs with *Candida albicans* (Gresnigt et al., 2012). The addition of neutrophils limited production of IL-1β and TNFα by PBMC. Transwell experiments found that this effect was driven by neutrophil proteases rather than by inhibition of phagocytosis and, unlike the scenario described above, this effect was independent of NADPH oxidase. *In vivo* experiments demonstrated that depletion of neutrophils led to elevated pro-inflammatory cytokine levels and aggravated zymosan-induced arthritis supporting the *in vitro* findings.

A study of cholesterol crystal-induced inflammation in the setting of atherosclerosis found a pro-inflammatory priming effect of NETs (Warnatsch et al., 2015). Partially cleaved NETs provided inflammasome priming in cholesterol-crystal stimulated monocytes *in vitro*. Monocytes are often used as a surrogate for tissue macrophages, but the responses of these cells to pro-inflammatory stimuli vary significantly (Netea et

al., 2009). In particular, monocytes can release IL-1β through a non-canonical mechanism when stimulated with LPS alone without the need for a traditional inflammasome agonist (Gaidt et al., 2016). Furthermore, MSU crystals may also activate monocytes in the absence of separate priming (Chung et al., 2016). This suggests the findings in monocytes may not be directly relevant to responses in tissue macrophages.

To test the role *in vivo*, PR3/NE deficient mice were crossed onto the *ApolipoproteinE-/-* mouse model of atherosclerosis (Warnatsch et al., 2015). NETs accumulated in atherosclerotic plaque in wild-type mice, but were absent from the PR3/NE deficient mice. DNase administration reduced atherosclerotic plaque size, potentially linking NETs with the chronic inflammatory process of atherosclerosis.

1.10.3 NETosis and other particles

The study of Mitroulis et al. described previously (1.7.4 - Autophagy) was the first examination of NETosis in response to non-infective particles. Since then, other reports have demonstrated that NETosis can be triggered by CPPD crystals (Pang et al., 2013), alum, silica (Brinkmann et al., 2012) and amyloid fibrils (Azevedo et al., 2012). NETosis was also elicited in a murine model of foreign body implantation (Jhunjhunwala et al., 2015).

NETosis is potentially an important response of neutrophils in infective and inflammatory conditions. Where NETosis fits in with the other forms of neutrophil cell death will now be discussed.

1.11 Neutrophil cell death and relevance to inflammatory conditions

The balance and modality of neutrophil cell death and disposal along with bone marrow neutrophil production are likely to be key parameters in maintaining a functional innate immune defence, whilst preventing spontaneous inflammation. Timely cell death is important for tissue homeostasis. Apoptosis appears to be an important type of cell death under steady-state conditions (Kerr et al., 1972) and is characterised by orderly and programmed dismantling of the cell and labelling the cell remnants for removal by phagocytes. This form of cell death is thought to be immunologically silent (Rongvaux et al., 2014; White et al., 2014). Macrophages that phagocytose apoptotic cells polarize to an anti-inflammatory phenotype (Fadeel et al., 1998). NETosis is another form of

neutrophil cell death and, as outlined previously, inappropriate NETosis may result in inflammatory disease in the absence of infection.

This section will compare, contrast and highlight potential interactions between different modes of neutrophil cell death.

1.11.1 Neutrophil turnover

Given the massive number of neutrophils produced in the bone marrow (around 10^{11} per day) (Cartwright et al., 1964), these cells need to be disposed of at a comparable rate to maintain the relatively stable levels seen in peripheral blood under steady-state conditions. Neutrophils enter the blood in terminally differentiated state without the capacity to proliferate. Both *in vitro* and *in vivo* studies suggest they are short-lived (Tofts et al., 2011).

1.11.2 Neutrophil lifespan *in vitro*

Neutrophils die rapidly through spontaneous apoptosis in cell culture conditions. After 18–20 hours' culture under standard culture conditions, the levels of apoptosis are reported to be in the range of 50–70% (Duffin et al., 2010). The presence of serum does not significantly alter neutrophil survival, unlike most other cell types (Xu et al., 2010). Serum contains a variety of growth factors capable of promoting cell survival. Removal of serum induces cytokine deprivation that is used in other cell types to induce apoptosis. Variability in reported rates of neutrophil apoptosis *in vitro* may be accounted for by differences in the source of neutrophils, the mode of isolation, media, assays used and time-points chosen (Hannah et al., 1998).

1.11.3 Neutrophil lifespan *in vivo*

Neutrophils are presumed to have a short life span *in vivo* as well as *in vitro*. The rapid onset of neutropenia following chemotherapy (between 3-5 days) when neutrophil production is suppressed supports this theory. Assessing neutrophil lifespan *in vivo* under physiologic conditions remains a challenge. Various labelling techniques have generated differing estimates of longevity. A recent study in humans employing deuterium-labelled water administration to healthy controls found a half-life estimated at 5.4 days, using a mathematical model (Pillay et al., 2010). This was far longer than previous estimates and debate continues (Tofts et al., 2011).

1.12 Mechanisms of spontaneous neutrophil apoptosis

Apoptosis occurs through either intrinsic or extrinsic pathways (Hotchkiss et al., 2009). The intrinsic pathway is triggered by a number of stimuli including cytokine and growth factor withdrawal, and genotoxic stress induced by stimuli such as chemotherapy, UV light and ROS (Danial & Korsmeyer, 2004). It is thought that mitochondrial leakage of cytochrome c activates apoptotic peptidase activating factor 1 (Apaf-1) and leading to assembly of the apoptosome (Li et al., 1997). This activates caspase-9, which in turn cleaves caspase-3, the executioner caspase. A family of pro- and anti-apoptotic molecules regulates this system.

The extrinsic pathway requires ligation of death receptors at the cell membrane, which leads to caspase-8 activation, and subsequent cleavage of caspase-3. Of note, there is also some amplification of the extrinsic pathway via caspase-8 cleavage of Bid that interacts with Bax to cause mitochondrial leakage and engagement of the intrinsic pathway.

Neutrophils appear capable of undergoing apoptosis through both pathways, although the exact mechanism of spontaneous neutrophil apoptosis remains unclear.

1.12.1 Intrinsic pathway

1.12.1.1 Mitochondria

Neutrophils are thought to have relatively few mitochondria and do not rely on mitochondrial respiratory function for survival or ATP production and there is very low cytochrome c expression in neutrophils (Maianski, Geissler, et al., 2004). In respect to cell death however, this appears to be compensated for by a heightened sensitivity to cytochrome c, assessed using cell free extracts and immuno-depleting residual cytochrome c (B. M. Murphy et al., 2003). Mitochondrial permeabilization also releases the serine protease high-temperature requirement A2 (HtrA2) and second mitochondria-derived activator of caspases (Smac) that in turn down-regulate the inhibitors of apoptosis (IAPs). It is not clear how important IAPs are in the case of neutrophils (Maianski, Roos, et al., 2004). It is also unclear whether neutrophil are dependent on recruitment of the intrinsic pathway for death receptor-mediated apoptosis.

1.12.2 Pro- and anti-apoptotic Bcl-2-family proteins

The B-cell lymphoma 2 (Bcl-2 family of proteins govern apoptosis and comprise pro- and anti-apoptotic family members. This review will highlight those that have been studied in neutrophils specifically. The founding member of the family, Bcl-2 itself, is not expressed in mature neutrophils (Iwai et al., 1994), which may rely on other Bcl-2 family members for survival.

1.12.2.1 Mcl-1

Myeloid leukaemia cell differentiation protein (Mcl-1) is thought to be the critical anti-apoptotic factor involved in neutrophil survival, particularly given the absence of Bcl-2 in mature neutrophils and it functions by restraining the activity of pro-apoptotic proteins (Iwai et al., 1994). Interestingly, when HL-60 myeloid leukaemia cells are cultured with retinoic acid, the cells develop a mature neutrophil phenotype and the cells undergo spontaneous apoptosis. During maturation, Bcl-2 expression is progressively lost (Watson et al., 1997) whereas Mcl-1 continues to be expressed. Mcl-1 has a very short half-life (only a few hours), owing to constitutive ubiquitination that marks the protein for proteasomal degradation. Myeloid-specific deletion of Mcl-1 in mice (Mcl-1 deficiency is embryonic lethal) leads to neutropenia (Dzhagalov et al., 2007) and elevated rates of apoptosis were observed in bone marrow neutrophils and *in vitro* cultured neutrophils. This suggests Mcl-1 is an important factor in the maintenance of neutrophil numbers at steady state.

The loss of Mcl-1 induces apoptosis and interventions that prolong or accelerate apoptosis are commonly associated with acceleration or slowing of Mcl-1 loss respectively (Derouet et al., 2006). For example, GM-CSF prolongation of neutrophil survival is associated with prolonged protein expression of Mcl-1 (Derouet et al., 2004) whereas treatment with flavones accelerates both Mcl-1 loss and neutrophil apoptosis (Lucas et al., 2013). Reduction of Mcl-1 is only partly explained by caspase cleavage, suggesting its loss is not merely a secondary phenomenon (Wardle et al., 2011). The assessment of the importance of Mcl-1 in mature neutrophil survival has been limited by the absence of effective chemical inhibitors for Mcl-1 (Brumatti & Ekert, 2013) and the inability to genetically manipulate mature neutrophils. One study using an siRNA approach found a survival role for Mcl-1, although it remains unclear whether this strategy is possible in terminally differentiated neutrophils (Leuenroth et al., 2000). A potent Mcl-1 chemical inhibitor was recently reported, providing a useful tool for future studies (Kotschy et al., 2016).

1.12.2.2 A1

Another anti-apoptotic protein, A1, was found to be important for neutrophil survival in mice (Hamasaki et al., 1998). Also, shRNA knockdown of A1 in the Hoxb8 system of neutrophil differentiation from immortalized murine progenitor cells resulted in increased apoptosis (Vier et al., 2016). A1 was important for both progenitor function and mature neutrophil survival. Transcription of A1 was up regulated by pro-inflammatory cytokines such as GM-CSF, but granulocyte colony stimulating factor (G-CSF) had minimal effect on A1 levels.

1.12.2.3 Pro-apoptotic Bcl-2 family members

Bax and Bak are the Bcl-2 family members responsible for mitochondrial outer membrane permeabilization (M. C. Wei et al., 2001). Bid, when truncated by caspase-8 to tBid can also engage Bax to induce mitochondrial permeabilization. Croker et al. explored the role of these proteins using murine knockout models (Croker et al., 2011). While Bax single knockout mice were unaffected, Bid knockout and Bax/Bak double knockout mice exhibited reduced Fas ligand (FasL)-mediated apoptosis, implicating the mitochondrial pathway in death receptor-induced apoptosis in neutrophils. Notably, there was little difference in spontaneous apoptosis rates in the knockouts. Overexpression of Mcl-1 and Bcl-2 resulted in reduced sensitivity to FasL and reduced spontaneous neutrophil apoptosis. Caspase-3 and -7 cleavage was delayed under the same conditions, although caspase-8 was not assessed. While a mitochondrial role for the poorly understood FasL-induced IL-1β release was inferred because Bid knockout neutrophils produced less IL-1β after priming and FasL treatment, the precise relationship between IL-1β production and apoptosis remains to be disentangled.

In a study of neutrophils from patients suffering a variety of inflammatory disorders, reduced apoptosis was observed and it was associated with low Bax expression (Dibbert et al., 1999). *In vitro* treatment of healthy donor neutrophils with anti-apoptotic pro-inflammatory cytokines including GM-CSF, G-CSF and IFNγ reproduced this reduced Bax expression and delayed apoptosis.

Bim and Noxa are counter-regulatory proteins responsible for reducing the inhibition provided by anti-apoptotic Bcl-2 family members. Both are expressed in neutrophils and have been reported to modify neutrophil apoptosis (Villunger et al., 2003) (Kirschnek et al., 2011) (Andina et al., 2009). Noxa in particular is an important inhibitor of Mcl-1 function (Oda et al., 2000). Phosphorylation of Bad, another pro-apoptotic Bcl-

2 family member, appears to mediate prolonged neutrophil survival (El Kebir et al., 2008).

1.12.3 Extrinsic pathway

Neutrophils are susceptible to death ligand-induced apoptosis – so-called extrinsic apoptosis. Fas ligand (FasL), TNFα and TNF-related apoptosis-inducing ligand (TRAIL) bind respective receptors to engage the death-receptor pathway and trigger caspase-8 cleavage (Reviewed in (Akgul & Edwards, 2003)).

1.12.3.1 Fas

Neutrophils express both Fas and FasL on the cell membrane (Liles et al., 1996), and FasL is known to induce apoptosis in murine and human neutrophils (Croker et al., 2011). What role Fas and FasL play in spontaneous neutrophil apoptosis is not clear. One study suggested that whilst death receptor signalling including formation of the death-inducing signalling complex (DISC) and caspase-8 cleavage is involved early in neutrophil apoptosis, it appeared to be independent of receptor ligation (assessed using blocking antibodies against FasL, TRAIL and TNF) (Scheel-Toellner et al., 2004). Spontaneous aggregation of death domains and assembly of the DISC (assessed by co-immunoprecipitating Fas-associated death domain protein) was mediated by ROS (Scheel-Toellner et al., 2002). Importantly, neutrophils from Fas-deficient and FasL-deficient mice exhibit normal survival (Fecho & Cohen, 1998). FasL-induced neutrophil apoptosis was inhibited by ZVAD-fmk, a broad-spectrum caspase inhibitor. In contrast, the same concentration of ZVAD-fmk did not reduce spontaneous neutrophil apoptosis (Harter et al., 2001).

1.12.3.2 TRAIL

Neutrophils express TRAIL receptors and ligation accelerates apoptosis (Renshaw et al., 2003). Apoptosis induced by TRAIL has been proposed to play a role in the removal of aging neutrophils from the circulation (Lum et al., 2005).

1.12.3.3 TNFα

TNFα has been demonstrated to have both pro- and anti-apoptotic effects on neutrophils. In general, pro-inflammatory cytokines prolong neutrophil survival (see 1.13.1). TNFα dose appears to be important, promoting survival at low dose and accelerating death at higher doses (Murray et al., 1997). Addition of cycloheximide may augment TNFα–induced apoptosis (Tsuchida et al., 1995).

The effects of TNFα on neutrophils may not rely on the canonical death receptor activation of caspase-8 during apoptosis, as it does in other cell types (Geering et al., 2011). Rather, TNFα may act through PI3K and ROS-mediated activation of caspase-3. Others have also proposed that TNFα can induce a caspase-independent form of neutrophil cell death (Maianski et al., 2003). However, concerns have been raised about the effectiveness of caspase inhibitors used in these studies of neutrophils, in particular ZVAD-fmk (see section on caspase dependence 1.12.5), which calls into question the conclusions drawn from studies using these compounds. Caspase-independent forms of cell death will be discussed below.

1.12.4 Morrbid – a novel long non-coding RNA modifying myeloid cell survival

A recently described long non-coding RNA, Morrbid, has been found to influence granulocyte (neutrophil, eosinophils, basophils and monocytes) survival by reducing the expression of the pro-apoptotic family member, Bim (Kotzin et al., 2016). As described above, Bim may have a role in regulating neutrophil apoptosis.

1.12.5 Caspase dependency

Caspases play a key role in apoptosis through the initiation and execution of the apoptotic program. The extrinsic apoptosis pathway begins with the non-redundant activation of caspase-8 in mice and caspase-8 deficiency results in embryonic lethality (Varfolomeev et al., 1998). In humans, caspase-10 may serve a similar role in the extrinsic pathway, providing some redundancy (Chun et al., 2002; Kischkel et al., 2001). It is unclear which caspases are critical for neutrophil apoptosis and no thorough genetic study in mice has been conducted. Interestingly, neutrophils from caspase-1 knockout mice have reduced spontaneous apoptosis (Rowe et al., 2002). Several of the caspase knockouts are embryonic lethal, necessitating foetal liver transplantation or cell type-specific knockouts to investigate further. As described earlier, chemical caspase inhibitors have been relied upon to determine the relative contribution of caspases to cell death, but may lack specificity (Callus & Vaux, 2007). One recent review highlighted this issue in experiments on neutrophils (Luo & Loison, 2008) as an explanation for the inconsistency between studies.

1.12.5.1 Chemical Caspase Inhibitors

ZVAD-fmk is a potent broadly acting caspase inhibitor that has been used extensively in apoptosis studies. ZVAD-fmk is relatively ineffective at reducing spontaneous

apoptosis in human neutrophils (Luo & Loison, 2008). In comparison, another broadly acting caspase inhibitor, QVD-OPh, potently suppresses spontaneous neutrophil death (Wardle et al., 2011).

The difference between these two inhibitors could relate to a number of factors. Luo and Loison (Luo & Loison, 2008) found variability between different preparations of ZVAD-fmk, citing varying cell-permeability as a possible determinant in effectiveness. Their laboratory initially published that ZVAD-fmk did not inhibit neutrophil apoptosis (Zhu et al., 2006), but subsequently used another preparation of the inhibitor, with the opposite result (Loison et al., 2014). Of note, QVD-OPh is a dipeptide inhibitor with characteristics conducive to cell penetration. Why this difference should be observed with neutrophils and not other cell types is not clear.

Another possibility for the difference is the caspase specificity of the different inhibitors. Z-VAD-fmk and Q-VD-OPh are both broad specificity inhibitors, although Q-VD-OPh may exhibit more potency toward caspase-3 (Chauvier et al., 2007). Another recent study exploring the induction of necroptosis in leukaemia cells found Z-VAD-fmk demonstrates superior caspase-8/cFLIP$_L$ blocking capability than QVD-OPh (Brumatti et al., 2016). However, precisely which caspases are involved in neutrophil apoptosis remains an open question.

1.12.5.2 Caspase-8

A key question is whether caspase-8 activity is required for spontaneous apoptosis in neutrophils, and if so, how it is activated. Apart from caspase-8 activation by death receptor signalling, studies have proposed a non-canonical activation of caspase-8 through a protease cascade involving cathepsin D (Conus et al., 2008). Genetic and chemical blockade of cathepsin D with a relatively specific inhibitor, Pepstatin A, prolonged neutrophil survival. Cathepsin D deficiency exacerbated inflammation in a mouse model of sterile peritonitis, potentially linking neutrophil apoptosis with inflammation resolution.

Activated Caspase-8 and caspase-3 may undergo phosphorylation in neutrophils. This is mediated by p38–mitogen-activated protein kinase (p38 MAPK), a recognised neutrophil survival factor whose activation is enhanced by cytokines such as GM-CSF. Phosphorylation of caspase-8 and caspase-3 inhibits proteolytic activity and delays apoptosis (Alvarado-Kristensson et al., 2004).

1.12.5.3 Caspase-9

Caspase-9 is activated through the intrinsic apoptosis pathway as described in section 1.12.1.

1.12.5.4 Executioner Caspases – Caspase-3 and Caspase-7

Caspase-3 and caspase-7 are generally considered the caspases responsible for dismantling cellular components during apoptosis (Janicke et al., 1998). Caspase-3 has been studied more extensively in neutrophils and is implicated in the 'demolition phase' of apoptosis in these cells, regardless of the upstream pathways involved. Activation of caspase-3 by proteinase 3 has been described in neutrophils and will be discussed later (Section 1.13.3.4.)

1.12.5.5 Caspase-10

Caspase-10 is expressed in human but not mouse cells. It appears to play a role similar to caspase-8 and can operate independently of it (J. Wang et al., 2001). Interestingly, it may not be blocked effectively by ZVAD-fmk (Lafont et al., 2010). Caspase-10 is expressed in neutrophils and may play a role in cell death (Goepel et al., 2004) although this study relied primarily on reportedly specific caspase-10 inhibitors to demonstrate its involvement.

1.12.6 Calpains

Calpains are a family of cysteine proteases distinct from caspases that are abundant in neutrophils. Studies have suggested these proteases play a role in spontaneous neutrophil apoptosis, although whether up- or down-stream of caspase activation is not clear (Knepper-Nicolai et al., 1998). Calpastatin is an endogenous inhibitor of calpains. Its expression reduces as neutrophils age, which may unleash the calpains to initiate apoptosis. Calpains do not play a role in Fas-mediated neutrophil cell death (Squier et al., 1999), but may activate pro-apoptotic Bax in neutrophils (Altznauer et al., 2004) and cleave and disable X-linked inhibitor of apoptosis (XIAP) (S. Kobayashi et al., 2002).

1.12.7 Reactive Oxygen species

Reactive oxygen species (ROS) have been implicated in spontaneous neutrophil cell death. ROS slowly accumulate in aging neutrophils and may inhibit pathways including the PI3Kγ/Akt pathway implicated in neutrophil survival (Xu et al., 2010). Inhibitors or scavengers of ROS, including glutathione (Yamamoto et al., 2002) and catalase

(Kasahara et al., 1997), are reported to inhibit apoptosis and addition of H_2O_2 appears to accelerate apoptosis (Lundqvist-Gustafsson & Bengtsson, 1999). N-acetyl cysteine (NAC), a commonly used antioxidant, has a variable effect, perhaps explained by its relatively short duration of action (Xu et al., 2010). Of note, DMSO-treated HL-60 cells mature into neutrophil-like cells that lack specific granules and the ability to assemble NADPH oxidase. These cells are also a sensitive to H_2O_2-induced apoptosis (Lundqvist-Gustafsson & Bengtsson, 1999). One study found the opposite effect of ROS, with inhibition of NADPH using DPI enhancing caspase activity during PMA stimulation (Fadeel et al., 1998).

Patients with CGD have defects in NADPH oxidase function and cannot produce ROS through this pathway. Some studies have found a delay in both spontaneous and FasL-induced apoptosis in CGD patients (Conus et al., 2008; Kasahara et al., 1997). Given these patients experience chronic inflammation, it remains unclear whether ROS are intrinsically important to neutrophil survival or other factors such as elevated pro-inflammatory cytokines drive survival. Of note in the Kasahara study candidate anti-apoptotic cytokines (G-CSF, GM-CSF and IL-6) were not elevated in serum from CGD patients. Another study found CGD patients had only slightly delayed spontaneous and Fas-induced apoptosis (Fadeel et al., 1998). Interestingly, a more recent study found that exposure of phosphatidylserine (PS) was delayed in CGD patients, but other markers of apoptosis including sub-diploid propidium iodide (PI) staining, trypan blue exclusion and Terminal deoxynucleotidyl transferase (TdT) dUTP Nick-End Labelling (TUNEL) were not (Sanford et al., 2006). Aging CGD neutrophils are poorly phagocytosed by macrophages that may lead to the inflammation and autoimmunity seen in CGD patients (Sanmun et al., 2009).

1.13 Pro and anti-apoptotic factors

1.13.1 Anti-apoptotic factors

Under conditions of disturbed homeostasis, such as sepsis (Keel et al., 1997) and trauma (Ertel et al., 1998) neutrophil lifespan is prolonged. Neutrophils obtained from peripheral blood and from the inflamed site in inflammatory disease patients also have prolonged survival (Dibbert et al., 1999). This prolongation in survival is due at least in part to the presence of soluble factors that prolong neutrophil survival *in vitro* (Dibbert et al., 1999). FasL can still induce apoptosis in neutrophils treated with anti-apoptotic factors such as GM-CSF (Renshaw et al., 2000).

1.13.1.1 Granulocyte Colony-Stimulating Factor (G-CSF)

G-CSF is a critical cytokine for neutrophil homeostasis, performing roles in neutrophil bone-marrow development, bone marrow egress, chemotaxis and activation (Cornish et al., 2009). It is also a potent inhibitor of neutrophil apoptosis *in vitro* (Homburg et al., 1995) and when administered *in vivo* (Leavey et al., 1998). The G-CSF gene deficient mouse is neutropenic with reduced granulopoiesis, but it is unclear whether there is also a defect in survival of circulating neutrophils (Lieschke et al., 1994).

Suggested mechanisms of G-CSF delayed apoptosis include: interference with Bid-mediated mitochondrial apoptosis (Maianski, Roos, et al., 2004) compared to caspase inhibition, which blocks apoptosis after this step (Maianski et al., 2002); increased expression of proliferating cell nuclear antigen (PCNA), a neutrophil anti-apoptotic factor (Witko-Sarsat et al., 2010); elevating neutrophil pH (Gottlieb et al., 1995); inhibition of calpain-mediated loss of XIAP (van Raam et al., 2008); increasing Akt activity (Zhu et al., 2006); and increasing cIAP2 expression (Hasegawa et al., 2003). The effect of G-CSF occurs independently of Bcl-2, Bcl-w, Bax, or Bim (Villunger et al., 2003). G-CSF signals through both the Erk and JAK-STAT3 pathways in neutrophils (Panopoulos et al., 2006) (Nguyen-Jackson et al., 2010).

1.13.1.2 Granulocyte-Macrophage Colony-Stimulating Factor (GM-CSF)

GM-CSF is another cytokine with multiple effects on neutrophil homeostasis and function, including delaying neutrophil apoptosis (A. Lee et al., 1993). Mechanisms suggested include signalling via Lyn kinase (S. Wei et al., 1996) and increasing the stability of Mcl-1 via PI3K/Akt and MEK/ERK signalling (Derouet et al., 2004). GM-CSF engages signalling pathways that both overlap and are distinct from G-CSF (Suzuki et al., 1999). GM-CSF was found to be the dominant cytokine in bronchioalveolar lavage fluid prolongation of neutrophil survival (Cowburn et al., 2011).

1.13.1.3 LPS and other TLR ligands

Lipopolysaccharide (LPS) or endotoxin activates neutrophils through TLR4 and prolongs survival (A. Lee et al., 1993). LPS may act through increased expression of the anti-apoptotic factor cIAP2 which ubuiqitinates and deactivates caspase-3 (Mica et al., 2004). LPS also increases Mcl-1 expression (Moulding et al., 1998).

In vitro studies with a panel of TLR agonists found heterogeneous effects on neutrophil apoptosis. LPS (TLR4), peptidoglycan (TLR2), R-848 (TLR7/8), and CpG-DNA (TLR9) were effective at delaying spontaneous apoptosis of neutrophils. PamCSK4 (TLR1/2),

macrophage-activating lipopeptide-2 (TLR2/6), flagellin (TLR5), and loxoribine (TLR7) were less effective or inactive (Francois et al., 2005). Pro-survival effects were inhibited by PI3K inhibition and NF-κB inhibition. Increased phosphorylation of Akt and increased levels of Mcl-1 and A1 were associated with survival.

1.13.1.4 Adiponectin

Adiponectin is an adipokine, which has anti-inflammatory actions and was demonstrated to delay neutrophil apoptosis. Pathways implicated in its effect include AMPK, Akt/PKB and ERK1/2 (A. Rossi & Lord, 2013).

1.13.1.5 Other anti-apoptotic factors

In inflamed tissues, the extracellular milieu is often perturbed. Hypoxia at levels demonstrated in the joints of patients with RA promotes neutrophil survival (Cross et al., 2006). An acidic environment, commonly seen in inflamed tissue, may also promote neutrophil survival (Cao et al., 2015).

1.13.1.6 Glucocorticoids

Glucocorticoids are potent anti-inflammatory and immunosuppressive agents and have been clinically used for many years to manage inflammatory conditions such as RA and gout – conditions where neutrophils are thought to play a significant role. Somewhat paradoxically, glucocorticoids delay neutrophil apoptosis *in vitro* (Cox, 1995; Liles et al., 1995). Under hypoxic conditions, however, glucocorticoids did not prolong neutrophil survival and may attenuate pro-survival signals (Marwick et al., 2013). Whether prolonged neutrophil survival with glucocorticoid treatment can be of clinical consequence remains to be established.

1.13.2 Pro-apoptotic factors

A number of compounds have been identified that accelerate neutrophil apoptosis *in vitro* (Duffin et al., 2010) and have been proposed as potential apoptosis-inducing anti-inflammatories *in vivo*.

The fungal metabolite, gliotoxin, induces neutrophil apoptosis. Gliotoxin may exert this effect through its ability to inhibit NFκB (Ward et al., 1999) and exhibited synergy with TNFα in inducing apoptosis. Pyocyanin is a toxin produced by *Pseudomonas aeruginosa,* an important human pathogen, including in cystic fibrosis. Pyocyanin can elicit neutrophil apoptosis, possibly via lysosomal dysfunction (Prince et al., 2008). Pyocyanin has also been reported to cause NETosis (Rada et al., 2013). Flavones,

plant-based compounds with anti-inflammatory properties, accelerate neutrophil apoptosis (40-50% apoptosis with multiple different flavones compared to 20% untreated at 6 hours) (Lucas et al., 2013) possibly via reduction in Mcl-1.

1.13.2.1 Blockade of transcription and translation

Blockade of transcription with Actinomycin D accelerated neutrophil apoptosis in one study (Moulding et al., 2001). Reduced transcription and expression levels of anti-apoptotic proteins, in particular Mcl-1, might account for this effect. Blockade of protein translation can induce apoptosis, especially in TNF-treated neutrophils (Moulding et al., 2001; Squier et al., 1999; Ward et al., 1999). Okadaic acid, a phosphatase inhibitor also induces apoptosis (Derouet et al., 2006) whereas inhibition of the proteasome with MG-132 delays apoptosis (Derouet et al., 2004)

1.13.2.2 Sulfasalazine

Sulfasalazine is an immunomodulatory drug comprising a salicylate moiety coupled to a sulfapyridine used in inflammatory arthritis and inflammatory bowel disease. Sulfasalazine induced rapid apoptosis in healthy control neutrophils at concentrations observed in human subjects (10-100μM) (Akahoshi et al., 1997). It is unclear whether this property accounts for the clinical effect of sulfasalazine. A related compound, sodium salicylate, also induces neutrophil apoptosis via caspase-dependent loss of Mcl-1 (Derouet et al., 2006).

1.13.3 Novel mediators of neutrophil apoptosis

A number of mediators of apoptosis specific to neutrophils have been identified. These are presented in a simplified schematic of apoptotic pathways (Figure 1.3 Neutrophil apoptotic pathways).

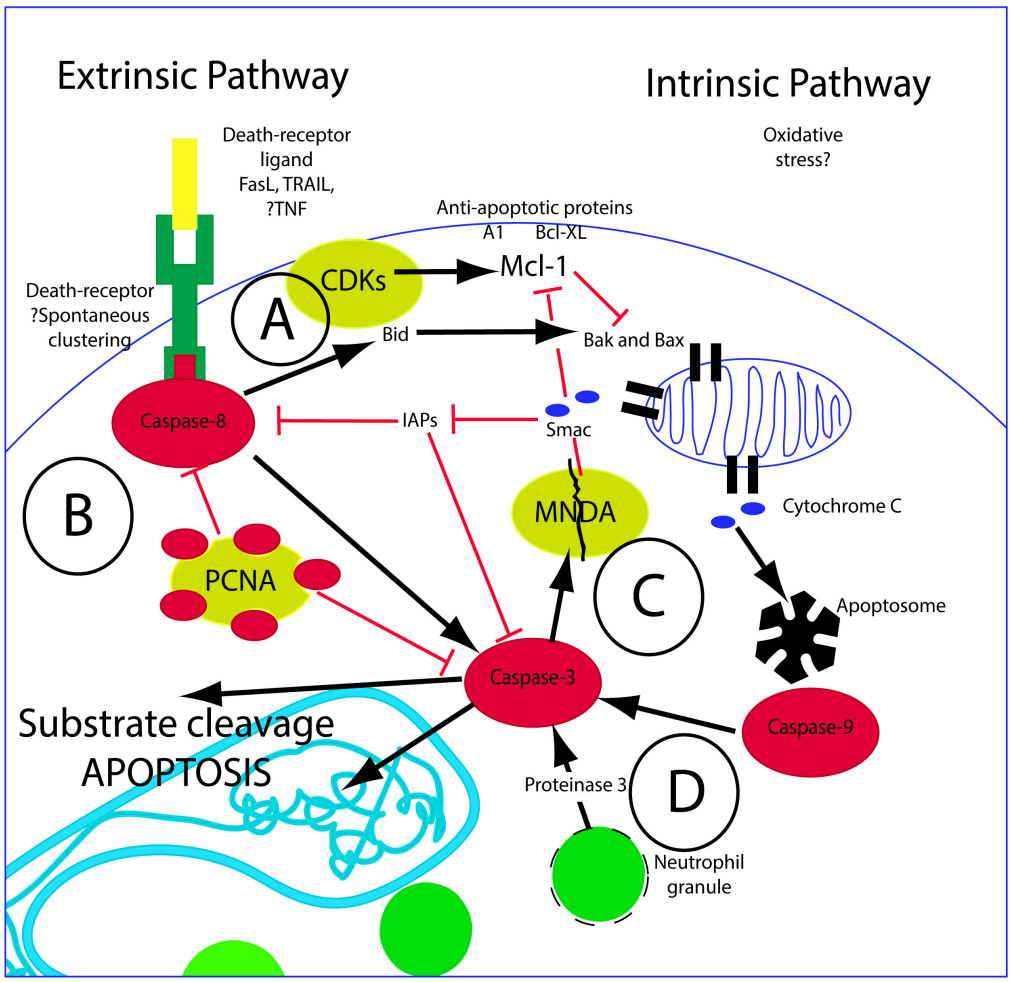


Figure 1.3 Neutrophil apoptotic pathways
A simplified schematic of the intrinsic and extrinsic pathways of apoptosis with specific emphasis on the main factors involved in neutrophil apoptosis. Novel mediators of neutrophil apoptosis are: A) Cyclin-dependent kinases (CDK) inhibit Mcl-1 degradation and reduce apoptosis; B) PCNA sequesters pro-caspases to prevent their activation; C) MNDA is cleaved by caspase-3 and the cleaved product promotes Mcl-1 proteasomal degradation; and D) Pr3 leaks from the granules of aging neutrophils to directly cleave caspase-3 and activate the apoptotic program.

1.13.3.1 Cyclin-dependent kinase inhibitors

Cyclin-dependent kinases (CDKs) have been primarily studied in the context of cell proliferation (Morgan, 1997). CDK7 and CDK9 also appear to play a role in neutrophil apoptosis. Roscovitine is a non-specific inhibitor of CDKs that has been found to induce neutrophil apoptosis (A. G. Rossi et al., 2006). Application of this compound in murine inflammatory models reduced severity of disease in a caspase-dependent manner, coupling neutrophil apoptosis with inflammation. While the mechanism is unclear, it has been proposed that CDK inhibition may reduce neutrophil transcription of anti-apoptotic proteins (Leitch et al., 2012).

Flavopiridol, a potent CDK9 inhibitor, also induces neutrophil apoptosis as a consequence of promoting rapid loss of Mcl-1 expression (K. Wang et al., 2012)). These agents also overcome the anti-apoptotic effect of GM-CSF.

1.13.3.2 Proliferating cell nuclear antigen (PCNA)

PCNA also appears to play an unexpected role in neutrophil apoptosis (Witko-Sarsat et al., 2010). PCNA, normally found in the nucleus of the majority of cell types, is located in the cytoplasm of neutrophils, where it is thought to sequester pro-caspases. Peptides derived from the endogenously expressed cyclin-dependent kinase inhibitor, p21, displace the pro-caspases from PCNA and facilitate activation to trigger neutrophil apoptosis. The p21 knockout mouse exhibits exacerbated neutrophilic inflammation (C. Martin et al., 2016)

1.13.3.3 Myeloid nuclear differentiation antigen (MNDA)

MNDA is another protein with roles in cell differentiation that has been discovered to influence neutrophil apoptosis (Fotouhi-Ardakani et al., 2010). Nuclear MNDA is cleaved by caspases early during apoptosis and translocates to the cytoplasm where it promotes proteasomal degradation of Mcl-1 accelerating apoptosis. Knock down of MNDA in HL-60 granulocytic cells decreased susceptibility to apoptosis.

1.13.3.4 Proteinase-3 (Pr3)

Pr3 is an abundantly expressed granule serine protease that has recently been found to play a role in spontaneous neutrophil apoptosis. Neutrophil serine proteases have been implicated in other processes attributed to caspases, including maturation of IL-1β, normally cleaved by caspase-1 (Guma et al., 2009). Leakage of PR3 from the granules of aging neutrophils can cleave caspase-3 directly and trigger spontaneous neutrophil apoptosis (Loison et al., 2014). Reportedly specific inhibitors of Caspase-8 (Z-IETD-fmk) and caspase-9 (Z-LEHD-fmk) did not reduce caspase-3 cleavage or activation, and did not inhibit spontaneous neutrophil apoptosis demonstrating that the classical intrinsic and extrinsic pathways to apoptosis were not involved. Di-isopropylfluorophosphate (DFP), a potent and irreversible serine protease inhibitor, was able to inhibit caspase-3 cleavage and neutrophil apoptosis and PR3 was identified as the likely target. Pr3 cleaved Pro-caspase-3 three amino acids upstream of the canonical caspase-9 cleavage site, resulting in a functional 20 kDa fragment.

Neutrophils from mice deficient in Pr3 demonstrated slower apoptosis than wild type. Furthermore, the authors transferred Pr3 -/- and wild-type neutrophils into the

peritoneum of mice primed with IP thioglycollate. Under those inflammatory conditions, the Pr3-deficient cells survived longer. Pr3 appears to leak from granules into the cytosol with prolonged incubation *in vitro*. Treatment with desferrioxamine that inhibits oxidative stress-induced lysosomal membrane permeabilization (Baird et al., 2006) and HSP70 that stabilizes lysosome lipid membranes (Kirkegaard et al., 2010) reduced the proteinase 3 leak and improved neutrophil survival. Exactly what leads to this leak is not clear but progressive accumulation of ROS was suggested to play a role.

1.13.4 Pathogens and neutrophil cell death

Phagocytosis through Fc receptors and complement receptors induce changes in gene expression in human neutrophils, including those involved with cell death pathways. It was found that phagocytosis via either receptor could induce neutrophil apoptosis (S. D. Kobayashi et al., 2002). Bacteria may further subvert this process. *Streptococcus pyogenes* alters the expression of neutrophil apoptosis-related gene transcripts including down-regulation of IAP2 and up regulation of Bax that may account for the acceleration of neutrophil apoptosis observed (Kobayashi et al., 2003). Lipopolysaccharide (LPS) is a potent pathogen-associated molecular pattern (PAMP), triggering signalling through toll-like receptor 4 (TLR4). It can delay neutrophil apoptosis, but can also promote NADPH-oxidase dependent neutrophil apoptosis in the context of bacteria-neutrophil adhesion (Blomgran et al., 2004). Viral infection with influenza may accelerate neutrophil apoptosis, possibly involving up-regulation of the Fas death pathway (Colamussi et al., 1999).

1.14 Impact of apoptosis on neutrophil functionality

In the latter phases of apoptosis, cells have markedly reduced functionality, consistent with “cell shutdown”. Aging neutrophils also have impaired critical functions, including chemotaxis, phagocytosis and release of ROS and granule enzymes (Whyte et al., 1993). A number of cell surface receptors are down regulated during apoptosis (Hart et al., 2000). Delaying apoptosis with anti-apoptotic cytokines prolongs the capacity of neutrophils to spread, undergo chemotaxis and release inflammatory mediators (A. Lee et al., 1993). Transgenic Bcl-2 over-expression in mice delayed neutrophil apoptosis, maintaining neutrophil functionality *in vitro* and deleteriously delayed the resolution of pneumococcal meningitis inflammation *in vivo* (Koedel et al., 2009).

Activation of caspases appears to be critical for this apoptosis-related functional decline. Inhibitors of the executioner caspases, caspase-3 and caspase-7 have been

demonstrated to both inhibit apoptosis and maintain cell functionality in neutrophils (D. Lee et al., 2000). Caspase-3 inhibition maintains the ability of UV-treated neutrophils to produce ROS (Sweeney et al., 2001). The targets of these executioner caspases are not clear. One example, protein kinase Cδ (PKCδ) is cleaved and activate by caspase-3 and plays a role in the downstream components of the apoptotic program (Pongracz et al., 1999).

While caspase activity is evidently central to neutrophil functionality, other factors may be involved. For example, inhibition of caspases failed to rescue the loss of calcium flux observed upon Fas treatment of neutrophils (Ayub et al., 2004). The extent of the involvement of caspase activity in regulating neutrophils remains a matter of enormous interest.

A major change that occurs with apoptosis is morphologic, culminating in the breakdown of the cell into apoptotic blebs. The actin cytoskeleton is crucial for maintaining cellular structure. Important actin regulators such as the protein tyrosine phosphatase, PTP-PEST, are targets of caspases, accounting for some of the structural changes of apoptosis (Halle et al., 2007). The calpains, non-caspase cysteine proteases, may also degrade cellular components during neutrophil apoptosis. Targets of calpains include proteins binding filamentous actin including ezrin and α-actinin (Knepper-Nicolai et al., 1998). Actin itself can be cleaved during neutrophil apoptosis (S. B. Brown et al., 1997). In different cell types, apoptosis induces breakdown of fibroblast cell-to-cell contact through caspase-3 cleavage of β-catenin that co-ordinates membrane actin assembly (Brancolini et al., 1997). Actin depolymerizes during apoptosis in adherent cells such as epithelial cells. Gelsolin is a caspase-3 substrate *in vitro* and in human neutrophils (Kothakota et al., 1997). The gelsolin fragments sever actin polymers with subsequent cytoskeletal breakdown and the development of apoptotic morphology.

1.15 Induction of apoptosis as an anti-inflammatory strategy

Given the important role of neutrophils in a number of inflammatory diseases, targeting neutrophils has been put forward as an attractive anti-inflammatory strategy (Cornish et al., 2009; Grayson et al., 2016). Inducing neutrophil apoptosis offers the potential to not only limit the inflammatory capacity of neutrophils, but can also trigger an anti-inflammatory program in phagocytic macrophages (Hampson et al., 2013). It may divert neutrophils away from other more inflammatory forms of cell death.

This strategy has been directly assessed in murine models of inflammation using the pro-apoptotic properties of CDK inhibition as outlined above. Rossi et al (A. G. Rossi et al., 2006) used models of inflammatory lung disease and arthritis and demonstrated a reduction in severity using R-Roscovitine *in vivo*. Furthermore, the anti-inflammatory effect was attenuated by treatment with the caspase inhibitor, ZVAD-fmk, providing an experimental link between apoptosis and inflammation resolution (A. G. Rossi et al., 2006). An alternative strategy was used in the K/BxN model of arthritis (Scatizzi et al., 2010) where an injectable mimetic peptide corresponding to the pro-apoptotic BH3 component of Bim (TAT-BH3) attenuated disease activity. They proposed myeloid cells were the primary target of TAT-BH3 and demonstrated myeloid cell apoptosis (both macrophages and neutrophils) *in vivo* (Scatizzi et al., 2010).

1.16 Non-apoptotic cell death in neutrophils

A number of forms of non-apoptotic cell death have been described in cells other than neutrophils. These include pyroptosis, necroptosis and cell death relating to autophagy.

1.16.1 Staurosporine-induced cell death

Staurosporine, a potent but relatively non-specific inhibitor of PKC and CDKs, induces neutrophil death with features bearing some similarities with intrinsic pathway apoptosis. However, staurosporine-treated neutrophils fail to express membrane phosphatidylserine during apoptosis and are also phagocytosed less efficiently by macrophages than conventionally apoptotic neutrophils (Franz et al., 2015).

1.16.2 Autophagic cell death

Another unusual form of neutrophil cell death involves the induction of autophagy. Autophagy is the regulated disassembly and destruction of cellular components that are dysfunctional or redundant. Cell death has been associated with excessive autophagy and proposed to be a specific cell death routine (Galluzzi et al., 2012). Neutrophils undergo a similar form of cell death, with formation of autophagic vacuoles when stimulated with pro-inflammatory cytokines such as GM-CSF in the presence of antibodies against CD44, a receptor mediating cell-matrix interactions (Mihalache et al., 2011). This pathway paradoxically involves the activation of PI3K, (normally associated with cell survival) and is also NADPH oxidase-dependent. Cell death was not abrogated by ZVAD-fmk and did not correlate with caspase-3 activation, but it is uncertain if it is truly caspase-independent. Engagement of other receptors such as

FcαRI may induce a similar form of cell death (Wehrli et al., 2014). The pathophysiologic relevance of this form of cell death is unclear. Neutrophils with morphologic features of autophagic cell death were found in inflamed human tissues (Mihalache et al., 2011). As outlined above, autophagy may be involved in NETosis (1.7.4 Autophagy)

1.16.3 Pyroptosis

It remains unclear whether neutrophils can die through pyroptosis, another caspase-mediated form of inflammatory cell death. Recent studies have delineated Gasdermin-D as a key molecule in the pyroptosis pathway (Kayagaki et al., 2015; J. Shi et al., 2015). Gasdermin D is cleaved by caspase-11 and possibly caspase-1 to generate an N-terminal cleavage product that forms a pore in the plasma membrane to facilitate "lytic" pyroptotic death. These studies have been conducted in macrophages and the role of gasdermin D in neutrophils has not been explored. Neutrophils do contain the machinery for inflammasome activation including caspase-1 (Mankan et al., 2012). In comparison to macrophages, neutrophils exhibit different responses to inflammasome agonists, with responses to the soluble stimulus, nigericin but minimal activation in response to particulate stimuli (K. W. Chen et al., 2016). *Salmonella* activates the NLRC4 inflammasome in macrophages and neutrophils to cleave caspase-1 and generate mature IL-1β. Macrophages can undergo pyroptosis, but neutrophils are resistant (K. W. Chen et al., 2014). This suggests that caspase activation and cell death may be dissociated in neutrophils.

1.16.4 Necroptosis

Necroptosis is a recently recognised form of caspase-independent form of cell death. It shares molecular pathways with death receptor-mediated apoptosis – namely involvement of the Receptor-interacting serine/threonine-protein kinases, RIPK1 and RIPK3 (Silke et al., 2015). Necroptosis is triggered in a range of cell-types by the death receptor pathway (usually with TNF), whilst blocking the inhibitors of apoptosis (IAPs). This combination drives the activation of RIPK1 and under normal conditions, the subsequent activation of Caspase-8 and apoptosis. In the presence of caspase inhibition, an alternative complex, the necrosome, is formed, resulting in the phosphorylation of RIPK3. RIPK3 subsequently phosphorylates the pseudokinase mixed-lineage kinase domain-like (MLKL). This unleashes the functional N-terminal domain responsible for MLKL membrane localisation and cell death. Whether MLKL is

sufficient for cell death alone or acts in concert with other proteins remains to be determined.

1.16.4.1 Necroptosis analysis

The demonstration of MLKL phosphorylation, multimerization and translocation from the cytoplasm to the membrane fraction is currently the best evidence for activation of the necroptosis pathway (Hildebrand et al., 2014). Phosphorylation of MLKL can be assessed in human cells by a recently described antibody (phospho s345 – EPR9515), providing the ability to stain tissue sections for evidence of necroptosis *in vivo* (H. Wang et al., 2014).

1.16.4.2 Necroptosis inhibitors

Necroptosis can be inhibited by a number of molecules. Compounds such as necrostatins and necrosulfonamide (NSA) have served as tools to explore necroptosis. However, the specificity of these compounds is uncertain. For example, necrostatin-1 also inhibits indoleamine 2,3-dioxygenase (IDO) which can have independent effects on inflammation and cell survival (Vandenabeele et al., 2013). NSA has reactive cysteine groups, and measurably bound non-specifically to proteins (Sun et al., 2012), precluding its utility in *in vivo* models.

1.16.4.3 Necroptosis and neutrophils

Necroptosis in neutrophils has been explored with the advent of necroptosis inhibitors but caspase-independent neutrophil cell death has been recognised prior to this. A number of early studies, performed before the first description of the necroptosis pathway, found that neutrophils underwent cell death with stimuli such as TNFα, in a caspase-independent manner. As above, there are caveats with these studies as they generally relied on ineffective caspase inhibition with ZVAD-fmk. One study found caspase inhibitors (ZVAD-fmk and Boc-D) that reduced neutrophil apoptosis induced by FasL and TNFα /cycloheximide accentuated the apoptosis induced by TNFα alone (Liu et al., 2003). The conclusions of this study have been tempered because of the high dose of ZVAD-fmk used (100 μM), which has off target effects, and the lack of a similar effect with caspase-8 and caspase-9 specific inhibitors (Cowburn et al., 2005). However, a separate paper described TNF-induced neutrophil cell death despite ZVAD-fmk treatment (Maianski et al., 2003). Parallel experiments demonstrated good suppression of FasL induced apoptosis at the same doses. The cell death had some atypical features including lack of DNA laddering (Maianski et al., 2003), and was

dependent on mitochondrial ROS but not NADPH oxidase ROS. The ability to engage the necroptosis pathway with TNF may be limited in neutrophils as a previous study demonstrated failure to activate caspase-8 with TNF (Geering et al., 2011).

More recent papers have used the inhibitors necrostatin-1 and necrosulfonamide to interrogate necroptosis in neutrophils. Following work in autophagic neutrophil death (see above - 1.16.2 Autophagic cell death), the same authors have gone on to describe possible involvement of the necroptosis pathway in neutrophil death induced by GM-CSF and a series of antibodies against adhesion receptors (X. Wang et al., 2016). The cell death was accompanied by MLKL phosphorylation assessed by immunocytochemistry of neutrophil cytospins, rather than more conventional Western blot analyses. Phosphorylation is a hallmark of MLKL activation (p-MLKL) and activation of the necroptotic pathway, but in this study staining for p-MLKL appeared to be cytoplasmic, rather than membrane located. ROS generation, p38 MAPK activation and cell death were all reduced by chemical inhibitors of: RIPK1 (Necrostatin-1 – 25 μM); RIPK3 (GSK872 10 μM and GSK843 50μM); and MLKL (GW806742X 5μM). Surprisingly NSA (5μM) that is a potent necroptosis inhibitor in human cells did not inhibit this form of cell death. These authors also demonstrated pMLKL staining in human tissues from patients with inflammatory diseases, including cutaneous vasculitis, ulcerative colitis and psoriasis. These findings suggest that an unconventional necroptosis pathway is operating upstream of ROS and p38 MAPK activation, which requires further examination. Commonly used chemical inhibitors of this pathway are known to possess significant off-target effects that may confound interpretation. For example, the MLKL inhibitor, GW806742X, was originally described as a VEGRF2 inhibitor (Hildebrand et al., 2014), and has been subsequently shown to also inhibit RIPK1 (Ma et al., 2016).

A rapid form of caspase-independent neutrophil cell death induced by *Staphylococcus aureus* and inhibited by high dose necrostatin-1 (40 μM) has been described (Greenlee-Wacker et al., 2014). Subsequently, with the use of alternative inhibitors of both RIPK1 and RIPK3, it appears this inhibition is being driven by factors other than the necroptosis pathway (Nauseef, conference presentation, 2016). Necrostatin-1 operates at concentrations of 10 μM or less to inhibit necroptosis and at this concentration, it had no effect on NETosis (Remijsen, Kuijpers, et al., 2011).

In a recent study of murine neutrophils, LPS was able to induce neutrophil cell death in XIAP gene deficient mice treated with caspase inhibition (QVD-OPh), consistent with necroptosis (Wicki et al., 2016). This study provided evidence of MLKL accumulation in the membranes, but not of MLKL phosphorylation and multimerization. The cell death was TNF-dependent, suggesting LPS caused neutrophil TNF release that acted on the cells in an autocrine manner. LPS and Compound A (CpA), a Smac mimetic that inhibits the apoptosis-suppressing IAP proteins, also drove caspase-independent death in wild-type neutrophils that was inhibited by necrostatin-1.

1.16.5 NETosis and alternate forms of cell death

NETosis does not have the characteristic hallmarks of apoptosis. Morphologically, there is no nuclear condensation and phosphatidylserine exposure occurs simultaneously with cell death, rather than preceding it (Fuchs et al., 2007). Neutrophils undergoing NETosis are not positive for TUNEL staining, a characteristic finding in apoptosis that reflects caspase mediated activation of nucleases. Mechanistically, neither caspase inhibition nor RIPK1 inhibition using necrostatin-1 inhibited NETosis (Remijsen, Vanden Berghe, et al., 2011), although subsequent studies have offered conflicting results using differing experimental conditions and very high concentrations of inhibitors.

Inhibitors of necroptosis have been used in NETosis studies with inconclusive results. Desai et al. found inhibition of RIPK1 (with necrostatin-1 or necrostatin-1s – used at 50 μM for 30 minute prior to stimulation) and MLKL (with necrosulfonamide (NSA) – 5μM, less so at 1μM) prevented MSU- or PMA-induced NET formation in human and mouse neutrophils (at the 2 hour time point) (Desai et al., 2016). The authors also observed phosphorylation of MLKL during PMA stimulation by Western blot. This was corroborated with genetic analysis using the RIPK3 knockout mouse to demonstrate reduced air pouch NET generation and crystal aggregation. In parallel, Amini et al. (Amini et al., 2016) reported no involvement of the necroptosis pathway during NETosis. Once again chemical inhibitors of the necroptosis pathway were used but failed to decrease NETosis in response to GM-CSF and C5a or E. coli. Neutrophils from the RIPK3 knockout mouse failed to release NETs after GM-CSF priming and treatment with C5a (Amini et al., 2016). This group focused on DNA release from living neutrophils and did not demonstrate increased rates of death associated with NET release. Assessment of PMA-stimulated neutrophils after 15 minutes is too early to see evidence of “lytic” NETosis as demonstrated by multiple previous papers suggesting

that the DNA release reported in this study is a different process (Fuchs et al., 2007; Remijsen, Vanden Berghe, et al., 2011).

The discrepancy in the findings has highlighted methodological issues when studying NETosis (Naccache & Fernandes, 2016). A lack of standardization of measurement of NETosis and the lack of reliable quantitative assays makes comparing studies difficult. In the case of the two necroptosis/NETosis studies, it's possible that the two different strategies of stimulation and timing of analysis measure two separate forms of NET release.

1.16.6 Other Caspase-independent forms of cell death

Cathepsin G mediates murine neutrophil cell death induced by Leu-Leu-OMe – only partially inhibited by caspase inhibitor, QVD-OPh (Baumann et al., 2013).

1.17 Conclusion

Understanding the role of neutrophil cell death in the context of inflammation is of potential importance in improving the management of human disease. Both the quality and quantity of neutrophil cell death are likely to play key roles in the initiation and resolution of inflammation. Studying the consequences of the different forms of cell death in a broad range of contexts will inform appropriate interventions to control inflammation in both infective and non-infective conditions. This thesis will explore neutrophil cell death in the context of gout, a human disease characterised by acute inflammation and spontaneous resolution and tissue deposition of crystalline urate.

2 DEVELOPMENT OF NOVEL QUANTITATIVE IMAGING APPROACHES TO MEASURE NEUTROPHIL EXTRACELLULAR TRAPS

2.1 Introduction

Measuring NETs and NETosis accurately and reproducibly is critical to understanding their biology and developing strategies to modify NETosis (Naccache & Fernandes, 2016). Quantifying *in vivo* NETosis poses an enormous challenge based on our current knowledge and technological limitations. Our understanding of NETosis has been built on various *in vitro* approaches comprising fixed cell imaging (Brinkmann et al., 2010), DNA release assays (Fuchs et al., 2007) and live cell fluorescence approaches (Remijsen, Vanden Berghe, et al., 2011). This chapter will outline the currently available techniques for assessing NETs and NETosis *in vitro*, with a focus on so-called “lytic” NETosis of human neutrophils. I will highlight shortcomings and the need for more robust technologies to monitor NETosis, before presenting the rationale and methodology for a novel quantitative live cell NETosis assay.

2.2 NETosis assays

The central components of NETosis are:

1. Caspase-independent cell death; and
2. Nuclear decondensation, with resultant cell spreading and release of DNA mixed with neutrophil granule proteins (NETs)

Investigations into NETosis first need to demonstrate that these processes are occurring and exclude an alternative death process, such as apoptosis with secondary necrosis. The next challenge is to quantify the rate of NETosis. Strategies employed to date have been: manually counting cells undergoing NETosis using morphology and imaging; and quantifying the release of DNA into supernatant of unfixed or nuclease-treated cells.

2.2.1 Neutrophil isolation and culture

2.2.1.1 Neutrophil source

This thesis is focused on human neutrophil analysis. In brief, NETosis has been studied in mice (Ermert et al., 2009), cows (Lippolis et al., 2006), fish (Palic et al.,

2007) and a related cell death process has been studied in plants (Hawes et al., 2016). There are important differences in studying neutrophils from other species, such as different kinetics of NETosis and morphologic differences in the released NETs (Ermert et al., 2009), however the principles and challenges of quantifying NETosis are common to all systems.

Healthy humans have on average between 2 and 6 x 10^6 neutrophils per ml in peripheral blood. This is a significantly higher cell concentration than in murine peripheral blood, although this may be an artefact of the relatively immature immune systems of laboratory mice (Beura et al., 2016). Obtaining reasonable volumes of peripheral blood from humans is a relatively simple procedure compared to the murine system. A number of techniques have been established to isolate neutrophils from peripheral blood, as detailed below in 1.2.1.2. Avoiding neutrophil activation and ensuring purity of the sample are key parameters to be considered in neutrophil isolation. In addition to peripheral blood, white blood cell filters (Loison et al., 2014) and buffy coats are alternate sources of human neutrophils, which use white cells that are otherwise discarded during blood donation.

To obtain neutrophils from whole blood, the blood needs to be anticoagulated. Options for anticoagulant include Heparin (which promotes anti-thrombin III activity, thus inhibiting the coagulation cascade), citrate and ethylenediaminetetraacetic acid (EDTA). The latter two sequester calcium, a critical cofactor for coagulation. The choice of anticoagulant has not been reported to make a major difference in neutrophil analysis although EDTA may improve the yields of neutrophil isolation (Freitas et al., 2008). Heparin has been demonstrated to exert biological effects on neutrophils *in vitro* (R. A. Brown et al., 2003). Of note heparin is not advised as the anticoagulant for PolymorphPrep density gradient separation. Extracellular calcium and magnesium are both chelated by EDTA and are important for a number of neutrophil functions (Gupta et al., 2014). Residual cation chelation with citrate or EDTA could potentially affect the study of these responses but with multiple washing steps, the amount present is negligible.

2.2.1.2 Neutrophil isolation

The majority of studies employ a combination of density gradient separation and red cell removal. Density gradient solutions include polysaccharides (e.g. Ficoll) and colloidal silica (e.g. Percoll). These take advantage of the density differences between

neutrophils and mononuclear leukocytes to separate them under centrifugation. Density gradients in general do not separate neutrophils from eosinophils, another relatively dense granulocyte. A simple gradient step also fails to resolve granulocytes from red cells (Clark & Nauseef, 1996).

Separation from red cells can be achieved using sedimentation or lysis strategies. Polysaccharides in density gradients such as Ficoll sediment red cells. Otherwise separate sedimentation and gradient separation steps can be employed with dextran aggregation of red cells causing them to sediment below the white cells. Lysis of red cells using hypotonic strategies or ammonium chloride-based lysis media removes red cells whilst maintaining the integrity of the white cells. Histopaque and PolymorphPrep use combined gradient sand sedimentation solutions to resolve mononuclear and polymorphonuclear cells and erythrocytes.

Magnetic bead isolation is another strategy to isolate neutrophils that obtains high purity neutrophils, excludes eosinophils and is reported to minimally activate neutrophils (Zhou et al., 2012). Negative bead selection strategies theoretically activate cells less than positive selection although the differences may not be great (Lyons et al., 2007). Bead selection strategies are however, much more expensive than gradient strategies.

Fluorescence-activated cell sorting or FACS can also be used to obtain very pure neutrophils. Negative staining strategies are possible but it does require *in vitro* manipulation of the cells, including red cell lysis and antibody labelling.

2.2.1.1 Isolation issues

The major concern with neutrophil isolation is the propensity of these cells to become activated. This can compromise analysis of *ex vivo* activation states and *in vitro* functional testing. During isolation, the material of the test tubes used, the process of pelleting, osmolarity shifts and fluctuations in temperature may all activate neutrophils to varying degrees (Zhou et al., 2012). Low-grade contamination of reagents by LPS may also contribute to neutrophil activation (Haslett et al., 1985). Measures of neutrophil activation include up-regulation of cell surface receptors including CD11b, CD16 and down-regulation of CD62L (Haslett et al., 1985).

2.2.1.2 Media

The media in which NETosis experiments are conducted may affect the interpretation of the results. Ideally media should mimic *in vivo* conditions, accepting the limitations imposed by the need to isolate the cells and remove them from a physiological context. Media may be tailored to the planned duration of the experiment – NETosis studies are undertaken with fresh neutrophils and the stimulation and assessment is usually complete within 12 hours of isolation. Media allows pH buffering and may contain nutrients such as amino acids, vitamins and glucose needed for longer-term incubations.

Typical media include Roswell Park Memorial Institute medium (RPMI) and Hanks' balanced salt solution (HBSS) supplemented with calcium and magnesium. RPMI and HBSS use a bicarbonate based buffering system, with RPMI specifically formulated for incubation in 5% CO_2.

Levels of electrolytes in media may have a significant impact on the interpretation of results. A recent example highlights the importance of phosphate levels in media (Munoz-Planillo et al., 2013). A previous study into the role of calcium in inflammasome responses used RPMI media supplemented with calcium to highlight a potential stimulatory role (G. S. Lee et al., 2012). A subsequent study found high levels of phosphate in RPMI relative to other media at certain concentrations of calcium leads to precipitation of calcium phosphate, which can stimulate the inflammasome (Munoz-Planillo et al., 2013).

2.2.1.3 Media supplementation

Supplementation of media is of major importance in studying NETosis. The addition of serum provides nutrients and growth factors for cells, particularly under long-term culture conditions. There are several issues with serum and NETosis. First, serum, including foetal calf serum that is frequently used for cell culture, degrades extracellular DNA, affecting the study of NET structures, as described in Chapter 1 (von Kockritz-Blickwede et al., 2009). Serum also inhibits PMA-induced NETosis but the mechanism remains unknown (Fuchs et al., 2007). As a result, most NETosis studies use low serum media as media without protein leads to high background rates of NETosis in unstimulated cells (Brinkmann et al., 2010). Other options include bovine serum albumin (BSA – 0.5% (Brinkmann et al., 2010)), human serum albumin (Gupta et al.,

2014) and low concentrations of foetal calf serum (Remijsen, Vanden Berghe, et al., 2011).

2.2.2 Fixed cell imaging quantification

Fixed cell imaging requires culture of neutrophils on slides or in culture plates. Stimuli to induce NETosis are added to the media and the cells are either imaged or fixed at varying times thereafter (Brinkmann et al., 2010). Fixed cells and NETs are subsequently stained with a fluorescent DNA dye. It is worth noting that some DNA dyes are cell permeable, including Hoechst 33342, while others are cell impermeable including 4', 6-diamidino-2-phenylindole (DAPI), Sytox Green, Propidium Iodide (PI) and Draq5, which require permeabilization of the fixed cells. Importantly, cell impermeable dyes used in non-permeabilized cells allows detection of extracellular DNA.

Fixed and permeabilized cells may also be immunostained for chromatin or histones (including citrullinated histones) and for neutrophil granule enzymes (typically neutrophil elastase and myeloperoxidase). Staining for these proteins is not strictly required for quantification of NETosis (Hakkim et al., 2011). An automated assay has been described that uses anti-chromatin antibodies that demonstrate greater affinity for NETs than condensed chromatin (Brinkmann et al., 2012). Immunostaining requires at least some washing steps that may lead to dislodgement of the relatively fragile NETs.

Fixed cells are subsequently imaged with a widefield or confocal fluorescence microscope. Neutrophils that have undergone NETosis are characterised by loss of the normal nuclear architecture with nuclear delobulation, decondensation and spreading observed. NET structures are made up of chromatin (containing histones) coated with neutrophil enzymes (e.g. neutrophil elastase and myeloperoxidase). Therefore, NETs comprise extracellular entities of DNA colocalized with histones and neutrophil granule enzymes.

Quantifying rates of NETosis on fixed cell images has been reported using manual and automated techniques. An assessor (ideally blinded to the experiment) manually counts the number of cells undergoing NETosis and expresses the rates of NETosis, with the total cell count as the denominator. Conventionally, a number (3-5) of high

power fields, ideally randomly, are taken from each condition for analysis and biological replicates are performed.

2.2.2.1 Automated NETosis analysis of fixed cells

Automated counting of NETosis has been reported in a study that screened for NETosis inhibitors (Hakkim et al., 2011). Sytox Green staining of unfixed cells in culture plates allowed quantification of cell death. Cells were subsequently fixed, permeabilized and imaged. A computer algorithm based on assessing fluorescent particle size and circularity allowed differentiation of the nuclear forms evident during NETosis. A similar analysis was used to report size and shape data from unfixed Sytox Green stained neutrophil microscopy images (Papayannopoulos et al., 2010). In the latter study, the mean area of each Sytox Green positive cell was plotted as a frequency distribution incorporating information about the rate of cell death and the amount of chromatin decondensation at a single time point.

Another type of analysis involves quantifying the percentage of DNA covering the microscopy field as a surrogate of the spreading of DNA induced during NETosis (Healy et al., 2016).

2.2.2.2 Fixed images – Advantages and disadvantages

This technique allows assessment of morphology of the NETs. However, this "classical" spreading morphology of NETs appears to be an artefact of the fixation, as unfixed cells that have undergone NETosis appear as diffuse clouds (Brinkmann & Zychlinsky, 2012) (examples of unfixed and fixed NETs in Figure 2.1). Fixation also allows staining for NET proteins as well as DNA, to provide further support for the conclusion that the mode of death is NETosis.

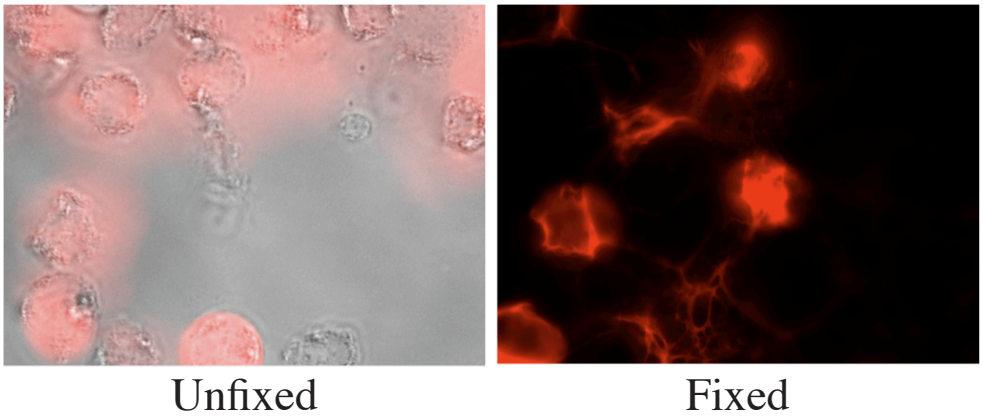


Figure 2.1 - Fixed versus Unfixed images of NETs

Neutrophils treated with PMA for four hours in culture plate. Unfixed cells and cells after fixation with 4% paraformaldehyde. Stained with 1 mcg/ml PI. Representative of two biological replicates.

Fixed imaging requires multiple handling steps that place the samples at risk of disruption and cell loss. Coating plates and coverslips with agents such as poly-lysine help reduce but cannot completely eliminate this risk. Treating the neutrophils with chemical inhibitors may affect the cell adherence, creating the appearance of reduced cell numbers that could be misinterpreted as decreased NETosis.

At higher cell densities, neutrophils undergoing NETosis adjacent to one another can overlap and connect, making counting difficult. With certain stimuli such as crystals, there is some aggregation of the cells, making it difficult count how many individual cells are undergoing NETosis.

Fixation and permeabilization of the cells means dead and living cells cannot be differentiated and a separate cell viability assay may need to be performed. Fixation also means that experiments are performed with defined time-points and it is technically difficult to conduct large numbers of comparisons at once.

2.2.3 DNA release assays

During NETosis, DNA becomes extracellular. Assays have been developed which take advantage of DNA fluorescent dyes that are not cell permeable, such as Sytox Green, to measure extracellular DNA. Sytox Green can be added at a single time-point or left in the media to allow a time-course of fluorescence to be established (Remijsen, Vanden Berghe, et al., 2011).

Another strategy to measure release of DNA into the extracellular space includes limited micrococcal nuclease treatment, which liberates the NETs into solution, without degrading the DNA signal (Fuchs et al., 2007). It is unclear whether the decondensed chromatin from cells that have died from NETosis is liberated more or less easily than cells that have died without chromatin decondensation (Fuchs et al., 2007). In DNA-release assays, the amount of released DNA is usually expressed as a percentage of total DNA able to be extracted from the same amount of neutrophils.

2.2.3.1 DNA release – Advantages and disadvantages

These analyses offer the advantage of being relatively simple and can be batched for higher throughput, quantitative analyses without the need for an independent observer. However, DNA is exposed with any form of cell membrane compromise, so these assays cannot distinguish between a cell undergoing NETosis or another form of death, such as secondary necrosis after apoptosis. For example, one study found Wortmannin restrained NETosis, but not cell death. The Sytox assay showed no difference with and without wortmannin in the amount of DNA released. It required separate imaging analysis to determine that the DNA had not decondensed (Remijsen, Vanden Berghe, et al., 2011). DNA release assays therefore need separate supportive structural information to exclude cell death processes other than NETosis.

Because these assays rely on fluorescence detection, they are prone to interference by reagents that fluoresce. An example of a pilot Sytox Green NET release assay experiment using suramin, a purine receptor antagonist is presented in Figure 2.2. It illustrates that suramin exhibits strong fluorescence emission in the same wavelength range as Sytox Green, which could lead to incorrect conclusions in the absence of complementary analyses.

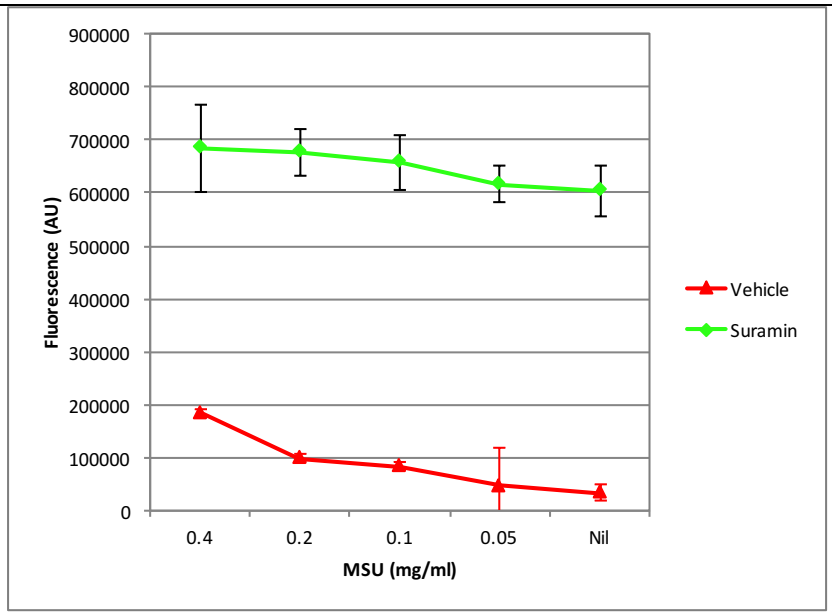


Figure 2.2 - Suramin exhibits fluorescent interference in the Sytox Green assay

Neutrophils (1 x 10^6/ml) stimulated with MSU at the indicated concentrations for 240 minutes. Sytox Green (50nM) was added and fluorescence was measured using the Tecan Genios (Excitation 485, emission 535 nm). Technical triplicate experiment from a single donor. Mean ± SEM.

2.2.4 Other NETosis assays

Flow cytometry has been used to quantify NETosis (Gavillet et al., 2015). The technique relies upon the staining of cells with citrullinated histone and MPO antibodies. Both murine and human neutrophils were studied with ionomycin as the stimulus. However, the extensive cellular disruption observed during PMA "lytic" NETosis makes FACS-based interpretation of NETosis problematic and this assay may be identifying earlier phases of NETosis (de Buhr & von Kockritz-Blickwede, 2016).

2.3 Cell death quantified with live cell imaging – rationale for live cell imaging of NETosis

Given the limitations in quantifying NETosis outlined above, I developed a live cell imaging approach incorporating computerised quantification. Live cell imaging has been used to assess other forms of cell death, such as apoptosis. Croker et al. labelled murine neutrophils with Cell Tracker Green and added PI to the media. Using time-lapse microscopy to assess apoptosis, these investigators computationally quantified cell death in the images to enable the rate of apoptosis to be calculated (Croker et al., 2011).

This technique served as a starting point that I have adapted to measure not simply cell death, but also chromatin decondensation, taking advantage of the strengths of time-lapse analysis and computerised quantification. The following section will outline the assay and its development.

2.3.1 Live cell imaging and Quantitative Image Analysis

2.3.1.1 Cell preparation

Neutrophils from healthy controls were isolated using PolymorphPrep as per manufacturer's instructions (see below for extended detail - section 2.4.1.1). Neutrophils were labelled with 1 μM Cell Tracker Green (CTG) (Invitrogen) and incubated for 30 minutes in a tissue culture incubator at 37°C in 5% CO_2. CTG is cell-permeable but becomes trapped inside the cell when the CTG chloromethyl group reacts with cellular thiol groups. CTG fluorescence is stably maintained until cell death when it is released. No extra wash steps were performed, as this was adequate to label the cells and remove enough CTG from the media to allow counting, thereby reducing the potential for cell activation with repeated pelleting of the cells. The cells were resuspended in culture media in human tonicity RPMI (HT-RPMI) without phenol red. Phenol red can interfere with fluorescent signals particularly in the cyan and green spectrum (Ettinger & Wittmann, 2014). The media was supplemented with 0.5% bovine serum albumin (BSA) to reduce background NETosis but not inhibit NET responses as previously described. Propidium Iodide (PI, 2 μg/ml) was added to the medium. It is not cell permeable so will only stain the DNA of cells that have died. The cells were passed through a 40 μm filter to remove clumped cells. The final cell concentration was 1 x 10^6/ml and inhibitors were added for one hour prior to stimulation with NET stimuli. 100 μl of cell suspension per well was incubated in a 96 well optical bottom plate with standard cell culture surface (Nunc).

2.3.1.2 Time-lapse microscopy

The culture plate was inserted into a plate holder and imaged on a Zeiss Axiovert Live Cell Observer or a Nikon Eclipse TiE inverted microscope. The interior of the microscope was maintained at a constant 37°C to avoid major temperature changes that can affect focus. Culture conditions were maintained in humidified air with 5% CO_2 using a plate cover.

A 10x objective lens was used and one image per well was acquired every 10 or 15 minutes. Fluorescent exposure was between 400 and 600 milliseconds for PI and

between 500 and 700 for CTG. Phase contrast images were also taken alongside each fluorescent image. Between 700 and 1000 cells were imaged per well. Experiments were performed with duplicate wells. Unstimulated cells were included for each condition to exclude non-specific toxicity of inhibitors. Stimuli, in 20 μl drops, were added using a multichannel pipette taking care not to disrupt adherent cells after an initial image was taken. Focus was optimised after stimulation.

Imaging revealed three distinct cellular appearances: 1. CTG positive cells, consistent with live cells; 2. loss of CTG signal, high intensity of PI staining and low diameter, consistent with cell death, but without chromatin decondensation; or 3. loss of CTG signal, low intensity of PI staining and a large diameter, consistent with a dead cell with chromatin decondensation (Figure 2.3). Z-stack demonstrated that these low PI intensity cells were not simply necrotic cells that had gone out of focus. There was no evidence of significant dual staining with CTG and PI.

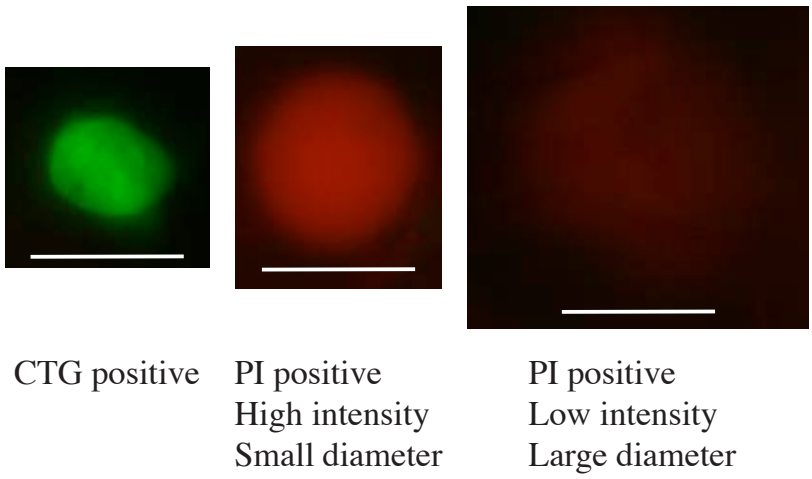


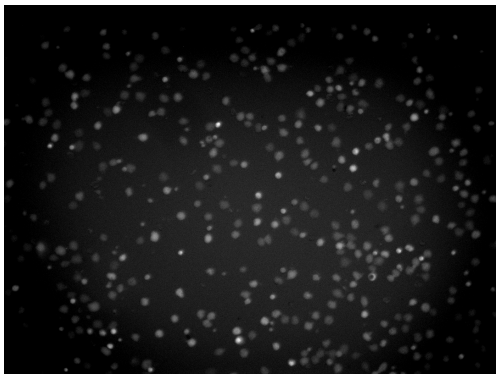
Figure 2.3 - Examples of cell appearances from live cell imaging

Representative examples of cell images taken from live cell time-lapse experiments. Scale bar = 10μm.

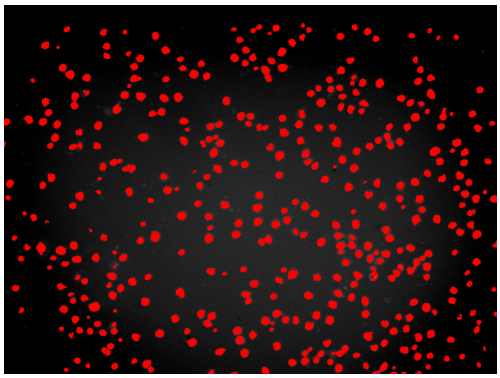
2.3.1.3 Computerized analysis of time-lapse images

Quantitative analysis of .tif image stacks of neutrophil images was performed using MetaMorph (v7.2.0, Molecular Devices). The “count nuclei” application module is a proprietary algorithm that counts fluorescent particles. The maximum and minimum expected cell diameter are entered to facilitate splitting clumps of cells into individual cells and excludes small non-cellular aggregates of fluorescent signal. Choosing diameters between 8 and 14 μm was effective at selecting cells. The difference in

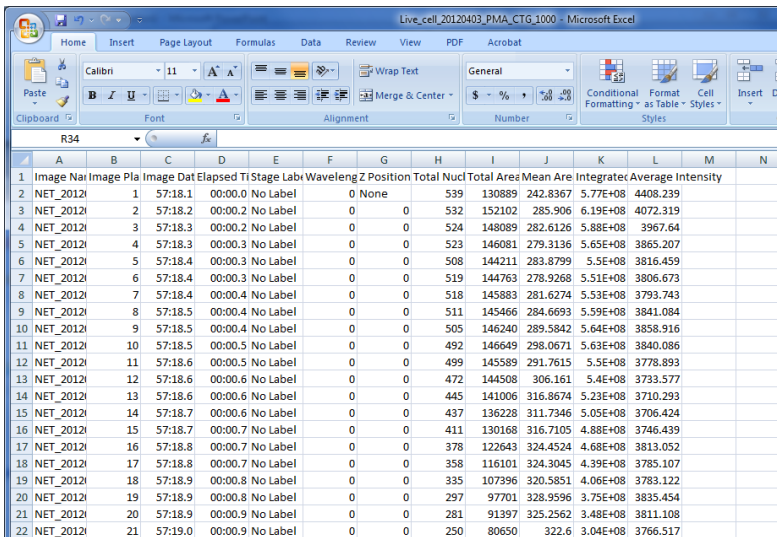
fluorescence intensity between the particles of interest and the adjacent media is estimated from selecting examples in a representative image. The “count nuclei” application also excludes cells on the edge of the field (Figure 2.4). A macro or “journal” was created that can be looped to count a series of time-lapse images as well as automatically count images from all of the wells. The output is an Excel file that can then be organised as necessary and calculations made.



CTG image



Metamorph count nuclei threshold image



Live_cell_20120403_PMA_CTG_1000 - Microsoft Excel

	A	B	C	D	E	F	G	H	I	J	K	L	M
1	Image Nar	Image Pla	Image Dat	Elapsed Ti	Stage Labe	Waveleng	Z Position	Total Nucl	Total Area	Mean Are	Integrated	Average Intensity	
2	NET_2012(	1	57:18.1	00:00.0	No Label	0	None	539	130889	242.8367	5.77E+08	4408.239	
3	NET_2012(	2	57:18.2	00:00.2	No Label	0	0	532	152102	285.906	6.19E+08	4072.319	
4	NET_2012(	3	57:18.3	00:00.2	No Label	0	0	524	148089	282.6126	5.88E+08	3967.64	
5	NET_2012(	4	57:18.3	00:00.3	No Label	0	0	523	146081	279.3136	5.65E+08	3865.207	
6	NET_2012(	5	57:18.4	00:00.3	No Label	0	0	508	144211	283.8799	5.5E+08	3816.459	
7	NET_2012(	6	57:18.4	00:00.3	No Label	0	0	519	144763	278.9268	5.51E+08	3806.673	
8	NET_2012(	7	57:18.4	00:00.4	No Label	0	0	518	145883	281.6274	5.53E+08	3793.743	
9	NET_2012(	8	57:18.5	00:00.4	No Label	0	0	511	145466	284.6693	5.59E+08	3841.084	
10	NET_2012(	9	57:18.5	00:00.4	No Label	0	0	505	146240	289.5842	5.64E+08	3858.916	
11	NET_2012(	10	57:18.5	00:00.5	No Label	0	0	492	146649	298.0671	5.63E+08	3840.086	
12	NET_2012(	11	57:18.6	00:00.5	No Label	0	0	499	145589	291.7615	5.5E+08	3778.893	
13	NET_2012(	12	57:18.6	00:00.6	No Label	0	0	472	144508	306.161	5.4E+08	3733.577	
14	NET_2012(	13	57:18.6	00:00.6	No Label	0	0	445	141006	316.8674	5.23E+08	3710.293	
15	NET_2012(	14	57:18.7	00:00.6	No Label	0	0	437	136228	311.7346	5.05E+08	3706.424	
16	NET_2012(	15	57:18.7	00:00.7	No Label	0	0	411	130168	316.7105	4.88E+08	3746.439	
17	NET_2012(	16	57:18.8	00:00.7	No Label	0	0	378	122643	324.4524	4.68E+08	3813.052	
18	NET_2012(	17	57:18.8	00:00.7	No Label	0	0	358	116101	324.3045	4.39E+08	3785.107	
19	NET_2012(	18	57:18.9	00:00.8	No Label	0	0	335	107396	320.5851	4.06E+08	3783.122	
20	NET_2012(	19	57:18.9	00:00.8	No Label	0	0	297	97701	328.9596	3.75E+08	3835.454	
21	NET_2012(	20	57:18.9	00:00.9	No Label	0	0	281	91397	325.2562	3.48E+08	3811.108	
22	NET_2012(	21	57:19.0	00:00.9	No Label	0	0	250	80650	322.6	3.04E+08	3766.517	

Figure 2.4 - Example of CTG labelled neutrophils counted using MetaMorph

CTG-labelled neutrophils 30 minutes post PMA stimulation. The image has had a threshold applied using the MetaMorph count nuclei application. The Excel output is shown below.

CTG positive cells are live cells and PI positive cells are dead. By setting the diameter and intensity parameters, PI positive cells with high PI intensity and small diameter were counted. This step excludes cells with large diameter and low PI density, which

are assumed to have undergone NETosis. The number of NET releasing cells was calculated at each time-point by deducting the CTG and PI positive cell counts from the initial total, using the following formula:

$$NET(t_x) = (CTG(t_0) + PI(t_0)) – CTG(t_x) – PI(t_x)$$

This approach assumes that minimal NETosis has occurred before image acquisition. Using prolonged exposure for PI staining to highlight decondensed chromatin, very few decondensed DNA structures were visible prior to stimulation (<1%). This technique also assumes stability of the field of view. No significant movement of cells from the field of view or detachment of cells was observed under the conditions described.

Examples of the assay and its graphical presentation are presented throughout Chapters 3 and 4 of this thesis.

2.3.1.4 Live cell imaging quantification of NETosis - Advantages and disadvantages

The assay measures the two key components of NETosis: 1) cell death; and 2) chromatin decondensation. It is the first reported that is able to do so in a time-lapse live cell setting. The data obtained includes the percentages of: 1) live cells; 2) dead cells not undergoing NETosis; and 3) cells undergoing NETosis. This approach can thus assess interventions that reduce NETosis either by preventing cell death or by preventing chromatin decondensation.

The assay does not involve any manipulation of the cells once the stimulus has been added, and cell counting is automated without the need to interpret morphology changes, which are issues with fixed cell imaging approaches. The assay is performed in a 96 well plate format, allowing the comparison of multiple stimuli and inhibitors of NETosis and it provides time-course information about NETosis. Experiments using the assay can determine, for example whether an inhibitor decreases NETosis or delays its onset. The assay also counts dead cells, allowing detection of non-specific toxicity of compounds. Live cell imaging also allows observation of other cell characteristics including cell shape change and aggregation of cells.

This technique requires access to sophisticated, well-calibrated microscopy facilities for long periods of time. For example, an assay to assess NETosis will typically take a minimum of five hours. Cell counting proved robust, but each experiment was visually

assessed exclude unexpected cell behaviour and to ensure that the counting is valid. As an example under certain conditions, neutrophil swarming (Kienle & Lammermann, 2016) may be induced, which results in large, densely aggregated clumps of neutrophils and the individual neutrophils cannot be differentiated. The presence of fluorescent interference of reagents may require adjustment of the counting parameters but generally can be accounted for. This NET readout is for DNA only, but it would be possible to adapt it for use with fluorophore-conjugated antibodies in live cell analysis to image other NET components.

2.4 Further methods

2.4.1 Human samples and cell isolation and culture

Synovial fluid samples, tophus aspirates and blood from healthy controls and a male patient with X-linked Chronic Granulomatous Disease were donated to the Royal Melbourne Hospital Inflammatory Disease Tissue Bank (Melbourne Health HREC 2005.056) and through the Volunteer Blood Donor Registry at the Walter and Eliza Hall Institute of Medical Research. Synovial fluid was aspirated as part of clinical care. The fluid was either used immediately for imaging or was centrifuged within 2 hours of aspiration at 3000 rpm for 10 minutes and stored at -80^{o}C until use. Clinically uninflamed tophi were aspirated using a 19-gauge needle under sterile conditions. Under suction, a core of tophus tissue was aspirated and used immediately or stored at -80^{o}C until use. All experiments were conducted under the auspices of the Melbourne Health and Walter and Eliza Hall Institute of Medical Research ethics committees. Sections of archived paraffin-embedded tophus tissue were provided by the Royal Melbourne Hospital Pathology department.

2.4.1.1 Neutrophil Isolation

Blood was taken using a vacutainer system into EDTA containing tubes (Becton and Dickinson, Franklin Lakes NJ). Neutrophils were isolated within 2 hours of blood taking using PolymorphPrep as per manufacturer's instructions. In brief, (Axis-Shield, Oslo, Norway) was used following manufacturer’s instructions. 7.5 ml peripheral blood samples in EDTA tubes were layered onto 6 ml of density gradient media. The tube was then centrifuged with 500xg, at 20°C without brake for 25-30 minutes in a Heraeus Megafuge 40R centrifuge. The plasma and PBMC layer were discarded or kept for further analysis and the granulocytes were harvested from the visible cell layer, down to the sedimented erythrocytes. Remaining erythrocytes were lysed with 3 ml of

human-tonicity red cell lysis buffer containing ammonium chloride and EDTA for 5 minutes at room temperature. The cells were resuspended in culture media. Cells were stained with Trypan Blue and cell viability was >95%. Cytospins were performed (Cytocentrifuge, Shandon, Pittsburgh, PA) during the pilot experiments, demonstrating >90% neutrophils with the primary contaminating cell being eosinophils (Figure 2.5).

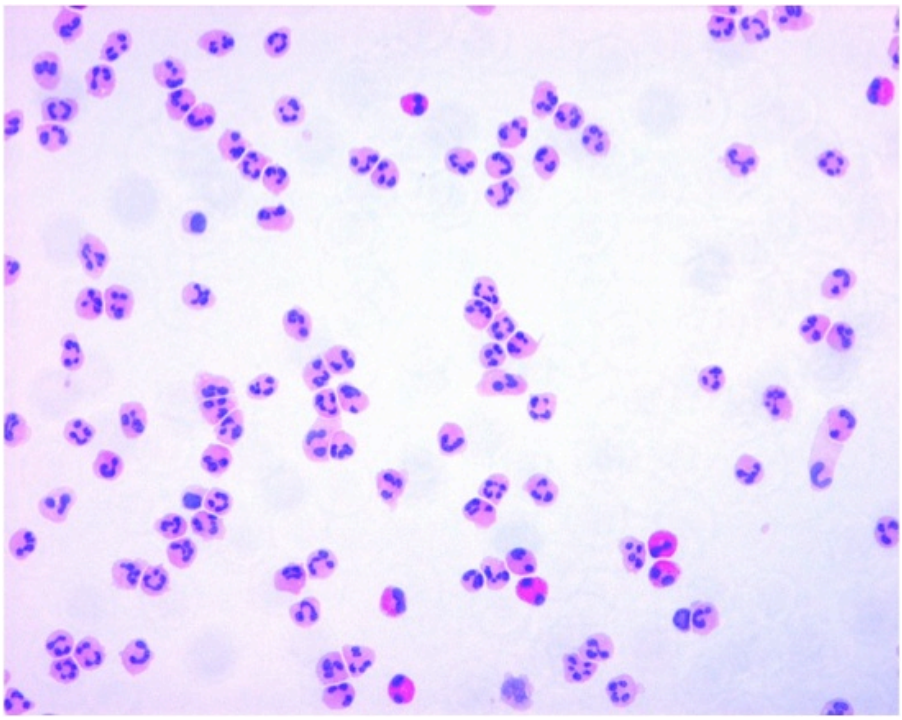


Figure 2.5 Cytospin of PolymorphPrep isolated neutrophils
Example of a cytospins of neutrophils isolated from human blood using PolymorphPrep. Stained with Haematoylin and Eosin. Representative of three biological replicates

2.4.1.2 Culture media

For NETosis experiments, HT-RPMI supplemented with 0.5% BSA was used. For fluorescent analysis, phenol red was omitted from the media to avoid fluorescence interference. Foetal calf serum and autologous human serum were used instead of BSA for some experiments, as indicated.

2.4.1.3 THP-1 cell co-culture

THP-1 cells were cultured in RPMI with 10% foetal calf serum and stimulated with 500 nM PMA for 3 hours to induce maturation and then washed three times to remove residual PMA. After culture overnight, cells were cultured in RPMI and 0.5% BSA at 0.5 x 10^6 cells/ml.

2.4.2 Preparation of stimuli

2.4.2.1 Preparation of MSU crystals

MSU crystals were formed as previously reported (Ortiz-Bravo & Schumacher Jr, 1993). Briefly 0.024 M uric acid in 0.024 M NaOH was heated to 70°C. NaOH was added as required to maintain pH between 7.1 and 7.2 and the solution was filtered and incubated at room temperature overnight to allow crystallization. The crystals were kept sterile, washed with ethanol, dried, autoclaved, re-suspended in PBS by sonication and were examined under phase and polarizing microscopy. Stock concentration of 10 mg/ml was prepared for use in experiments.

2.4.2.2 Preparation of Candida hyphae

Candida albicans were transferred from limiting media and resuspended at 10^7 cells per ml in RPMI medium supplemented with 10% foetal calf serum and cultured in 5% CO_2 at 37°C to induce formation of hyphae. Hyphae induction was over 50% assessed by phase contrast microscopy and stimulations were performed at a multiplicity of infection (MOI) of 0.4. Hyphae were incubated in 50% autologous serum for 30 minutes and washed with media prior to use.

2.4.2.3 Latex beads

Latex beads of various sizes (0.8μm, 3μm or 10μm in diameter, Sigma Aldrich) were added to neutrophils with and without incubated with 50% autologous serum for 30 minutes and washed in media prior to use. Bead concentrations were calculated to expose neutrophil to defined numbers of beads per cell.

2.4.2.4 Fas Ligand

Recombinant FcFasL (a trimeric form of FasL) protein was purified from FcFasL-transfected HEK-293 cell culture supernatant by affinity chromatography using the MabSelect resin (GE Healthcare), followed by size-exclusion chromatography on a Superdex 200 column (GE Healthcare). FasL isolation was performed by Lorraine O'Reilly and the cell line was kindly provided by Pascal Schneider (University of Lausanne, Switzerland).

2.4.3 Imaging

2.4.3.1 Synovial fluid and tophus microscopy and fixed cell imaging

Joint fluid and tophus aspirates were immediately stained with 2 μg/ml Propidium

Iodide (PI) (Sigma) without washing and examined unfixed on a microscope slide with wide field (Nikon Ti Eclipse) or confocal microscopy (Leica SP8). Tophus aspirates were pressed onto glass slides and fixed with paraformaldehyde (4%, Sigma). Primary antibodies used were rabbit anti-neutrophil elastase antibody and mouse anti-myeloperoxidase antibody as listed (Table 2.3 Antibodies) or the primary antibody was omitted. Secondary antibodies were goat anti-rabbit Ig Fab fragment Alexa488 and a goat anti-mouse Ig Alexa568. DNA was stained with DAPI and slides mounted in Polymount mounting medium (Polysciences, Nijkerk, Netherlands).

2.4.3.2 Fixed cell imaging of in vitro stimulated neutrophils

Fixed cell imaging of *in vitro* stimulated neutrophils was performed as previously described (Brinkmann et al., 2010). Neutrophils were incubated at 0.4 x 10^6/ml on poly-L-lysine (0.001%, Sigma) coated 13mm No.1.5 glass coverslips in a 24 well culture plate. Stimuli were added to the wells and the cells fixed at indicated times with an equal volume of 8% paraformaldehyde (Sigma) for 15 minutes. Cells were permeabilized with Triton X-100 (0.1%, Sigma) either before or after staining as indicated. Washes and incubations were performed by inverting the coverslips on drops of wash buffer on parafilm coated test-tube racks as per Brinkman et al. (Brinkmann et al., 2010). Urate-supersaturated PBS was used for washes and incubations to reduce dissolution of crystals. No new crystal formation was observed using this solution.

Primary antibodies used were rabbit anti-NE antibody, mouse anti-MPO antibody, mouse anti-CD63 antibody and mouse anti-β actin. Secondary antibodies were as used for tophus staining in addition to goat anti-rabbit Ig conjugated to Alexa647 and secondary antibodies are listed in Table 2.3 Antibodies. DNA was stained with DAPI or Hoechst 33342 as indicated.

DQ ovalbumin (10 μg/ml, Thermo Fisher Scientific) was added to the media prior to neutrophil stimulation to image intracellular protease activity. Phalloidin FITC (50μM) was used to stain F-actin (Thermo Fisher Scientific).

2.4.3.3 Microscope

Coverslips were imaged using: Deltavision Elite widefield microscope (GE Healthcare Life Sciences) with post-acquisition deconvolution; Zeiss LSM780 confocal microscope; and Leica SP8 confocal microscope with resonance scanning. Images

were taken with Z-stacks and presented either as individual images or as maximum intensity projections as indicated.

2.4.3.4 Live cell imaging

Wide field live cell imaging is as previously described above (2.3.1.2 Time-lapse microscopy).

Live cell imaging to demonstrate nuclei of intact cells was performed by adding 1μg/ml of Hoechst 33342, a cell permeable DNA dye. Annexin V labelled with Alexa 488 was used to measure phosphatidylserine exposure

Live cell imaging of neutrophils labelled with DQ ovalbumin (10 μg/ml, Thermo Fisher Scientific) was performed in an 8 well chamber microscope slide (Nunc) taking multiple Z-sections using a Leica SP8 confocal laser microscope with resonance scanning under culture conditions.

Live cell imaging of THP-1 cells was performed as for neutrophil assays. The THP-1 cells were labelled with CTG before the addition of unlabelled neutrophils and stimulation with crystals. Cell death was calculated from CTG positive population counts.

2.4.3.5 Immunohistochemistry of tophi sections

Slides of paraffin-embedded tophus tissue underwent heat-induced antigen retrieval Roche Ventana Ultra Cell Conditioning Solution and were stained using a Roche Ventana Benchmark Ultra immunohistochemistry stainer. The primary antibody was a polyclonal rabbit anti-human myeloperoxidase antibody (Dako, A0398). Secondary antibody HRP labelled and counterstained with haematoxylin (Roche).

2.4.3.6 Transmission Electron Microscopy

Initial cell preparation for electron microscopy was performed by myself. Sarah Ellis and the microscopy staff at the Victoria Comprehensive Cancer Centre performed subsequent preparation following the initial fixation. I performed imaging of the prepared samples.

Neutrophils ($1x10^6$/ml) were cultured in HT-RPMI + 0.5% BSA in Eppendorf tubes under culture conditions. After stimulation, the cells were spun at 1500 rpm for 5 minutes and resuspended in 2.5% glutaraldehyde 2% paraformaldehdye in cacodylate Buffer (0.1M) and fixed for one hour.

Cells were rinsed twice for 15 minutes in 0.1M cacodylate buffer and post-fixed with 1% osmium tetroxide, 1.5% potassium ferrocyanide in 0.1M sodium cacodylate, pH 7.4 in the dark for 1 hour in a fume hood. After two further rinses in distilled water, the cells were dehydrated through a graded alcohol series: 50%, 70%, 90%, 95%, 100%, and 100% for 15 minutes each. After two final rinses in acetone, the pellet was embedded in Spurrs resin into embedding moulds. Spurrs resin was polymerised overnight in a laboratory oven at 70°C overnight. Ultrathin sections were cut with a diamond knife (Diatome, Austria) using a Leica Ultracut S or UC7 ultra-microtome, mounted on copper grids and treated with methanolic uranyl acetate and aqueous lead citrate for contrast.

Imaging was performed in a JEOL 1011 transmission electron microscope with a MegaView III CCD cooled digital camera (Soft Imaging Systems, Münster, Germany).

2.4.3.7 Neutrophil-crystal interaction analysis

To assess crystal-neutrophil membrane interaction, segmentation images from the 'count nuclei' function of CTG labelled neutrophils were used. Cells at the edge of the image were excluded. An intensity threshold was applied to the segmentation image and the subsequent image was submitted for integrated morphometric analysis. The shape factor was then applied to the cells. The shape factor, defined as $4\pi A/P^2$ (A and P are the nuclear area and perimeter, respectively), approaches 1 for a rounded cell and approaches 0 for an elongated cell. Average circularity of the cells was calculated prior to stimulation and then 15 minutes after the addition of the crystals. A reduction in circularity reflects a deformity of the neutrophil shape that acts as a surrogate for interaction with the crystals, but is not a direct measure of crystal phagocytosis. Examples of cells with different circularity indexes are shown (Fig. 2.6).

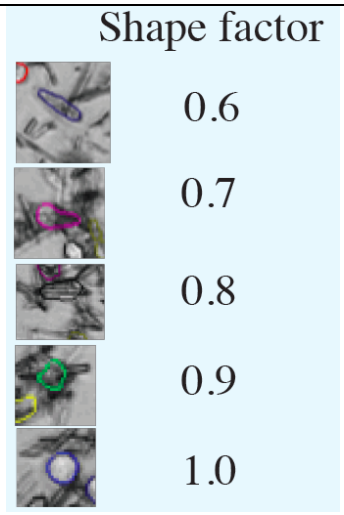


Figure 2.6 - Neutrophil shape analysis examples

Examples of neutrophils of various circularity indices. The outline is the outline of the CTG labelled neutrophil.

2.4.4 MPO-DNA measurement

The MPO-DNA assay was developed by an Honours student, Kathrin Grebe, and myself and the following experiments were performed by myself. MPO-DNA conjugates were measured in synovial fluid. Black 96 well microplates (Nunclon delta surface) were coated in 5 μg/ml of anti-human MPO antibody (clone 4A4, ABD-Serotec) overnight, shaking at 4°C. Plates were washed and blocked with 1% BSA. Samples were incubated at room temperature for 2 hours.

After washing, proteinase K (2.5 mg/ml, Sigma) was added and incubated at 37°C with shaking for one hour to reduce the protein content that can interfere with fluorescent measurement of nucleic acid. PicoGreen (Life Technologies), a nucleic acid binding fluorescent reagent, was added to the proteinase K digested sample to measure the DNA content. Fluorescence was measured using a Tecan Genios Microplate reader with excitation at 485 nm and emission measured at 535 nm. Results are expressed in Arbitrary Fluorescent Units (AFU). Coefficient of variation with *in vitro* NETs and serum samples were <10%.

2.4.5 Luminol-enhanced chemiluminescence

Neutrophils in HT-RPMI and 0.5% BSA were incubated in a black 96 well plate with Luminol (200 μM, Sigma). Stimuli were added and luminescence measurements were taken every minute using a Chameleon plate reader (Hidex).

2.4.6 NET protein studies

2.4.6.1 Neutrophil protein for Western blotting

Neutrophils with and without inhibitors, as indicated, were incubated in Eppendorf tubes at 1 x 10^6 cells per ml. At selected time points after stimulation, the cells were centrifuged at 8000xg for 5 minutes to pellet the cells. Supernatants were removed and 150 μl of 2x SDS loading buffer was added, cells resuspended and immediately boiled for 5 minutes. Samples for non-reducing PAGE were resuspended in 2x SDS without 2-mercaptoethanol. Samples were sonicated for 20 seconds at 50% duty cycle (one second on, one second off) and 30% amplitude with a digital sonifier (Branson) and boiled again before freezing at -80^{o}C. Samples were resolved by SDS-polyacrylamide gel electrophoresis (PAGE) (8-14% Tris, Novex), transferred to nitrocellulose (0.45 μm pore, GE Healthcare) or PVDF membranes (0.45 μm pore, Millipore) for one hour at 100V, blocked in PBST plus 5% skim milk powder for 1 hour, and labelled with primary antibodies. Primary antibodies were diluted in PBST with 1% skim milk powder and 0.02% sodium azide and incubated overnight at 4°C. Antibodies are listed in Table 2.3 Antibodies. After washing, the membranes were incubated with appropriate secondary horseradish peroxidase–conjugated antibodies for 30-60 minutes at room temperature. After further washes, blots were developed with chemiluminescent HRP substrate (Immobilon, Millipore) and images were taken with ChemiDoc Touch Imager (Biorad).

2.4.6.2 NET proteomics

NET protein was isolated following the protocol published by Urban et al (Urban et al., 2009). Neutrophils in HT-RPMI with 0.5% BSA were cultured in a 12 well culture plate at 1.7 x 10^6 per ml at 37°C in a 5% CO_2 and activated with either PMA (27nM) or MSU (0.2 mg/ml) for 4 hours. Each well was carefully washed twice for 10 minutes with warm HT-RPMI and non-EDTA containing protease inhibitor P1860 (1:200,Sigma) (no dislodgement of the NET structures was observed microscopically). The NETs were then digested for 20 minutes in 1 ml HT-RPMI with 5 U/ml micrococcal nuclease (Worthington). Nuclease activity was stopped by addition of EDTA pH 8.0 at 5mM final concentration. The samples were centrifuged at 300xg to remove whole cells and then

at 16,000xg to remove debris. Proteins were acetone precipitated. Four matched samples from different wells were pooled together and transferred to 30 ml polypropylene tubes and 16 ml of ice-cold acetone (-20°C) was added. Precipitation samples were incubated overnight at -20°C and then centrifuged at 10,000xg for 30 min at 4°C. The protein pellet was washed with 1 ml 80% acetone buffered in 20 mM Tris-HCl pH 8.0 and solubilized in 120 μl 2x Laemmli sodium dodecyl sulphate (SDS) sample buffer (1 well or 1.7 x 10^6 cells) for SDS-PAGE or prepared for mass spectrometry (MS)(4 wells or 6.8 x 10^6 cells, two independent experiments).

2.4.6.3 Gel excision, in-gel digestion and Nano-LC-MS/MS

Mass spectrometry and mass spectra database searching was performed by Tom Nebl as outlined in sections 2.4.6.3. and 2.4.6.4.

20 μl aliquots of NET preparations were separated on a preparative SDS-PAGE gel, stained with Sypro Ruby Red (SRR), and 12 equal slices were excised per lane. All gel samples were reduced with 10mM Dithiothreitol (DTT, Sigma) for 30 min, alkylated for 30 min with 50mM iodoacetamide (Sigma) and digested with 375ng trypsin gold (Promega) for 16 hrs at 37°C. The extracted peptide solutions were then acidified (0.1% formic acid) and concentrated to 10 ml by centrifugal lyophilisation using a SpeedVac AES 1010 (Savant). Extracted peptides were injected and fractionated by reversed-phase liquid chromatography on a nanoACQUITY UHPLC system (Waters, USA) using a nanoACQUITY C18 150 mm × 0.15 mm I.D. column (Waters, USA) developed with a linear 60-min gradient with a flow rate of 250 nl/min from 100% solvent A (0.1% Formic acid in Milli-Q water) to 60 % solvent B (0.1% Formic acid, 100% acetonitrile, (Thermo Fisher, USA) 40% Milli-Q water). The nano-UHPLC was coupled on-line to a Q-Exactive Orbitrap mass spectrometer equipped with a Proxeon nano-electron spray ionization source (Thermo Fisher, USA) for automated MS/MS. High mass-accuracy MS data was obtained in a data-dependent acquisition mode with the Orbitrap resolution set at 75,000 and the top-ten multiply charged species selected for fragmentation by higher-energy collisional dissociation (single and doubly charged species were ignored). The ion threshold was set to 15,000 counts for MS/MS. The capillary electrophoresis voltage was set to 27.

2.4.6.4 Mass spectra database searching

For protein identification, LC-MS/MS data were searched against a non-redundant protein decoy database comprising sequences from the latest version of

MSPnr100_Q215 (selected for Homo sapiens species plus contaminants) as well as their reverse sequences. Mass spectra peak lists were extracted using extract-msn as part of Bioworks 3.3.1 (Thermo Fisher Scientific) linked into Mascot Daemon (Matrix Science, UK). Peak lists for each nano-LC-MS/MS run were searched using MASCOT v2.2.04 (Matrix Science, UK), provided by the Australian Proteomics Computational Facility (www.apcf.edu.au). The search parameters consisted of carbamidomethylation of cysteine as a fixed modification (+57 Da), with variable modifications set for NH2-terminal acetylation (+42 Da) and oxidation of methionine (+16 Da). A precursor mass tolerance of 20 ppm, #13C defined as 1, fragment ion mass tolerance of ±0.04 Da, and an allowance for up to three missed cleavages for tryptic searches was used. Scaffold v4.4.3 (Proteome Software, Inc., USA) was used to validate protein identifications derived from MS/MS sequencing results (False discovery rate FDR<1%).

2.4.6.5 Cell membrane isolation and Blue Native Page

Preparation of cell membranes and cytosol and Blue Native PAGE (BN-PAGE) analysis of the proteins was performed as previously described (Hildebrand et al., 2014). In brief, 3 x10^6 neutrophils were treated as indicated. At various time-points, the cells and supernatant were harvested and centrifuged for 5 minutes at 1500 rpm. The washed cells were treated with 0.025% digitonin in buffer (20 mM Hepes (pH 7.5), 100 mM KCl, 2.5 mM $MgCl_2$, and 100 mM sucrose) supplemented with protease and phosphatase inhibitors (Roche) and 2 µM N-ethyl maleimide (NEM). After a further 13000rpm spin for 5 minutes, the supernatant representing the cytosolic fraction was added to 4x SDS loading buffer for conventional Western blotting. The BN-PAGE sample was supplemented with digitonin to a final concentration of 1%. The pellet was resuspended in 1% digitonin containing buffer. This solution represents the whole membrane fraction and used for BN-PAGE and added to 2x SDS loading buffer for Western blotting.

Samples were resolved by BN-PAGE (Life Technologies) for 45 minutes at 150V after adding BN-loading buffer. Proteins were transferred to PVDF for 3 hours at 50V and the membrane briefly destained with 50% methanol and 25% acetic acid. The membranes were subjected to denaturing for 1-2 hours with 6M GuHCL, 10mM Tris-Cl pH 7.0 and 5mM 2-ME, before the membrane was washed with water and then PBS and Western blotting performed as described above.

2.4.7 NET degradation assays

2.4.7.1 Macroscopic and microscopic analysis of NET degradation

Neutrophils were cultured at $1x10^6$ cells/ml in a 6 well culture plate and stimulated with 0.2mg/ml crystals, shaken to form neutrophil-crystal aggregates. Nuclease (MNase (Worthington) or bovine pancreatic DNase 1 (Roche) or protease proteinase K (Roche, 2.5 mg/ml) were added and images were taken with an Olympus SZX16 stereomicroscope using top illumination. Neutrophils were incubated on coverslips for fixed cell imaging. Autologous serum at 10% was added and incubated for 6 hours prior to fixation. DNA was stained with DAPI.

2.4.7.2 DNA release assay

DNA release assays were performed as previously described (Hakkim et al., 2010). In brief, PMA and MSU stimulated (4 hours) neutrophils were incubated for 60 minutes with varying doses of MNase and DNase 1 and the reaction terminated with EDTA 5 mM. Picogreen was used to measure the DNA content of the supernatants. DNA release was expressed relative to the amount released by MNase 500 mU/ml after an hour.

2.4.7.3 Time-lapse fluorescent imaging of the nuclease degradation

For time-lapse fluorescent imaging of DNA degradation, PI-labelled PMA- and MSU-induced NETs were generated in Eppendorf tubes. NETs were resuspended by brief vortexing and then centrifuged at 8000xg for 5 minutes to generate discrete clumps. These were then dislodged with gentle pipetting and placed in a 96 well microscopy culture plate (Nunc). Nuclease or serum was added at the indicated concentrations with duplicate wells. EDTA was added at a final concentration of 5mM for certain conditions. Uricase treatment (Worthington, 10U/ml) was performed for two hours at 37°C prior to nuclease treatment. Images were acquired every 15 minutes with the Nikon Eclipse TiE microscope under culture conditions. Image analysis was performed using ImageJ (US National Institutes of Health) by measuring the intensity of PI signal from the whole image. Data are expressed as a percentage of the starting PI intensity.

2.4.8 Inflammasome and IL-1β studies

2.4.8.1 THP-1 cell co-culture

THP-1 cells matured with PMA were washed and stimulated for 6 hours with MSU crystals alone or crystals that had been incubated with neutrophils (1×10^6/ml) for 4 hours prior to induce NETosis. DNase treatment (10 U/ml) was added an hour prior to

stimulation to disrupt the NETs. Nigericin (10 μM) was added 1 hour prior to harvest. Supernatants were aspirated and spun at 5000rpm for 5 minutes. Supernatant was frozen at -80°C until analysed by ELISA for IL-1β.

2.4.8.2 IL-1β ELISA

The IL-1β concentration in solution was measured using the human IL-1β Duo-set ELISA kit (R&D Systems), as per manufacturer's instructions.

2.4.9 Inhibitors

Inhibitors were dissolved in DMSO unless otherwise indicated and used at concentration indicated in the main text. DMSO concentrations were less than 0.5% and concentrations up to 1% did not interfere with NETosis. Of note, formal biochemical validation of all of the inhibitors was not undertaken. This is an important caveat in interpreting the results obtained and the conclusions drawn. Genetic analysis of the roles of target molecules is ideal but difficult to achieve in primary human neutrophils.

Table 2.1 Stimuli and Inhibitors

Compound	Manufacturer	Compound	Manufacturer
ABAH	*Cayman*	Mito-TEMPO	*Sigma-Aldrich*
Bafilomycin A1	*Sigma-Aldrich*	Monosodium Urate crystals	*In-house*
BAPTA-AM	*Sigma-Aldrich*	N-acetyl cysteine	*Sigma-Aldrich*
CA-074-Me	*Enzo Lifesciences*	Na Acetate	*Sigma*
Calcium pyrophosphate crystal	*Invivogen*	Na Azide	*Sigma*
Caspase 3 Inhibitor II Z-DEVD-fmk	*Calbiochem*	Na Butyrate	*Sigma*
Caspase 8 Inhibitor 1 IETD-CHO	*Calbiochem*	Na Propionate	*Sigma*

Caspase 9 Inhibitor II LEHD-CHO	*Calbiochem*	Necrostatin-1	*TetraLogic*
Cl amidine	*Calbiochem*	Necrosulfonamide	*Abcam*
Colchicine	*Sigma-Aldrich*	Nigericin	*Enzo Life Sciences*
Colchicine	*Sigma*	Nocodazole	*Sigma-Aldrich*
Cucurbitacin	*Enzo Lifesciences*	PD98059	*Calbiochem*
Cytochalasin D	*Sigma-Aldrich*	Piceatannol	*Enzo Lifesciences*
Dexamethasone	*Sigma-Aldrich*	PMA	*Sigma-Aldrich*
Diphenylene Iodonium (DPI)	*Enzo Lifesciences*	Potassium Chloride	*Sigma-Aldrich*
EDTA	*Sigma-Aldrich*	PP2	*Alexis*
EGTA	*Sigma-Aldrich*	Pyrocatechol	*Sigma-Aldrich*
G-CSF	*Amgen Australia*	Q-VD-Oph	*MP Biochemicals*
Glybenclamide	*Sigma-Aldrich*	R-Roscovitine	*Cayman*
GM-CSF	*Prospec Bio, Rehovot, Israel*	Rapamycin	*Invivogen*
GSK 484	*Cayman*	SB203580	*Calbiochem*
GSK832 - RIPK3 inhibitor	*In house*	Silica Dioxide	*Sigma-Aldrich*
GW311616A	*Sigma-Aldrich*	Simvastatin	*Sigma-Aldrich*
GW806742X	*In-house*	Sivelestat	*Sigma-Aldrich*
Hit #14	*Otava Chemicals*	Staurosporine	*Enzo Lifesciences*
Indomethacin	*Sigma-Aldrich*	Suramin	*Enzo Lifesciences*
Jasplakinolide	*Enzo Lifesciences*	WEHI781	*In house*
Latrunculin B	*Enzo Life Sciences*	WEHI929	*In house*

LPS	*Sigma Aldrich*	Wortmannin	*Enzo Lifesciences*
LY294002	*Cayman*	ZVAD-fmk	*Enzo Lifesciences*

2.4.10 Other Reagents

Table 2.2 Other reagents

Reagent	**Manufacturer**
Bovine serum albumin	Sigma-Aldrich
Cell tracker green	Invitrogen
Cholera toxin Alexa-488	Thermo Fisher Scientific
DAPI	Sigma-Aldrich
Dextran-Alexa647	Invitrogen
DQ ovalbumin	Thermo Fisher Scientific
Gelsolin	Cytoskeleton
Hoechst 33342	Thermo Fisher Scientific
Leu-Leu-Ome	Sigma-Aldrich
Lucifer Yellow	Sigma-Aldrich
Luminol	Sigma-Aldrich
Phalloidin-FITC	Sigma-Aldrich
PicoGreen	Life Technologies
Poly-lysine	Sigma-Aldrich
Propidium Iodide	Sigma-Aldrich
Sytox Green	Life Technologies
Proteinase K	Sigma-Aldrich
Uric Acid	Sigma-Aldrich

Micrococcal nuclease	Worthington
Bovine pancreatic Deoxyribonuclease 1	Roche
Annexin V Alexa 488	Molecular Probes
Annexin V Alexa 647	Molecular Probes

2.4.11 Antibodies

Table 2.3 Antibodies

Antibody	**Species**	**Clone/ Catalogue number**	**Manufacturer**	**Concentration**
Neutrophil Elastase	Rabbit	Ab21595	Abcam	1 in 1000
Myeloperoxidase	Mouse	A0398	Dako	1 in 500
CD63	Mouse	RFAC4	Millipore	1 in 500
Histone 3	Rabbit	Ab1791	Abcam	1 in 1000
Histone 4	Rabbit	Ab7311	Abcam	1 in 1000
Citrullinated Histone 3	Rabbit	Ab5103	Abcam	1 in 1000
Myeloperoxidase	Mouse	4A4	ABD-Serotec	MPO-DNA
MLKL	Rat	3H1	In house	1 in 1000
β-actin	Mouse	AC-74	Sigma Aldrich	1 in 5000 WB 1 in 200 IFA
S100-A8	Mouse	sc-20174	Santa Cruz	1 in 500

Caspase-8 p18	Rabbit	H-134 SC-7890	Santa Cruz	1 in 1000
Cleaved Capase-3	Rabbit	Asp175) (5A1E)	Cell Signalling	1 in 100
Rabbit Ig Fab Alexa 488	Goat		Thermo Fisher Scientific	1 in 1000
Mouse Ig Alexa 568	Goat		Thermo Fisher Scientific	1 in 500
Rabbit Ig Alexa 647	Goat		Thermo Fisher Scientific	1 in 500
Rabbit Ig HRP	Donkey		GE Healthcare Life Sciences	1 in 15000
Goat Ig HRP	Donkey		GE Healthcare Life Sciences	1 in 10000
Rat Ig HRP	Donkey		GE Healthcare Life Sciences	1 in 10000
Mouse Ig HRP	Donkey		GE Healthcare Life Sciences	1 in 10000

2.4.12 Statistical analysis

Statistical analysis of discrete time-points was performed using paired or unpaired Mann-Whitney U tests as indicated. For time-lapse experiments, two way repeated measures ANOVA with time and treatment as factors was used. Analyses were performed at a nominal significance level p value <0.05 (two-tailed). Statistics and graphical representations were generated with GraphPad PRISM™ statistics software package (Ver. 2.0; San Diego, CA).

3 NEUTROPHILS SEQUESTER PRO-INFLAMMATORY CRYSTALS USING DNASE-RESISTANT "SAFETY NETS"

3.1 Introduction

Crystals have been implicated in a number of human diseases, including gout (monosodium urate crystals (MSU)), pseudogout (calcium pyrophosphate dehydrate crystals (CPPD)), silicosis (silica crystals) and atherosclerotic disease (cholesterol crystals) (Franklin et al., 2016). Gout is induced by MSU depositing within and around joints, leading to the classical features of acute inflammation – namely severe joint pain, swelling, erythema and loss of function. An untreated attack of gout, however, typically resolves within 7-10 days despite the ongoing presence of crystals (Pascual, 1991). Furthermore, recurrent attacks of gout can lead to formation of tophi - dense crystal deposits surrounded by fibrotic tissue (Dalbeth et al., 2010) that can cause disfigurement, bone destruction and disability, but curiously are not inflamed. Macrophages are thought to play a crucial role in driving the inflammation of gout (W. J. Martin et al., 2009). MSU-induced NLRP3-dependent inflammasome activation and release of interleukin-1β has been well characterised (Martinon et al., 2006). The role of neutrophils, which are potent pro-inflammatory cells (Popa-Nita & Naccache, 2010) and are abundant in the joint fluid during acute gout, is less clear. Of note, intact neutrophils are conspicuously absent from established tophi (Dalbeth et al., 2010).

A recently described neutrophil response to various pro-inflammatory stimuli is a form of cell death called NETosis, wherein cells release decondensed nuclear DNA coated with neutrophil granule enzymes, such as neutrophil elastase (NE) and myeloperoxidase (MPO), to generate neutrophil extracellular traps, or NETs (Brinkmann et al., 2004). NETosis has been extensively investigated *in vitro* using the convenient, but non-physiological stimulus, phorbol myristate acetate (PMA). PMA-

induced NET release is dependent on NADPH oxidase-generated reactive oxygen species (ROS) (Fuchs et al., 2007). ROS trigger translocation of NE from azurophil granules to the nucleus, where NE degrades histones, causing chromatin decondensation prior to cell death and the subsequent release of NETs (Papayannopoulos et al., 2010). Fungal hyphae also induce NETosis in an NADPH oxidase-dependent manner in both mice and humans (Bianchi et al., 2009; Branzk et al., 2014). More recently, crystals - including MSU, CPPD and cholesterol - have been identified as NET-inducing stimuli, but with inconsistent reports on the role of ROS (Mitroulis et al., 2011; Pang et al., 2013; Warnatsch et al., 2015).

In this study, we demonstrate that NETs are not only present in the inflamed synovial fluid of gout patients, but also surround the crystals in non-inflamed tophi. Using a novel, live cell imaging assay, we show that MSU and other physiologically relevant crystals induce NETosis with features distinct from PMA- or *Candida*-induced NETosis. MSU-induced NETs are actin-enriched and resistant to serum nucleases, facilitating aggregation of MSU crystals in a DNA-dependent manner. Furthermore, NETosis reduces the inflammatory potential of MSU crystals, generating DNA-coated crystal aggregates similar to a tophus. These results demonstrate that NETosis serves to coat and sequester noxious particles in diseases such as gout, reducing ongoing, futile inflammation.

3.2 RESULTS

3.2.1 DNA associated with neutrophil granule enzymes is present in acute gout synovial fluid and non-inflamed tophi from patients with chronic gout

Microscopy of unfixed synovial fluid taken during acute gout and stained with PI demonstrated the presence of extracellular DNA, which was closely associated with clumps of MSU crystals (Figure 3.1).

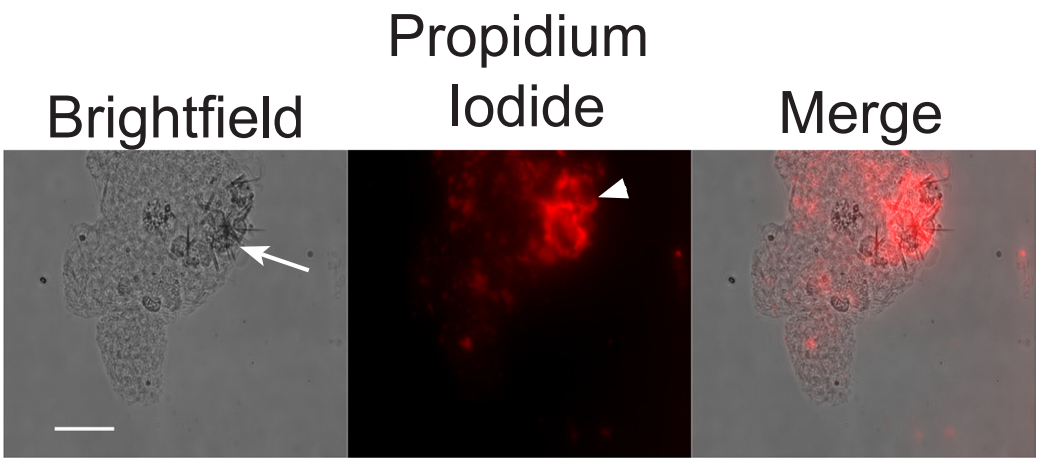


Figure 3.1 Synovial fluid from gout patients contains aggregates of crystals and extracellular DNA
Synovial fluid from a patient with gout immediately stained with propidium iodide (PI). Brightfield, fluorescent image and merged. Scale bar represents 20 μm. Arrow indicates crystals. Arrowhead indicates extracellular DNA. Representative of four separate patient samples.

We also measured DNA complexes associated with MPO, in synovial fluid, using a novel immunocapture and DNA fluorimetry technique. MPO-DNA fluorescence levels were higher in cell-free synovial fluid taken from patients with acute gout compared to patients with non-inflammatory osteoarthritis (Figure 3.2). These findings suggest local DNA release from synovial neutrophils occurs in acute gout.

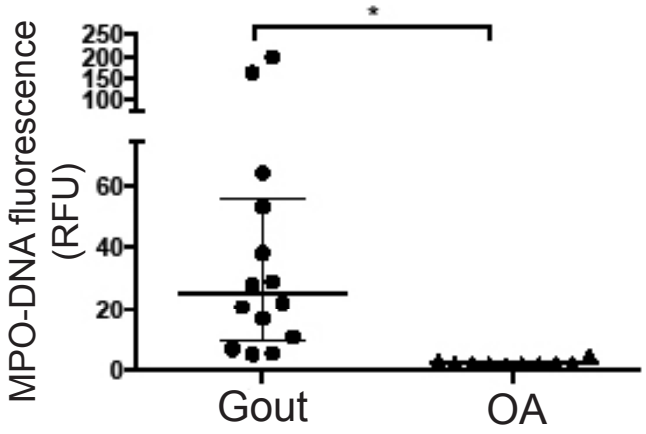


Figure 3.2 Synovial fluid from gout patients contains more MPO-DNA complexes than from OA patients

Synovial fluid samples from patients with either acute gout or osteoarthritis (OA) (Gout, n=14, OA, n=10). MPO-captured DNA levels (MPO-DNA) expressed as relative Picogreen fluorescent units (RFU). Data represented as median and interquartile range. *P<0.01 for the difference between groups using the Mann-Whitney U test.

Surprisingly, aspirates from clinically uninflamed tophi also displayed abundant crystal-associated DNA (Figure 3.3). At higher magnification, the DNA appeared to coat the crystals (lower panel).

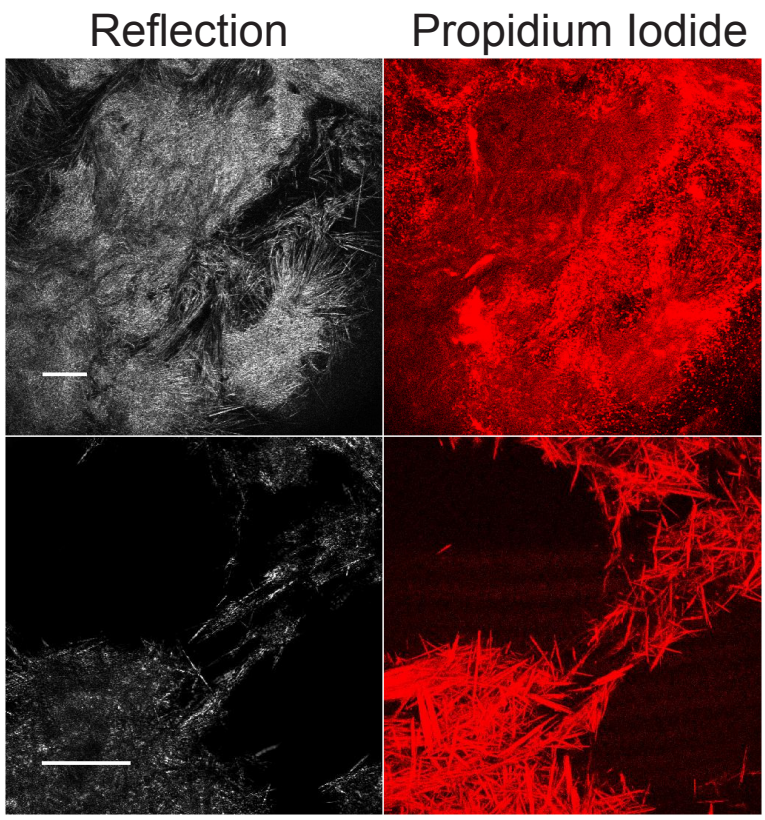


Figure 3.3 Crystals from tophi of gout patients are coated in DNA
Needle aspiration of a tophus stained with PI (red). Images were taken with a confocal microscope, using reflected light to image crystals. Upper panel – single z section. Lower panels - maximum intensity projection of z stack. Scale bar = 20 μm. Representative of six individual patients.

Immunofluorescence staining revealed colocalization of NE, MPO and DNA (Figure 3.4). There was a degree of low level non-specific staining in the omitted primary control but in a pattern distinct from that seen with primary antibodies. The non-specific binding was associated with dense clumps of crystals. Unfortunately, a number of strategies failed to reduce background staining including using goat serum (same as the source of secondary antibodies) in addition to bovine serum albumin prior to antibody staining and increasing the duration and number of washes. In keeping with previous observations (Dalbeth et al., 2010), there were few intact neutrophils in the tophaceous material. These finding

implicate NETosis as part of the pathophysiological response to MSU crystals. This data provides important surrogate evidence that these ex vivo samples demonstrate neutrophil derived-DNA, but does not exclude that some of the DNA is derived from other cell types.

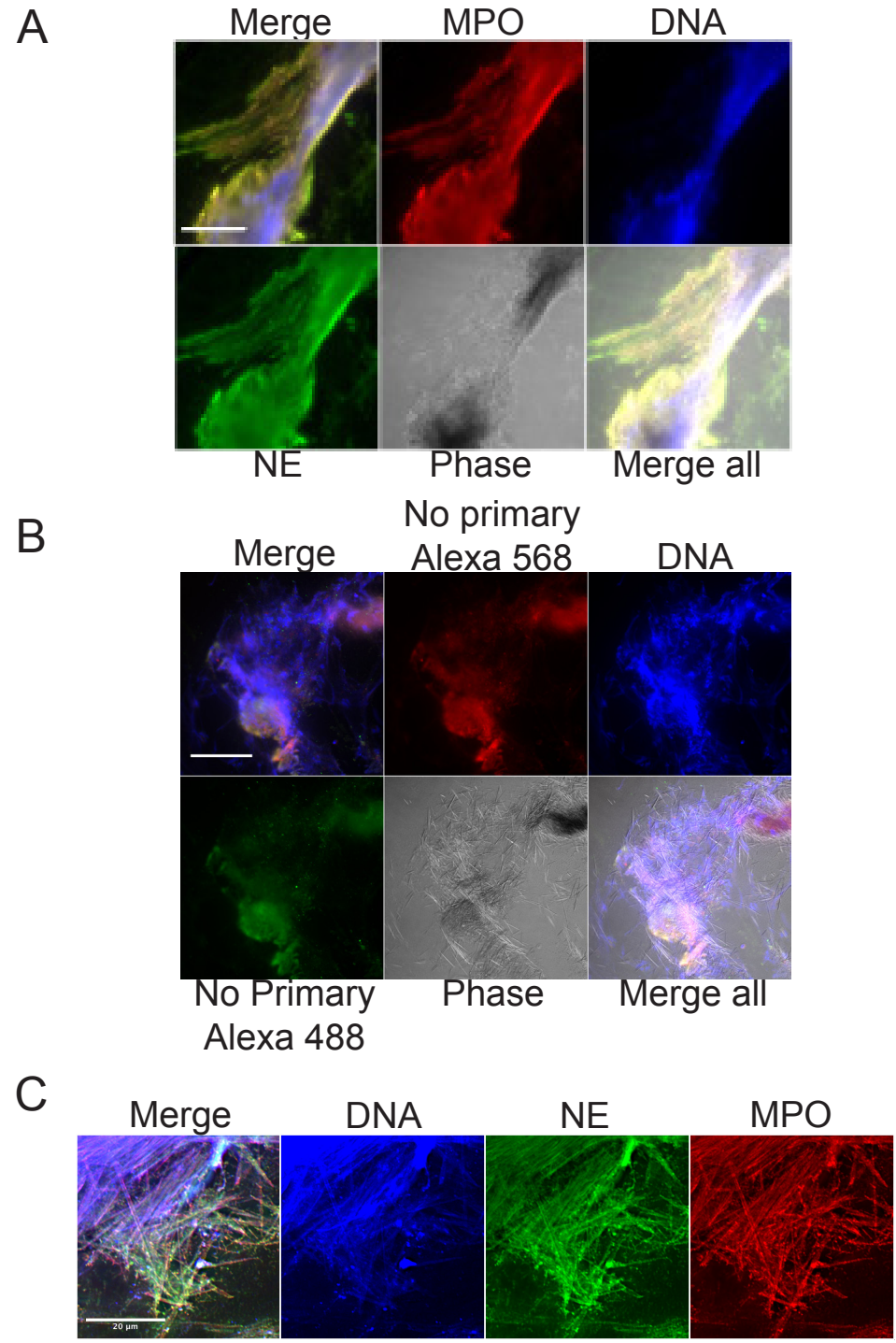


Figure 3.4 Immunofluorescence staining of tophus reveals the presence of neutrophil granule proteins and DNA

Immunofluorescence of an aspirate of a tophus. Samples stained for MPO (red), NE (green), and DNA staining with DAPI (blue). Crystals imaged with phase contrast. All steps were performed with urate-saturated PBS to prevent dissolution of the crystals. A) Scale bar represents 20 µm. B) Images from staining with the primary antibody omitted. C) Higher power image. Scale bar represents 20 µm. Representative of 3 separate experiments.

To support this finding and reduce the likelihood of artefacts created by needle aspiration, sections of paraffin-embedded surgically removed tophi were stained for MPO, with staining evident for crystal containing areas that are devoid of intact cells (Figure 3.5).

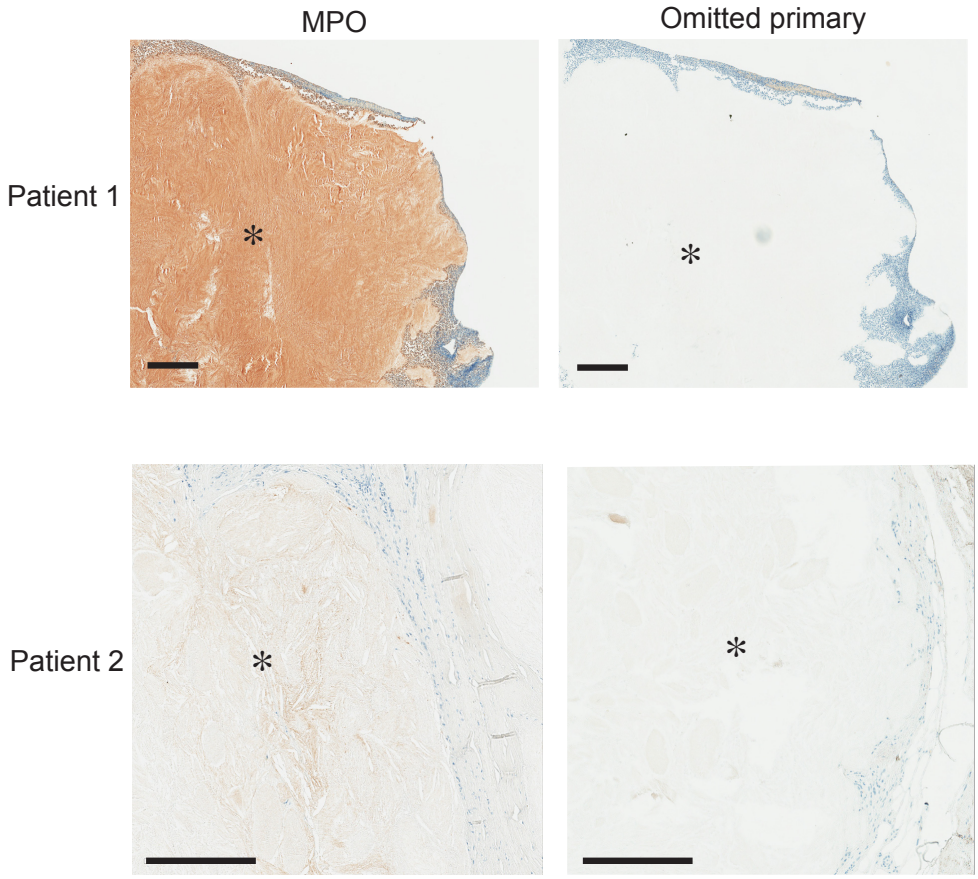


Figure 3.5 Immunohistochemistry staining for MPO in surgically removed tophi
Sections of paraffin embedded surgically removed tophi stained for MPO or with the primary antibody omitted with haematoxylin counterstaining to highlight nuclei. Two patients of seven analysed are demonstrated. An asterisk highlights the crystal-containing core of the tophus. Scale bar represents 300 μm

3.2.2 Live cell imaging of human neutrophils demonstrates stimulus-dependent kinetics of NETosis

To further examine neutrophil responses to MSU and other stimuli, we established a novel quantitative, live cell time-lapse imaging assay as described in Chapter 2. Briefly, Cell Tracker Green (CTG) quantifies live cells. Simultaneous PI DNA staining, which

only occurs after cell death, allows assessment of chromatin condensation (Figure 3.6 and Supplementary Movie S1 - file attached and described in the Appendix).

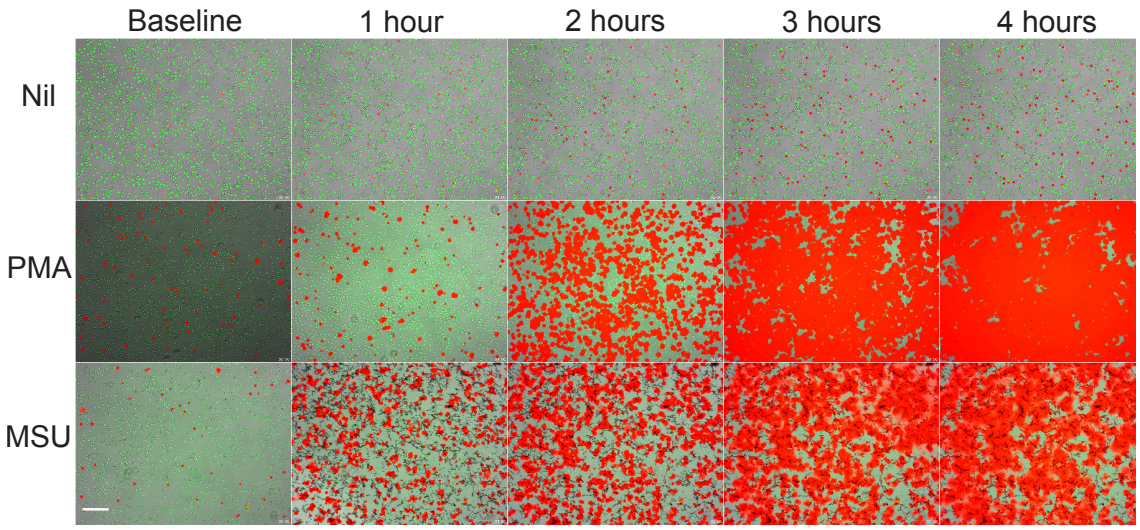


Figure 3.6 Montage of time-lapse live cell imaging of NETosis
Time-lapse imaging of PMA- and MSU-induced NETosis. Neutrophils were labeled with Cell Tracker Green (CTG, green) and PI (red) was added to the media. Fluorescent and phase contrast images were taken 15 minutely after stimulation. Montage of representative time-points as indicated. See supplementary Video 1. Scale bar represents 100 μm.

By subtracting the CTG positive (i.e. live cells) and high intensity, low diameter PI cells (i.e. dead cells not undergoing NETosis) from the initial total cell count, those cells undergoing NETosis can be quantified (Figure 3.7).

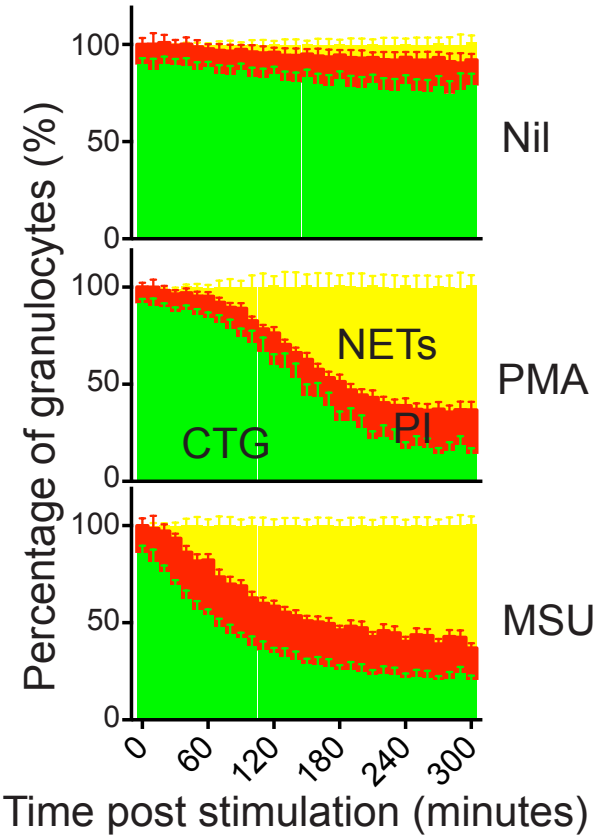


Figure 3.7 Computerized quantification of live cell imaging assay of NETosis
Computerized quantification of live-cell imaging cell counts presented as cumulative bar graphs. Green – percentage of CTG positive live cells. Red – PI positive dead cells with condensed nuclei. Yellow – calculated cells that had undergone NETosis. Data represent mean ± SEM, n=14. Cell counts per field between 700-1000.

PMA induced NETosis after a latent period of an hour. In contrast, MSU crystals induced more rapid NET release, with little latency as highlighted by the first derivative curve demonstrating rate of NETosis over time. Of note, unstimulated cells undergo minimal NETosis (Figure 3.8).

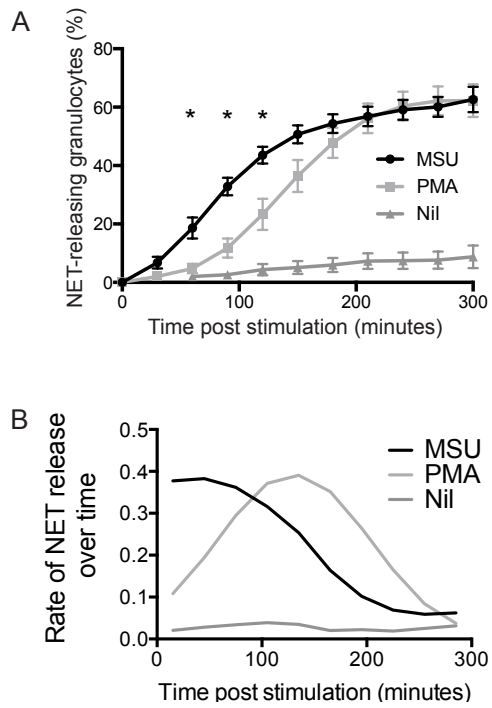


Figure 3.8 MSU crystals induce NETs more rapidly than PMA
A) MSU crystals induce NETosis more rapidly than PMA. Data represent mean ± SEM, n = 14. *P <0.01 at time-points 30 minutes, 60 minutes and 90 minutes post stimulation. B) First derivative curve calculated from the data in A) demonstrating the rate of NETosis changing over time

The individual curves for each stimulus demonstrate significant variability in NETosis rates between individuals (Figure 3.9).

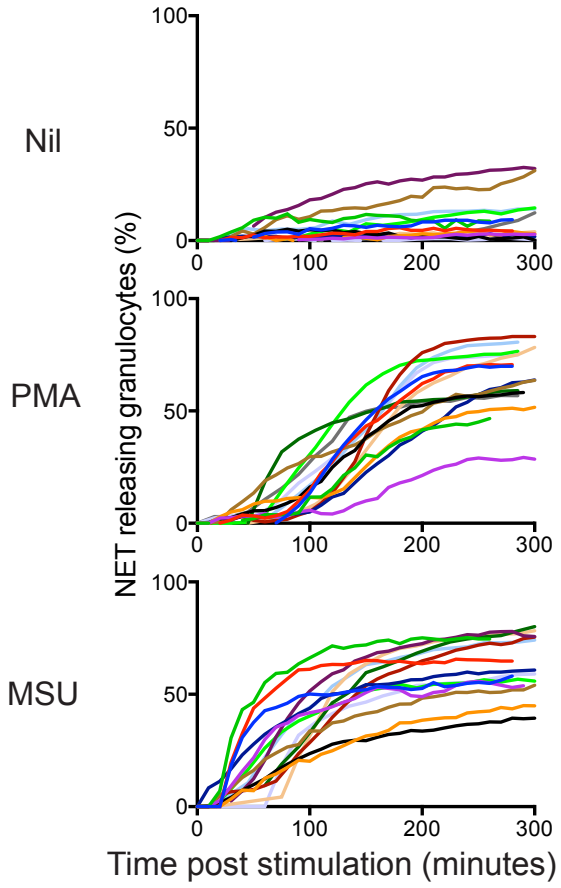


Figure 3.9 Individual curves from NETosis time-lapse experiments
Individual time-lapse quantification of NETosis data from the summary curve in Figure 3.8. n = 14

The frequency, but not the kinetics, of NETosis varied with the stimulus concentration (Figure 3.10).

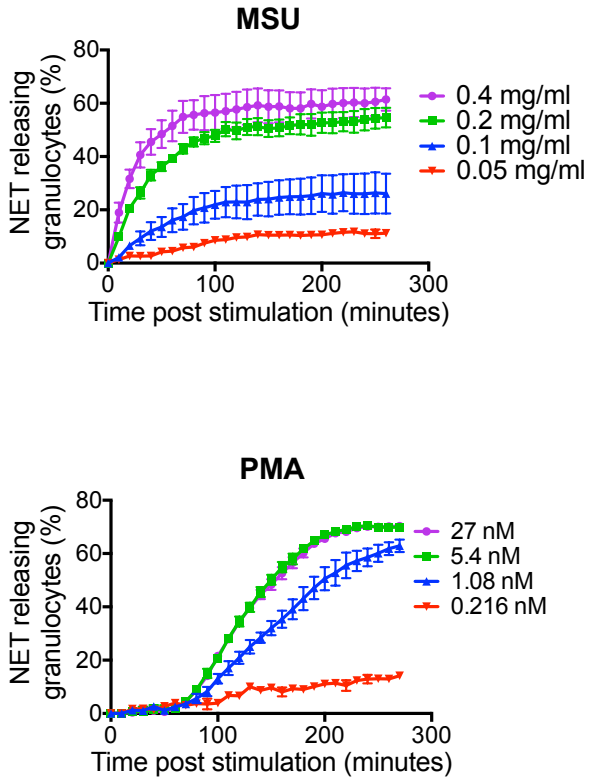


Figure 3.10 PMA and MSU NETosis are dose-dependent
Live cell imaging time-lapse curves of NETosis for different doses of PMA and MSU. n = 4.

Live cell experiments also showed a different sequence of DNA decondensation and cell death between these stimuli. Staining with cell-permeable Hoechst 33342 (red) to label the nucleus within live cells clearly demonstrated chromatin decondensation before death (indicated by PI positive, green) in response to PMA. In contrast, DNA decondensation only occurred after death with MSU (Figure 3.11 and Supplementary Video 2 file attached and described in the Appendix).

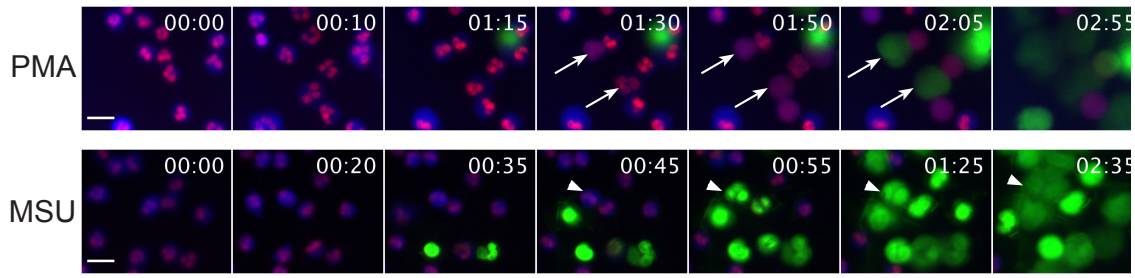


Figure 3.11 Time-lapse demonstrates the timing of nuclear decondensation relative to cell death
Time-lapse montage demonstrating nuclear decondensation changes relative to time of cell death (Red – Hoechst 33342 cell-permeable DNA dye, Blue – CTG, Green – PI). Time-points demonstrate the phases of NETosis. PMA - Arrows point to viable neutrophils (PI negative) with decondensed nuclei that progress to cell death. MSU – arrowhead demonstrates a neutrophil undergoing cell death prior to nuclear decondensation. Scale bar represents 10 μm. Times as indicated hh:mm. Representative of three independent experiments.

3.2.3 Crystal-induced NETosis is NADPH-oxidase independent

We next sought to determine whether MSU-induced NETosis was dependent on NADPH-oxidase function by treating healthy control neutrophils with the NADPH oxidase inhibitor diphenylene iodonium (DPI) prior to stimulation and comparing their response to the neutrophils from a patient with Chronic Granulomatous Disease (CGD) with genetic deficiency of NADPH oxidase function (Figure 3.12). PMA-induced and fungal-induced NETosis is dependent on NADPH oxidase function (Bianchi et al., 2009; Fuchs et al., 2007). In keeping with these previous reports, DPI significantly inhibited PMA- and *Candida*-induced NETosis (Figure 3.12A). In contrast, three chemically distinct crystals (MSU, CPPD and silica) induced NETosis despite treatment with DPI (Figure 3.12A). DPI profoundly inhibited luminol-enhanced chemiluminescence induced by PMA, *Candida*, MSU and CPPD crystals, indicating suppression of ROS production (Figure 3.12B). However, silica crystals did not induce significant ROS despite adequate phagocytosis.

Neutrophils isolated from a CGD patient did not produce ROS with any of the stimuli tested, as expected (Figure 3.12B) and did not undergo NETosis with PMA or *Candida*. However, when stimulated with crystals, CGD neutrophils underwent NETosis with comparable kinetics to healthy controls (Figure 3.12A).

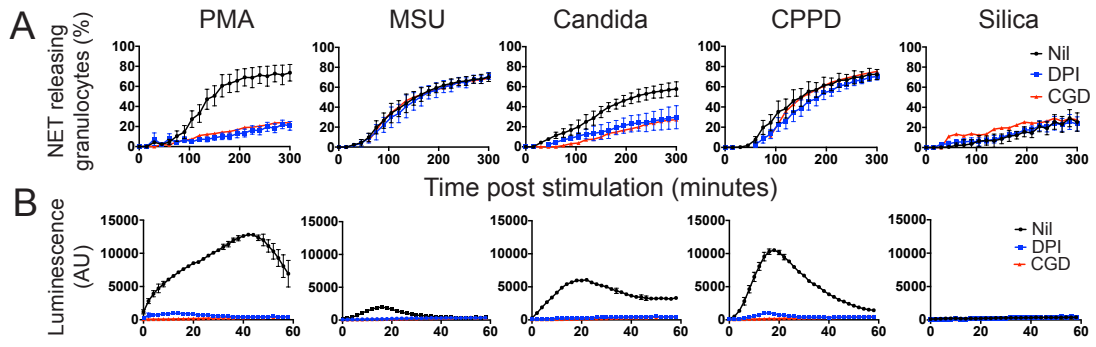


Figure 3.12 NADPH oxidase function is required for PMA- and *Candida*-induced NETosis but not Required for Crystal-induced NETosis
(A) Quantitative time-lapse live cell imaging demonstrates reduced PMA- and *Candida*-induced NETosis in DPI treated healthy control neutrophils and neutrophils from a CGD patient but no difference in crystal- (MSU, CPPD, and Silica) induced NETosis. Values represent mean ± SEM. n = 3-7, CGD patient n = 1. Significant difference between untreated and DPI treated neutrophils for PMA ($P<0.01$) and *Candida* ($P<0.05$) as assessed by two way ANOVA with repeated measures. (B) Luminol-enhanced chemiluminescence is induced by PMA, *Candida*, CPPD and MSU crystals but not by silica crystals and this is inhibited by DPI treatment and absent in CGD patient neutrophils. Representative curves from three separate experiments with inhibitor, data from a single experiment with a CGD patient. Values represent mean ± SEM from three technical replicates of a single donor.

The live cell data were supported by the findings of fixed cell imaging, which demonstrated colocalized staining of DNA, NE and MPO – consistent with NETosis (Figure 3.13).

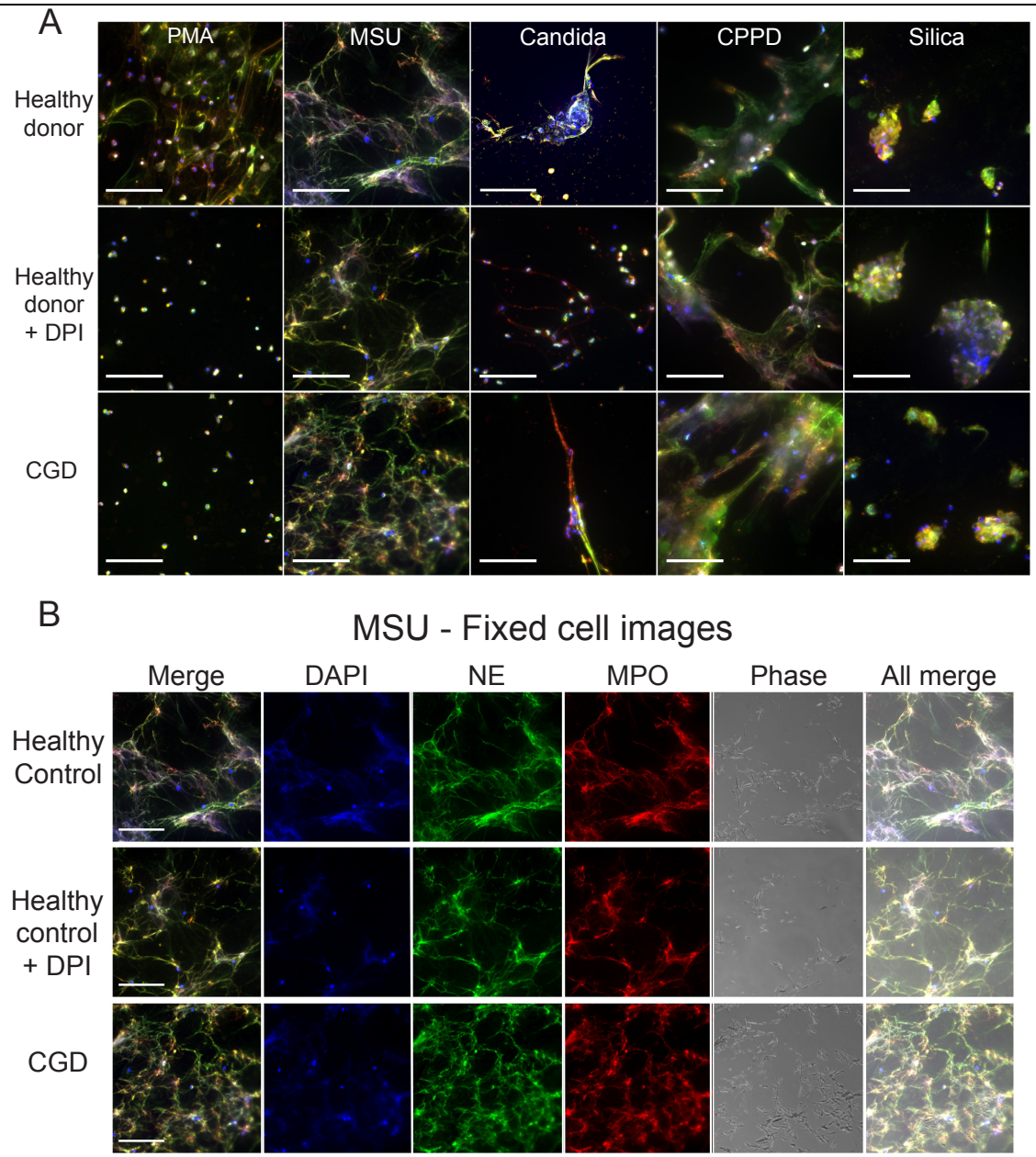


Figure 3.13 Fixed cell immunofluorescence imaging of neutrophils treated with different stimuli

A) Fixed cell immunofluorescent images of stimulated neutrophils from healthy controls with or without DPI and CGD patient neutrophils. Images are maximum intensity projections of z stacks. Scale bar represents 100 µm. Merge of DAPI (blue), NE (Green) and MPO (Red). Representative of three biologic replicates. B) Example of individual fluorescent channels and phase contrast images corresponding to the fluorescent merged images in the MSU (0.2 mg/ml) treated neutrophils in Figure 3C. Fluorescent channel merge (Merge), DNA stain (DAPI), Neutrophil Elastase (NE), myeloperoxidase (MPO), phase contrast (phase) and merge including phase contrast (All merge). Scale bar represents 100 µm.

Inhibition of NETosis in response to PMA and *Candida* was due to inhibition of cell death (Figure 3.14) without chromatin decondensation.

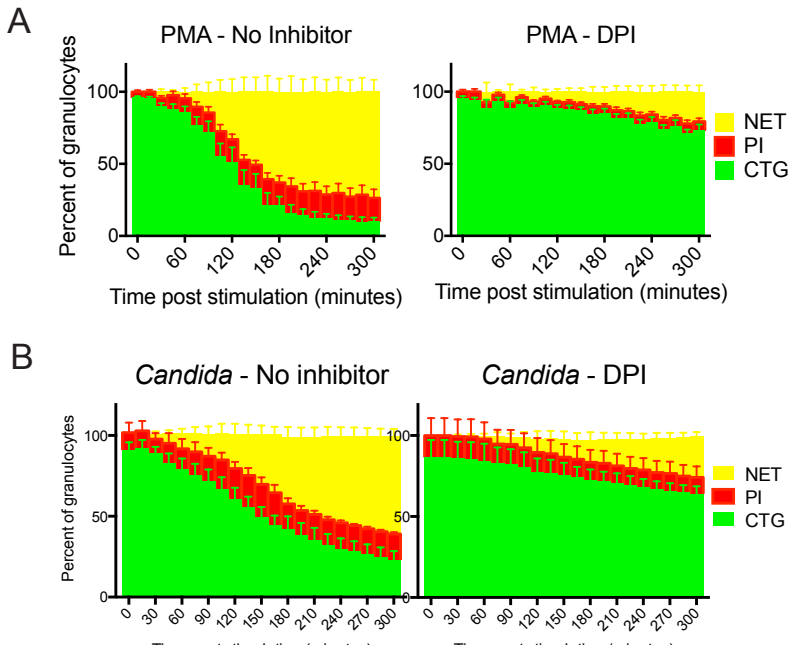


Figure 3.14 DPI treatment reduces NETosis through reducing cell death
(A) Quantitative time-lapse live cell imaging demonstrates reduced PMA-induced NETosis and cell death in neutrophils treated with DPI 10 μM. Green −CTG. Red − PI. Yellow − cells that had undergone NETosis. Values represent mean ± SEM, n = 7. B) Corresponding data for neutrophils stimulated with *Candida* hyphae. Values represent mean ± SEM, n = 3.

There have been concerns raised about potential toxicity and off target effects of DPI (Bauernfeind et al., 2011) however during the NETosis experiments no excess cell death was observed in unstimulated neutrophils treated with DPI (Figure 3.15).

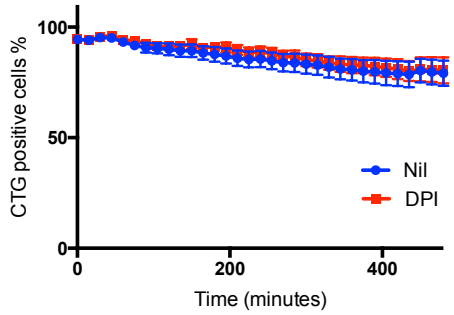


Figure 3.15 DPI does not increase cell death over 8 hours
Quantitative time-lapse live cell imaging demonstrates no difference in neutrophil survival with or without 10 μM. Values represent mean ± SEM. n = 7

Repeating the experiments using Pyrocatechol, a ROS scavenger (Harbort et al., 2015), demonstrated dose-dependent reduction of PMA-induced NETosis, but no effect on MSU-induced NETosis (Figure 3.16).

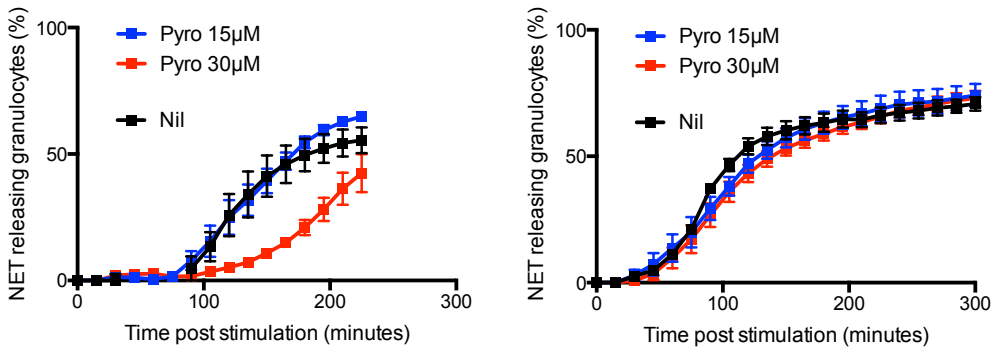


Figure 3.16 The ROS scavenger, Pyrocatechol, inhibits PMA- but not MSU-induced NETosis
Quantitative time-lapse live cell imaging demonstrates reduced PMA- but not MSU-induced NETosis in Pyrocatechol (Pyro) treated healthy control neutrophils at concentrations indicated. Values represent mean ± SEM. n = 3, Significant difference between untreated and Pyrocatechol-treated neutrophils for PMA ($P<0.01$) as assessed by two way ANOVA with repeated measures.

Of note, treatment with MitoTEMPO, a scavenger of mitochondrial rather than NADPH oxidase ROS, did not alter either PMA- or MSU-induced NETosis (Figure 3.17).

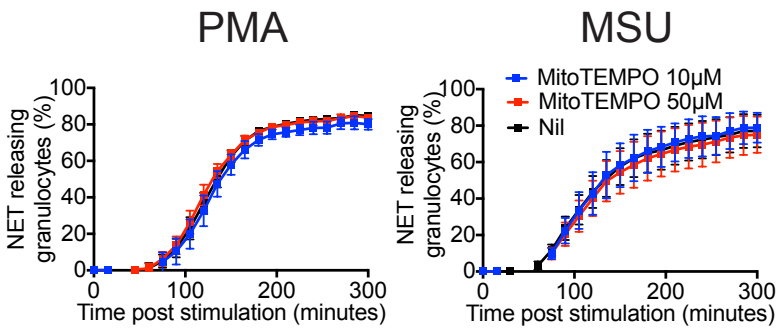


Figure 3.17 MitoTEMPO, mitochondrial ROS scavenger does not effect NETosis induced by either PMA or MSU
Quantitative time-lapse live cell imaging demonstrates no reduction in PMA- or MSU-induced NETosis in MitoTEMPO treated healthy control neutrophils at concentrations indicated. Values represent mean ± SEM. n = 3

Serum inhibits PMA-induced NETosis and cell death (Fuchs et al., 2007), (Figure 3.18), but had no effect on MSU-induced NETosis, further distinguishing the two pathways. Heat-inactivating the serum led to a non-significant reduction in MSU NETosis, but inhibited PMA-induced NETosis.

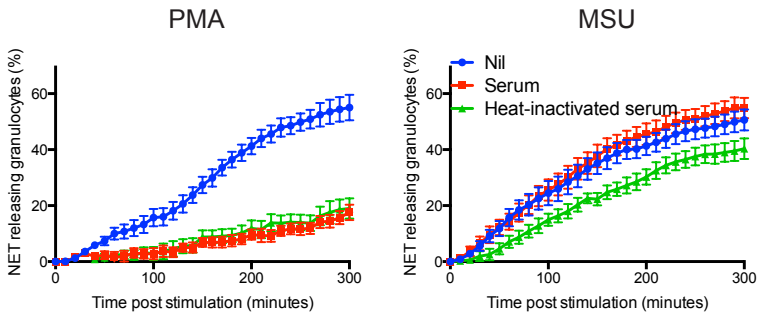


Figure 3.18 Autologous serum inhibits PMA- but not MSU- induced NETosis
Quantitative time-lapse live cell imaging of PMA- and MSU-induced NETosis in the presence or absence of 10% autologous human serum with or without heat-inactivation. Values represent mean ± SEM, n = 5. Significant difference between untreated and serum-treated neutrophils for PMA ($p<0.01$) but not MSU as assessed by two way ANOVA with repeated measures.

Of note, latex beads (3 to 15µm in diameter) opsonized with serum failed to induce NET release, despite efficient phagocytosis (Figure 3.19), suggesting the nature of the particle is important rather than phagocytosis itself.

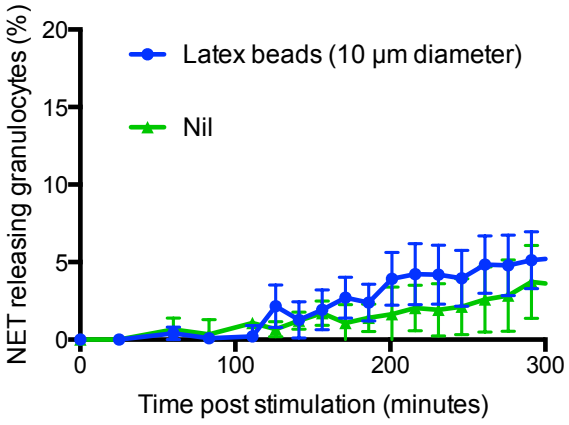


Figure 3.19 Latex beads do not induce NETosis
Time-lapse live cell imaging analysis of neutrophils stimulated with latex beads (10µm diameter) opsonised in serum at 10 beads per neutrophil concentration. Values represent mean ± SEM, n = 3

Histone degradation mediated by NE leads to chromatin decondensation in PMA-induced NETosis (Papayannopoulos et al., 2010). Protein extracts from PMA- and MSU-treated neutrophils at various time-points were therefore probed for histone proteins (Figure 3.20). Signal corresponding to full length Histone 3 (~18kDa, arrow) reduced with both stimuli over a four-hour time course, while a lower molecular weight band (~12 kDa, arrowhead) appeared, consistent with degradation. The amount of another core histone, Histone 4, also decreased. Treatment with DPI prevented PMA-induced histone degradation, but not that induced by MSU. Of note, actin commonly used as a loading control for experiments is also actively degraded during neutrophil cell death. A Ponceau stained membrane is provided demonstrating the loading.

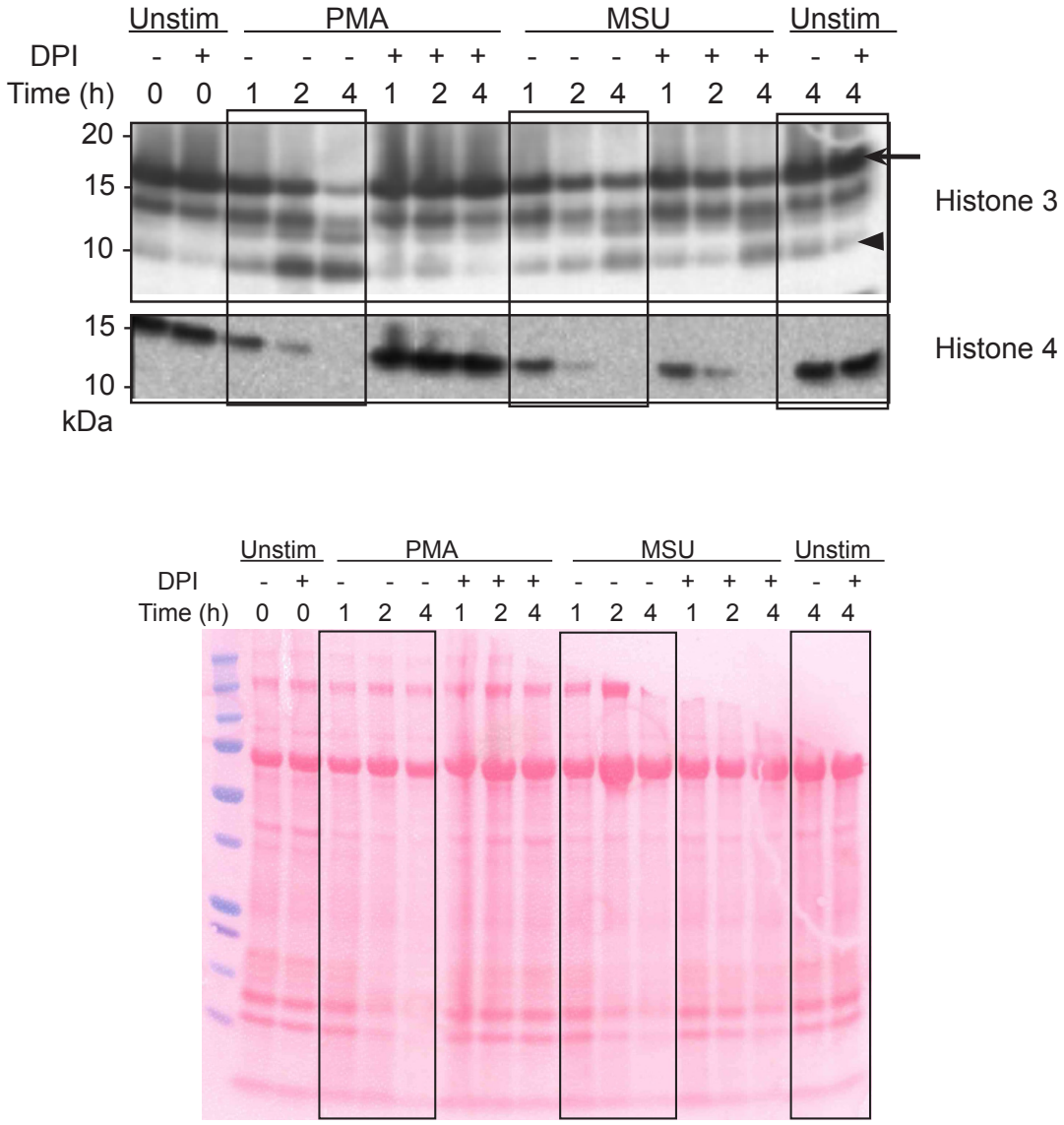


Figure 3.20 Western blotting for histones in lysates of PMA and MSU-treated neutrophils with and without DPI

Histone degradation occurs during PMA- and MSU-induced NETosis. DPI inhibits PMA but not MSU induced histone degradation. Western blot of lysates of neutrophils with and without DPI treatment following stimulation with PMA or MSU and unstimulated (Unstim) harvested at indicated time-points probed for Histone 3 and Histone 4. Arrow indicates expected full length Histone 3 and the arrowhead indicates a degradation product. Representative of three experiments from different donors.

3.2.4 Neutrophil Elastase mediates nuclear decondensation, but not cell death, in response to crystal and non-crystal stimuli

Treatment with NE inhibitor (NEi), GW311616a, significantly reduced NETosis in PMA- and *Candida*-treated neutrophils (Figure 3.21), but did not change the kinetics of cell death. Similarly, chromatin decondensation, but not cell death, was reduced in MSU-stimulated neutrophils in the presence of NEi, suggesting a common terminal pathway.

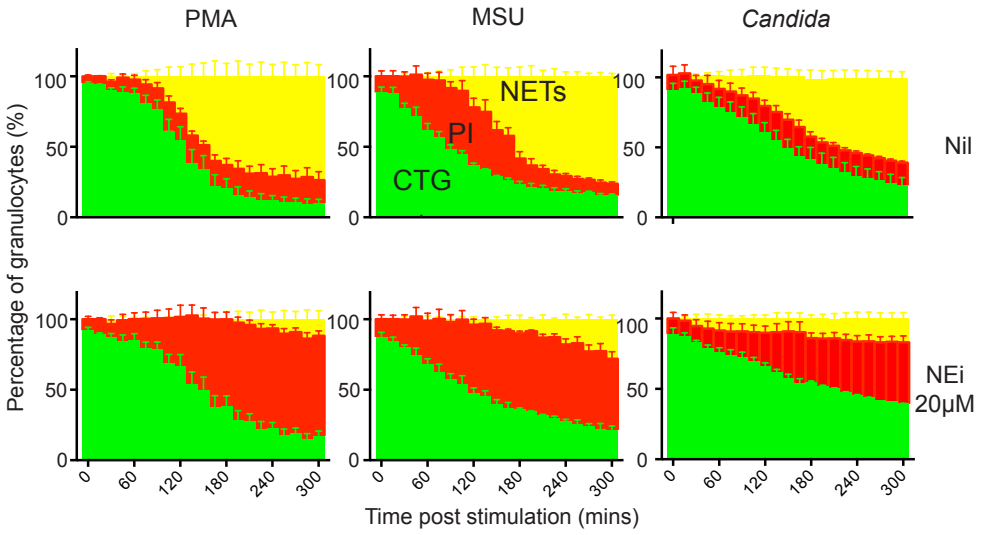


Figure 3.21 Neutrophil Elastase inhibitor reduces NETosis but does not change the kinetics of cell death
Quantitative time-lapse live cell imaging demonstrates reduced PMA, MSU-and *Candida*-induced NETosis in NE inhibitor (NEi 20 μM) treated healthy control neutrophils. Green – CTG. Red – PI. Yellow – cells that had undergone NETosis. Values represent mean ± SEM, n = 4 separate donors. Differences in NETosis percentage between untreated and NEi-treated neutrophils for PMA (P<0.01) and MSU (P<0.01) assessed with two way ANOVA with repeated measures.

PI stained nuclei of cells treated with NEi remained condensed (Figure 3.22), suggesting NEi inhibited chromatin decondensation, but not cell death induced by PMA.

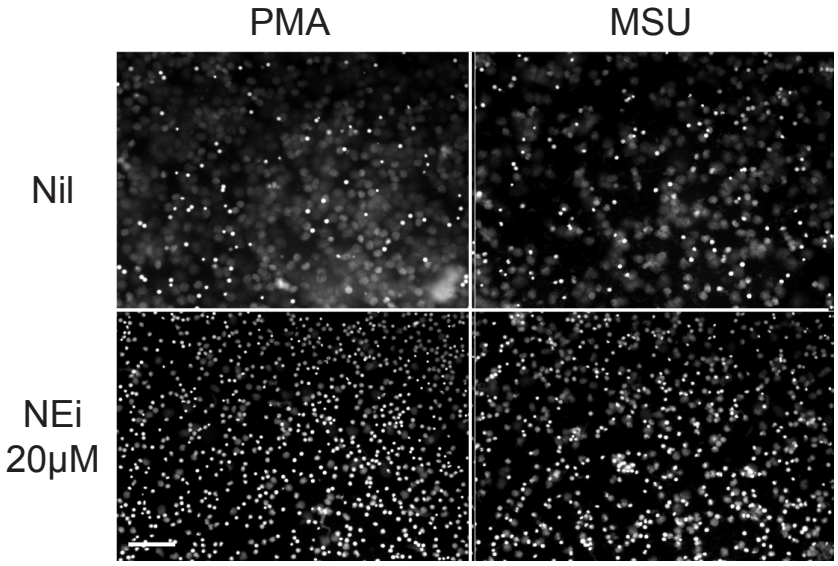


Figure 3.22 PI staining reveals NE inhibitor prevents nuclear decondensation during NETosis
Images taken from time-lapse at 240 minutes after stimulation with PMA or MSU in neutrophils treated with and without NEi (20 μM). PI staining of dead cell nuclei. Scale bar represents 100 μm.

Of note, NEi prevented Histone 3 and 4 degradation induced by both PMA and MSU (Figure 3.23).

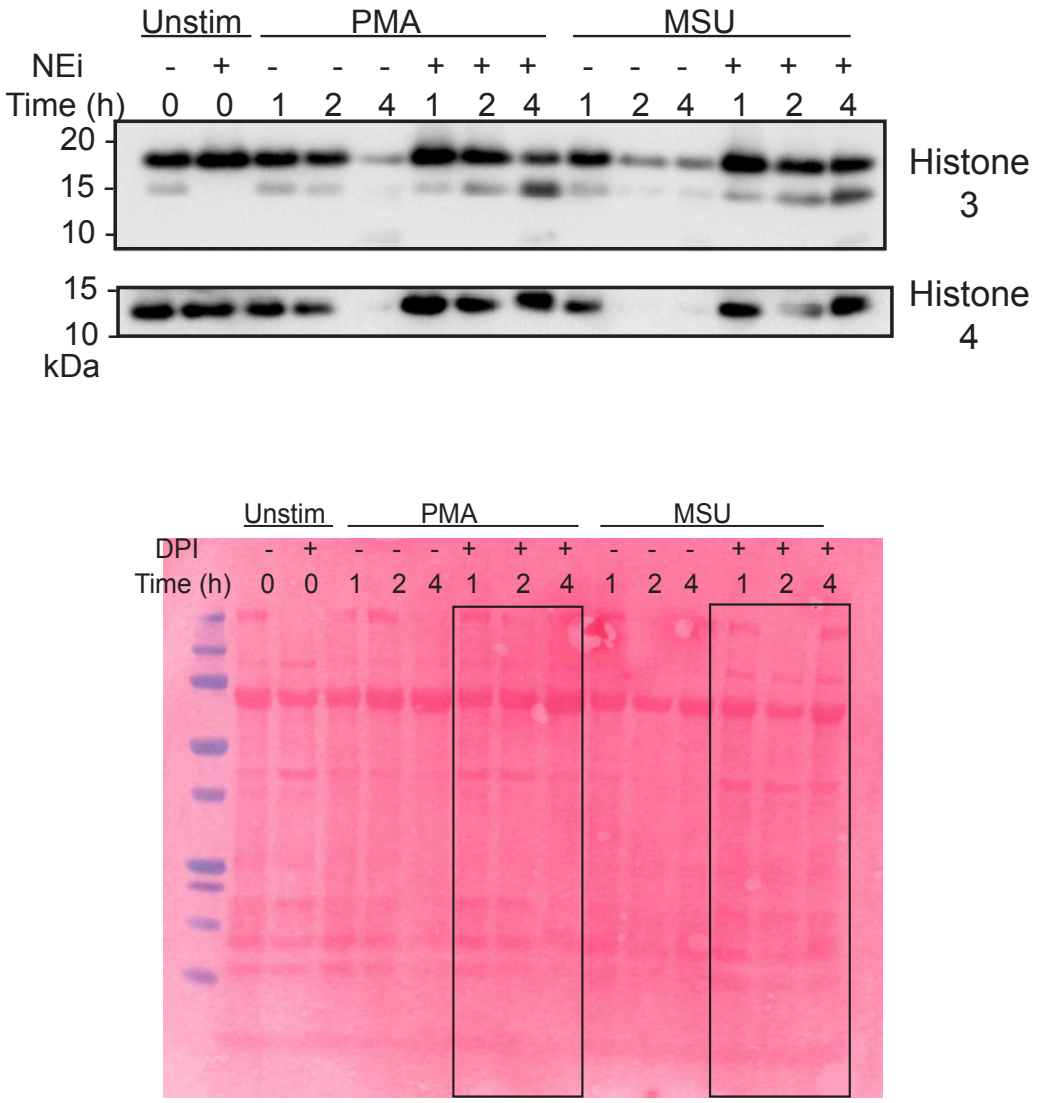


Figure 3.23 NE inhibitor prevents degradation of histones during NETosis
PMA- and MSU-induced histone degradation is inhibited by NE inhibitor (NEi). Western blots of lysates of neutrophils with and without DPI treatment following stimulation with PMA or MSU and unstimulated (Unstim) - harvested at indicated time-points and probed for Histone 3 and Histone 4. Representative of three independent experiments from separate donors.

NE is normally sequestered in the azurophilic granules of unstimulated neutrophils and during phagocytosis is delivered to the phagosome, where it interacts with the ingested particle (Nordenfelt & Tapper, 2011). When neutrophils attempt to phagocytose fungal hyphae, phagosome maturation fails and NE translocates to the nucleus in a ROS-dependent manner, leading to NETosis (Branzk et al., 2014). Given nuclear chromatin

decondensation occurred post-mortem with MSU, we assessed the dynamics of NE translocation during NETosis. NE was labelled before and after Triton-X100 permeabilization, using different fluorescent detection secondary antibodies, allowing membrane impermeability to provide a surrogate for cell viability (Figure 3.24). Extracellular NE in NETs was accessible to staining prior to permeabilization, but intact unstimulated cells only stained for NE after Triton and the NE remained separate from the nucleus.

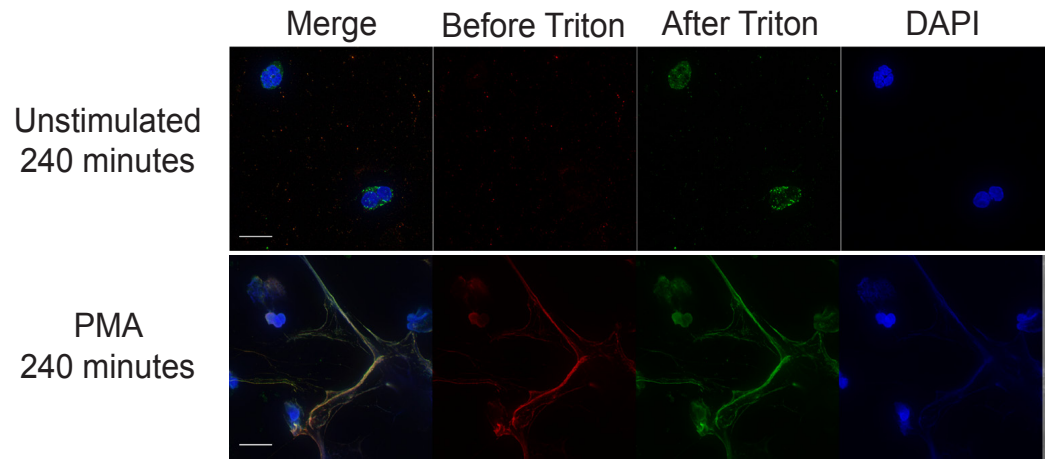


Figure 3.24 Immunofluorescence staining of neutrophils and relationship to cell permeability
NE-stained neutrophils and relationship to cell permeability. Neutrophils were unstimulated or stimulated with PMA and were fixed at indicated time-points. NE staining was performed before and after triton permeabilization with DAPI staining for DNA. Scale bar represents 10 μm. Representative of three experiments from different donors.

Viable PMA-treated neutrophils exhibited NE translocation to condensed nuclei prior to NETosis (Figure 3.25, 120 minutes), as previously reported (Papayannopoulos et al., 2010), with evidence of chromatin decondensation in viable cells at later time-points (Figure 3.25, 180 minutes). This finding is consistent with NE-mediated chromatin decondensation prior to cell death, as demonstrated with live-cell imaging (Figure 3.11 Time-lapse demonstrates the timing of nuclear decondensation relative to cell death).

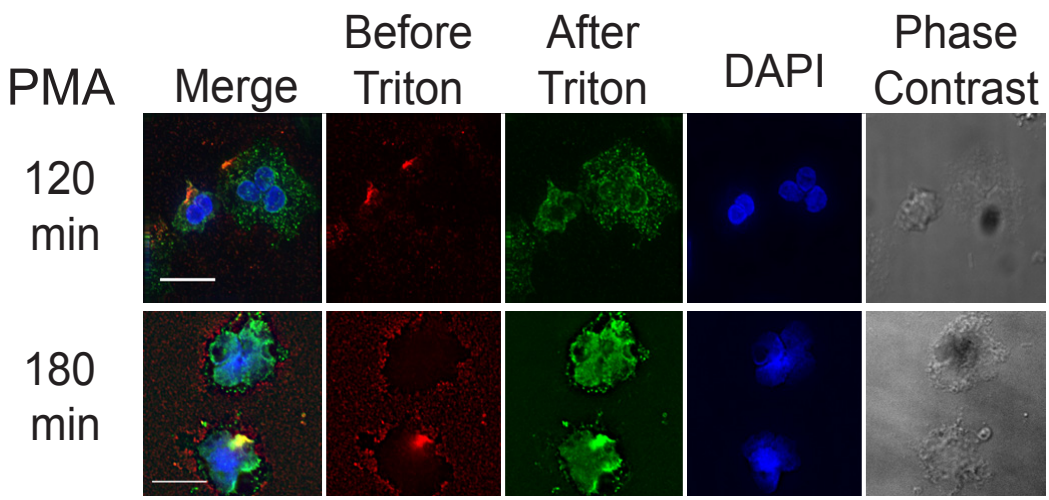


Figure 3.25 Neutrophil elastase translocates to the nucleus prior to cell permeability during PMA NETosis
NE-stained neutrophils and relationship to cell permeability. Neutrophils were stimulated with PMA and were fixed at indicated time-points. NE staining was performed before and after triton permeabilization with DAPI staining for DNA. Scale bar represents 10 μm. Representative of three experiments from different donors.

In contrast, in MSU-stimulated neutrophils, NE nuclear translocation was evident at earlier time-points (Figure 3.26, 30 minutes). NE translocation in condensed nuclei was seen in both viable and dead cells (Figure 3.26, 60 minutes), but no examples of viable neutrophils with decondensed chromatin were observed. These findings suggest that during MSU-induced NETosis, NE translocates either immediately before or after cell death and chromatin decondensation occurs after death.

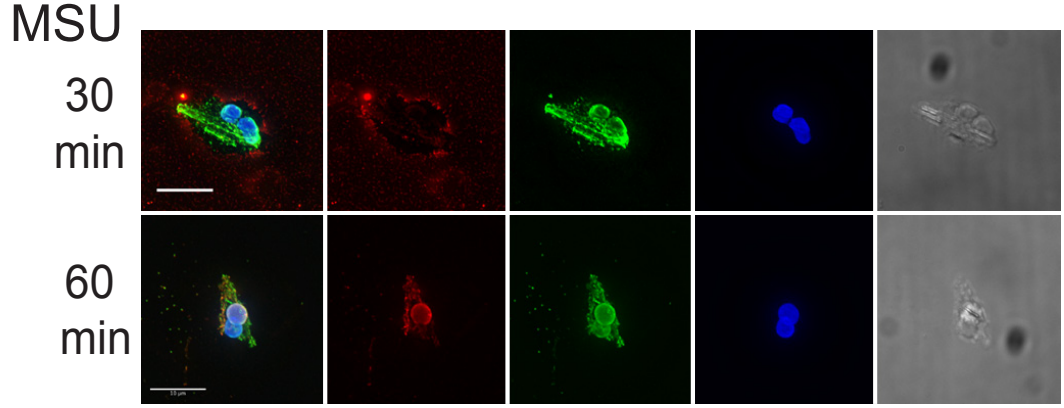


Figure 3.26 NET translocates to the nucleus either shortly before or after cell permeabilization during MSU NETosis
NE-stained neutrophils and relationship to cell permeability. Neutrophils were stimulated with MSU and were fixed at indicated time-points. NE staining was performed before and after triton permeabilization with DAPI staining for DNA. Scale bar represents 10 µm. Representative of three experiments with different donors.

At earlier time points, MSU-stimulated neutrophils demonstrated phagosome maturation, assessed by staining with the azurophil granule marker, CD63 and NE around the ingested crystal (Figure 3.27, arrow indicates crystal position). DQ ovalbumin is a self-quenching fluorescent protein conjugate that becomes fluorescent after proteolytic degradation (Hornung et al., 2008). DQ ovalbumin staining was consistent with proteolytic activity around the crystal (Figure 3.27).

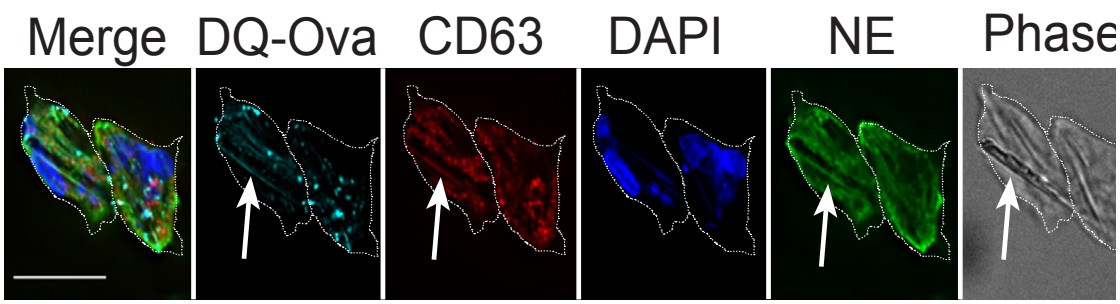


Figure 3.27 MSU-containing phagosomes undergo maturation
MSU-containing neutrophil phagosomes undergo maturation. MSU treated neutrophils that were incubated with DQ ovalbumin (cyan) were fixed at 15 minutes post stimulation. Immunostaining was performed for CD63 (red) and NE (green) and phase contrast microscopy was performed. Representative of three independent experiments with different donors. Scale bar represents 10 μm.

Compounds that reduce acidification of lysosomal contents such as the vacuolar-type H+-ATPase inhibitor Bafilomycin A1 can disrupt phagosomal maturation and Nocodazole, a microtubule inhibitor that may disrupt intracellular trafficking of organelles. Neither of these inhibitors reduced MSU crystal-induced NETosis (Figure 3.28).

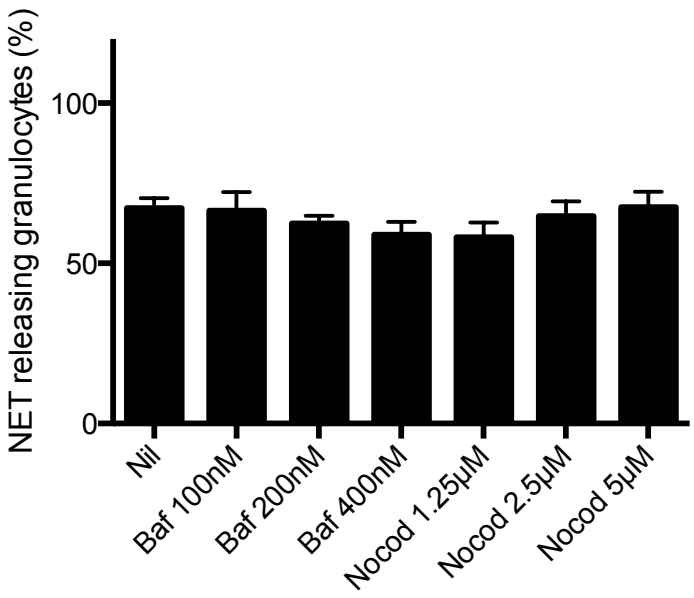


Figure 3.28 Bafilomycin A and Nocodazole do not inhibit MSU induced NETosis
NET release at 240 minutes from time-lapse imaging quantification. Neutrophils were incubated for 1 hour prior to stimulation with Bafilomycin A1 (Baf) and Nocodazole at the concentrations indicated. Values represent mean ± SEM, n = 3

On fixed cell imaging, there was still evidence of phagosomal maturation (i.e. phagosome labelling with CD63, NE and cleavage of DQ Ovalbumin) in the presence of these two agents (Figure 3.29), arguing against an effect on phagosome maturation. In neutrophils, phagosome maturation is accompanied by alkalinization rather than acidification (A. P. Levine et al., 2015), and ROS generation prevents accumulation of the vacuolar H+-ATPase on phagosome membranes (El Chemaly et al., 2014), perhaps accounting for the lack of efficacy of Bafilomycin A1. Whether microtubule function is required for neutrophil granule mobilization is also unclear, with earlier studies suggesting that it is not important (Pesanti & Axline, 1975).

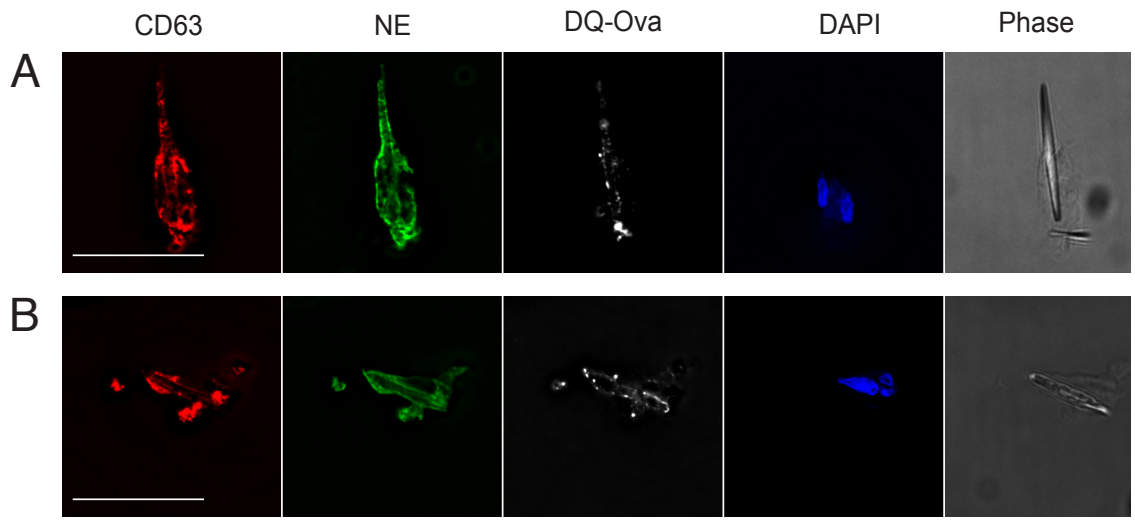


Figure 3.29 Bafilomycin and Nocodazole do not inhibit phagosome maturation
Neutrophils were incubated with DQ ovalbumin (cyan) and A) Bafilomycin A 400 nM or B) Nocodazole 5μM were fixed at 15 minutes post stimulation with MSU crystals (0.2 mg/ml). Immunostaining was performed for CD63 (red) and NE (green) and phase contrast microscopy was performed. Representative of two independent experiments with different donors. Scale bar represents 10 μm.

To further establish the sequence of events, a live cell strategy was used with DQ ovalbumin (Figure 3.30 Live cell imaging with DQ ovalbumin and Supplementary Videos 3 and 4 files attached and described in the Appendix). Stimulated cells accumulated DQ ovalbumin both in punctate structures and around phagocytosed crystals. Approximately ten minutes prior to cell death (time-point 01:48 - PMA) in PMA-treated neutrophils, DQ ovalbumin fluorescence changed to a diffuse, most likely nuclear distribution (indicated by arrows Figure 3.30). In contrast, MSU-treated cells showed no diffuse staining prior to death, with the DQ ovalbumin associated with the crystal until cell death. These findings suggest that proteolytic activity in PMA-treated neutrophils is not confined to the granules or lysosomes prior to death, enabling pre-morbid chromatin decondensation. On the other hand, MSU-treated neutrophils demonstrate proteolytic activity that is confined to phagosomes and translocates to the nucleus either immediately before or after cell death.

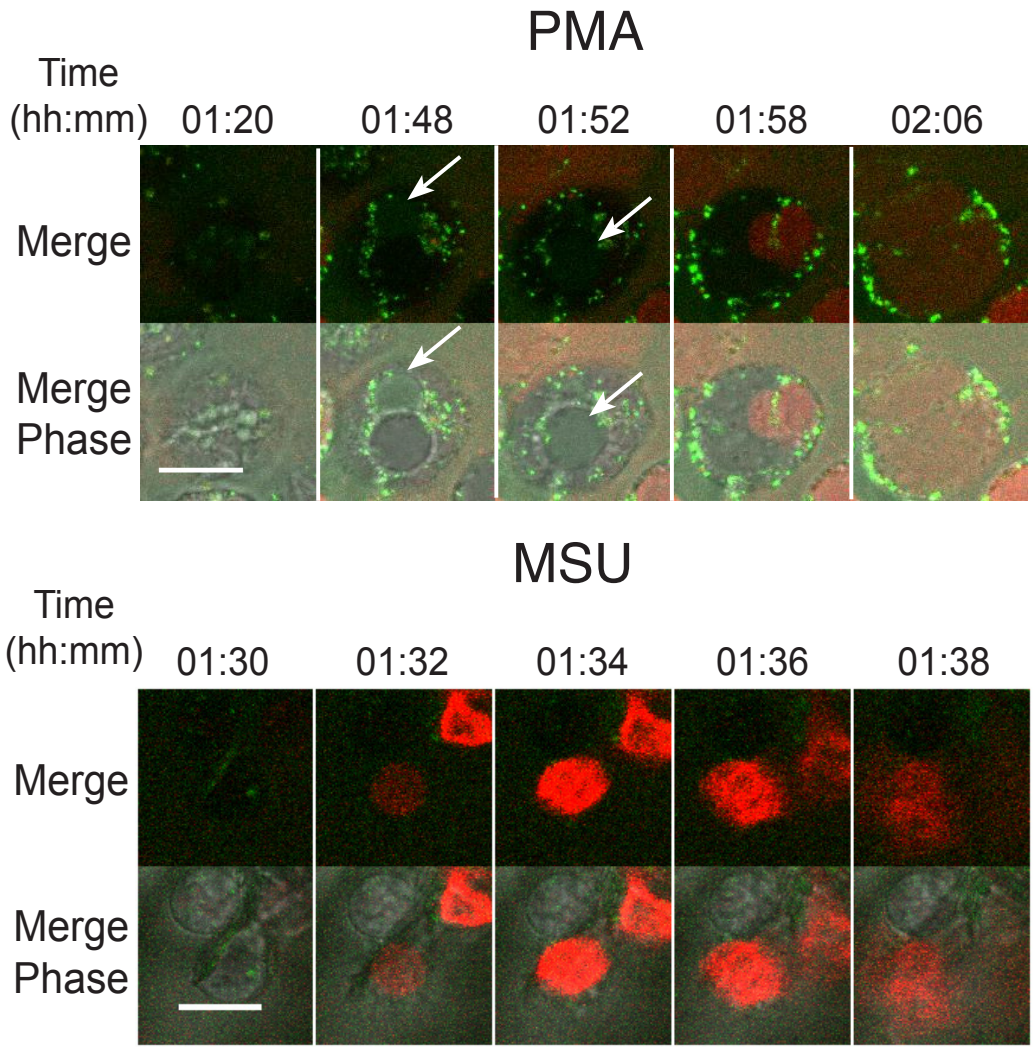


Figure 3.30 Live cell imaging with DQ ovalbumin
DQ ovalbumin signal becomes diffuse prior to cell death in PMA- but not MSU-treated neutrophils. Montage of time-lapse images taken every two minutes with confocal resonance scanner. DQ ovalbumin (green), PI (red) and phase contrast. Time-points as indicated leading up to and after cell death. Arrows highlight areas of diffuse DQ ovalbumin staining. See supplementary Video 3 (PMA) and 4 (MSU) files attached and described in the Appendix. Representative of three donors

3.2.5 Myeloperoxidase

Myeloperoxidase inhibition with 4-aminobenzoic acid hydrazide (ABAH) delayed PMA induced NETosis by slowing the kinetics of cell death. MPO had minimal effect on MSU induced NETosis (Figure 3.31). However, ABAH inhibition of MPO was incomplete, reflected by failure to completely suppress luminol-enhanced chemiluminescence in

comparison to DPI (Figure 3.31B). ABAH inhibited NETosis by inhibiting cell death in contrast to inhibition of NEi that does not alter cell death (Figure 3.31C).

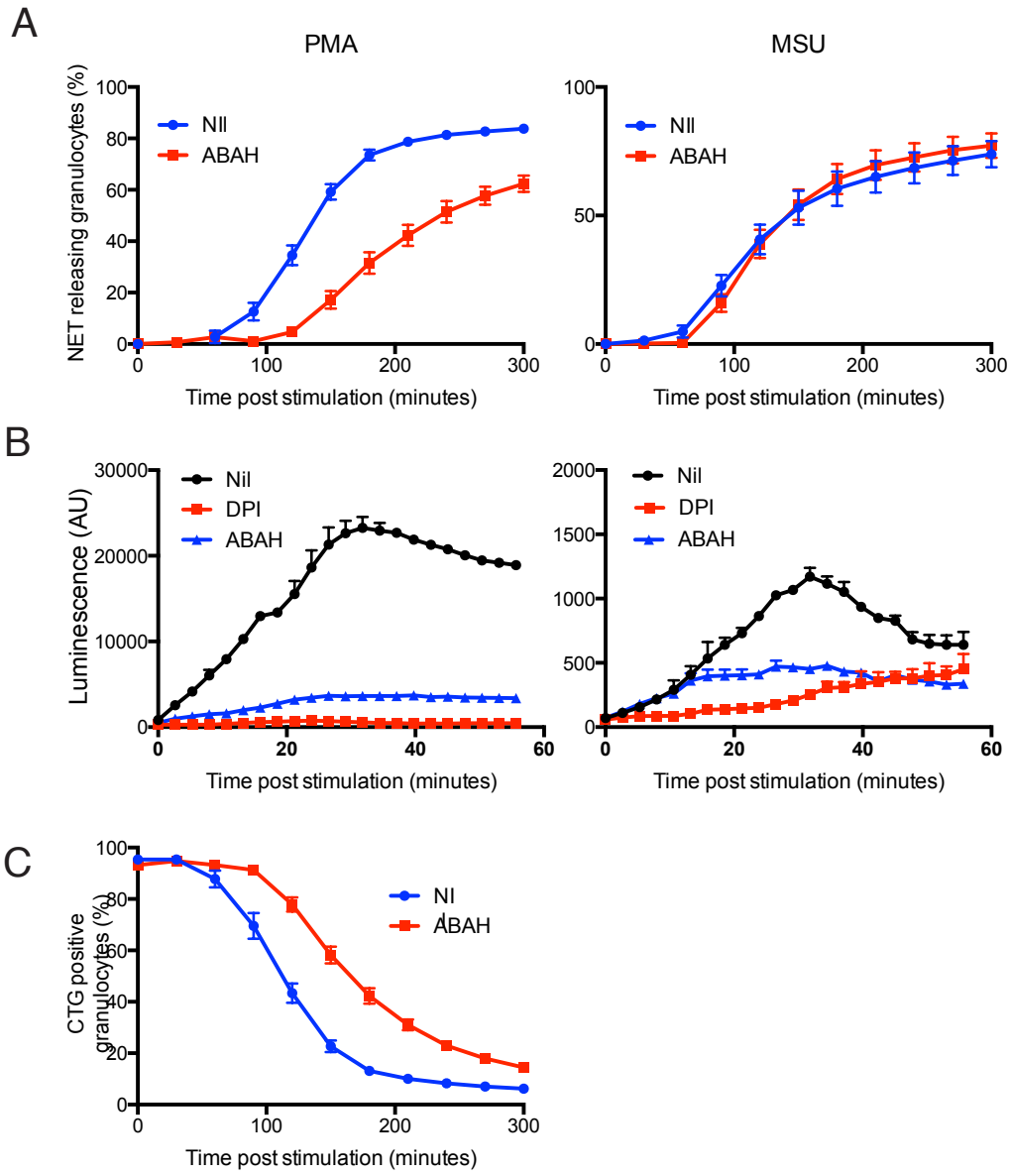


Figure 3.31 Inhibition of MPO with ABAH partially inhibits PMA NETosis but not MSU NETosis

A) Quantitative time-lapse live cell imaging demonstrates reduced PMA NETosis but not MSU induced NETosis in ABAH (200 μM) treated healthy control neutrophils. Values represent mean ± SEM, n = 4. Differences in NETosis percentage between untreated and NEi-treated neutrophils for PMA (*P*<0.01) assessed with two way ANOVA with repeated measures. B) ABAH inhibits PMA and MSU induced luminol-enhanced chemiluminescence but not as profoundly as DPI (10μM). C) ABAH inhibits PMA-induced cell death. From the same time-lapse data as A), demonstrating the percentage of CTG positive live cells.

During PMA NETosis, NE translocates to the nucleus early, but MPO becomes colocalized with DNA later in the course of NETosis (Papayannopoulos et al., 2010). MSU-treated neutrophils with evidence of nuclear NE also had MPO-staining of the nucleus, suggesting the two granule proteins translocated around the same time with MSU NETosis (Figure 3.32).

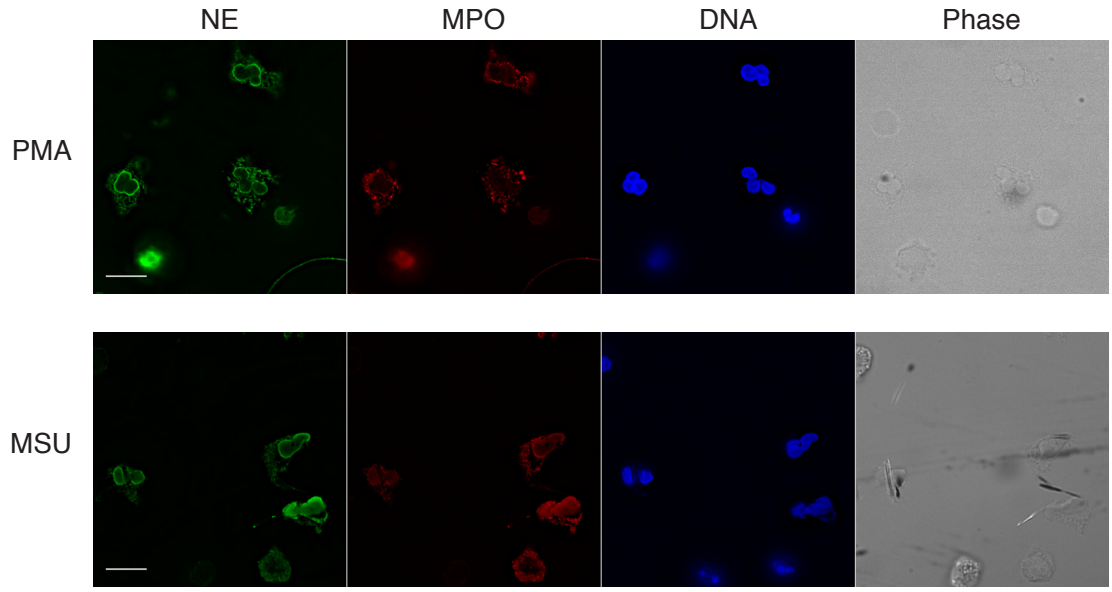


Figure 3.32 NE and MPO nuclear translocation with MSU and PMA stimulation
Neutrophils were stimulated with PMA (60 minutes) or MSU (30 minutes). Immunostaining was performed for MPO (red) and NE (green) and phase contrast microscopy was performed. Representative of two independent experiments with different donors. Scale bar represents 10 μm

3.2.6 Lysosomal detergent LLOme induces NETosis, but crystal-induced NETosis is not mediated by inflammasome activation

The involvement of phagosomes in MSU-induced NETosis parallels lysosome involvement in crystal-induced inflammasome activation in macrophages (Hornung et al., 2008). Previous electron microscopy studies have demonstrated that MSU crystals escape neutrophil phagosomes (Schumacher & Phelps, 1971). The lysosomal detergent, L-Leucyl-L-leucine methyl ester (LLOMe) can be used to chemically disrupt lysosomes in cells expressing the protease dipeptidyl peptidase I (McGuire et al., 1993). LLOme is cleaved by DPPI (also known as Cathepsin C). Once cleaved, it attains detergent-like properties resulting in membrane lysis. In the case of neutrophils,

this presumably occurs in neutrophil azurophil granules that contain DPPI, directly liberating their contents. This is an assumption and it remains unclear whether such granule membrane lysis would be sufficient to allow release of active proteases. Cationic neutrophil granule enzymes may be sequestered by the negatively charged proteoglycan, serglycin (Pham, 2006, 2008). Alkalinization of the granule contents as occurs in the maturing phagosome may also be important for the optimal activation of serine proteases.

We found that LLOMe induced NETosis in a dose-dependent fashion (Figure 3.33).

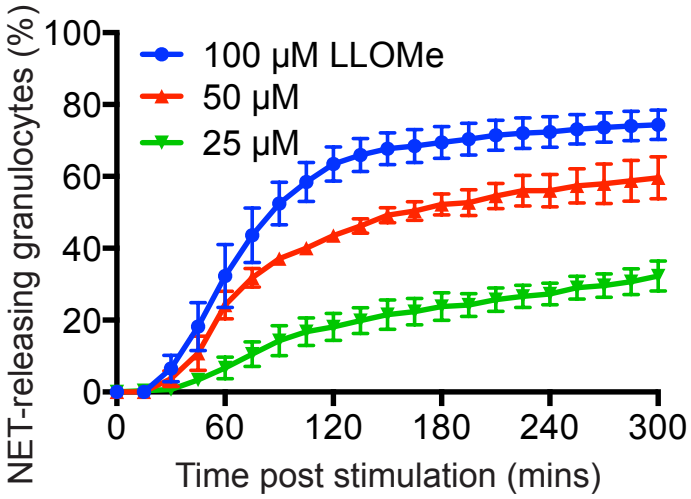


Figure 3.33 Leu-Leu-OMe induces NETosis in a dose dependent fashion
Leu-Leu-OMe (LLOMe) induces NETosis in a dose-dependent fashion. Time-lapse imaging data acquired as previously described. Values represent mean ± SEM, n = 6.

NE translocated to the nucleus within 15 minutes of Leu-Leu-OMe exposure (Figure 3.34).

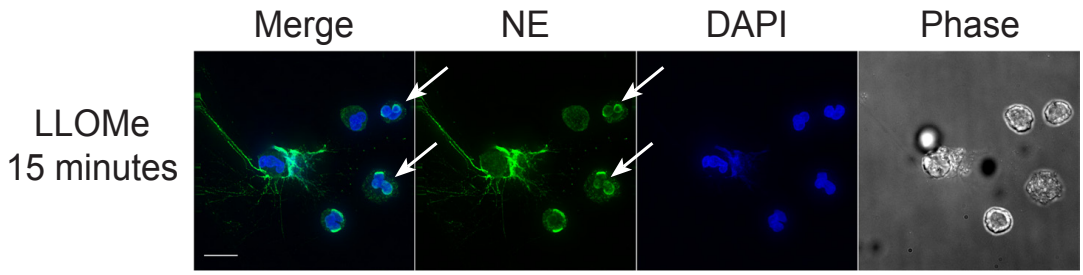


Figure 3.34 Leu-Leu-OMe induces NE nuclear translocation
NE-stained neutrophils. Neutrophils were stimulated with Leu-Leu-OMe (100 μM) and were fixed after 15 minutes. Cells were DAPI stained for DNA and phase contrast. Scale bar represents 10 μm. Representative of three experiments with different donors.

Despite involvement of lysosomes, MSU-induced NETosis was unaffected by multiple inhibitors of pathways implicated in the activation of the inflammasome and pyroptosis (Figure 3.35). However, Cytochalasin D, an inhibitor of actin polymerization, did inhibit MSU-induced NETosis. Of note, ZVAD-fmk despite profoundly inhibiting caspase-1 processing of IL-1 during inflammasome activation may not efficiently reduce caspase-1 induced cell death (Broz et al, 2010).

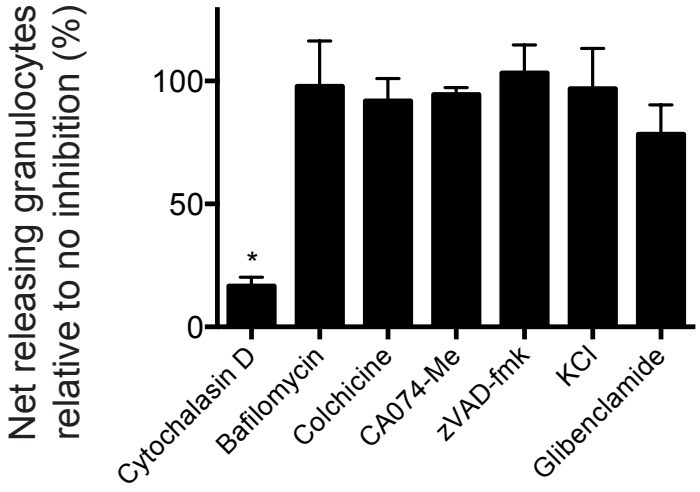


Figure 3.35 Inhibitors of inflammasome activation apart from Cytochalasin D do not inhibit MSU NETosis

Inhibitors of inflammasome activation do not inhibit NETosis but inhibition of actin polymerization does. Neutrophils were incubated with inhibitor for one hour prior to stimulation. Cytochalasin (10 μM), Bafilomycin A (100 nM), Colchicine (10 μM), CA074-Me (20 μM), zVAD-fmk (10 μM), KCl (45 mM) and Glibenclamide (50 μM). NET release at 240 minutes expressed as a percentage of the NET release in the absence of inhibitor from the matching experiment. Values represent mean ± SEM, n = 3-5. *p<0.05.

Latrunculin, an inhibitor of actin polymerization and two inhibitors of actin depolymerization (jasplakinolide and cucurbitacin (Figure 3.36)) also inhibited MSU-induced NETosis. Using other inhibitors also revealed likely roles for calcium flux (EDTA, EGTA and BAPTA-AM) and several tyrosine kinases in MSU-induced NETosis in keeping with previous reports on mediators of neutrophil crystal interactions (Ng et al., 2008; Popa-Nita & Naccache, 2010)(Figure 3.36).

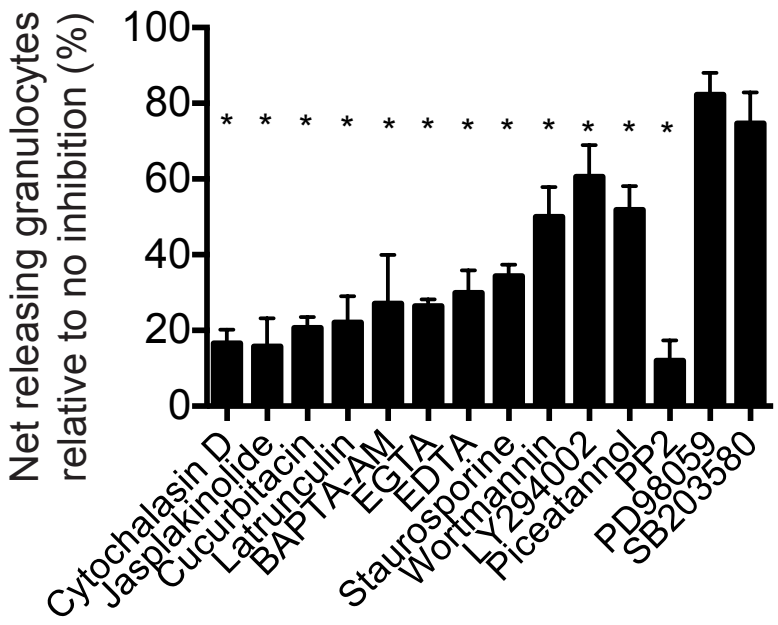


Figure 3.36 Chemical inhibitors of MSU-induced NETosis
Inhibitors of MSU-induced NETosis. NET release at 240 minutes expressed relative to the uninhibited NET release from the matching experiment. Neutrophils were incubated for 1 hour prior to stimulation. Cytochalasin D (10 μM), Jasplakinolide (2 μM), Cucurbitacin (10.2 nM), Latrunculin (1 μM), BAPTA-AM (10 μM), EGTA (5mM), EDTA (4mM), Staurosporine (100nM), Wortmannin (1 μM), LY294002 (20 μM), Piceatannol (50 μM), PP2 (50 μM), PD98059 (50μM) and SB203580 (50 μM). Values represent mean ± SEM, n = 3-7. * $p < 0.05$

However, an important cautionary note with these studies is that several of the inhibitors that blocked NETosis prevented neutrophils from interacting with crystals. This was obvious by microscopy, with neutrophils remaining rounded rather than undergoing shape change induced by the presence of the crystals (example of Cytochalasin D (Figure 3.37)).

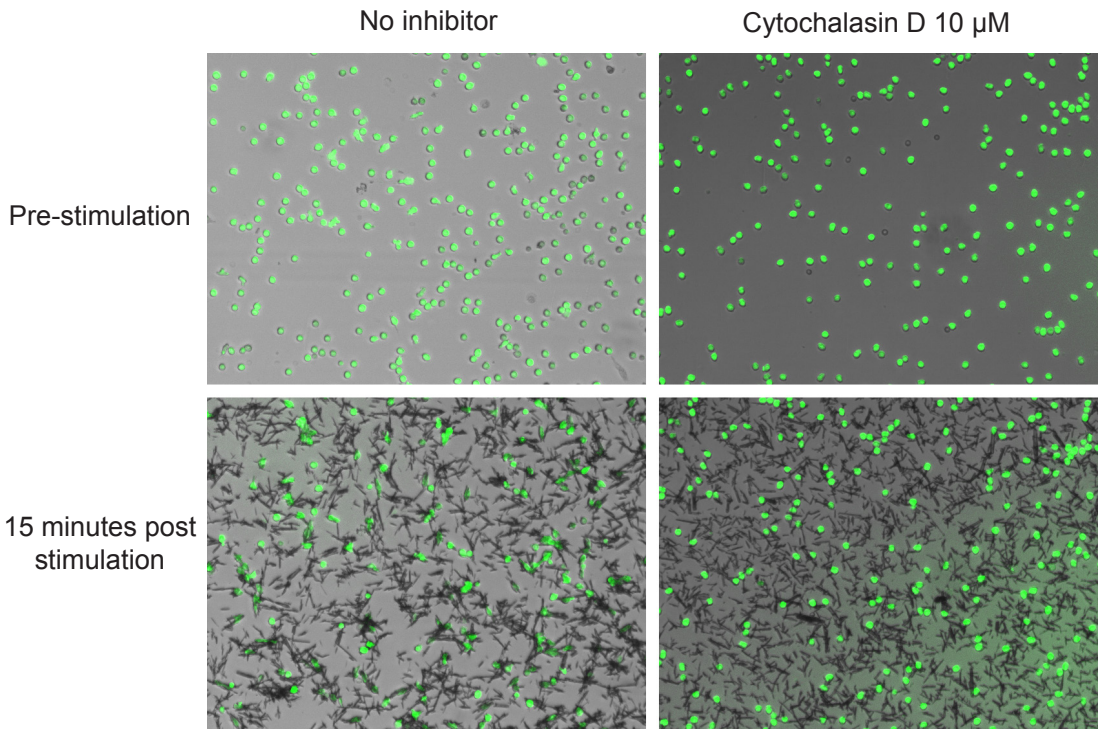


Figure 3.37 Cytochalasin D reduces neutrophil shape change induced by MSU crystals
Pre and post stimulation time-points from time-lapse imaging of MSU stimulated neutrophils incubated with and without Cytochalasin D. Neutrophils were labeled with Cell Tracker Green (CTG, green). Merged CTG fluorescent and phase contrast images.

Neutrophil-crystal interaction was further quantified using average cell circularity before and after stimulation (Figure 3.38). The majority of inhibitors that reduced NETosis also reduced the change in cell circularity induced by the crystals. Whilst this parameter does not directly measure phagocytosis, it suggests an important part of the MSU crystal induction of NETosis is mediated by neutrophil crystal interaction. Two kinase inhibitors that did not inhibit NETosis (MEK inhibitor (PD98059) and p38 MAPK inhibitor (SB203580)) also had little effect on cell circularity. Others had a large effect on circularity, but less inhibitory effect on NETosis (PI3K (Wortmannin) and Syk (Piceatannol)). Interestingly EDTA, EGTA and Staurosporine inhibit NETosis but had little effect on cell circularity, suggesting an inhibitory effect downstream of the initial crystal interaction.

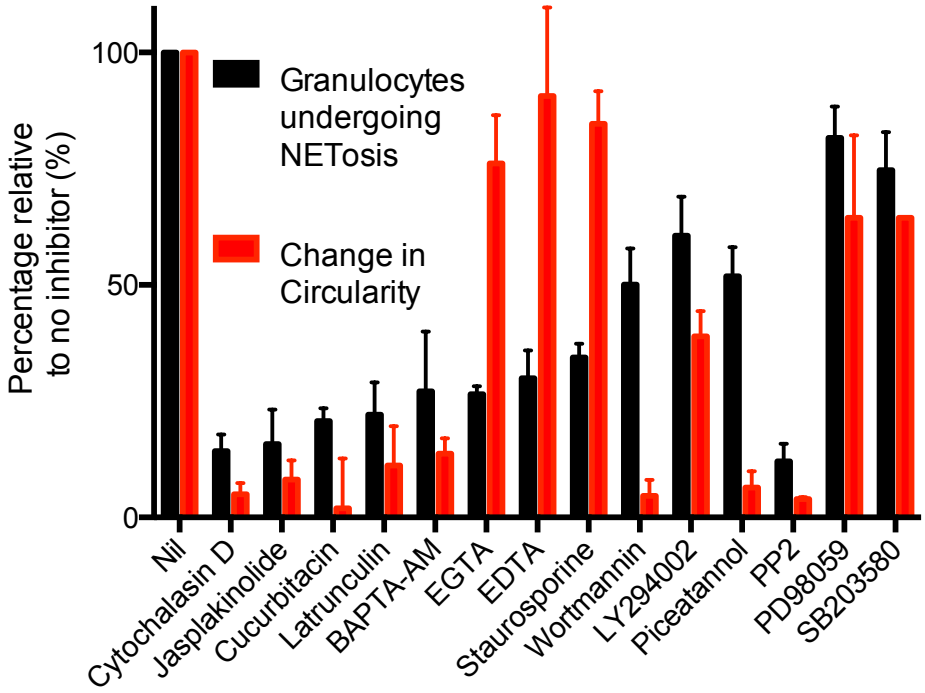


Figure 3.38 NETosis inhibitors and effects of neutrophil circularity induced by MSU crystals
Change in circularity (Average cellular circularity before minus after crystal stimulation expressed as a percentage of baseline and expressed relative to the change in the absence of inhibitor). Data is overlaid with the effect on NETosis. For change in circularity, Values represent mean ± SEM, n = 3-4 analysed for shape change.

3.2.7 MSU-containing phagosomes have irregular surrounding membranes

The previous experiments demonstrate: (i) the importance of crystal neutrophil interaction in NETosis; and (ii) lysosome compromise is a potential candidate to explain the translocation of NE. We attempted to determine whether the phagosome membranes were compromised. Reagents used in a previous study (Hornung et al., 2008) to study phagosome compromise - such as fluorescently-labelled cholera toxin to label membranes and fluorescently-labelled dextran that is taken up by cells during phagocytosis - demonstrated non-specific binding to MSU crystals. Neutrophils were stimulated with MSU crystals or latex beads and labelled with anti-CD63 antibodies to demonstrate phagolysosome fusion with azurophil granules. Phagosomes containing latex beads exhibited uniform staining surrounding the ingested particle. Neutrophils phagocytose serum-coated latex beads avidly but they do not undergo NETosis

(Figure 3.19). In contrast, MSU-containing phagosomes demonstrated irregular CD63 staining (Figure 3.39).

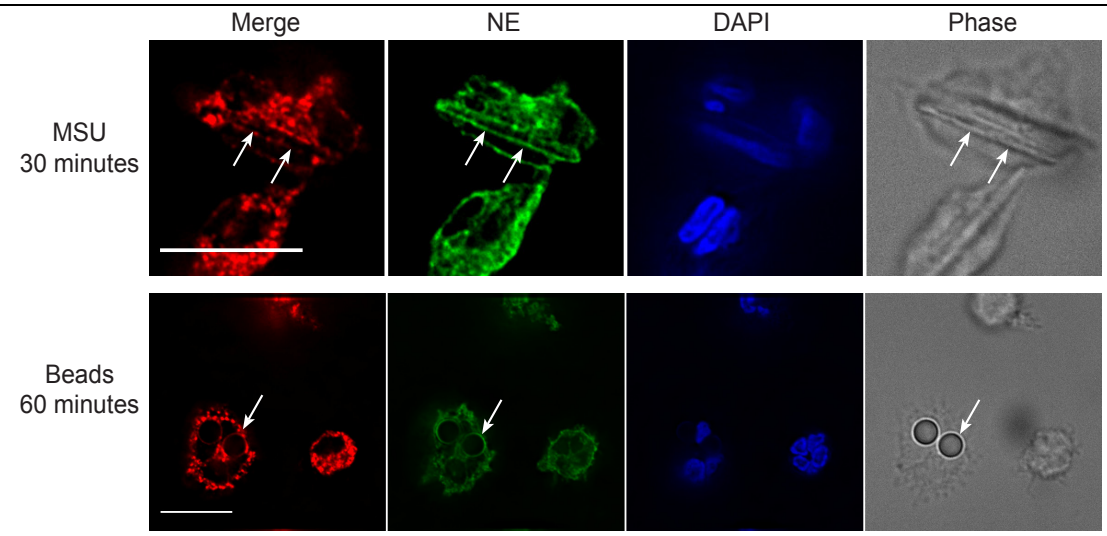


Figure 3.39 CD63 immunofluorescence staining of bead and MSU containing phagosomes
CD63 staining around MSU crystals is discontinuous compared to the regular staining around bead-containing phagosomes. Neutrophils that were fixed at indicated time-points post stimulation with MSU (0.2mg/ml) or beads (Opsonized with autologous human serum,10^7 beads/ml). Immunostaining was performed for CD63 (red) and NE (green) and phase contrast microscopy was performed. Representative of two independent experiments with different donors. Scale bar represents 10 μm

Discontinuity of the phagosome membranes was present even in the absence of neutrophil elastase nuclear translocation. To further characterize the phagosome membranes, transmission electron microscopy was performed with assistance from Sarah Ellis. The phagosomes formed around the beads demonstrated a distinct membrane structure that was continuous (Figure 3.40).

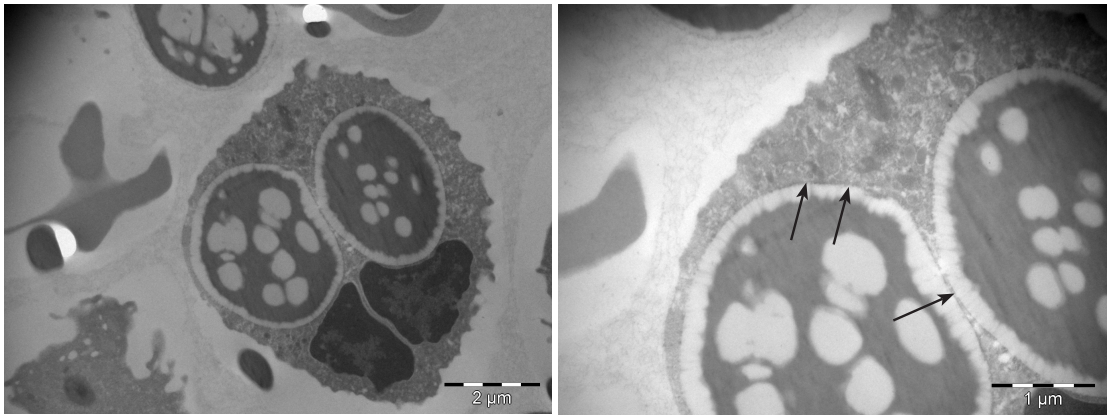


Figure 3.40 Transmission electron microscopy of a neutrophil that has phagocytosed latex beads

Neutrophils were incubated with serum coated 3µm latex beads (10^7 beads/ml) and fixed after 60 minutes. The pellets of the stimulated neutrophils were prepared for scanning electron microscopy and contrasted with uranyl acetate and lead citrate. Lower and higher power of the same cell presented. Scale bars as indicated. Representative of two donors.

Neutrophils fixed five minutes after stimulation demonstrated MSU crystals within relatively well-circumscribed phagosomes although the edges were not as distinct as those surrounding the beads. At 15 minutes, some MSU crystal-containing cells showed the phagosome membranes were partially intact, but not continuous, with areas without clear membrane. At 60 minutes, an example is shown of a cell undergoing cell death. The phagosome membranes are discontinuous, with evidence of breaks in the membrane (Figure 3.41).

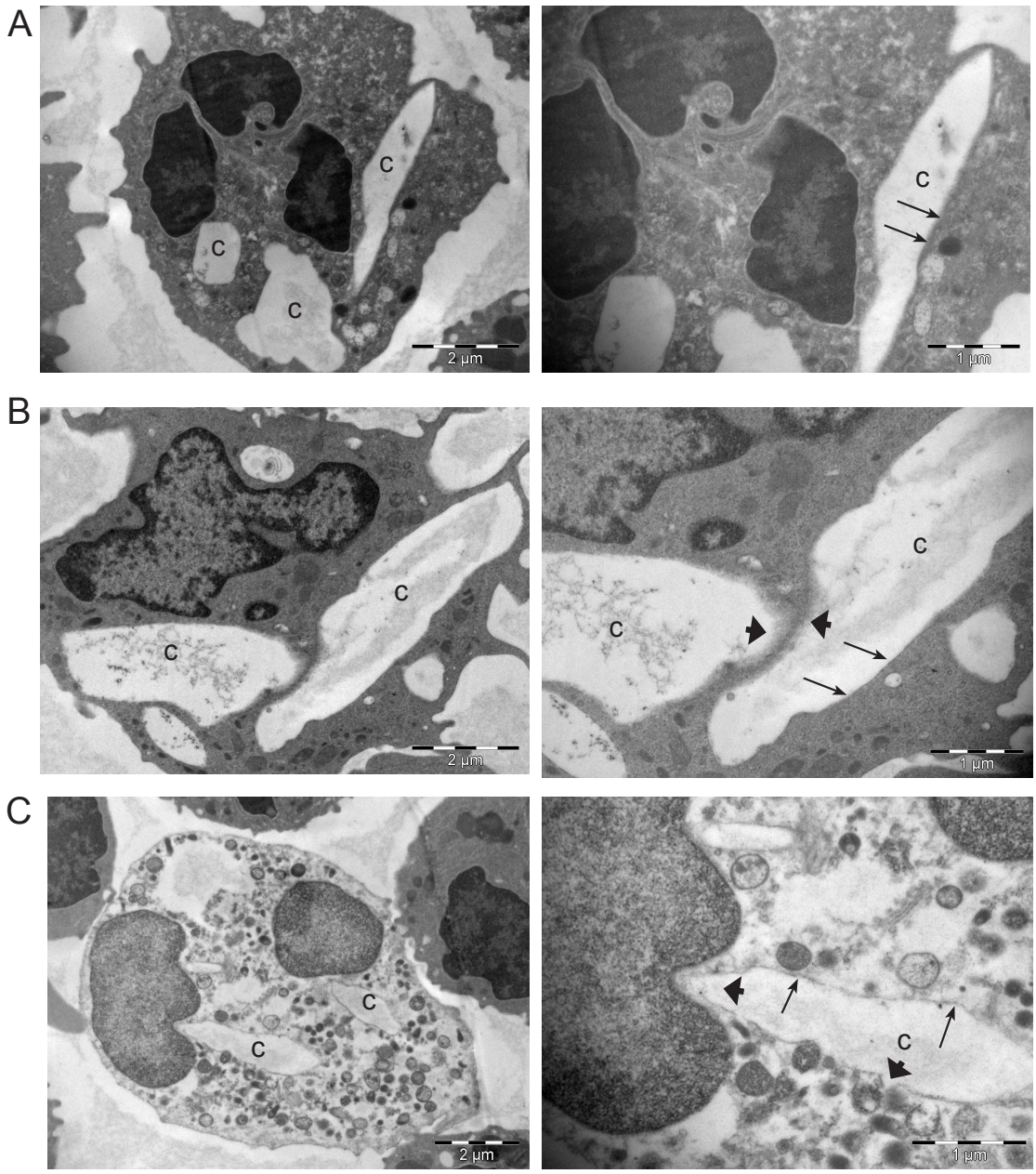


Figure 3.41 Transmission electron microscopy of neutrophils stimulated with MSU crystal
Neutrophils were incubated with MSU crystals (0.2 mg/ml) and fixed after A) 5 minutes, B) 15 minutes and C) 60 minutes. The pellets of the stimulated neutrophils were prepared for scanning electron microscopy and contrasted with uranyl acetate and lead citrate. Lower and higher power of the same cell presented. Long arrows indicate intact phagosomal membranes and the arrowheads demonstrate breaks in the membrane. The crystals are labelled “c”. Scale bars as indicated. Representative of two donors.

This imaging data suggests that the phagosome membrane around MSU crystals is not continuous, although does not directly demonstrate escape of enzymes from the phagosome.

3.2.8 MSU-induced NETosis and relationship to other forms of cell death

As reported for PMA-induced NETosis (Fuchs et al., 2007), MSU crystal-induced NETosis is distinct from apoptosis as it was caspase-independent (zVAD-fmk and QVD-OPh, Figure 3.42) and annexin V binding did not occur before cell death (Figure 3.43). Furthermore, MSU-induced NETosis was not reduced by inhibitors of necroptosis, including Necrostatin 1 (inhibitor of RIPK1), a RIPK3 inhibitor (GSK832 (Kaiser et al., 2013)), nor two structurally distinct MLKL inhibitors (necrosulfonamide (Sun et al., 2012) and GW806742X (Hildebrand et al., 2014)) (Figure 3.42). MSU-induced NETosis was also not inhibited by therapeutic agents used to treat gout, including indomethacin, dexamethasone (Figure 3.42) and colchicine (Figure 3.35).

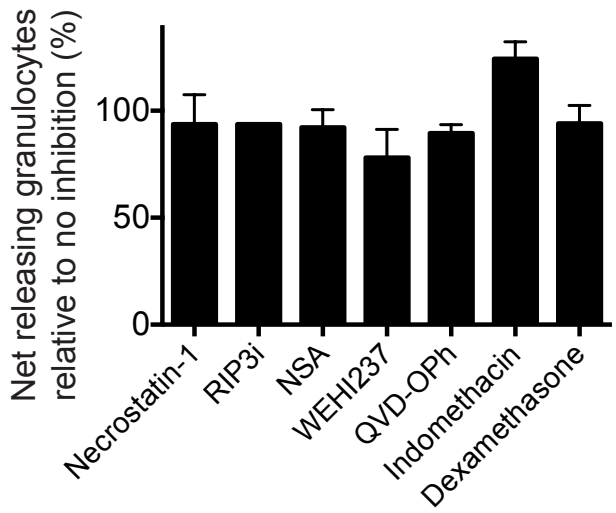


Figure 3.42 Inhibitors of alternative forms of regulated cell death and clinical inhibitors of gouty inflammation do not inhibit NETosis
Neutrophils were incubated for 1 hour prior to stimulation. NET release at 240 minutes expressed relative to the uninhibited NET release from the matching experiment. Necrostatin-1 (25 μM); RIP3 inhibitor GSK840 (2 μM); Necrosulfonamide (NSA, 10 μM); MLKL inhibitor WEHI237 (2 μM); QVD-oph (2.5 μM); Indomethacin (10 μM) and Dexamethasone (10μM). Values represent mean ± SEM. n=3

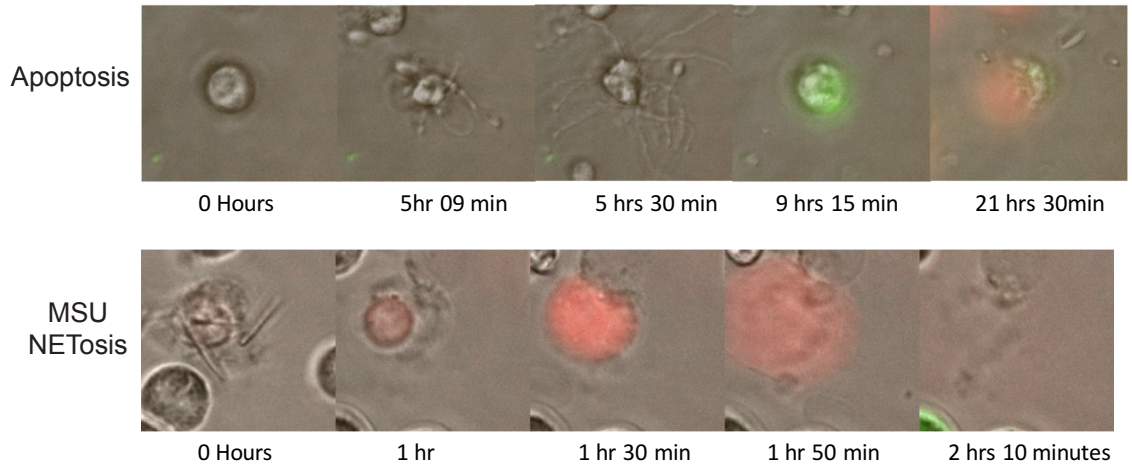


Figure 3.43 Annexin V binding occurs before cell death in apoptosis and after in MSU NETosis
Live cell time-lapse montage of neutrophils incubated in media containing Alexa488-labelled Annexin V and PI and stimulated with MSU crystals or unstimulated and allowed to undergo spontaneous apoptosis. Representative of two independent experiments with different donors

In addition, a potent and selective PAD4 inhibitor, which inhibits calcium ionophore-induced NETosis, GSK484 (Lewis et al., 2015), failed to alter the rate or kinetics of either PMA- or MSU-induced NETosis (Figure 3.44A). Immunofluorescence of neutrophils in duplicate at multiple time-points demonstrated positive staining for citrullinated histones at low levels in PMA-treated neutrophils, with higher percentages in MSU-treated neutrophils (Figure 3.44B C). Interestingly, the percentage increased up to an hour after stimulation and then progressively decreased. If confirmed, this finding suggests that citrullination of histones occurs during MSU-induced NETosis, but is not sufficient to cause it. The loss of staining with time might reflect degradation of the citrullinated histones.

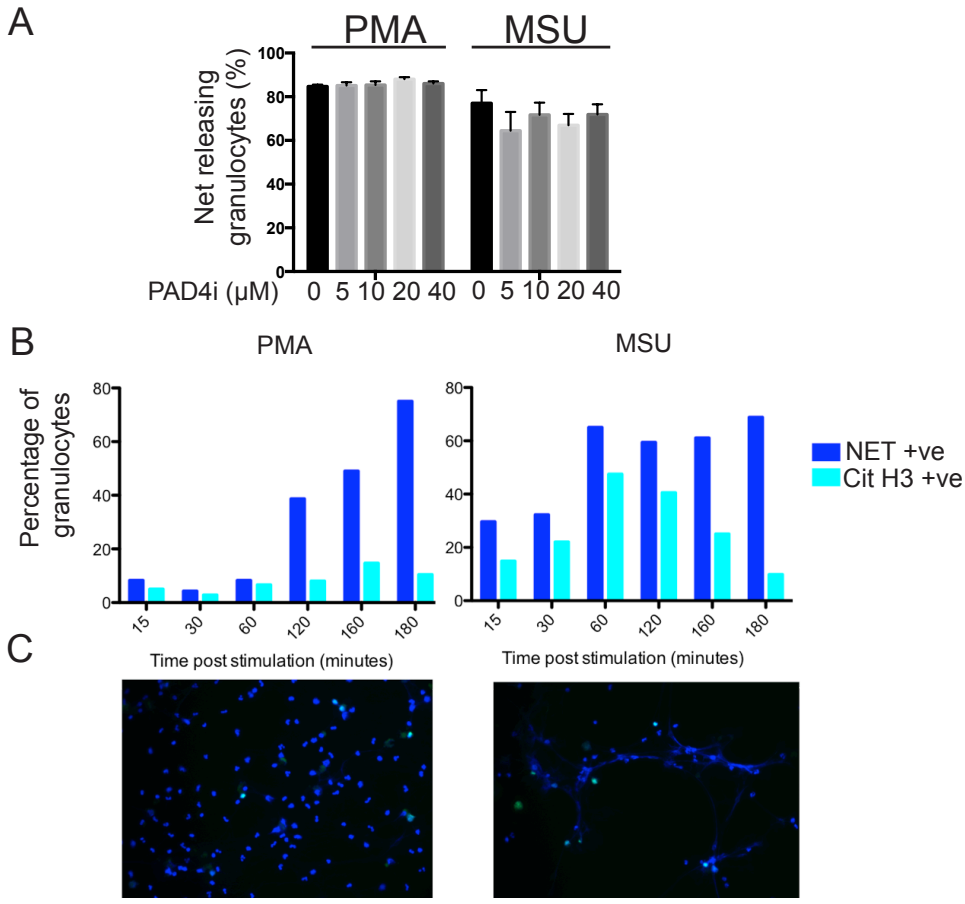


Figure 3.44 Histone citrullination occurs during PMA and MSU-induced NETosis but is not required
A) PMA and MSU-induced NET release at 240 minutes expressed relative to the uninhibited NET release from the matching experiment in neutrophil treated with PAD4 inhibitor (GSK484) at indicated concentrations. Values represent mean ± SEM, n=4. B) Immunofluorescence staining of PMA and MSU treated neutrophils for citrullinated histone 3 (Abcam5103) and DAPI staining. Manual counts of cells undergoing NETosis (NET) and cells labelled with citrullinated histone antibody (Cit3) expressed as a percentage of total cells. Data represent the mean of the counts from two experimental replicates from a single donor. C) Representative fluorescent image from 120 minutes post stimulation (Blue = DAPI, green = anti-citrullinated histone).

3.2.9 MSU crystal-induced NETs are less susceptible to Deoxyribonuclease 1 and serum degradation than PMA NETs

The presence of cell-free DNA in gout patient samples was unexpected as NETs induced by PMA are susceptible to degradation by serum nucleases, primarily Deoxyribonuclease (DNase) 1 (Hakkim et al., 2010). DNA was critical for the capacity

of NETs to maintain crystals in aggregates, as demonstrated by disruption with high dose deoxyribonuclease 1 (DNase) and micrococcal nuclease (MNase), but not Proteinase K (Figure 3.45).

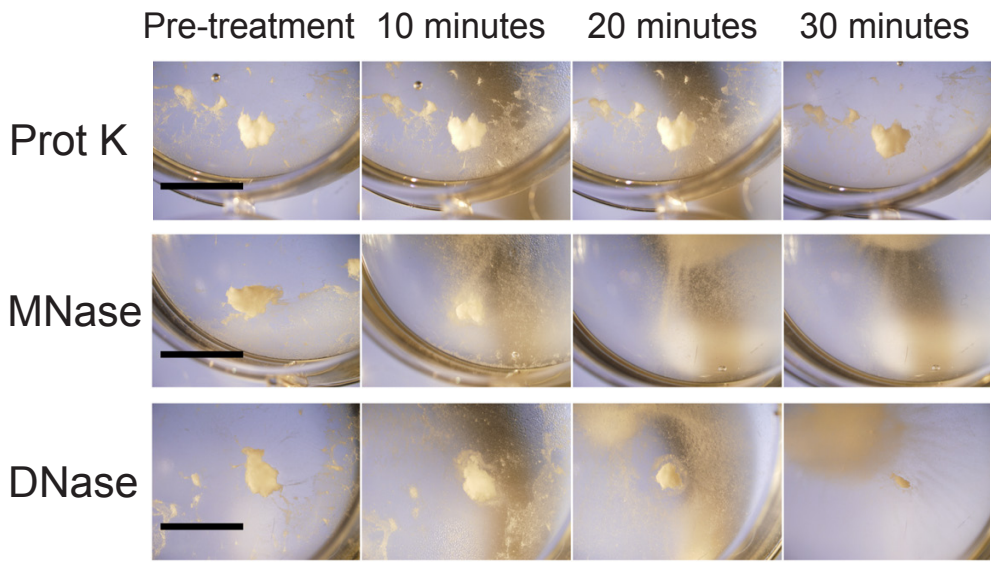


Figure 3.45 DNA provides the structural component of NET crystal aggregates
Time-lapse images of *in vitro* generated macroscopic neutrophil-crystal aggregates (described in Methods section) treated with Proteinase K (Prot K, 2.5 mg/ml) or nuclease (Micrococcal nuclease (MNase, 5 U/ml) or deoxyribonuclease 1 (DNase, 5 U/ml)). Representative of three independent experiments from different donors. Scale bar represents 1 cm.

Incubation with serum caused microscopic degradation of PMA-induced NETs (PMA-NETs), but had minimal effect on MSU-induced NETs (MSU-NETs) (Figure 3.46).

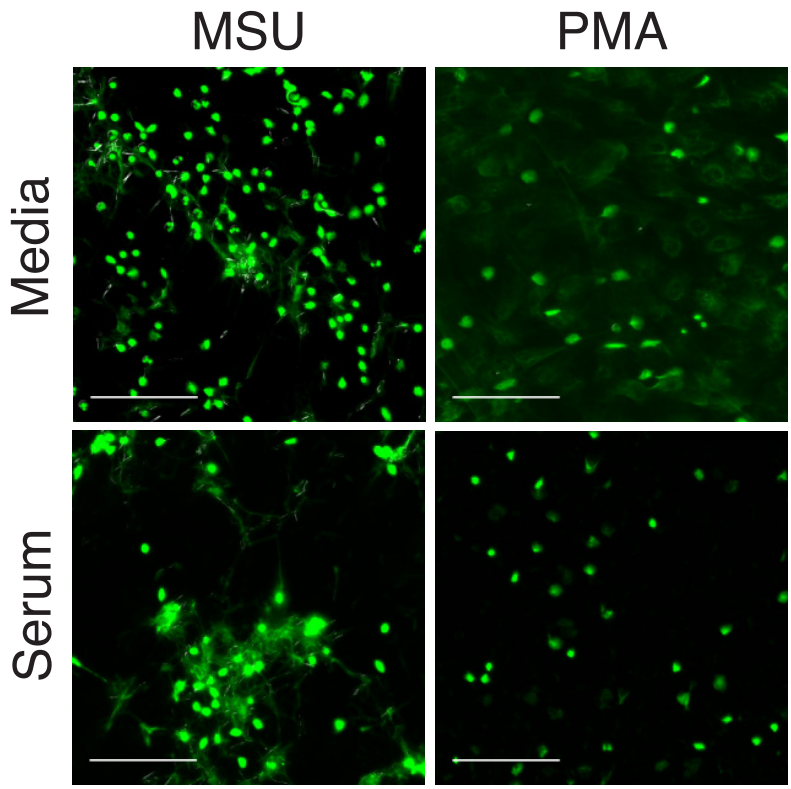


Figure 3.46 Serum degrades PMA NETs more effectively than it degrades MSU NETs
PMA- and MSU-treated neutrophils incubated with 10% autologous serum or media control for 6 hours prior to fixation and staining. Merged images – DAPI (Green) and phase contrast. Representative of three experiments from different donors. Scale bar represents 100 μm.

Using a DNA release assay (Hakkim et al., 2010), less DNA was released over 60 minutes from MSU-NETs than from PMA-NETs over a range of DNase concentrations, while there was no difference in susceptibility to MNase (Figure 3.47).

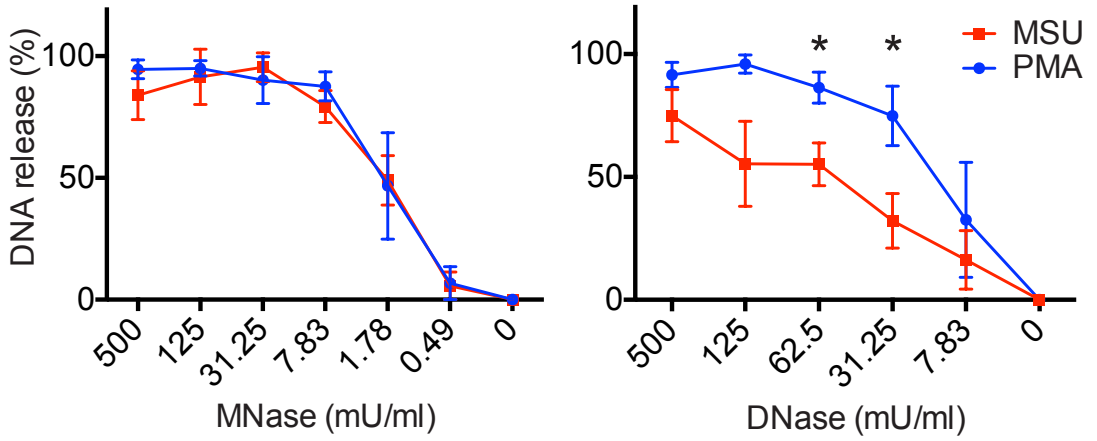


Figure 3.47 MNase degrades PMA and MSU NETs equally, but DNase degrades PMA NETs more efficiently than MSU NETs
The amount of DNA released from PMA and MSU NETs after an hour of treatment with the indicated concentrations of MNase or DNase. DNA in supernatants was measured using Picogreen fluorescent dye. The values are expressed as a percentage of the amount released using MNase 500 mU/ml for 1 hour representative of the maximal release. Values represent mean ± SEM. * $P<0.05$, n=5.

Susceptibility to DNase was further assessed by generating aggregates of PMA- and MSU-NETs and then monitoring reduction in PI signal over time (Supplementary Video 5 file attached and described in the Appendix). DNA degradation was nuclease dose- and time-dependent (Figure 3.48). MSU-NETs were less sensitive to degradation than PMA-NETs across a range of DNase concentrations. At higher concentrations, the difference in sensitivity was minimal, suggesting a threshold to overcome an inhibitory factor.

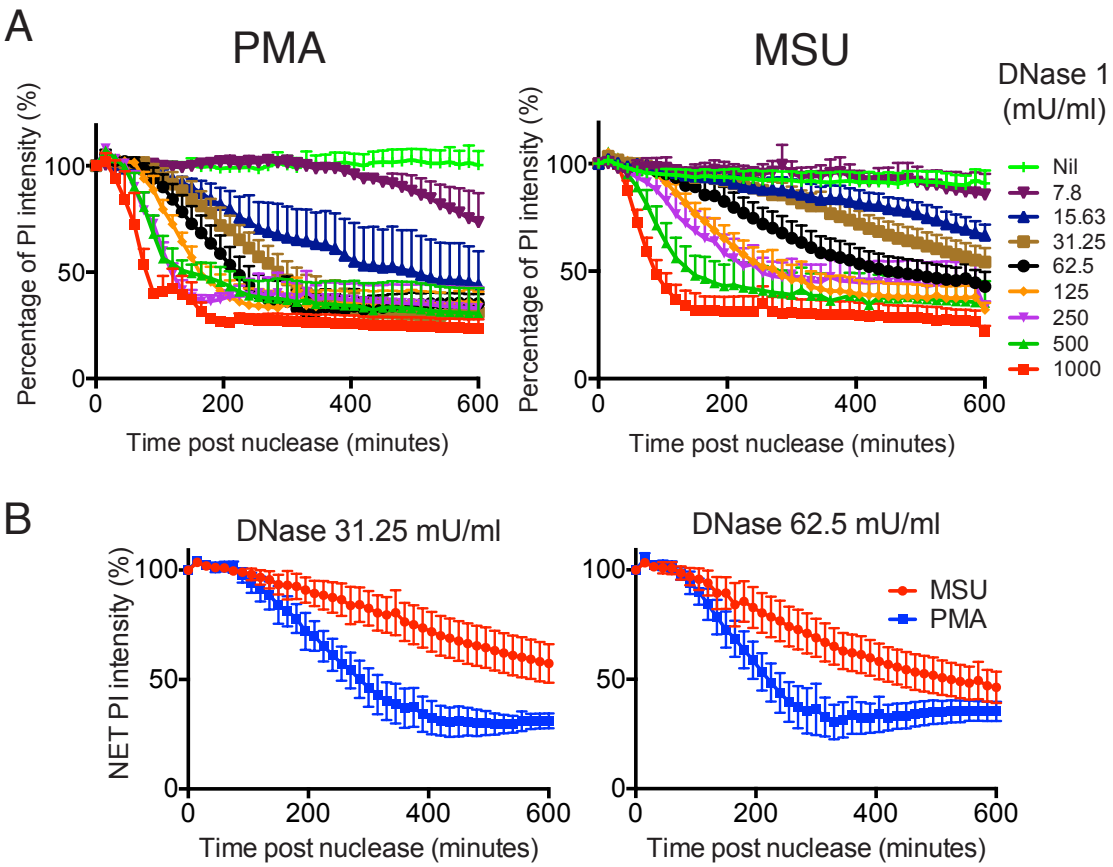


Figure 3.48 DNA from PMA NETs is more rapidly degraded by DNase than that from MSU NETs

(A) NET DNA degradation by DNase is time- and dose-dependent. PI stained MSU NETs and PMA NETs were transferred to a 96 well microscope plate and imaged every 15 minutes after addition of DNase at the indicated concentrations. Computerized analysis of total PI intensity was calculated at each time point. Data are expressed as a percentage of the starting intensity. Values represent mean ± SEM, n=5. B) PMA compared to MSU at the same DNase concentration from the data in A). Values represent mean ± SEM, n=5. Significant difference (P<0.05) between PMA and MSU as measured by two-way ANOVA at both concentrations.

Using this assay, PMA-NETs were more sensitive to serum degradation than MSU-NETs (Figure 3.49).

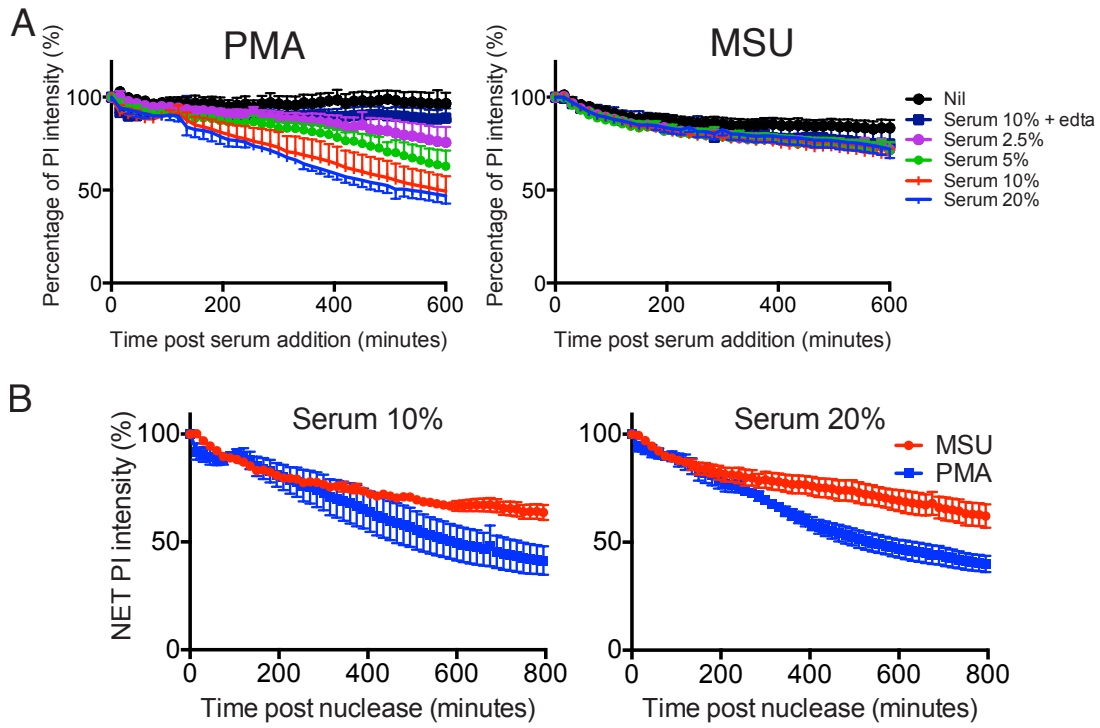


Figure 3.49 DNA from PMA NETs is more rapidly degraded by serum than that from MSU NETs

NET DNA degradation by autologous serum is time- and dose-dependent. A) Data generated as per Figure 3.48. Values represent mean ± SEM, n=5. B) PMA compared to MSU at the same serum concentration from the data in A). Significant difference (P<0.05) between PMA and MSU as measured by two-way ANOVA at both concentrations.

EDTA inhibited serum nuclease activity, consistent with the requirement of cations for DNase 1 function (Figure 3.50A). Dissolving the crystals using uricase did not significantly enhance the susceptibility of MSU-NETs to DNA degradation (Figure 3.50B).

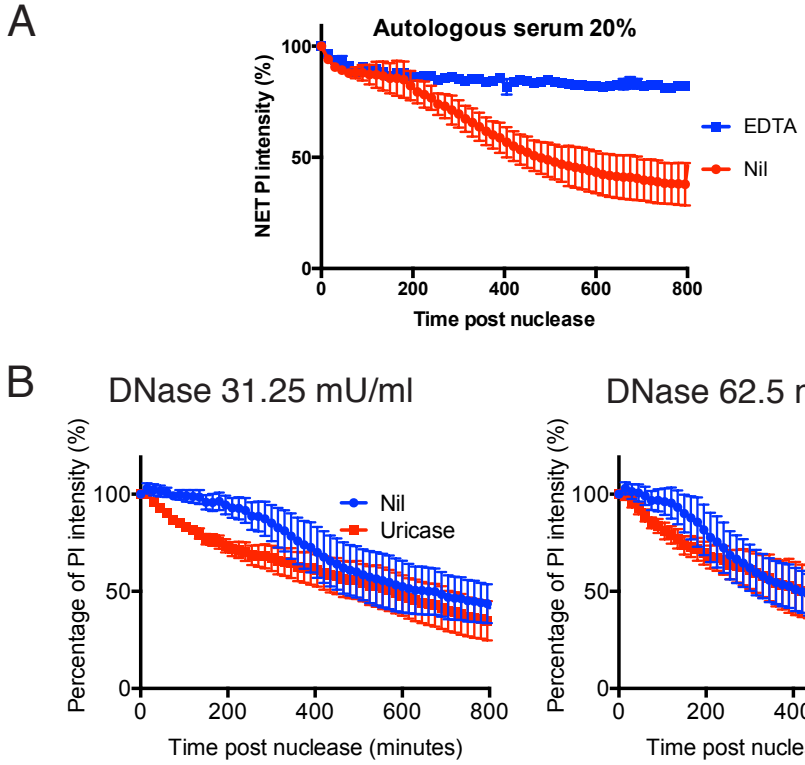


Figure 3.50 EDTA inhibits serum nuclease and uricase treatment does not affect DNase degradation of MSU NET
A) EDTA inhibits serum-mediated degradation of NETs. PMA NETs incubated with 20% autologous serum with or without EDTA (5mM). Time-lapse data as per Figure 3.49. Values represent mean ± SEM, n=5. B) Uricase treatment does not alter MSU NET degradation by DNase 1. PI stained MSU NETs and PMA NETs were transferred to a 96 well microscope plate and treated with Uricase (10 U/ml) for 1 hour and then imaged every 15 minutes after addition of DNase 1 at the indicated concentrations. Computerized analysis of total PI intensity was calculated at each time point. Data are expressed as a percentage of the starting intensity. Values represent mean ± SEM, n = 3.

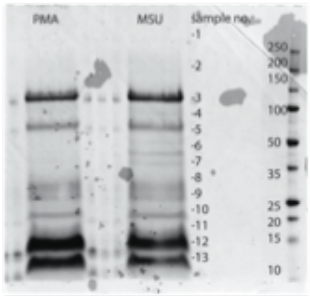
3.2.10 MSU NETs are enriched with actin and actin-binding proteins.

Given these functional differences, we investigated the composition of MNase-liberated NETs using proteomics. A similar pattern of protein bands between PMA- and MSU-NETs was found, but additional bands between 37 and 50 kDa were present in the MSU NETs (Figure 3.51). Proteomic analysis found a shared NET proteome (Figure 3.51B, Supplementary Table 1 in the Appendix), enriched for histones and neutrophil granule proteins, as previously described (Urban et al., 2009). HMGB1 and LL-37 previously reported to be NET components (Lande et al, 2011) were not identified,

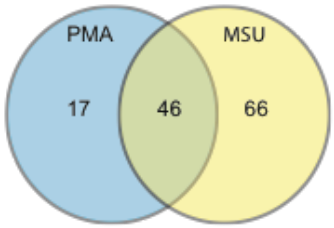
possibly due to relative low abundance. A number of anti-inflammatory molecules were also identified including Annexin A1 and SerpinB1.

MSU-NETs had higher levels of several proteins, the most abundant of which was β-actin. Among the proteins in the top 20 most abundantly expressed proteins associated with MSU-NETs included actin-binding proteins: myosin-9, α-actinin, plastin-2 and filamin-A (Figure 3.51C).

A



B



C

MSU		PMA	
Protein	Spectral count	Protein	Spectral count
Lactotransferrin	167	Myeloperoxidase	210
Myeloperoxidase	133	Lactotransferrin	208
Actin	100	Histone H4	74
Histone H4	67	Hemoglobin beta	55
Lactoferrin	67	Lactoferrin	54
Myosin-9	47	MNDA	38
Histone H2B	41	Histone H2B	26
Alpha-enolase	36	Cathepsin G	26
Leukocyte elastase inhibitor	33	Profilin-1	21
Annexin A1	33	Leukocyte elastase inhibitor	20
Cathepsin G	30	Actin	17
MNDA	28	Eosinophil peroxidase	17
Alpha-actinin-1	25	Alpha-enolase	15
GAPDH	24	Triosephosphate isomerase	14
Annexin A3	22	Peroxiredoxin-2	13
Plastin-2	22	Annexin A1	12
Filamin-A	22	Transketolase	12
Eosinophil cationic protein	19	Eosinophil cationic protein	12
Hemoglobin beta	17	GAPDH	11
Transketolase	17	Protein S100	9

Figure 3.51 NET proteomics demonstrated both shared and differential protein expression between PMA and MSU NETs
A) Sypro Ruby staining of an SDS-Page gel of nuclease-liberated PMA and MSU NETs. Note bands present between 35 and 50 kDa present in MSU but not PMA NETs. Representative of two experiments. (B) Mass spectrometry identified 46 shared proteins associated with NETs derived from neutrophils stimulated with PMA or MSU. 17 unique proteins were attributed to PMA, while MSU stimulation resulted in 66 unique proteins associated with NETs. (C) Lists of the 20 most abundant NET proteins in order of spectral counts for PMA and MSU induced NETs. MNDA = Myeloid cell nuclear differentiation antigen. GAPDH = Glyceraldehyde-3-phosphate dehydrogenase. See supplementary Table 1 in the Appendix for complete list.

Actin enrichment was confirmed with Western blotting of the isolated NETs (Figure 3.52A). Fixed-cell imaging revealed β-actin staining associated with extracellular DNA in MSU-treated neutrophils (Figure 3.52B - MSU). Higher power images demonstrated

that colocalization was most evident adjacent to crystals (Figure 3.52B – MSU High magnification). β-actin staining of PMA-treated neutrophils occurred in a distribution suggestive of cell remnants, rather than association of β-actin with extracellular DNA strands (Figure 3.52B - PMA).

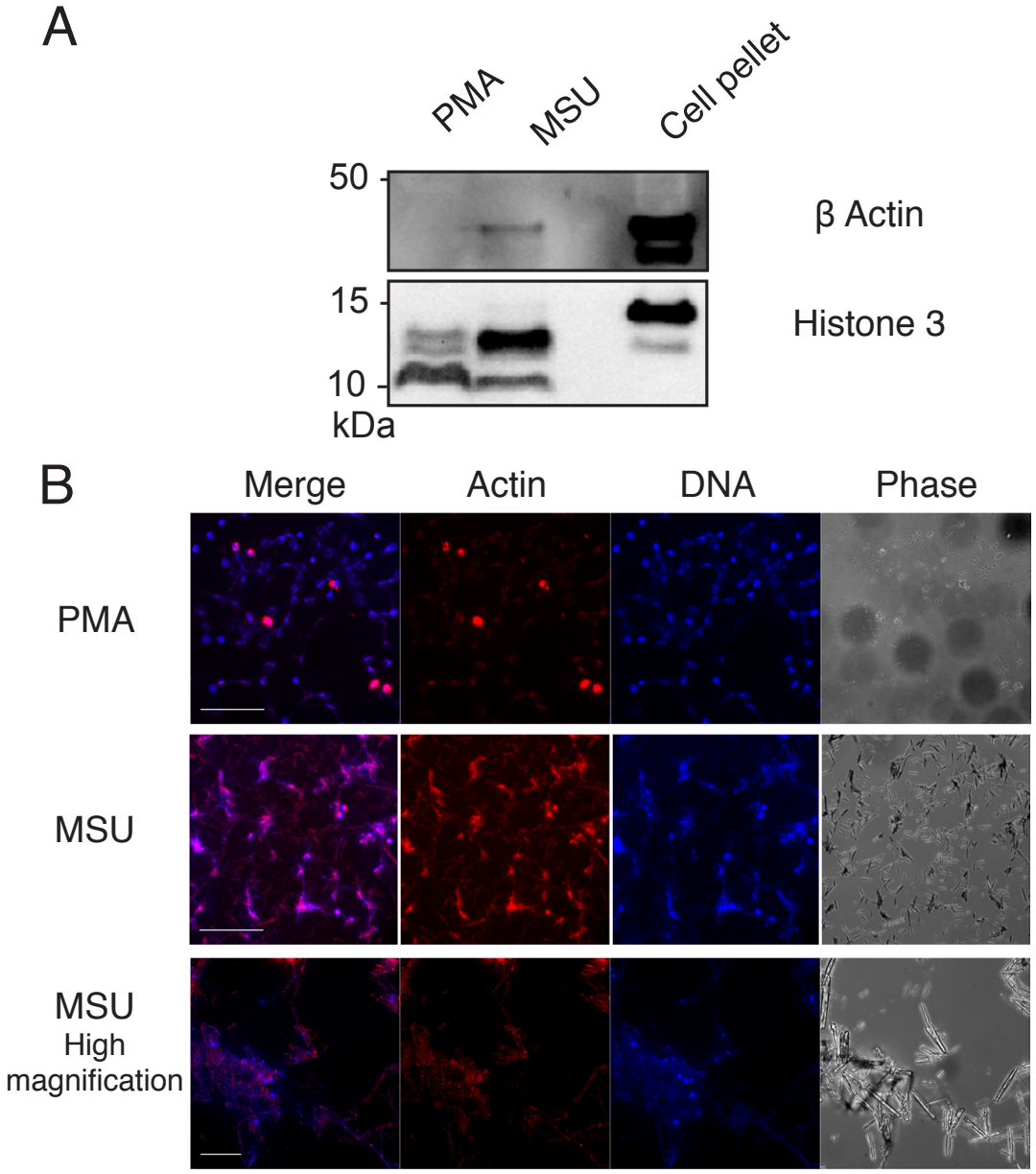


Figure 3.52 MSU-NETs are enriched for β-actin
(A) MSU-NETs contain more actin than PMA-NETs. PMA- and MSU-NET protein western blot for β-actin and Histone 3. Note Histone 3 is a lower molecular weight in NETs than in intact neutrophils. Example of three separate experiments with different donors. (B) Actin partially colocalizes with DNA strands in MSU-NETs but not PMA-NETs. Neutrophils were stimulated for 4 hrs before fixation and immunofluorescent imaging. Images are maximum intensity projections of z stacks. Scale bar represents 100 μm for low magnification images and 10 μm in high magnification image. Merge of β-actin (red), and DAPI (blue) with phase contrast. Representative of three separate experiments with different donors. See supplementary Figure 6 for high power image.

MSU-NETs also demonstrated staining with phalloidin-FITC, suggesting at least some actin is polymerized F-actin (Figure 3.53).

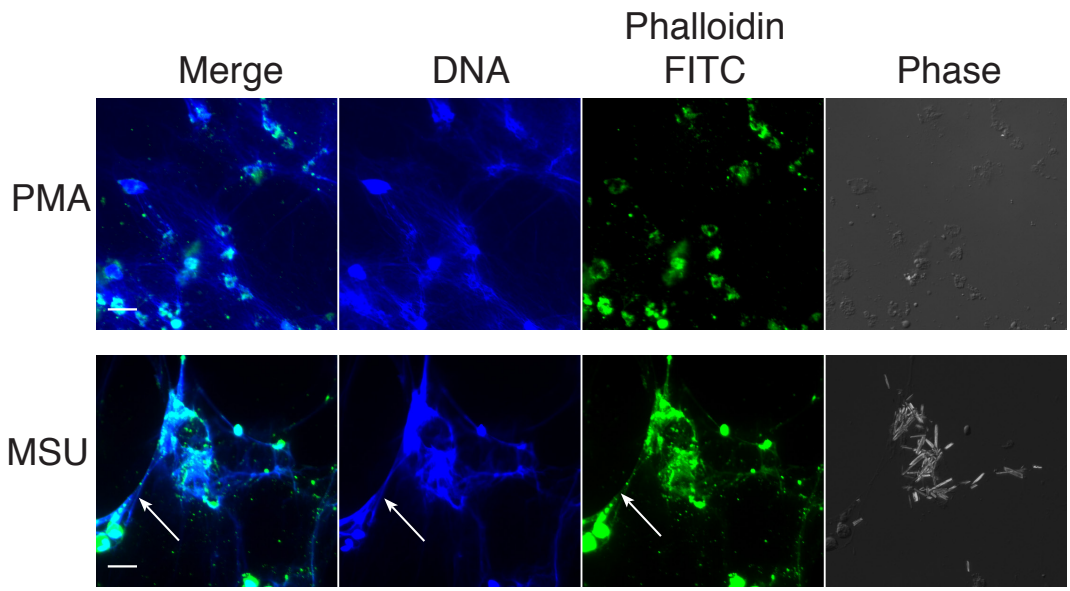


Figure 3.53 F-actin colocalizes with DNA in MSU-NETs
Representative fixed cell immunofluorescent images of PMA and MSU stimulated neutrophils after four hours. Images are maximal intensity projections of z stacks. Scale bar represents 10 μm. FITC-conjugated phalloidin (green), and DAPI (blue) with phase contrast. Arrow highlights strands of DNA colocalising with phalloidin FITC. Representative of three separate experiments with different donors.

Actin is a physiologic inhibitor of DNase (Lazarides & Lindberg, 1974), but has no effect on MNase (Hakkim et al., 2010). Gelsolin reduces this inhibition by cleaving actin and displacing it from DNase 1 (Davoodian et al., 1997). Consistent with enriched actin in MSU-NETs, we found gelsolin increased the speed of MSU-NET degradation by DNase (Figure 3.54). The rate of DNA degradation was not as rapid as with PMA-NETs suggesting other factors contribute to the DNase resistance of MSU-NETs.

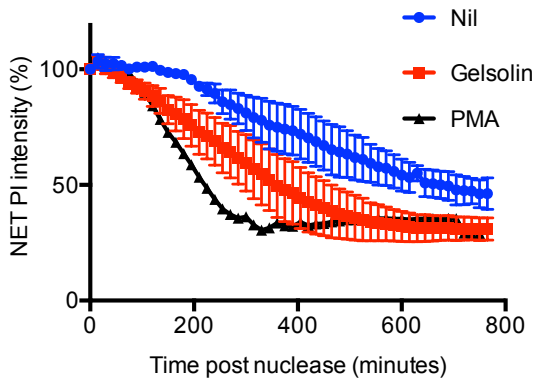


Figure 3.54 Gelsolin increases the susceptibility of MSU-NETs to DNase degradation
Gelsolin (120 nM) treatment of MSU NETs increases susceptibility to DNase degradation (62.5 mU/ml). Data obtained as per Figure 5C. Values represent mean ± SEM, n=3. Significant difference (*P*<0.05) between Gelsolin and untreated MSU NETs as measured by two-way ANOVA. The curve for PMA without error bars is presented for comparison.

3.2.11 NETosis reduces the pro-inflammatory potential of MSU-crystals

Given the presence of NETs in inflamed gout synovial fluid and in uninflamed tophi, we sought to determine the effect of NETosis on the inflammatory potential of MSU crystals. Tissue resident macrophage production of interleukin-1β (IL-1β) is thought to drive acute gout (W. J. Martin et al., 2009). PMA-primed human THP-1 (macrophage-like) cells were therefore co-incubated with MSU crystals and neutrophils to assess the ability of NETs to enhance or suppress the release of interleukin-1β (IL-1β). MSU alone induced IL-1β production, as expected, but when MSU crystals were pre-incubated with neutrophils, IL-1β release was reduced (Figure 3.55). Release of IL-1β from THP-1 cells was restored by DNase treatment of the NETs, at concentrations sufficient to disaggregate the crystals. In contrast, a soluble NLRP3 agonist, nigericin, potently induced IL-1β release that was not inhibited by the presence of neutrophils. Of note, neutrophils alone did not release IL-1β, either with or without MSU stimulation. An alternative crystal stimulus would be important to support this as a general effect of neutrophil on THP-1 cell crystal responses.

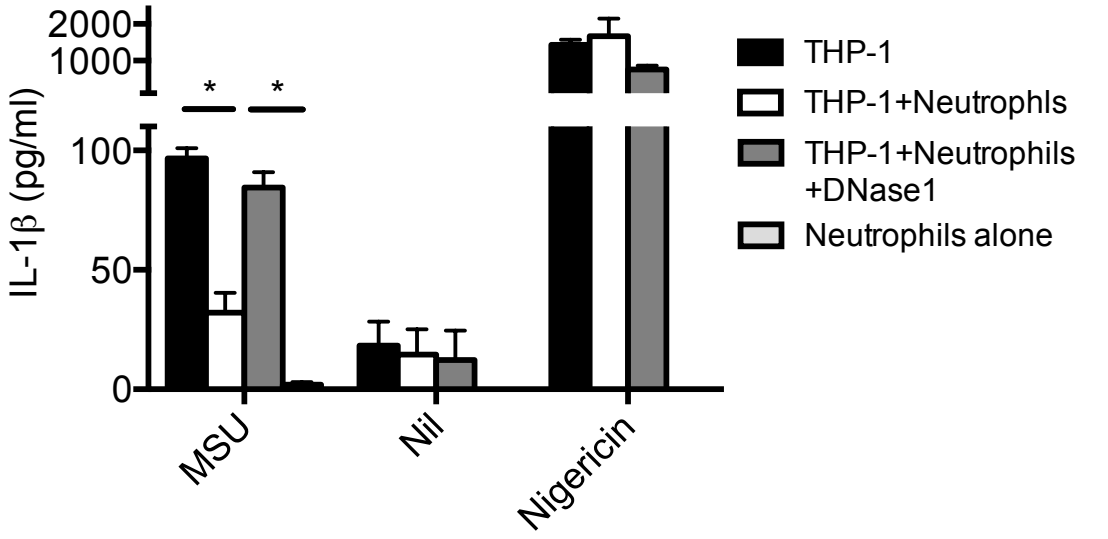


Figure 3.55 Neutrophils reduce THP-1 IL-1 in response to MSU crystals in a DNA-dependent manner
THP-1 cells were stimulated for six hours with MSU crystals (0.2 mg/ml), media or nigericin (10μM) that had been incubated in the presence or absence of neutrophils for four hours, with and without DNase treatment. Neutrophils alone were also stimulated in the absence of THP- cells. IL-1β was measured in the supernatants by ELISA. Values represent mean ± SEM. *P<0.05, n = 3 independent experiments

Cell death appears to be important in the ability of some cells to release IL-1β (Cullen et al., 2015). MSU crystals induced THP-1 cell death, measured using live cell microscopy (Figure 3.56). Neutrophils incubated with THP-1 cells prior to the addition of crystals underwent robust NETosis but there was significantly reduced THP-1 cell death. These findings suggest NETosis attenuates MSU-induced cell death and IL-1β release in macrophage-like cells. The resolution of the images is not sufficient to determine whether the crystals are coated with DNA and further experiments pre-incubating the crystals with NETs to coat them would help clarify the mechanism.

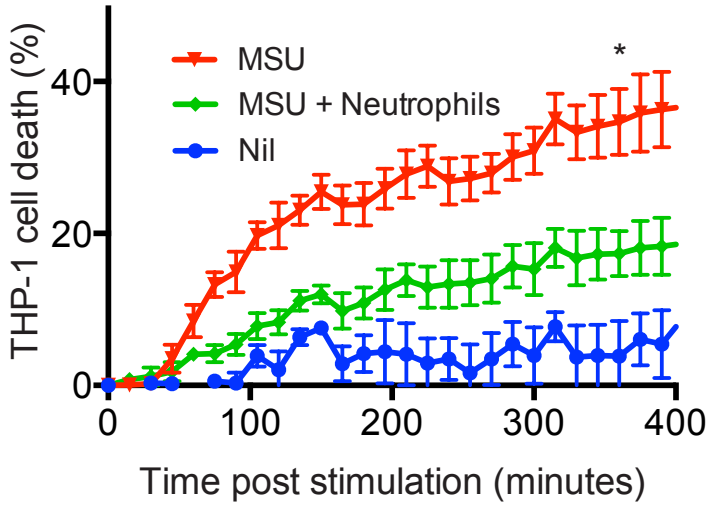


Figure 3.56 Neutrophils reduce MSU-crystal induced THP-1 cell death
THP-1 cells were incubated with MSU crystals (0.2 mg/ml) in the presence or absence of neutrophils. THP-1 cell death was measured using CTG vital staining and time-lapse microscopy. Data are presented as the loss of CTG stained cells. Values represent mean ± SEM. *P<0.05 for the difference in cell death at 360 minutes (same time-point as IL-1β ELISA) P=0.07 for the treatment difference between MSU and MSU with neutrophils as measured by two-way ANOVA with repeated measures (n=3).

3.3 DISCUSSION

Neutrophil cell death and chromatin release, or NETosis, has most likely evolved as a mechanism to counteract pathogens and the inflammatory response to the deposition of MSU, CPPD, cholesterol and silica crystals within host tissues appears to mimic this response. To date, NETosis has been studied with relatively crude tools, including the use of a non-physiological inducer – PMA – and single point in time enumeration of neutrophil morphology *in vitro*. Here, we developed new time-lapse approaches to provide strong evidence that MSU crystals induce NETosis through a pathway that is distinct from PMA-induced NETosis. This pathway results in a nuclease resistant, actin-rich DNA coating of sequestered crystals that limits further activation of the inflammatory response in macrophage-like cells. This same phenomenon is demonstrable within tophi from patients with gout.

Quantifying NETosis has been a challenge, both *in vitro* and *in vivo* (Naccache & Fernandes, 2016). We describe a novel assay that permits simultaneous assessment of both cell death and chromatin condensation - the essential components of “lytic” NETosis (Yipp & Kubes, 2013) - in a high throughput format, allowing kinetic assessment of multiple stimuli and inhibitors. Using this approach, we have uncovered alternative pathways to NETosis. We demonstrate that NADPH oxidase activation leads to neutrophil cell death and NETosis in response to PMA and *Candida,* but is dispensable for crystal-induced NETosis.

NE was a critical mediator of the histone degradation common to both crystal and PMA-induced NETosis. We demonstrate that NE nuclear translocation and nuclear protease activity occurs prior to cell death with PMA, consistent with the concept of ‘misdirected’ NE activity previously demonstrated with *Candida* hyphae (Branzk et al., 2014). Conversely, NE and protease activity rapidly localized to mature, crystal-containing phagosomes in neutrophils stimulated with MSU, where it remains until immediately prior to or after cell death. Following cell death, NE translocates to the nucleus, most likely via disruption of the crystal containing phagosome, only then causing chromatin decondensation. Non-particulate induction of lysosome disruption with LLOMe also resulted in NETosis. MSU crystals may therefore permeabilize phagosome membranes, in keeping with the “lysis from within” hypothesis (Weissmann & Rita, 1972). In contrast to macrophages, crystal-induced NETosis did not involve inflammasome activation.

Whether MSU-induced NETosis represents simple toxic disruption or a form of programmed cell death is still unclear, but our data certainly suggest NETosis differs from established forms of cell death. Caspase inhibition had no effect on MSU-induced NETosis, thereby distinguishing it from apoptosis and pyroptosis. Despite conflicting reports of the role of caspase-independent necroptosis (Amini et al., 2016; Desai et al.,

2016), we found that blockade of the necroptosis pathway with multiple chemical inhibitors had no effect on MSU-NETosis.

MSU-NETs were also functionally distinct from PMA-NETs, exhibiting resistance to DNase and importantly, serum degradation. This finding is in keeping with the presence of NETs in clinical samples from gout patients. We demonstrated through proteomic analysis that actin is an intrinsic component of NETs generated in response to this pathophysiologic stimulus. Resistance to endogenous nucleases may thus facilitate durable crystal entrapment by DNA within tissues and this may represent a protective mechanism in other crystal-associated diseases.

The exact inflammatory consequences of NETosis are unclear. Inappropriate NETosis may promote or perpetuate inflammation in infective conditions and in particular autoimmune diseases (Branzk et al., 2014; Grayson et al., 2016). In contrast, and in keeping with our current study, an anti-inflammatory, pro-resolving role for NETs was suggested in a murine model of MSU crystal-induced peritonitis (Schauer et al., 2014). Using very high concentrations of neutrophils, the investigators proposed that large, NADPH oxidase-dependent NET/crystal aggregates cause local degradation of pro-inflammatory cytokines, including IL-1β, through neutrophil-derived serine proteases (Schauer et al., 2014). In contrast, we could not demonstrate a role for NADPH oxidase activity in MSU-induced NETosis. This discrepancy could relate to a specific role for NADPH oxidase in the formation of large macromolecular aggregates, rather than involvement in the mechanism of NETosis *per se*. ROS generation may also shield neutrophil serine proteases against serum inhibitors, such as α2-macroglobulin (Abbink et al., 1991), perhaps accounting for the otherwise unexplained dose-dependent enhancement of serine protease activity in aggregated NETs. Examining the consequences of NETosis *in vivo* is challenging as the phenotypes of specific gene knockouts, such as PAD4, NE, NADPH components etc., all extend beyond neutrophils

and NETosis. Using a simplified, *in vitro* co-culture system, we found NETosis reduced THP-1 cell IL-1β release in response to MSU crystals in a DNA-dependent manner and that neutrophils reduced MSU-induced THP-1 cell death. The coating and clumping of MSU crystals we demonstrated by live cell and fixed imaging approaches suggest that NETs sequester crystals away from macrophages, providing a striking parallel to the DNA coated, non-inflamed tophi we found in patients with tophaceous gout. This hypothesis needs further exploration, as does the potential cytokine-degrading role of neutrophil serine proteases as proposed by Schauer et al. Other potential anti-inflammatory roles of neutrophils could include the production of anti-inflammatory mediators, such as Annexin A1 as well as promoting the development of an anti-inflammatory phenotype in surrounding macrophages. The role of NETs is likely to be disease dependent, but in the context of gout, our data suggest that NETs sequester MSU crystals from tissue macrophages. This sequestration helps resolve acute gout and prevents persistent inflammation, albeit at the expense of progressive accumulation of crystals, causing chronic, but non-inflammatory tophaceous gout.

4 THE RELATIONSHIP BETWEEN NETOSIS, NECROPTOSIS AND APOPTOSIS

4.1 Introduction

Timely cell death is vital for tissue homeostasis. Under steady-state conditions, apoptosis is an important form of programmed cell death (Kerr et al., 1972). It is characterised by orderly dismantling of the cell and labelling of cell remnants for removal by phagocytes. Recently, other forms of regulated cell death distinct from apoptosis have been recognised, including pyroptosis and necroptosis. These forms of cell death have different mechanisms and consequences (Tait et al., 2014). By virtue of being lytic, non-apoptotic cell death may be accompanied by release of cellular contents, including danger associated molecular patterns (DAMPs), capable of inciting inflammation.

Apoptosis requires the activation of a cascade of cysteine proteases called caspases, commencing with initiator caspases (Nicholson, 1999). Initiation of apoptosis may occur through one of two pathways. The extrinsic pathway is initiated by the binding of death receptor ligands (e.g. FasL, TNFα or TRAIL) to the cognate death receptor that activates caspase-8. The intrinsic pathway is triggered by cellular stress or growth factor withdrawal (Danial & Korsmeyer, 2004) leading to the mitochondrial leakage of cytochrome c that activates apoptotic peptidase activating factor 1 (Apaf-1). This leads to assembly of the apoptosome (Li et al., 1997) and activation of caspase-9. Both caspase-8 and caspase-9 cleave and activate executioner caspases, such as caspase-3, which that dismantle the cell and flag the cell for disposal (for example, by changes in cell membrane constituents, such as exposure of phosphatidylserine), whilst preventing spillage of cellular contents and activation of immune pathways (White et al., 2014).

Pyroptosis requires the inflammatory caspase-11 or caspase-1, activation, leading to cleavage of the death effector protein, gasdermin D, which results in cell permeabilization and consequent DAMP release (Ding et al., 2016; Kayagaki et al., 2015; J. Shi et al., 2015). A recent study has demonstrated a parallel pyroptotic pathway with chemotherapy-induced caspase 3 activation resulting in cleavage of Gasdermin E and liberation of membranolytic fragments (Wang et al. 2017). Apoptosis and necroptosis share elements of the extrinsic apoptosis pathway with both forms of

cell death initiated by the ligation of death receptors and activation of Caspase-8. Necroptosis occurs when caspase-8 activity is inhibited. Proteins from viruses such as cytomegalovirus can inhibit caspase-8 and may serve to enhance viral pathogenesis by preventing apoptosis (Mocarski et al., 2011). Caspase-8 activity may also be inhibited experimentally using chemical inhibitors or genetically using Caspase-8 gene deficient mice (Silke et al., 2015). Caspase-8 inhibition under these conditions leads to the formation of the necrosome, a molecular platform containing receptor-interacting protein kinase 1 (RIPK1), receptor-interacting protein kinase 3 (RIPK3) and mixed lineage kinase domain-like (MLKL) (J M Murphy & Silke, 2014). This triggers necroptosis, a caspase-independent form of regulated cell death with cell membrane compromise and release of DAMPs that can drive inflammation (Rickard et al., 2014).

Another recently identified form of cell death is NETosis – the death of neutrophils in the context of neutrophil extracellular trap (NET) release (Brinkmann et al., 2004). NETosis is believed to occur independently of caspases, and phosphatidylserine exposure occurs only after cell death, consistent with non-apoptotic cell death (Fuchs et al., 2007). The relationship between NETosis and other forms of cell death remains unclear. It is unlikely NETosis is related to pyroptosis as caspase inhibitors (e.g. ZVAD-fmk) do not prevent NETosis (Remijsen, Vanden Berghe, et al., 2011) and should adequately suppress caspase-1 and -11 function. Inhibitors of necroptosis have been used in previous NETosis studies with inconclusive results. Necrostatin-1 (10 μM) failed to inhibit PMA-induced NETosis (Remijsen, Vanden Berghe, et al., 2011). Desai *et al.* found inhibition of RIPK1 with necrostatin-1 or necrostatin-1s at 50 μM with 30 minute incubation prior to stimulation, or MLKL with necrosulfonamide (NSA) at 5μM, with less pronounced protection at 1μM, prevented monosodium urate crystal- (MSU) or PMA-induced NET formation in human and mouse neutrophils at a 2 hour time point (Desai et al., 2016) The authors also demonstrated phosphorylation of MLKL during PMA stimulation. This was corroborated with genetic analysis using *Ripk3*$^{-/-}$ mice to demonstrate reduced air pouch NET generation and crystal aggregation. However, Amini *et al.* simultaneously reported no involvement of the necroptosis pathway during NETosis. Once again chemical inhibitors of the necroptosis pathway were used but failed to decrease human neutrophil NETosis in response to a series of stimuli including GM-CSF and complement factor 5a (C5a), *E. coli* and PMA after 45 minutes. Neutrophils from the *Ripk3*$^{-/-}$ mouse failed to release NETs after GM-CSF priming and treatment with C5a (Amini et al., 2016). This study focused on DNA release from living neutrophils and did not demonstrate increased rates of death associated with NET

release. Assessment of PMA stimulated neutrophils after 45 minutes is unlikely to encapsulate any cell death or "lytic" NETosis, because previous studies have shown these processes to occur after a minimum of one hour after stimulation (Fuchs et al., 2007).

The discrepancy in the findings has highlighted a major problem in the nascent NETosis field: methodological differences in mechanistic studies can give rise to vastly different conclusions (Naccache & Fernandes, 2016). A lack of standardization of measurement of NETosis and the lack of reliable, quantitative and kinetic assays makes comparing studies difficult. In the case of the two aforementioned necroptosis/NETosis studies that reached contrasting conclusions (Desai et al. and Amini et al.), differences in strategies of stimulation and experimental timeframes also raise the possibility that different forms of NET release may be being monitored.

With this in mind, we revisited the controversial role of the necroptosis pathway and chemical inhibitors thereof in NETosis, using the quantitative, live cell assay described in Chapter 2. Unexpectedly, we found that some, but not all, tested inhibitors did indeed reduce NETosis. In particular, two structurally distinct compounds previously demonstrated to target MLKL, Hit #14 (Sun et al., 2012) and GW806742X (Hildebrand et al., 2014) as well as a more potent derivative of GW806742X reduced NETosis. NETosis reduction was caspase-dependent, highlighting two important phenomena:

(i) caspases govern the ability of neutrophils to respond to PMA, suggesting that commitment to the apoptosis pathway precludes NETosis

(ii) some drugs targeting MLKL clearly accelerate apoptosis in neutrophils, although the mechanism involved is yet to be determined.

4.2 Results

4.2.1 Chemical inhibition of the cell death pathways and NETosis

4.2.1.1 Inhibitors of the necroptosis pathway do not inhibit PMA-induced NETosis when added 1 hour prior to stimulation

Given the controversy surrounding the role of the necroptosis pathway in NETosis, healthy control neutrophils were treated for one hour with inhibitors of key members of the necroptosis pathway prior to stimulating with PMA (Figure 4.1) including: a RIPK1 inhibitor, necrostatin-1; a RIPK3 inhibitor, GSK832 (Kaiser et al., 2013); the MLKL

inhibitor, necrosulfonamide (NSA) (Sun et al., 2012), and the RIPK1/MLKL dual inhibitor, GW806742X (Hildebrand et al., 2014). None of the inhibitors altered the frequency or kinetics of NETosis.

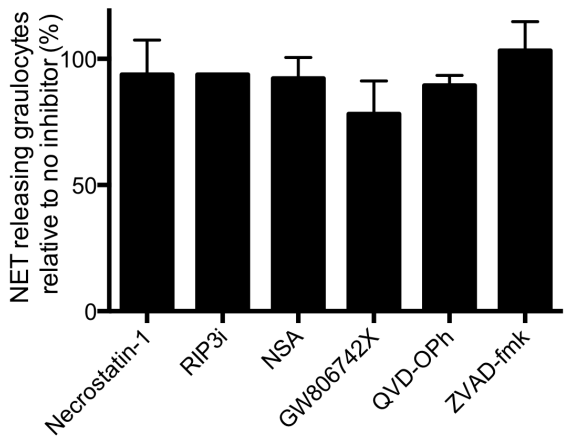


Figure 4.1 Inhibitors of the necroptosis pathway do not inhibit PMA-induced NETosis

Neutrophils were incubated with inhibitor for one hour prior to stimulation. Necrostatin-1 (10 μM, n=3), GSK832 (RIP3i - 10 μM, n=3), necrosulfonamide (NSA - 10 μM, n=4), GW806742X (2 μM, n=4), QVD-OPh (1.67 μM, n=4) and ZVAD-fmk (10 μM, n=3). NET release at 240 minutes expressed as a percentage of the NET release in the absence of inhibitor from the matching experiment. Values represent mean ± SEM

Coupled with my earlier findings in MSU-induced NETosis (Figure 3.42), these results suggest that necroptosis is not directly implicated in PMA-induced NETosis or MSU-induced NETosis. Of note, inhibition of caspases with either QVD-OPh or ZVAD-fmk (Figure 4.1) did not decrease PMA-induced NETosis, consistent with NETosis being a non-apoptotic form of cell death.

4.2.1.2 Hit #14, an MLKL inhibitor, inhibits apoptosis in a time-dependent manner

Hit #14 is an inhibitor of MLKL and is the initial compound from which NSA was derived (Sun et al., 2012). Hit #14 had a minimal effect on NETosis when incubated for one hour prior to addition of PMA. Unexpectedly, prolonged incubation for three hours with Hit #14 prior to PMA stimulation did reduce NETosis (Figure 4.2). More prolonged incubation for 5 hours prior to PMA resulted in complete inhibition of NETosis and this effect was dose-dependent.

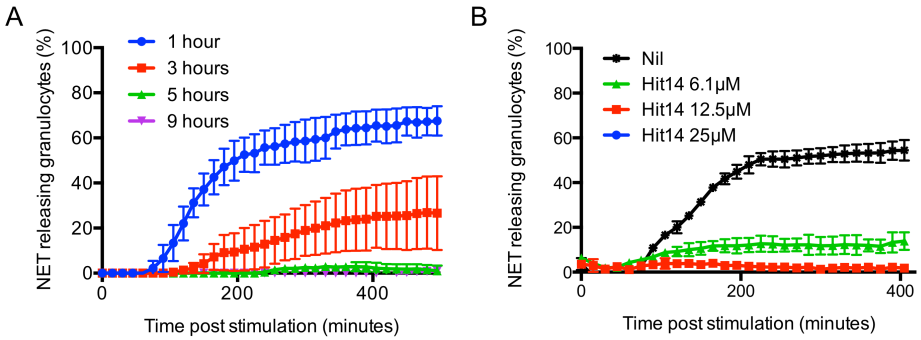


Figure 4.2 Hit #14, an inhibitor of necroptosis, inhibits PMA-induced NETosis in a time- and dose-dependent fashion

Quantitative time-lapse live cell imaging demonstrates PMA-induced NETosis in neutrophils A) incubated with Hit #14 (25μM) for indicated times prior to stimulation. Values represent mean ± SEM, n = 3 separate donors. Significant differences in NETosis percentage between 1 hour incubation versus 3 hours, 5 hours and 9 hours ($P<0.01$) assessed with two way ANOVA with repeated measures. B) Hit #14 at indicated concentrations for 5 hours prior to stimulation. n = 2 duplicates mean ± SEM.

Of note, this effect on NETosis was not evident with NSA (Figure 4.3), which in studies of TNF-α, Smac mimetic, and ZVAD-fmk-induced necroptosis in HT-29 cells is 5-fold more potent than Hit #14 (Liao et al., 2014). Incubation for 3 hours with the RIPK1 inhibitor, necrostatin-1 and a RIPK3 inhibitor, GSK832 also failed to reduce NETosis in a similar fashion (Figure 4.3). Hit #14 and necrosulfonamide bind MLKL via covalent modification of Cys86 to form a disulphide bond (Liao et al., 2014). No off-target effects have been reported as yet but the reactive nature of the compound suggests there is potential for further reactions with other proteins and hence off-target effects.

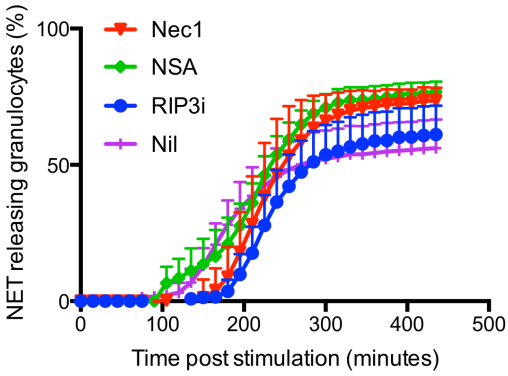


Figure 4.3 Prolonged incubation with inhibitors of RIPK1, MLKL and RIPK3 does not inhibit NETosis

Quantitative time-lapse live cell imaging demonstrates PMA-induced NETosis in neutrophils incubated for three hours with Necrostatin-1 (Nec-1, 10 μM), GSK832 (RIP3i, 10 μM), necrosulfonamide (NSA, 10 μM) for indicated times prior to stimulation. Values represent mean ± SEM, n = 3.

4.2.1.3 MLKL inhibitors targeting the ATP binding site also inhibit NETosis in a time-dependent fashion

To explore this possible effect on MLKL further, we used MLKL targeting compounds generated in-house at WEHI. GW806742X is the first generation compound that targets the nucleotide-binding site of both murine and human MLKL and inhibits necroptosis robustly at 1 μM (Hildebrand et al., 2014). This compound was initially identified as a VEGFR2 inhibitor and does demonstrate off-target effects, inhibiting RIPK1 in particular. Given the lack of effect of Necrostatin-1 in this assay, it is unlikely that the RIPK1 inhibitory activity of these compounds would account for their efficacy in reducing NETosis. Only at 4 μM did GW806742X demonstrate a modest non-significant reduction in NETosis after 3-hour incubation (Figure 4.4). A structurally related compound, termed “WEHI-929”, which does not inhibit necroptosis in cultured mouse or human cells, did not inhibit NETosis.

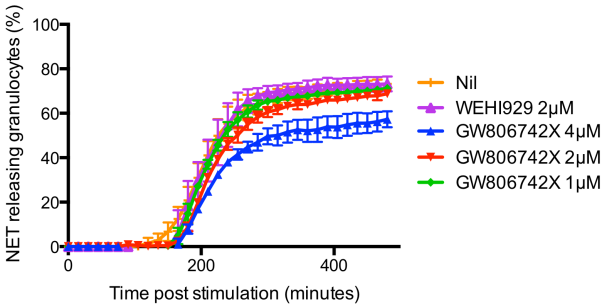


Figure 4.4 Prolonged incubation with a MLKL inhibitor does not inhibit NETosis

Quantitative time-lapse live cell imaging demonstrates PMA-induced NETosis in neutrophils incubated for three hours with GW806742X at the indicated concentrations. Difference between GW806742X at 4 μM and untreated p=0.09 assessed with two way ANOVA with repeated measures. Values represent mean ± SEM, n = 2.

WEHI781 is a second-generation compound that inhibits necroptosis with higher potency than GW806742X (James Murphy, personal communication). At 2 μM, WEHI781 inhibited NETosis when incubated for two hours, with a more apparent effect after five hours (Figure 4.5).

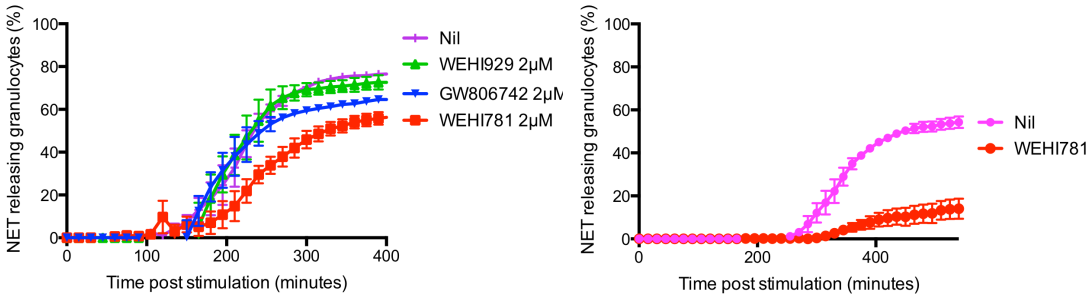


Figure 4.5 Prolonged incubation with a more potent MLKL inhibitor inhibits NETosis

Quantitative time-lapse live cell imaging demonstrates PMA-induced NETosis in neutrophils incubated for (A) three hours and (B) five hours with GW806742X at the indicated concentrations. Difference between WEHI781 and untreated p<0.01 assessed with two way ANOVA with repeated measures. Values represent mean ± SEM, n = 2.

These data suggest that a number of compounds reduce the ability of neutrophils to undergo NETosis, herein termed “NET competence”. The compounds that diminish NETosis ostensibly target MLKL, whereas inhibitors of other components of the necroptosis pathway did not reduce NET competence. While this implicates MLKL specifically in NETosis, we cannot exclude the possibility that these compounds impact NETosis through off target effects.

4.2.2 Ability to undergo NETosis, or "NET competence" diminishes with time

It was noted that the ability of neutrophils to undergo NETosis in response to PMA diminished with time in culture, even in the absence of any inhibitor (Figure 4.6). After five hours, the rate of NETosis had reduced to around half of that observed in the same neutrophils stimulated after one hour. This dropped to around 25% after nine hours.

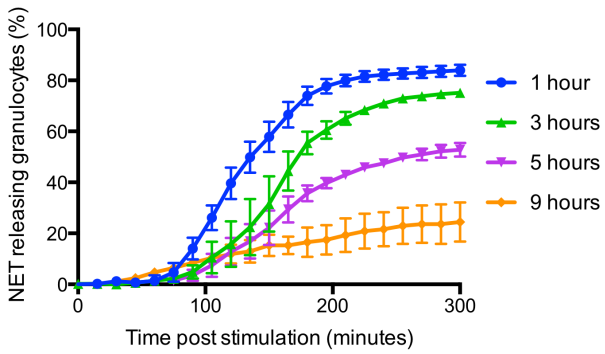


Figure 4.6 The ability of neutrophils to undergo PMA-induced NETosis diminishes with time in culture

Quantitative time-lapse live cell imaging demonstrates NETosis in neutrophils stimulated with PMA at various times as indicated after incubation in culture media. Values represent mean ± SEM, n = 3. Significant differences in NETosis percentage between 1-hour incubation versus 3 hours, 5 hours and 9 hours ($P<0.05$) assessed with two way ANOVA with repeated measures.

Microscopic observation of the aged neutrophils revealed failure to undergo the flattening, spreading and vacuolization normally observed with PMA stimulation (Figure 4.7). The Hit #14 and WEHI781 treated neutrophils similarly fail to spread and remained rounded. A simple metric of this failure to spread was the change in average neutrophil diameter, measured during the cell count of CTG fluorescence. This example shows an increase in diameter with PMA after 15 minutes that fails to occur with Hit #14 treatment, suggesting that neutrophils treated in this way were no longer responsive to PMA.

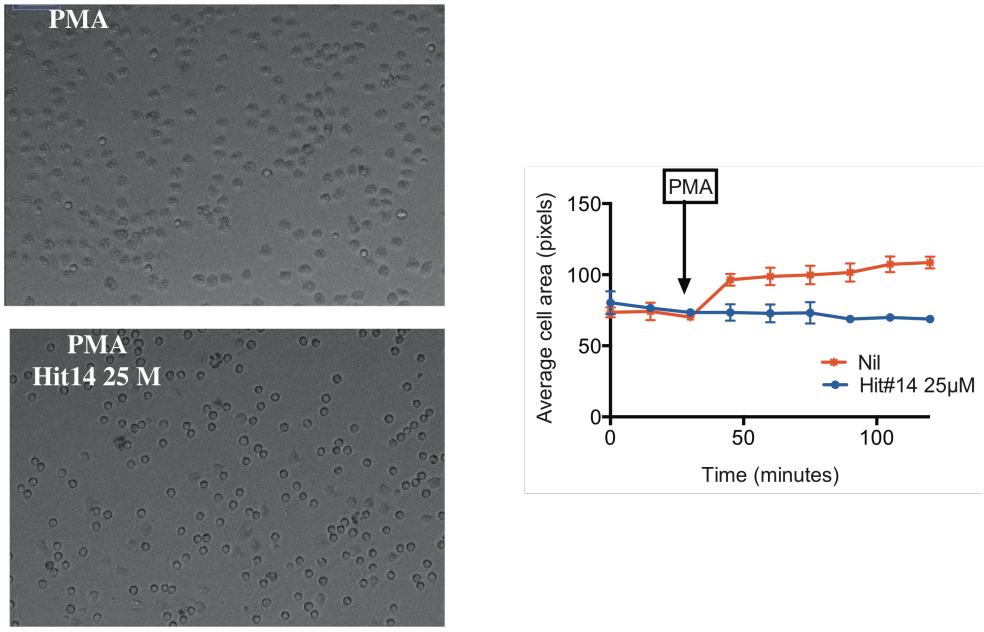


Figure 4.7 Neutrophils fail to spread in response to PMA when pre-treated with Hit #14

A) Phase contrast images taken at 1 hour after PMA stimulation (taken from time-lapse experiments) with and without Hit #14 (25 μM) treatment for 2 hours.
B) Average diameter of cell-tracker green labelled neutrophils from time-lapse experiments with PMA stimulation in neutrophils pre-incubated with and without Hit #14 (25 μM) treatment for 2 hours. Values represent mean ± SEM, n=2.

PMA-induced ROS generation, as detected over 24 minutes by luminol-enhanced chemiluminescence, was also suppressed with Hit #14 and again the suppression was more prominent with time (Figure 4.8).

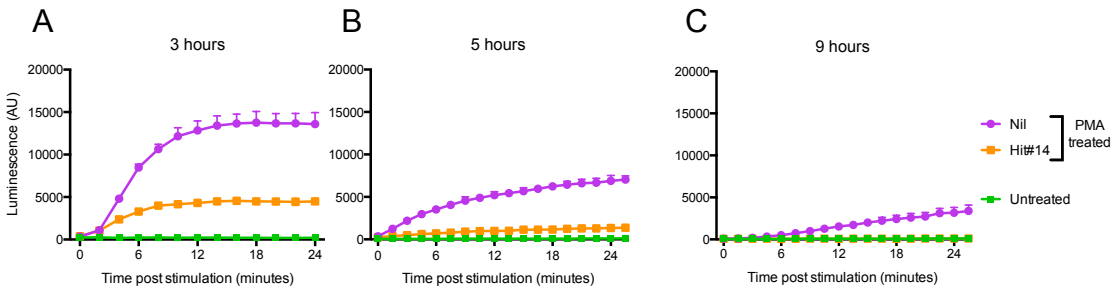


Figure 4.8 Neutrophils demonstrate reduced reactive oxygen species generation in response to PMA over time, further reduced when pre-treated with Hit #14

Luminol-enhanced chemiluminescence induced by PMA is inhibited by Hit #14 treatment incubated for (A) 3 hours, (B) 5 hours and (C) 9 hours prior to stimulation. Representative curves from two separate experiments with different donors. Values represent mean ± SEM from the triplicate experiment.

4.2.2.1 Loss of NET competence is associated with accelerated apoptosis

The time-dependent reduction in functionality suggested that neutrophils were undergoing apoptosis. Neutrophils are known to undergo spontaneous apoptosis in cell culture, regardless of the presence or absence of serum (Xu et al., 2010). Using the live cell platform, apoptosis was assessed by adding fluorescent annexin V to the media to label phosphatidylserine, which is exposed at the cell surface during apoptosis (Khosla et al., 2005; S. J. Martin et al., 1995; W. Shi et al., 2017). Both Hit #14 and WEHI781 conditions led to a higher percentage of Annexin V positive cells than untreated controls at 9 hours, with no difference in a measure of cell death, PI positivity (Figure 4.9). Caspase inhibition with QVD-OPh prevented PS exposure at 9 hours. At 9 hours, a time-point when the majority of neutrophils treated with Hit #14 have lost ”NET competence” in separate experiments, only 20% of Hit #14 treated neutrophils expressed phosphatidylserine. This suggests that NET competence is lost prior to phosphatidylserine exposure and is an early consequence of apoptosis.

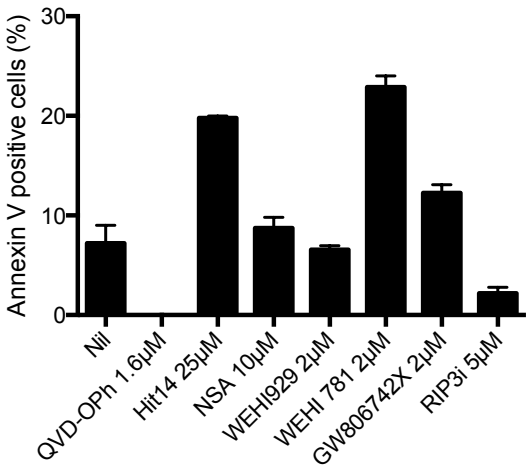


Figure 4.9 Hit #14 and WEHI781 accelerate neutrophil apoptosis

Annexin V positive cells measured using live cell imaging as a percentage of total neutrophils after 9 hours of incubation with QVD-OPh (1.67 μM, n=4), Hit #14 (25 μM), necrosulfonamide (NSA - 10 μM, WEHI929 (2 μM), WEHI781 (2 μM), GW806742X (2 μM) and GSK832 (RIP3i - 10 μM). Values represent mean ± SEM, n=2 .

4.2.2.2 Loss of NET competence is caspase-dependent

Given the evidence that the compounds that decrease NET competence were also inducers of apoptosis, the role of caspases was investigated. QVD-OPh-treated

neutrophils retained NET competence out to 9 hours (Figure 4.10). This suggests time-dependent loss of NET competence was due to caspase activation.

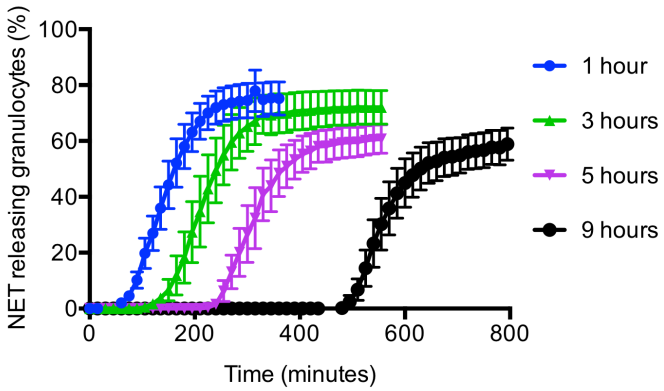


Figure 4.10 Caspase inhibition prevents the time-dependent loss of NET competence

Quantitative time-lapse live cell imaging demonstrates NETosis in neutrophils stimulated with PMA at various times after incubation with QVD-OPh (1.67 μM, times as indicated). Values represent mean ± SEM, n = 3.

G-CSF is a cytokine with known neutrophil anti-apoptotic activity REF. Here, we observed that G-CSF also prolonged NET competency, albeit not as potently as QVD-OPh (Figure 4.11). G-CSF alone did not induce NETosis.

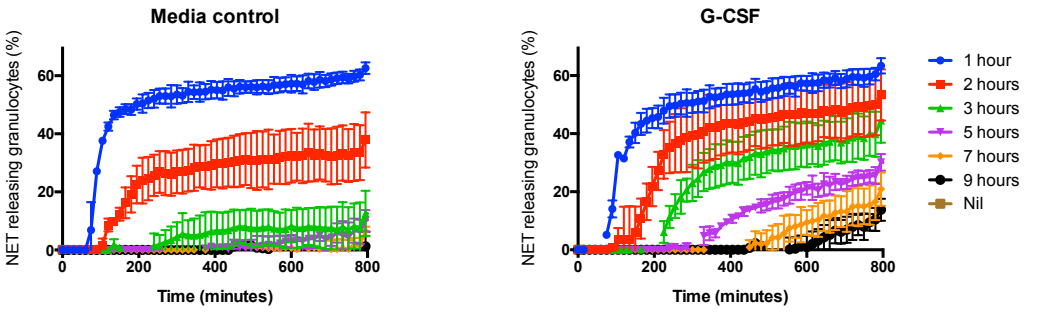


Figure 4.11 G-CSF delays the time-dependent loss of NET competence

Quantitative time-lapse live cell imaging demonstrates NETosis in neutrophils stimulated with PMA at various times after incubation with G-CSF (50 ng/ml, times as indicated). Values represent mean of experimental duplicates ± SEM, single donor

4.2.2.3 The effect of WEHI781 and Hit #14 on NET competence is mediated via caspase activation

Given the prominent effect of caspase activation on NET competence, we hypothesized that the observed effect of Hit #14 and WEHI781 may be dependent on caspase activation. QVD-OPh completely prevented the NETosis inhibitory effect of both compounds (Figure 4.12). This finding suggests these compounds are accelerating apoptosis and the mechanism on NETosis inhibition is indirect.

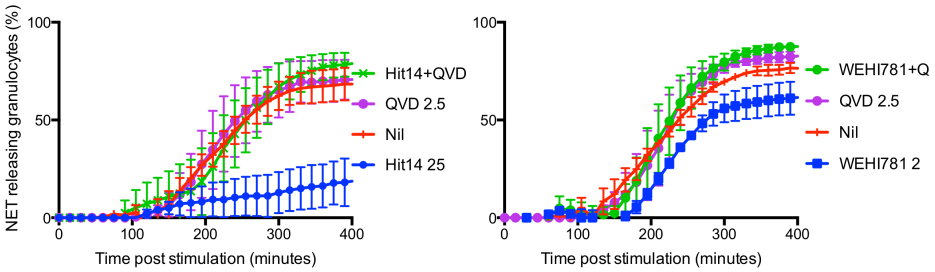


Figure 4.12 Hit #14 and WEHI781-induced loss of NET competence is caspase-dependent

Quantitative time-lapse live cell imaging demonstrates PMA-induced NETosis in neutrophils incubated for 3 hours with (A) Hit #14 (25 μM) or (B) WEHI781 (2 μM) with or without QVD-OPh (1.67 μM). Values represent mean ± SEM, n = 2. Significant differences in NETosis percentage between Hit #14 or WEHI781 versus the compound and QVD-OPh $P<0.05$ assessed with two way ANOVA with repeated measures.

Interestingly, another broad specificity caspase inhibitor, ZVAD-fmk, failed to preserve NET competence, in contrast to our observations using QVD-OPh (Figure 4.13). This finding is consistent with a report that ZVAD-fmk poorly inhibits spontaneous neutrophil apoptosis compared to QVD-OPh (Wardle et al., 2011).

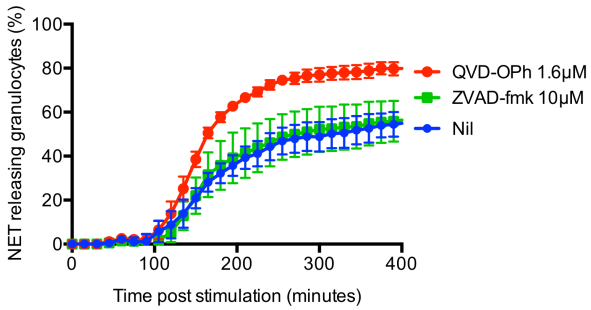
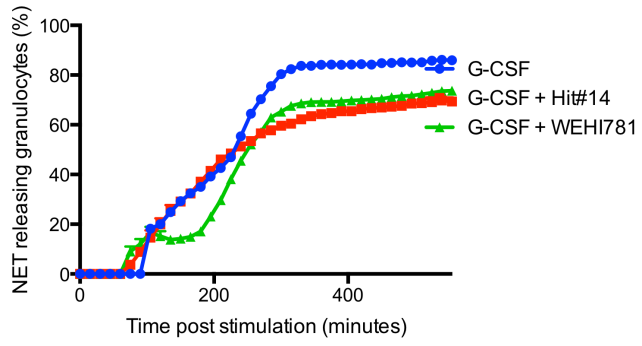


Figure 4.13 QVD-OPh but not ZVAD-fmk prevents time-dependent loss of NET competence

Quantitative time-lapse live cell imaging demonstrates PMA-induced NETosis in neutrophils incubated for 5 hours QVD-OPh (1.6 μM) or ZVAD-fmk (10 μM). Values represent mean ± SEM, n = 4.

Neutrophil apoptosis is delayed in inflammatory contexts (such as an inflamed joint of a patient with rheumatoid arthritis (Dibbert et al., 1999)), where mediators such as cytokines and DAMPs can exert an anti-apoptotic effect. In neutrophils incubated with G-CSF, a pilot experiment suggests WEHI781 and Hit #14 can reduce NET competence (Figure 4.14).



vers

Figure 4.14 Hit #14 and WEHI781 may subtly reduce NETosis in G-CSF-primed neutrophils

Quantitative time-lapse live cell imaging demonstrates PMA-induced NETosis in neutrophils incubated for 3 hours with (A) Hit #14 (25 μM) or (B) (WEHI781, 2 μM) with G-CSF (50 ng/ml). Values represent mean, n = 1.

4.2.2.4 Inhibition of Caspase-3 but not caspases-8 or -9 may maintain NET competence

Which caspases are involved in spontaneous neutrophil apoptosis remains unclear (Hampson et al., 2013). We assessed the role of the extrinsic pathway, the intrinsic

pathway and the common executioner pathway using inhibitors of caspase-8 (IETD-CHO, also inhibits Granzyme B), caspase-9 (LEHD-CHO, may also inhibit caspase 4 and 5) and caspase-3 (z-DEVD-fmk, also inhibits caspase 6, 7, 8, and 10 less potently) respectively. Only QVD-OPh and the caspase-3 inhibitor significantly retained NET competency in a pilot experiment (Figure 4.15), supporting the possibility that caspase3 is an important mediator of loss of NET competence. The lack of evidence for either the intrinsic or extrinsic pathways requires confirmation, but supports alternative activation of caspase-3 in neutrophils. One candidate protease, Proteinase 3, a neutrophil granule enzyme has been proposed to cleave caspase-3 and lead to spontaneous neutrophil apoptosis (Loison et al., 2014).

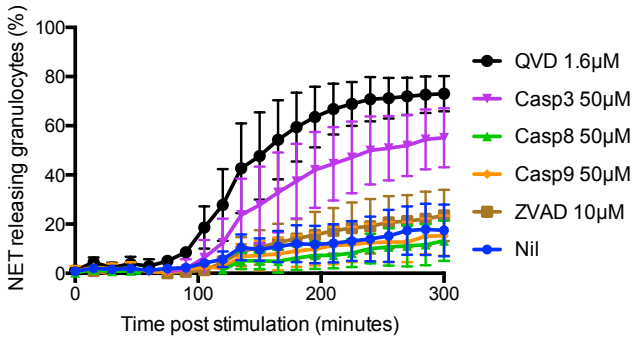


Figure 4.15 QVD-OPh and a caspase-3 inhibitor prevent loss of NET competence

Quantitative time-lapse live cell imaging demonstrates PMA-induced NETosis in neutrophils incubated for 3 hours with caspase-8 inhibitor (Casp8), caspase-3 inhibitor (Casp3), caspase-9 inhibitor (Casp9), QVD-OPh or ZVAD. Values represent mean of duplicates ± SEM, single donor.

4.2.2.5 Triggering extrinsic apoptosis with FasL attenuates NET competence in a caspase-dependent manner

To examine whether activation of the extrinsic pathway of apoptosis could abrogate NET competence, the death receptor agonist Fas ligand (linked to Fc (Croker et al., 2011)]) was added one hour before, ten minutes before or simultaneously with PMA. Treatment with FcFasL an hour prior to PMA completely abrogated NETosis and partial reduction in NETosis was evident when the FcFasL was added at the same time as the PMA. This effect was inhibited with QVD-OPh (Figure 4.16). Interestingly, QVD-OPh/FasL alone without PMA stimulation appeared to induce neutrophil cell death, without chromatin decondensation (Figure 4.1B). These observations raise interesting questions about the mode of cell death that will be the focus of future studies.

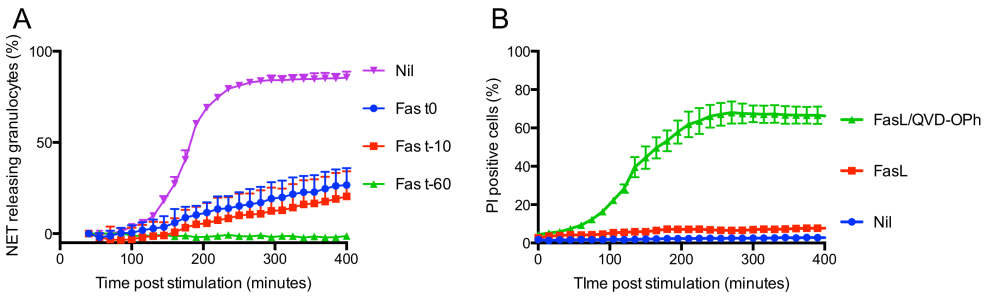


Figure 4.16 Fas ligand prevents NETosis in a caspase-dependent manner

Quantitative time-lapse live cell imaging of PMA-induced NETosis. (A) Neutrophils were treated with FasL at various times before stimulation with PMA (time t is the minutes before PMA stimulation). (C) FasL and QVD-OPh induce non-NETosis cell death. Values represent mean of duplicates ± SEM, single donor.

4.2.2.6 Inhibition of other protein kinases does not diminish NET competence

One reason to be circumspect about the results is the concern about off-target effects of these compounds. Small molecules often exhibit inhibitory effects against multiple enzymes and several tyrosine kinases have been suggested to play roles in neutrophil survival. We examined whether protein kinases might play a role by conducting a screen of chemical inhibitors for effects on NET competency, although none of the examined inhibitors exerted any obvious reduction (Figure 4.17). Only WEHI781 reduced NETosis, whilst QVD-OPh maintained NET competence.

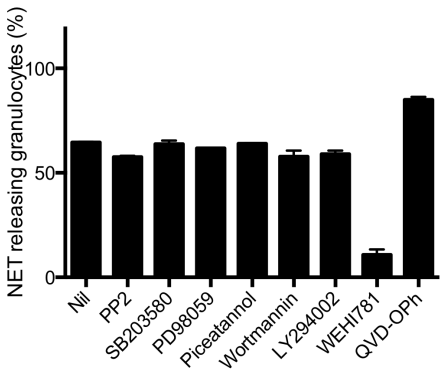


Figure 4.17 A panel of kinase inhibitors does not reduce NET competence

Neutrophils were incubated with inhibitor for five hours prior to stimulation. PP2 (Src kinase inhibitor, 50μM), SB203580 (p38MAPK inhibitor, 50μM), Piceatannol (Syk inhibitor, 50μM), Wortmannin (PI3K inhibitor, 1μM), LY294002 (PI3K inhibitor, 20μM), WEHI 781 (2 μM), QVD-OPh (1.67 μM). NET release at 240 minutes from time-lapse experiments. Values represent mean ± SEM, n=2.

4.2.2.7 Roscovitine, a cyclin-dependent kinase inhibitor has a modest effect on NET competence

Roscovitine is an inhibitor of cyclin dependent kinases that has previously been shown to have a cell-specific effect on enhancing neutrophil apoptosis (A. G. Rossi et al., 2006). After five hours of incubation, Roscovitine had minimal effect on NET competence at concentrations up to 40 μM (Figure 4.18).

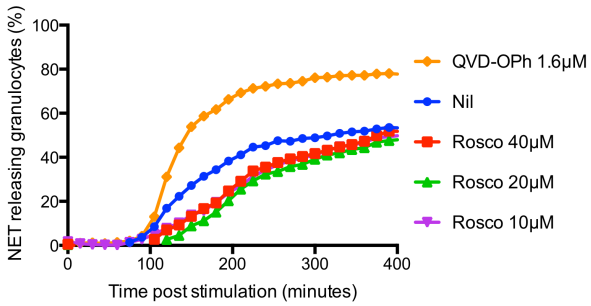


Figure 4.18 Effect of Roscovitine on NET competence

Quantitative time-lapse live cell imaging demonstrates PMA-induced NETosis in neutrophils incubated for 5 hours with Roscovitine at indicated concentration and QVD-OPh (1.67 μM). Mean values from a single donor.

4.2.3 Analysis of MLKL distribution

Given these unexpected findings, we attempted to assess the distribution of MLKL in human neutrophils during apoptosis. MLKL is isolated from the cytoplasmic compartment in macrophages and fibroblasts and moves to membranes during necroptosis (Hildebrand et al., 2014). Immunohistochemistry of endogenous MLKL also suggests a cytoplasmic distribution initially followed by nuclear translocation (Yoon et al., 2016). In a study of Concavalin A-induced hepatitis, murine hepatocytes from the inflamed liver contained cytoplasmic punctate MLKL staining at early time-points that became membrane associated at later time-points, consistent with changes of necroptosis (Gunther et al., 2016). There is little information on the expression and distribution of MLKL in primary human cells.

When phosphorylated by RIPK3, MLKL multimerizes and becomes associated with membranes (Hildebrand et al., 2014). Increasing evidence suggests that this activated MLKL itself is sufficient to induce membrane permeability (Dondelinger et al., 2014; Linkermann et al., 2014; Su et al., 2014; Tanzer et al., 2017; H. Wang et al., 2014). A recent paper suggested that MLKL, RIPK1 and RIPK3 translocate to the nucleus in

HT29 cells upon necroptosis induction, prior to moving to the membrane (Yoon et al., 2016), although the ubiquity of this phenomenon remains unclear.

4.2.4 Immunofluorescence analysis

Immunofluorescence staining was performed using the anti-MLKL antibody clone 3H1, generated at the Walter and Eliza Hall Institute (J. M. Murphy et al., 2013) and validated in *Mlkl*$^{-/-}$ cells. Staining of neutrophils incubated for 1 hour on coverslips demonstrated punctate staining throughout the cell that was not apparent when the primary antibody was omitted (Figure 4.19).

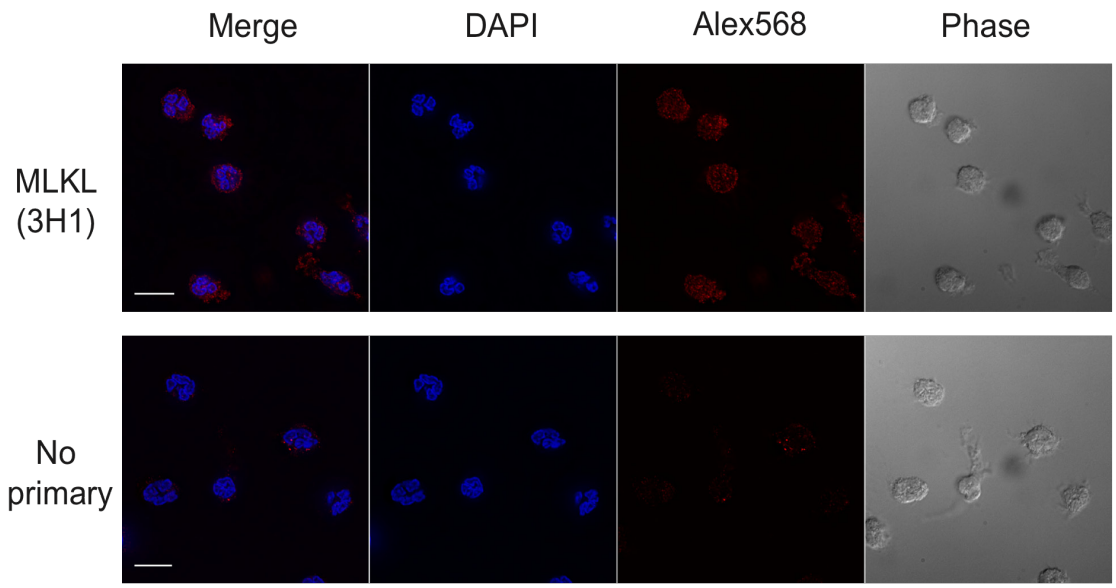


Figure 4.19 Immunofluorescence imaging of MLKL

High power fixed cell immunofluorescent images of unstimulated neutrophils from a healthy control. Images are a single representative slice of a z stack taken with the Deltavision Elite microscope with post acquisition deconvolution. Scale bar represents 10 μm. Fluorescent channels and phase contrast as labelled. Representative of experiments with two different donors.

PMA treatment did not induce any marked redistribution of the MLKL signal to suggest membrane localisation at 120 minutes, the time-point just prior to NETosis (Figure 4.20).

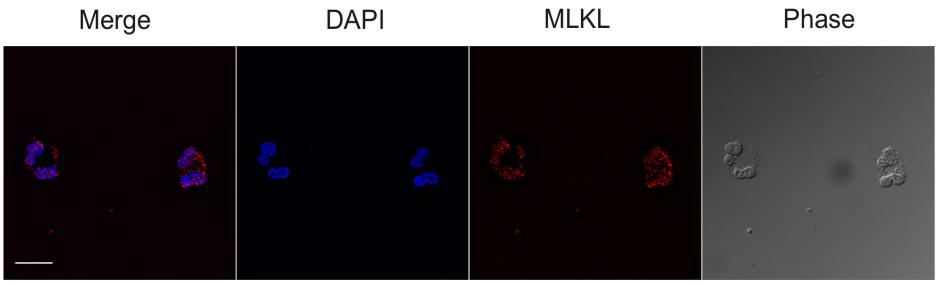


Figure 4.20 PMA does not induce major microscopic changes in MLKL distribution

High power fixed cell immunofluorescent images of PMA-treated neutrophils after 120 minutes of PMA stimulation. Images are a single representative slice of a z stack taken with the Deltavision Elite microscope with post acquisition deconvolution. Scale bar represents 10 μm. Fluorescent channels and phase contrast as labelled. Representative of experiments with two different donors.

Hit #14 and WEHI781 treated cells develop apoptotic nuclear morphology (Figure 4.21) after as little as four hours of incubation nuclear changes consistent with apoptosis with chromatin condensation and morphologic changes. These changes were only evident at later time-points in untreated neutrophils (24hrs). Of interest was the development of margination of the chromatin within the nucleus and the presence of a cavity without DNA in the centre of the nucleus, consistent with pyknosis (Majno & Joris, 1995).

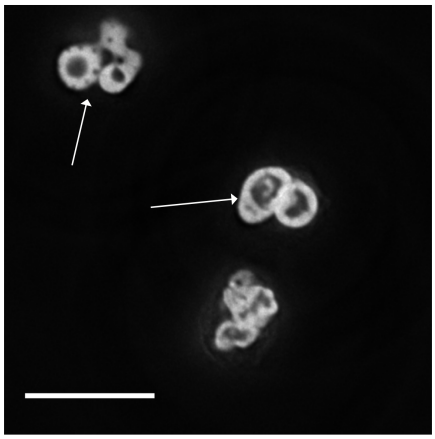


Figure 4.21 Hit #14-treated cells develop pyknotic nuclei

High power fixed cell immunofluorescent images of PMA-treated neutrophils after 4 hours in culture with Hit #14 25μM. The DAPI image is a single representative slice of a z stack taken with the Deltavision Elite microscope with post acquisition deconvolution. Scale bar represents 10 μm. Arrows indicate neutrophils with pyknotic nuclei, the remaining cell having a normal nucleus. Representative of experiments with four different donors

4.2.4.1 *Hit #14 fluorescence localises to the nucleus with prolonged incubation and this is paralleled by anti-MLKL staining*

Hit #14 caused remarkable fluorescence of the neutrophils in the absence of any immunofluorescence staining in a similar spectrum to Alexa488. The fluorescence underwent rapid photo-bleaching, which limits its usefulness for extensive imaging. However, at early time-points, the presumed Hit #14 fluorescence was evident in the cytosol. At later time points, Hit #14 fluorescence became concentrated in the nucleus, particularly in the DNA-free spaces within the pyknotic nuclei (Figure 4.22).

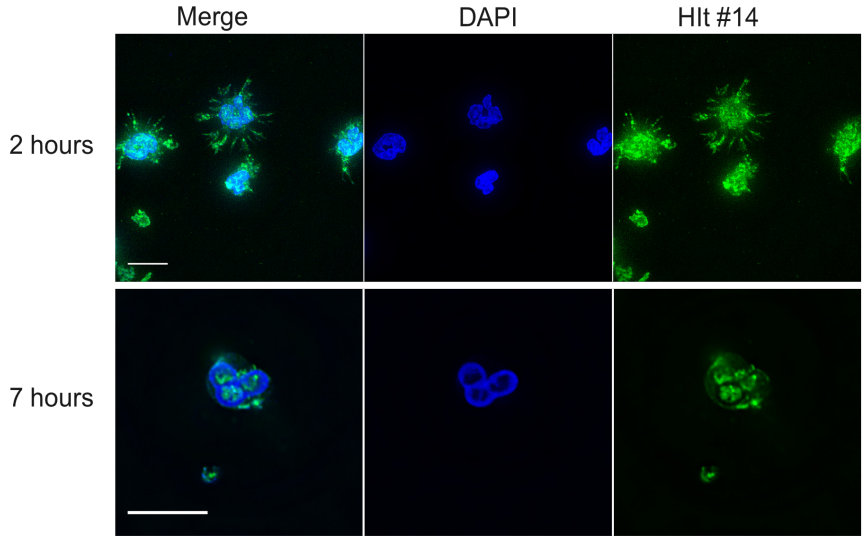


Figure 4.22 Fluorescent imaging analysis of Hit #14 and MLKL

Hit #14 fluorescence is evident throughout the neutrophils after 2 hours and becomes concentrated within the nuclei after 7 hours. Hit #14 fluorescence measured using the FITC excitation and emission parameters. Deltavision Elite single section from a z stack. Representative of experiments with four different donors.

Staining with anti-MLKL antibody at these later time-points demonstrated some localisation to the pyknotic nuclei, in particular in the spaces in the middle of the marginated chromatin. At 4 hours, MLKL at least partially localised to the nucleus in a distribution similar to Hit #14. The colocalization was not complete, however, with the Hit #14 signal more diffuse whilst anti-MLKL staining was punctate (Figure 4.23).

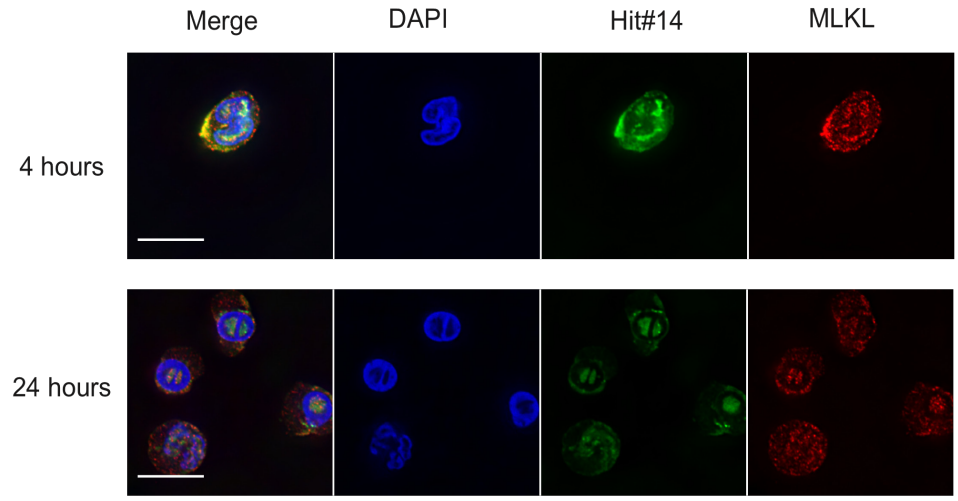


Figure 4.23 Fluorescent imaging of anti-MLKL-labelled neutrophils with Hit #14 fluorescence

Fixed cell microscopy visualising DAPI and anti-MLKL staining with Hit #14 fluorescence at 4 hours and 24 hours. Hit #14 fluorescence measured using the FITC excitation and emission parameters. Deltavision Elite maximum intensity projection of a limited z stack through the middle of the cell. Representative of experiments with three different donors.

4.2.4.2 MLKL nuclear localisation is seen with WEHI781 treatment and in spontaneous neutrophil apoptosis and is prevented by QVD-OPh

To determine whether the nuclear localisation of anti-MLKL staining was specific to Hit #14 treated cells, WEHI781-treated neutrophils were imaged after 7 hours and untreated neutrophils after 24 hours (Figure 4.24). Of note, at 24 hours, the adhesion of apoptotic cells is poor, so cytospins were performed as an adjunct. WEHI781 treated cells developed apoptotic morphology with similar accumulation of anti-MLKL signal in the nucleus. A plot of the intensity profile highlights that the MLKL signal, whilst nuclear, is not associated with the DNA signal. Neutrophils incubated for 24 hours without Hit #14 or WEHI781 also developed apoptotic morphology and the anti-MLKL signal was also enriched in the pyknotic nuclei. Some cells at 24 hours also developed features consistent with secondary necrosis.

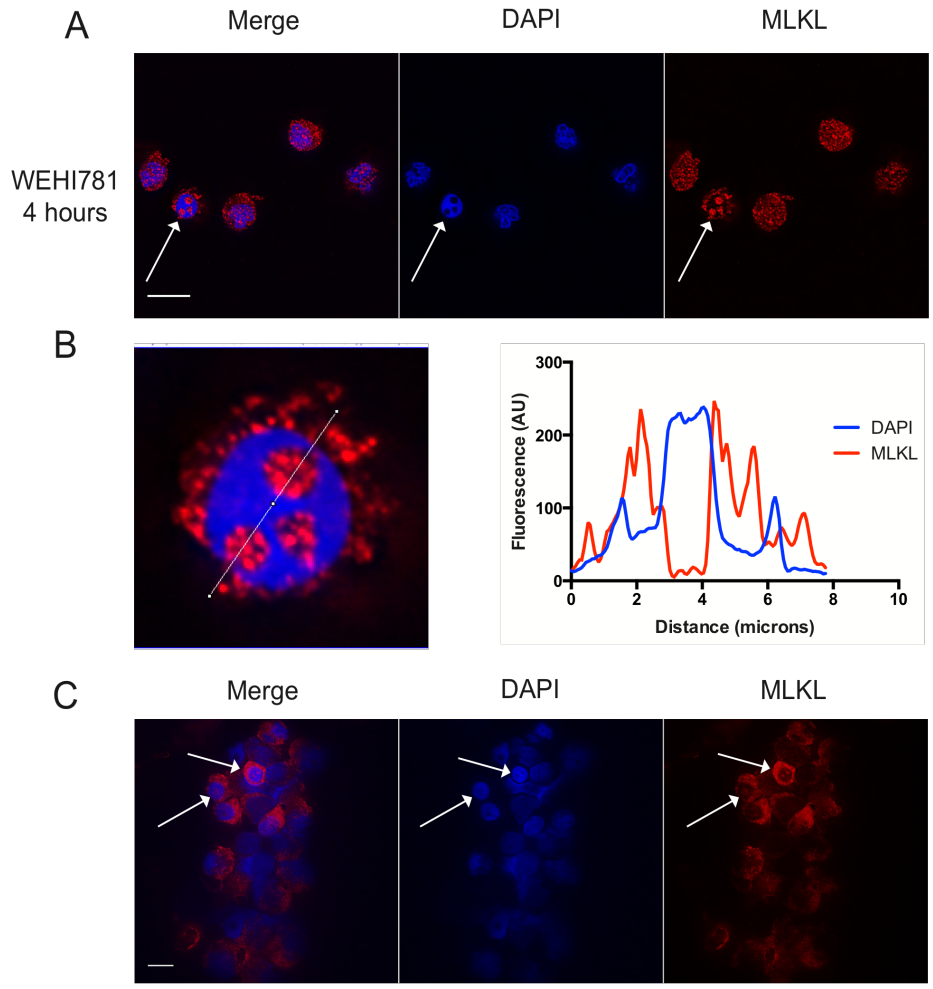


Figure 4.24 Fluorescent imaging of MLKL in WEHI781 and untreated neutrophils

Fluorescent imaging of neutrophils with DAPI and anti-MLKL antibody. A) WEHI781 treated neutrophils were fixed after 7 hours and stained as indicated. Arrow highlights a neutrophil with a pyknotic nucleus. B) The cell indicated in A) is enlarged and the profile of fluorescent intensity along a section is plotted. C) Cytospins of untreated neutrophils after 24 hours of incubation stained as indicated. Arrows highlight neutrophils with pyknotic nuclei. Representative of two separate experiments with different donors.

The localisation of MLKL in the nucleus was evident in pyknotic nuclei and suggests that the appearance is a consequence of apoptosis. QVD-OPh treatment abrogated Hit #14-induced nuclear pyknosis at eight hours and the MLKL signal appeared to remain cytoplasmic, forming larger aggregates (Figure 4.25).

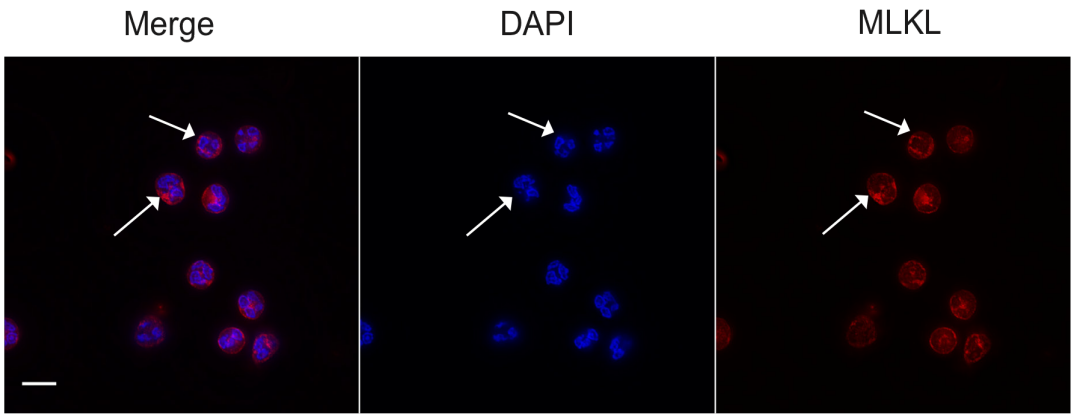


Figure 4.25 Fluorescent analysis of MLKL in Hit #14 and QVD-OPh-treated neutrophils

Anti-MLKL staining is evident in the cytoplasm of neutrophils treated with Hit #14 (25 μM) and QVD-OPh (1.6 μM) 4 hours. Extra-nuclear aggregates are indicated with arrows. Representative of two separate experiments with different donors.

4.2.5 Conclusions - Imaging studies of MLKL distribution of human neutrophils

The primary hypothesis tested in this chapter is whether NETosis shares the characteristics and machinery of cell death mediated by necroptosis. The lack of MLKL redistribution to the cell membrane in the context of NETosis and the lack of impact of RIPK1 and RIPK3 inhibitors on NETosis, are consistent with NETosis being distinct from necroptosis. The imaging findings in apoptotic neutrophils are interesting preliminary evidence that MLKL may be involved in processes other than necroptosis. The specificity of the antibody has been tested in murine models but it is not clear whether it might have off-target binding in human neutrophils. Competitive binding with MLKL protein titration would help to resolve this question. In other cell types, knockdown strategies could be employed to demonstrate specificity.

Accepting the important caveats of antibody specificity, MLKL appears to exhibit a punctate cytoplasmic distribution in human neutrophils. It is not clear what physical structures the MLKL antibody is staining. In caspase-dependent apoptosis, the MLKL staining is more pronounced within pyknotic nuclei, but not associated directly with DNA. This differs to the diffuse DNA associated staining seen in HT-29 undergoing necroptosis (Yoon et al., 2016). Whether this nuclear localisation is of mechanistic importance or simply an epiphenomenon will require further exploration.

The fluorescence exhibited by Hit #14 followed a similar pattern to the MLKL staining, becoming localised within pyknotic nuclei with time. Whilst some overlap between Hit

#14 and MLKL was observed, it was not complete and provides some evidence that Hit #14 is targeting MLKL specifically.

4.2.6 Western blotting demonstrates neutrophil MLKL expression

To further examine the distribution of MLKL with particular focus on membrane localisation, Western blotting was performed (Figure 4.26). Initially, neutrophils were all incubated with and without Hit #14 for a total of three hours with treatment with PMA 30 minutes and 60 minutes prior to the end of that 3-hour period. Cellular fractionation was performed to isolate cytoplasmic and membrane fractions, and the lysates then probed for expression of MLKL. Whole cell lysates from U937 cells served as positive controls for MLKL blotting. Expression of MLKL in neutrophils was predominantly cytoplasmic with limited membrane staining in any of the tested conditions. PMA did not appear to cause membrane redistribution of MLKL as observed during necroptosis. S100A8, an abundant neutrophil anti-bacterial protein served as the cytoplasmic loading control (molecular weight 11 kDa). Staining for membrane loading control remains to be optimised.

A lower molecular weight band was present in both neutrophils and U937 cells between 37 and 50 kDa. This band was not present in the PMA-treated neutrophils. Faint bands between 25 and 37 kDa were also seen, once again without PMA.

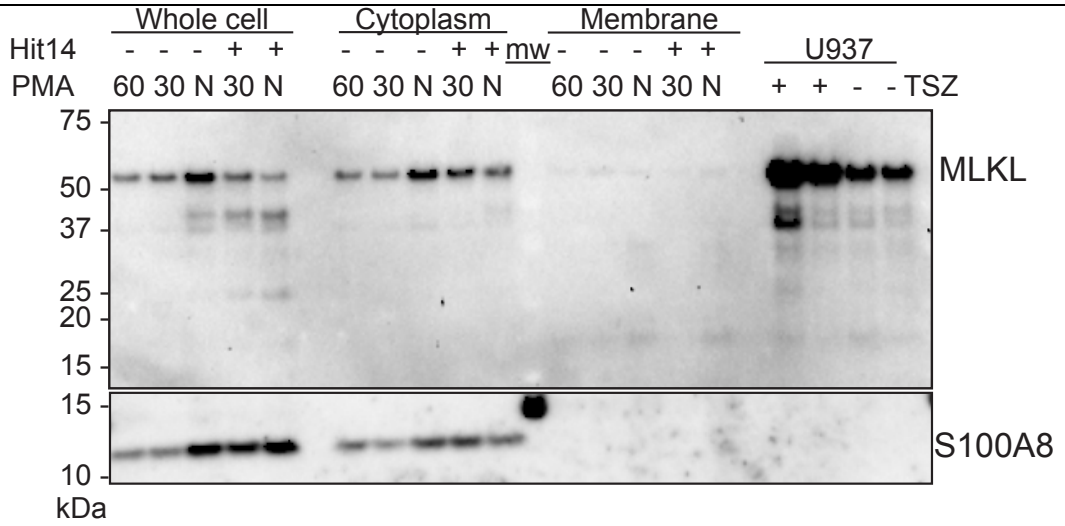


Figure 4.26 MLKL Western blots of fractionated neutrophil proteins

Neutrophils were incubated with or without Hit #14 (25 μM) for three hours. PMA stimulation was added at 30 or 60 minutes prior to harvest or the cells were non-stimulated (N). The cells were fractionated and the lysates were run on a reducing SDS-PAGE gel and probed with antibodies as indicated. U937 cell lysates were included as a control with and without TNF (T, 100ng/ml), smac mimetic (S, 500 nM) and Z (Z-VAD, 10mcM). Representative of two experiments with different donors.

Given the evidence for apoptosis in the effect of Hit #14, membranes were probed for Caspase-8 (Figure 4.27). Interestingly, caspase-8 appeared enriched in the membrane fraction. The low molecular weight band consistent with cleaved caspase-8 was most evident in unstimulated neutrophils with no clear difference with or without Hit #14.

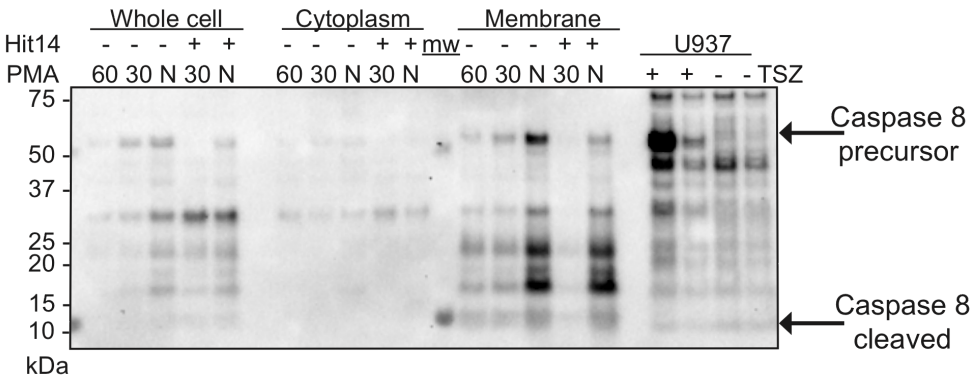


Figure 4.27 Caspase-8 Western of fractionated neutrophil proteins

Neutrophils were incubated with or without Hit #14 (25 μM) prior to PMA stimulation or non-stimulated (N). At indicated time points, neutrophils were harvested and underwent fractionation. The lysates were run on a reducing SDS-page gel and probed with Caspase-8 antibody (H-134, Santa Cruz). Caspase-8 precursor = 55 kDa. Cleaved form = 10 kDa Representative of two experiments with different donors.

4.2.6.1 Non-reducing SDS-Page reveals MLKL multimers in neutrophil lysates

Previous studies have highlighted that MLKL can form multimers during necroptosis. Two forms of multimerization have been reported: one from cells lysates resolved under non-reducing conditions (Cai et al., 2014; X. Chen et al., 2014) and another observed using Blue-Native PAGE (Hildebrand et al., 2014). Given the absence of the effect of the inhibitors on PMA-induced NETosis directly but a clear time and Hit #14-dependence on NET competence, a time-course with and without Hit #14 was undertaken. Initially whole cell lysates with and without reducing agent were generated in neutrophils aged over eight hours (Figure 4.28). Once again, in reducing conditions MLKL expression was seen and remained relatively stable or possibly increased over time. No difference in MLKL abundance or migration was observed between the Hit #14 treated and untreated neutrophils.

A higher molecular weight band was evident under non-reducing conditions just above the 100 kDa marker. This is of smaller size compared to a previously published multimer seen under non-reducing conditions at around 150 kDa and has been assumed to represent a trimeric form (Cai et al., 2014). Multimers have been described only in cells undergoing necroptosis to date (Hildebrand et al., 2014; H. Wang et al., 2014). Of note, the band where the monomeric form would be expected was commensurately decreased in intensity in the non-reducing conditions. A lower molecular weight band around 37 kDa was seen and remained stable throughout the

time course. The lower band was more evident under non-reducing conditions. The significance of these lower molecular weight forms is unclear. Two isoforms of MLKL have been identified (Arnez et al., 2015): full length MLKL, termed MLKL isoform 1, and MLKL isoform 2 (MLKL2), which lacks much of the regulatory pseudokinase domain and migrates at a lower molecular weight. MLKL2 is a much more potent inducer of cell death than full length human MLKL (isoform 1; MLKL1) in ectopic expression studies in HEK293T cells. Of note in that cell line, MLKL2 is expressed at much lower levels than MLKL1.

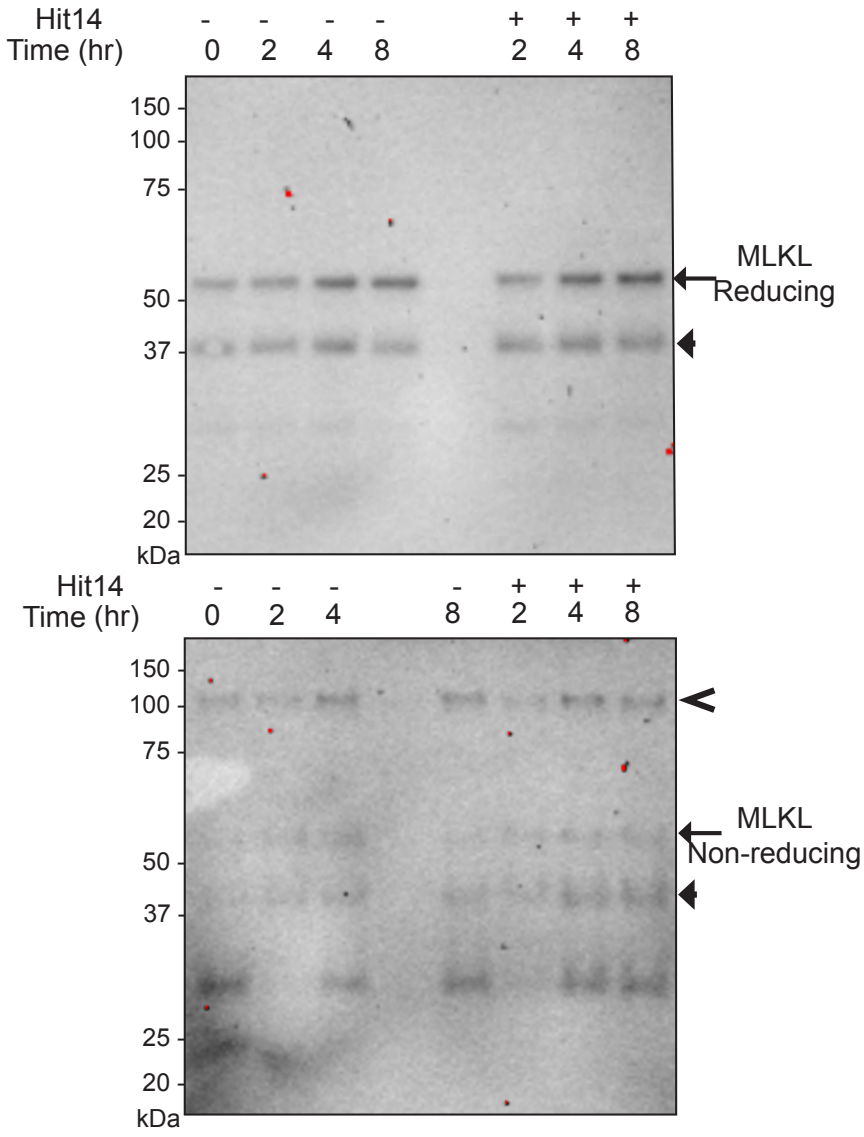


Figure 4.28 MLKL Western blots of neutrophil protein under reducing and non-reducing conditions
Neutrophils were incubated with or without Hit #14 (25 μM). At indicated time points, neutrophils were harvested. Note the difference in the conditions loaded. Neutrophils were lysed in either reducing or non-reducing SDS-loading buffer, run on SDS-PAGE gel and probed with anti-MLKL antibody. Long arrows indicate full-length MLKL. Short arrow a lower molecular weight band around 37 kDa and the arrowhead a higher molecular weight multimer. Experiments from a single donor.

4.2.6.2 Non-reducing SDS –PAGE of fractionated neutrophils demonstrates MLKL multimers in membranes

Lysates from fractionated cells were also assessed under non-reducing conditions (Figure 4.29). Only a small amount of MLKL was observed in the membranes in neutrophils that had been immediately processed (Time 0 hour) with the majority

evident in the cytoplasmic fractions. Under non-reducing conditions, a high molecular weight band was again evident. It was most prominent in the membrane fraction in freshly isolated neutrophils when a small amount was also seen in the cytoplasmic fraction. Of note, the normal molecular weight band evident in the reducing condition was no longer apparent, suggesting that the high molecular weight band was indeed a multimer. The effect of Hit #14 was not clear and awaits replication.

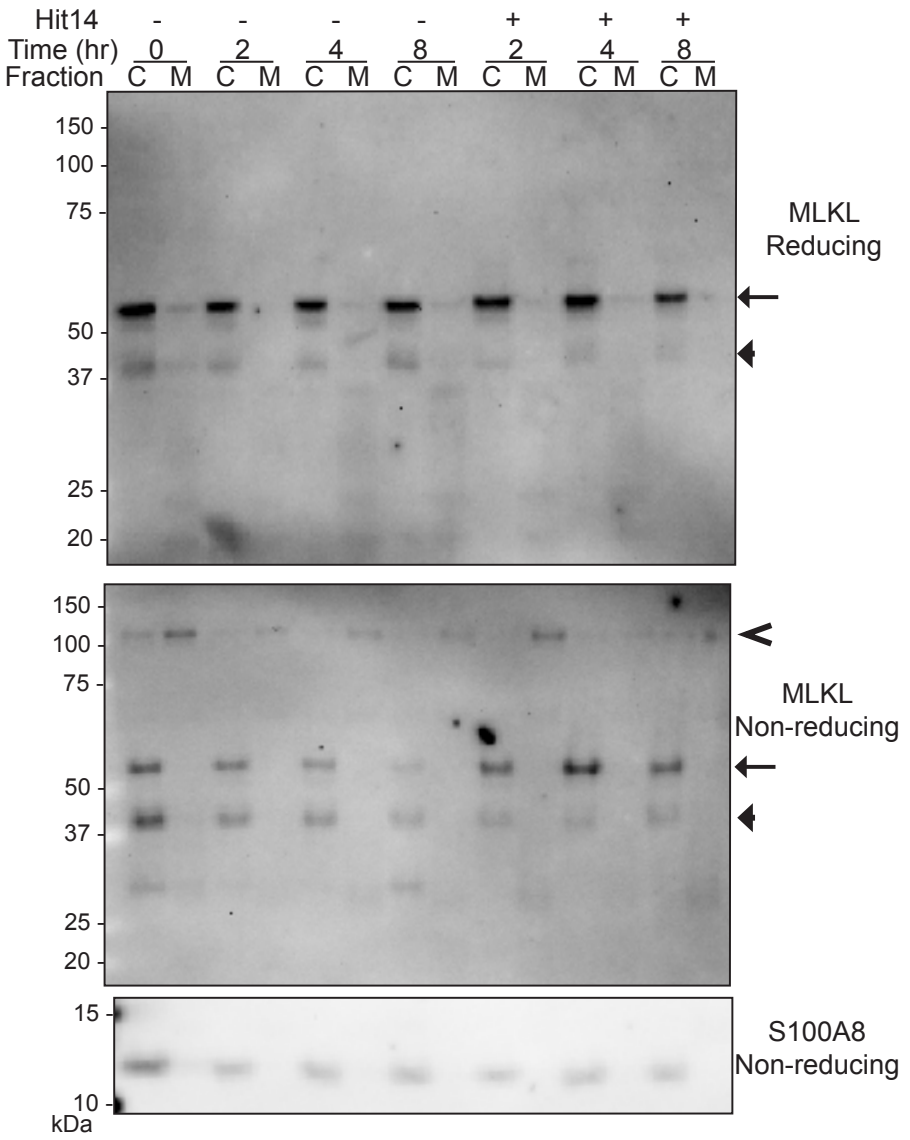


Figure 4.29 MLKL Western blots of fractionated neutrophil proteins under reducing and non-reducing condition
Neutrophils were incubated with or without Hit #14 (25 μM). At indicated time points, neutrophils were harvested and fractionated (C=cytoplasm, M = membrane). Neutrophils were lysed in either reducing or non-reducing SDS-loading buffer, run on SDS-PAGE gel and probed with anti-MLKL antibody and S100A8 for cytoplasmic control. Long arrows indicate full-length MLKL at 57 kDa. Short arrow a lower molecular weight band around 37 kDa and the arrowhead a higher molecular weight multimer. Experiments from a single donor.

These results suggest that MLKL is present in the membranes of freshly isolated unstimulated neutrophils in a multimeric state at the membrane. No clear perturbation of MLKL amount or distribution was seen with Western blotting over time although immunofluorescence suggested nuclear translocation as the cells become apoptotic

(either with time or accelerated with Hit #14 or MLKL781). It remains to be seen whether this multimeric form is phosphorylated.

Non-reducing conditions preserve some protein interactions, in particular disulphide bonds. These disulphide bonds may form under oxidative conditions and may not represent *in vivo* conditions. The addition of N-ethylmaleimide (NEM) during the cell lysis as done in these experiments provides some protection against *de novo* disulphide bonds being created and artefactual multimerization (Cai et al., 2014). If the multimerization is an artefact, it is unclear why it is appearing in the membrane primarily. BN-PAGE employs the charge applied by Coomassie Blue dye rather than using the potent and structurally disruptive anionic detergent SDS to charge label the proteins and may better assess the native state of proteins (Hildebrand et al., 2014). An initial pilot experiment demonstrated MLKL expression at around 146 kDa as previously observed in fibroblasts assess using BN-PAGE (Hildebrand et al., 2014)(Figure 4.30). Unfortunately, subsequent probing of the membrane for GAPDH as a loading control was not successful. No formation of multimers in PMA-treated neutrophils was observed (Figure 4.30). The multimers observed in the non-reducing SDS-PAGE analysis were from freshly isolated neutrophils. This pilot analysis was performed on neutrophils that had been in culture for three hours and repeat BN-PAGE of freshly isolated neutrophils would support the non-reducing SDS-PAGE observation.

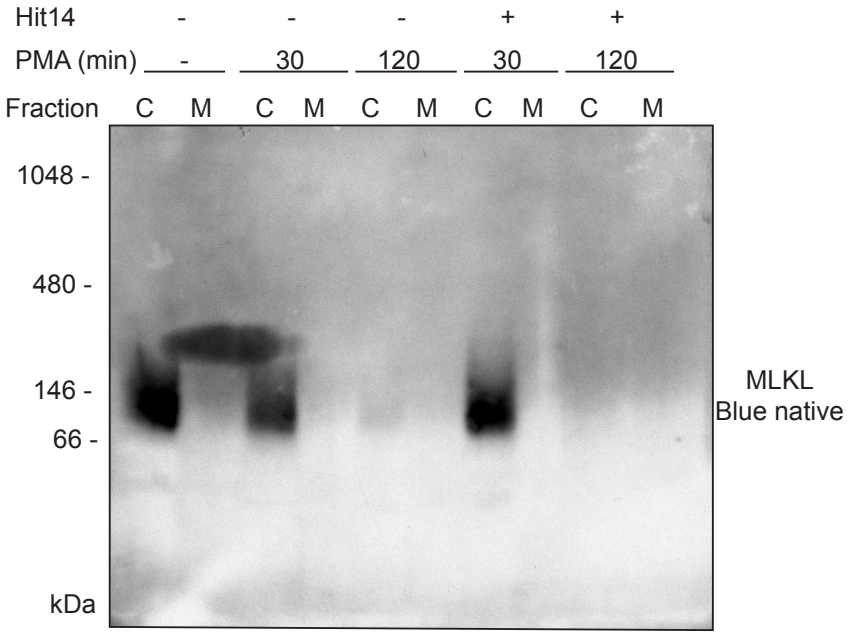


Figure 4.30 BN-PAGE MLKL Western blot
Neutrophils were incubated with or without Hit #14 (25 μM) for 3 hours. PMA stimulation was added 30 or 60 minutes prior to harvest. Neutrophils were harvested and fractionated (C=cytoplasm, M = membrane). Lysate preparations were resolved on Blue Native PAGE and probed with anti-MLKL antibody (3H1, In-house). Experiments from a single donor.

4.2.6.3 Western blotting demonstrates more rapid cleavage of caspase-3 with Hit #14 consistent with more rapid apoptosis

Fractionated neutrophil samples were probed for cleaved caspase-3, the active form of the executioner caspase, which revealed more rapid cleavage with Hit #14, evident in the cytoplasmic fraction only (Figure 4.31). This is consistent with the live cell data demonstrating accelerated apoptosis with Hit #14.

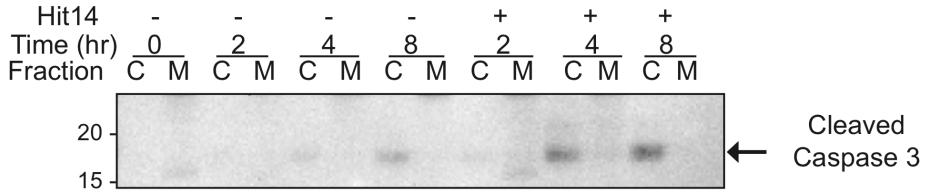


Figure 4.31 Cleaved Caspase-3 Western blots of fractionated neutrophil proteins

Neutrophils were incubated with or without Hit #14 (25 μM). At indicated time points, neutrophils were harvested and fractionated (C=cytoplasm, M = membrane). Neutrophils were lysed in reducing SDS-loading buffer, run on SDS-PAGE gel and probed with anti-cleaved caspase-3 antibody (Asp175, Cell Signalling). Arrows indicate cleaved caspase-3 (17 kDa). Experiments from a single donor.

4.2.6.4 Actin redistributes from the membrane to the cytoplasm with Hit #14 treatment

Staining for actin revealed both cytoplasmic and membrane associated actin (Figure 4.32). Remarkably, with Hit #14 treatment, actin became almost completely redistributed to the cytoplasmic fraction.

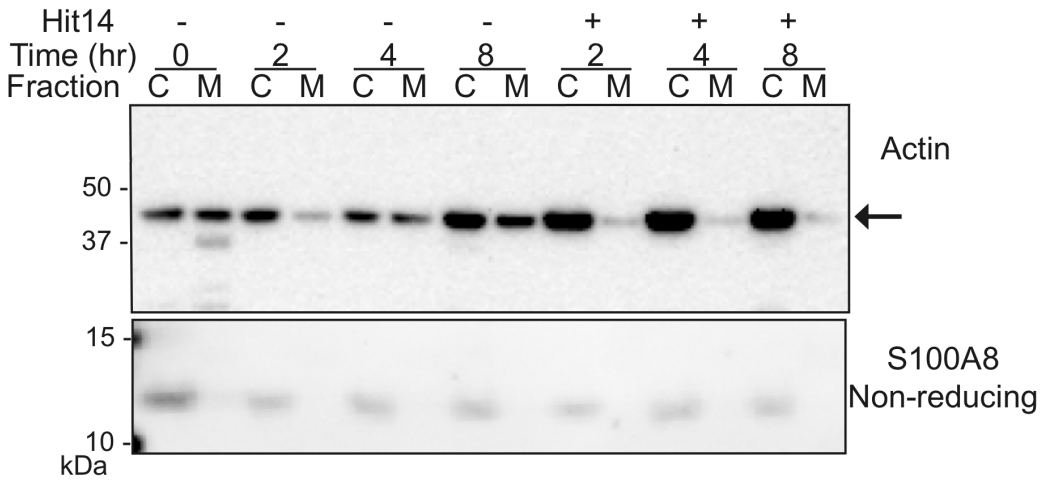


Figure 4.32 Actin Western blot of fractionated neutrophil proteins

Neutrophils were incubated with or without Hit #14 (25 μM). At indicated time points, neutrophils were harvested and fractionated. The lysates were run on a reducing SDS-PAGE gel and probed with anti-β actin antibody (AC-74, Sigma). Experiments from a single donor.

Immunofluorescence using anti-β-actin staining in untreated neutrophils reveals cytoplasmic staining as well as signal close to the cell membrane (Figure 4.33). Four hours of WEHI781 treatment substantially reduced the NET competency of neutrophils through induction of caspase activation. At this time, those cells that had begun to adopt an apoptotic nuclear morphology no longer exhibited prominent membrane-related actin staining. A cell in the same field with normal nuclear morphology (indicated by arrow) contained the same actin distribution as seen in the untreated cells.

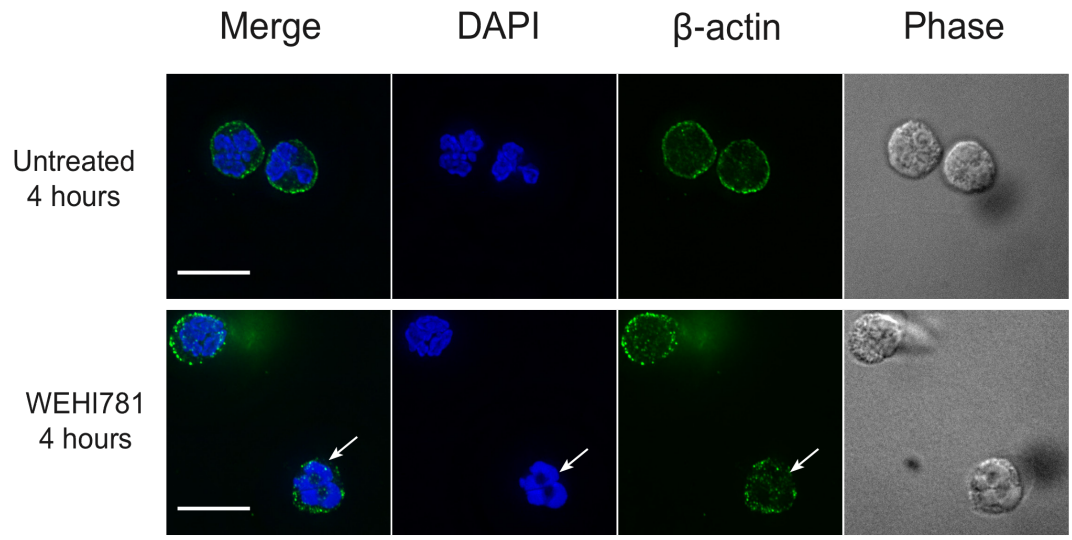


Figure 4.33 Actin immunofluorescence staining moves from a cortical to cytoplasmic distribution with WEHI781 treatment

Neutrophils were incubated with or without WEHI781 (2 μM) for four hours and then fixed and permeabilized. Images are a single representative slice of a z stack taken with the Deltavision Elite microscope with post acquisition deconvolution. Scale bar represents 10 μm. Fluorescent channels and phase contrast as labelled. Representative images from two experiments with different donors.

4.2.7 Induction of cell death with FasL but not WEHI781 or Hit #14 may cause release of IL-1β

Cell death has the potential to be pro-inflammatory, as in the case of necroptosis and pyroptosis, or anti-inflammatory, as is generally thought to be the case for apoptosis. Studies have suggested, however, that FasL may not only trigger apoptosis but cause IL-1β release in a caspase-1-independent manner *in vivo* (Miwa et al., 1998). Neutrophils that have been LPS-primed also release IL-1β when treated with FasL *in vitro* (Croker et al., 2011). The pathway responsible for IL-1β cleavage and release remains to be explored but caspase-1, caspase-8 and neutrophil serine proteases may all contribute (Gabay et al., 2010).

Neutrophils were treated with FcFasL and the two pro-apoptotic compounds, Hit #14 and WEHI781, with or without LPS priming, and the supernatants assayed for IL-1β (Figure 1.34 IL-1β release from neutrophils treated with inducers of apoptosis). In this preliminary experiment performed in duplicate, LPS alone drove IL-1β production without a second stimulus. Intriguingly, this production was not attenuated by QVD-OPh. ZVAD-fmk is more commonly used to suppress caspase-1 activity but the two inhibitors exhibit comparable *in vitro* efficacy (Chauvier et al., 2007). Notably, human

but not murine monocytes have recently been shown to release IL-1β upon stimulation with LPS alone in a caspase-1 dependent manner without the need for a second inflammasome agonist (Gaidt et al., 2016). Like LPS-treatment, FasL induced IL-1β release without additional stimulation, but in contrast to LPS, FasL-induced IL-1β release was inhibited by QVD-OPh. Hit #14 and WEHI781 in contrast did not induce significant IL-1β release and modestly reduced LPS-induced IL-1β release. QVD-OPh in this context restored the LPS effect. Silica is a particulate stimulus capable of activating the inflammasome in macrophages. It modestly increased IL-1β release in LPS-primed cells, which once again was not attenuated by QVD-OPh. Neutrophils are capable of processing IL-1β independently of caspase-1 (Guma et al., 2009). The amount of IL-1β released was relatively low compared to MSU-crystal and nigericin-stimulated macrophages and monocytes at equivalent cell concentrations (IL-1β concentration 100-1000 pg/ml - see Chapter 3 Figure 3.55).

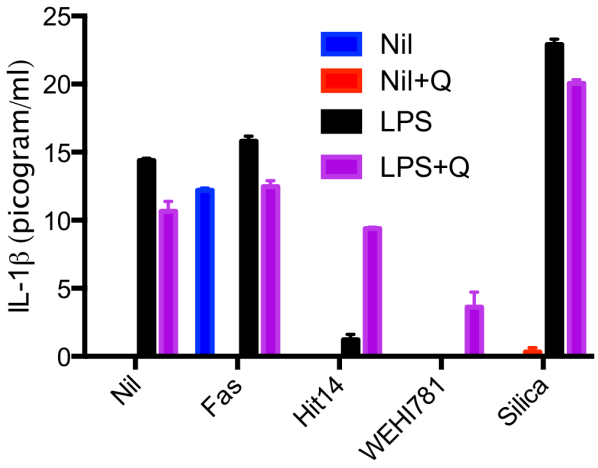


Figure 4.34 IL-1β release from neutrophils treated with inducers of apoptosis

Neutrophils were incubated with or without LPS (1μg/ml) for one hour before the addition of the compounds (Hit #14 and or WEHI781) or FasL (1:1000) or silica (0.5mg/ml). After a further 8 hours the supernatants were taken and IL-1β was measured by ELISA. Values represent mean ± SEM of experimental duplicates. Single donor.

This finding is interesting preliminary evidence for differential release of IL-1β with different apoptotic stimuli and warrants further investigation. FasL induces caspase-8 dependent apoptosis and appears to be able to cause IL-1β release that is caspase-dependent (although the responsible caspase remains to be deduced). The two pro-

apoptotic compounds do not appear to cause IL-1β release and may inhibit LPS-induced cytokine release in a caspase-dependent manner. This suggests the apoptotic program triggered by these compounds is different to the extrinsic pathway triggered by FasL. From the inhibitor studies, it is possible that caspase-8 activation is the main point of difference.

4.3 Discussion

Understanding the relationship between forms of cell death and manipulating cell death pathways is emerging as an important potential avenue to manage inflammatory conditions (K. R. Martin et al., 2015). NETosis may play a number of roles in inflammatory conditions (Grayson et al., 2016), but the relationship between NETosis and other forms of cell death is unclear. The initial finding of this study is that there was no evidence of direct involvement of the necroptosis pathway in PMA-induced NETosis. In particular, inhibition of RIPK1, RIPK3 and, in part, MLKL were ineffective at suppressing NETosis. There was no imaging or Western blot evidence of PMA-induced MLKL redistribution, indicating that if MLKL were to be involved, it may be through an unconventional mechanism. Instead, we have uncovered a reciprocal relationship between NETosis and apoptosis. The ability of neutrophils to respond to PMA by releasing NETs or "NET competence" is governed by caspase activation, with the commitment to apoptosis diverting the neutrophils away from NETosis when stimulated with PMA. Driving apoptosis with FasL rapidly extinguishes neutrophil capacity to release NETs.

Furthermore, we have identified several compounds that increase the rate of neutrophil apoptosis. These compounds decrease NET competence via caspase activation. Whilst this does not reconcile the previous inconsistencies in the NETosis/necroptosis literature, it does highlight that NETosis inhibitors may be operating indirectly through caspase activation and this effect is crucially time dependent.

4.3.1 NETosis does not require activation of the necroptosis pathway

This study represents the fourth examination of the role of the necroptosis pathway and NETosis, as outlined in the introduction. Methodologically, it is consistent with the study of Remijsen et al. in regard to inhibitor dose and PMA concentration and the findings in regard to Necrostatin-1 are the same (Remijsen, Vanden Berghe, et al., 2011). The more recent studies have important methodological differences from that study and the

current one. Desai et al. (Desai et al., 2016) used necrostatin at 50 μM rather than the more commonly used 10 μM, the concentration at which necroptosis is inhibited in other murine and human cell types (Vandenabeele et al., 2013). Whilst relatively specific for RIPK1, Necrostatin-1 does have known off-target effects (Christofferson et al., 2012) including indoleamine 2,3-dioxygenase (IDO) (Vandenabeele et al., 2013). Amini et al. (Amini et al., 2016) studied DNA release at an early time point without any observed cell death, which suggests the process measured was distinct from PMA induced "lytic" NETosis. Analysis of the phosphorylation of MLKL will be important to evaluating the role of MLKL in neutrophil cell death.

4.3.2 Apoptosis and NETosis

Apoptosis and NETosis have been previously explored in one study, which identified the Akt pathway as an important molecular switch between apoptosis and NETosis (Douda et al., 2014). Two different inhibitors of Akt incubated for only 30 minutes prior to PMA stimulation reduced NETosis, but not ROS generation, and appeared to drive apoptosis evidenced by manual assessed changes in nuclear morphology and cleavage of caspase-3 on using immunofluorescence (Douda et al., 2014).

This study demonstrates a time-dependent loss of neutrophil function, primarily assessed as a loss of NET competence that was caspase-mediated and is consistent with the neutrophils undergoing spontaneous time-dependent apoptosis. This study was conducted using isolated peripheral blood human neutrophils and the isolation and culture conditions may impact their survival and activation status. Caution is warranted when extending the conclusions to neutrophil cell death *in vivo,* although neutrophils also have a relatively short lifespan *in vivo* (Tak et al., 2013).

This study also demonstrates that induction of apoptosis can mimic a direct inhibitory effect on NETosis. Recognising apoptosis in the setting of the relatively short-term experiments examining NETosis is challenging, as loss of NET competence occurs prior to the appearance of conventional apoptosis markers such as phosphatidylserine exposure. In our study, co-administration with QVD-OPh allowed assessment of the contribution of caspases to NETosis inhibition by novel agents.

4.3.3 Caspase-mediated loss of neutrophil functionality

Apoptosis has previously been associated with reduced cell functionality and this appears to be governed by the action of caspases (D. Lee et al., 2000). Apoptosis may

be responsible for the functional “shut-down” of neutrophils *in vitro* and *in vivo* (Koedel et al., 2009). The mechanism of caspase-mediated reduction of NET competency remains the subject of ongoing work. The most striking preliminary finding was the redistribution of actin from the membrane to the cytosol with Hit #14 (Western blotting) and WEHI781 (IFA) within two hours of incubation. This actin redistribution needs to be evaluated in the presence of caspase inhibition. Actin can be cleaved during neutrophil apoptosis (S. B. Brown et al., 1997), however the findings of Western blotting in our study suggest the principle process is redistribution rather than cleavage. Anchorage of actin to the membrane is complicated with several actin-binding proteins, including moesin and ezrin, implicated in neutrophils specifically (Pestonjamasp et al., 1995). Apoptosis induces breakdown of fibroblast cell-to-cell contact through caspase-3 cleavage of β-catenin, the coordinator of membrane actin assembly (Brancolini et al., 1997). Caspase-3 may also activate gelsolin during apoptosis to sever actin polymers with subsequent cytoskeletal breakdown and the development of apoptotic morphology (Kothakota et al., 1997). Assessment of actin polymerization state under the current experimental conditions would help narrow down the mechanism.

4.3.4 MLKL inhibitors and Apoptosis

The compounds that accelerate neutrophil apoptosis share the common target, MLKL. Hit #14 was effective but NSA, its more potent derivative also targeting MLKL, was not. There is no straightforward mechanism to account for this discrepancy but potential issues could relate to cell permeability into neutrophils and the potential for oxidative alteration of the compound given its reactive cysteine. Compounds structurally unrelated to Hit #14 that target MLKL at its ATP binding site had a similar effect. WEHI781 is a more potent inhibitor of necroptosis than GW806742X and demonstrated superior efficacy in inducing neutrophil apoptosis. These two compounds do have off-target effects, including against RIPK1 and RIPK3, but specific inhibitors of either kinase were not effective in the same assays.

Off-target effects of chemical compounds are common, particularly with potentially “promiscuous” compounds such as Hit #14 and NSA (although none have so far been reported) (Conrad et al., 2016). The compound GW806742X was initially described as an inhibitor of VEGFR2 and the effect of VEGFR2 inhibition on neutrophils is not known. A recent paper called into question the ability of compounds that target the ATP-binding site to inhibit necroptosis (Ma et al., 2016) and reported off-target effects of GW806742X, including inhibition of both RIPK1 and RIPK3. A new MLKL inhibitor

has been reported with nanomolar potency and no reported RIPK1 and RIPK3 effects (Yan et al., 2017) with the proposed binding site being the cysteine, Cys-86, as for NSA.

Further work should ideally include genetic analysis of MLKL. The *Mlkl*$^{-/-}$ mouse is viable and does not demonstrate any major perturbation of neutrophils (J. M. Murphy et al., 2013; J. Wu et al., 2013). One concern about purely focusing on mouse genetics is the disparate structure and function of MLKL in mice and humans (Tanzer et al., 2016), highlighted by the lack of effect of Hit #14 and NSA in mouse neutrophils on account of species differences in the reactive cysteine target, Cys-86 (Sun et al., 2012). Human genetic strategies are limited because neutrophils are mature non-proliferative cells and are not easily amenable to genetic knockdown approaches. To date, no known functional human MLKL genetic abnormalities have been reported in the literature. Exploring whether these compounds demonstrate similar effects in neutrophil like cell-lines (e.g. differentiated HL-60 cells) would open further avenues to explore.

Another strategy would be to use extensive medicinal chemistry approaches to investigate the target of the compounds. One strategy would be to use chemical pull-down strategies similar to those employed by Sun et al. in identifying MLKL as the target of NSA (Sun et al., 2012). This could provide evidence for the target of these compounds (be it MLKL or another protein). Unfortunately, NSA was ineffective in this current study, so the biotinylated version used in the Sun et al. study is unlikely to be helpful. Furthermore, using primary human cells for these types of screens presents a major challenge.

4.3.5 MLKL – involvement in apoptosis

These findings raise the possibility that MLKL may act as a tonic inhibitor of neutrophil apoptosis, without any involvement of the rest of the necroptosis pathway. There is no precedent for MLKL to have involvement with the apoptosis pathway and there is no known function for MLKL outside its role in necroptosis. MLKL activation without involvement of the other necrosome components has been described in a recent *in vivo* study where autoimmune hepatitis was found to be dependent on MLKL, even in the absence of RIPK3 expression (Gunther et al., 2016). Additionally, a number of organisms are known to express MLKL, but no RIPK3 ortholog, consistent with other mechanisms of MLKL activation having co-evolved (Tanzer et al., 2016).

In terms of necroptosis pathway proteins and neutrophil apoptosis, a recent paper has suggested an unexpected role for RIPK1 in neutrophil apoptosis (Jie et al., 2016). Necrostatin-1 at doses up to 100 μM were found to modestly accelerate caspase-dependent neutrophil apoptosis, but not apoptosis of other peripheral blood cells or tested cell lines. Necrostatin-1 was able to override anti-apoptosis signalling from survival factors, such as GM-CSF and LPS. Administered *in vivo*, Necrostatin-1 also attenuated neutrophil driven inflammation in the mouse. Once again, it is unclear what the mechanism of Necrostatin-1 might be at these high doses.

How MLKL could be playing a role in neutrophil apoptosis inhibition is unclear and the findings of the descriptive component in this study remain preliminary. A direct inhibitory effect on caspases seems unlikely given extensive study in other cell types has not suggested this. Neutrophil cell death is less well studied than that of other cell types, but what is known suggests that neutrophils can differ substantially (Geering & Simon, 2011). It remains of major interest how proteins normally implicated in cellular proliferation play a role in neutrophil survival, particularly given neutrophils are non-proliferative. These proteins include the cyclin-dependent kinases (A. G. Rossi et al., 2006) and the proliferating cell nuclear antigen or PCNA (Witko-Sarsat & Ohayon, 2016). The reported mechanism of this latter molecule serves as an interesting paradigm. It provides a sequestering scaffold for pro-caspases that inhibits their function in a way unique to neutrophils. MLKL forms a multi-protein complex in the setting of necroptosis, with some evidence that this occurs in the nucleus prior to MLKL moving to the cell membranes (Yoon et al., 2016). The relevance of nuclear MLKL remains to be determined, but provides some support for nuclear localisation seen in the current study. Further studies should include confirmation of the imaging MLKL redistribution to the nucleus via cell fractionation and Western blotting.

The other perplexing result from the current study is the expression of membrane-associated multimers of MLKL in freshly isolated neutrophils that appears to decrease with time. Multimeric MLKL present in cell membranes has been strongly associated with MLKL activation during necroptosis (Cai et al., 2014) and biochemical studies suggest that this leads to cell membrane permeabilization (Dondelinger et al., 2014). It is still not clear whether MLKL activation is sufficient to cause death or whether other partner molecules are required (Hildebrand et al., 2014). The presence of multimers in neutrophils needs to be confirmed using BN-PAGE and the phosphorylation state of both monomeric and multimeric MLKL need to be assessed (H. Wang et al., 2014).

The ability to robustly induce neutrophil apoptosis is a potential potent anti-inflammatory strategy (K. R. Martin et al., 2015) and has been successfully employed in murine models (A. G. Rossi et al., 2006). Clarifying the apoptosis inducing-mechanism of the MLKL-targeting compounds may provide insights into the cell death programs in neutrophils. It will also inform about potential toxicities of MLKL-targeting compounds that are being developed as novel therapeutic agents.

5 DISCUSSION

Cell death has emerged as a critical process in many facets of human disease, ranging from cancer to inflammation to cardiovascular disease (Hotchkiss et al., 2009). With improved understanding of cell death comes the potential to inhibit or enhance it for therapeutic gain. Depending on the physiological context, it is also clear that different cell death modalities can play important homeostatic and anti-inflammatory roles. One such modality, NETosis, is a form of cell death with potential implications in a wide range of human conditions but, at present, understanding of the mechanisms of NETosis and its physiologic and pathological consequences is limited. Finding the key mechanisms underlying NETosis will illuminate the roles for NETosis in human diseases and animal models of these conditions, and provide targets for intervention.

5.1 Measurement facilitates understanding of NETosis

The ability to quantify cellular processes is a key step in allowing the effect of experimental perturbations to be established. Measuring NETosis and NET biology presents a number of challenges and multiple assays have been developed, each with strengths and weaknesses (Konig & Andrade, 2016; Naccache & Fernandes, 2016). This thesis presents new strategies to measure NETosis and assess NET biology. The live cell time-lapse imaging assay does not replace existing techniques, but does generate complementary information about NETosis. My work has highlighted different kinetics and characteristics of NETosis in response to different stimuli, revealing that multiple pathways can converge on NET release and neutrophil cell death.

The assay measures both cell death and decondensation in a time-lapse fashion, allowing systematic interrogation of both aspects of NETosis. The utility of this assay was highlighted when examining the effect of neutrophil elastase inhibition on NETosis. NE inhibition prevents NETosis through an effect on chromatin decondensation, rather than cell death. The assay also counters a number of the difficulties with fixed imaging strategies that require multiple manipulations of the cells. Using a relatively small amount of blood, up to 96 wells can be used to investigate stimuli and inhibition. Live-cell imaging is increasingly accessible and offers powerful insights into cellular biology. Increasing throughput and computerized quantification can turn images into data that can be analysed and compared. Consensus around NET measurement in the literature is likely to help the field move forward and reduce variability in results. The other

important conclusions from my work are (i) to reinforce the concept of a split between “lytic” and “vital” NETosis (Yipp & Kubes, 2013) and (ii) that release of DNA from neutrophils may occur as part of multiple biologic processes (Jorch & Kubes, 2017). Identifying which type of NETosis is actually occurring will once again facilitate comparison, rather than create confusion, in this emerging field.

Another challenge with the study of NETosis is the need to use primary human neutrophils, which limits interrogation of molecular mechanisms to the use of chemical inhibitors and observational data. Cross-validation of the efficacy of compounds using different assays (e.g. ROS generation assays for ROS inhibitors) and cell types is one way to improve the confidence around results. Further development of relevant cell-lines faithfully reproducing NETosis would be an important step forward. The HL-60 cell line has been used in multiple NETosis studies, but it is questionable whether these cells can undergo NETosis that compares to primary neutrophils (Yaseen et al., 2017). Use of murine neutrophils *ex vivo* harnesses the experimental strength of gene knockouts and use of the live-cell assay would provide a potential platform for analysing murine NETosis. *In vivo* study is a powerful way to assess the biology and physiologic relevance of biologic processes. Measuring NETosis in this setting provides even greater challenges. Further work needs to be done to compare human and murine NETosis in order to establish how well murine models reflect human responses (Rosen, 2013). To date, interventions to reduce NETosis in animal models have been relatively non-specific - such as NADPH oxidase deficiency (Schauer et al., 2014) and neutrophil granule enzyme deficiency (Warnatsch et al., 2015). Whilst it may not ultimately matter whether these knockouts reduce other cell functions apart from NETosis, the ability to target NETosis specifically may have fewer off-target effects.

The assays presented here also offer new ways to assess NETosis in humans suffering from various diseases as a potential biomarker. For larger scale comparative studies of NETosis rates between groups of patients and controls, assays with the ability to batch analyses offer practical advantages. The live cell assay could provide considerable depth in these situations. As evident among the data presented herein, there is substantial donor variability in NETosis, which needs to be understood when determining the significance of population differences.

5.2 Crystal-induced NETosis – another pathway to cell death and chromatin decondensation and relevance to gout

The neutrophil response to pathologically relevant crystals was investigated using the live cell assay and complementary techniques. It was systematically compared to PMA, the best-characterised NETosis stimulus, but one of limited direct physiologic significance. *Candida* hyphae appear to induce NETosis with comparable characteristics to PMA and served as a more physiological comparator (Metzler et al., 2014). The crystal NETosis pathway diverged from the PMA pathway in terms of kinetics, sequence of cell death and ROS-dependence. Crystal-induced NETosis retained the cardinal features of "lytic" NETosis - cell death and chromatin decondensation – but appears to achieve this through a distinct pathway, with cell death preceding chromatin decondensation. The crystal-induced NETosis pathway does not involve several of the components required for crystal-induced inflammasome activation in other cell types. The experimental findings implicate formation and compromise of a crystal-containing phagosome in NETosis.

One possibility is that the differences seen during PMA and MSU-NETosis relate to differential release and activation of neutrophil elastase during NETosis. The following figure demonstrates a proposed schematic for PMA and MSU-induced NETosis, highlighting differences (Figure 5.1 Schema for PMA and MSU-induced NETosis). The PMA/*Candida* pathway has been well described and requires ROS-mediated NE release from granules, leading to nuclear translocation and histone degradation (Metzler et al., 2014). It is still unclear what triggers cell membrane compromise and cell death in response to PMA. Neutrophil elastase inhibition alone does not prevent cell death, suggesting chromatin expansion causing physical compromise of the cell is not the mechanism of cell death.

My findings do not completely exclude NE liberation in MSU-induced NETosis. Evidence against this so-called "azurosome" pathway in MSU-induced NETosis includes: (i) lack of dependence on ROS; (ii) no effect from a modestly potent MPO inhibitor (which did reduce PMA NETosis); and (iii) early nuclear translocation of MPO. Furthermore, a proposed proximal trigger of *Candida*-induced NETosis is frustrated phagocytosis and inadequate formation of phagosomes (Branzk et al., 2014). Phagocytosis of MSU crystals occurred despite their relatively large size and a NE-containing phagosome was formed. Examining the membranes of MSU-containing

phagosomes revealed features suggestive of membrane discontinuity by electron microscopy, potentially allowing leakage of NE during MSU NETosis.

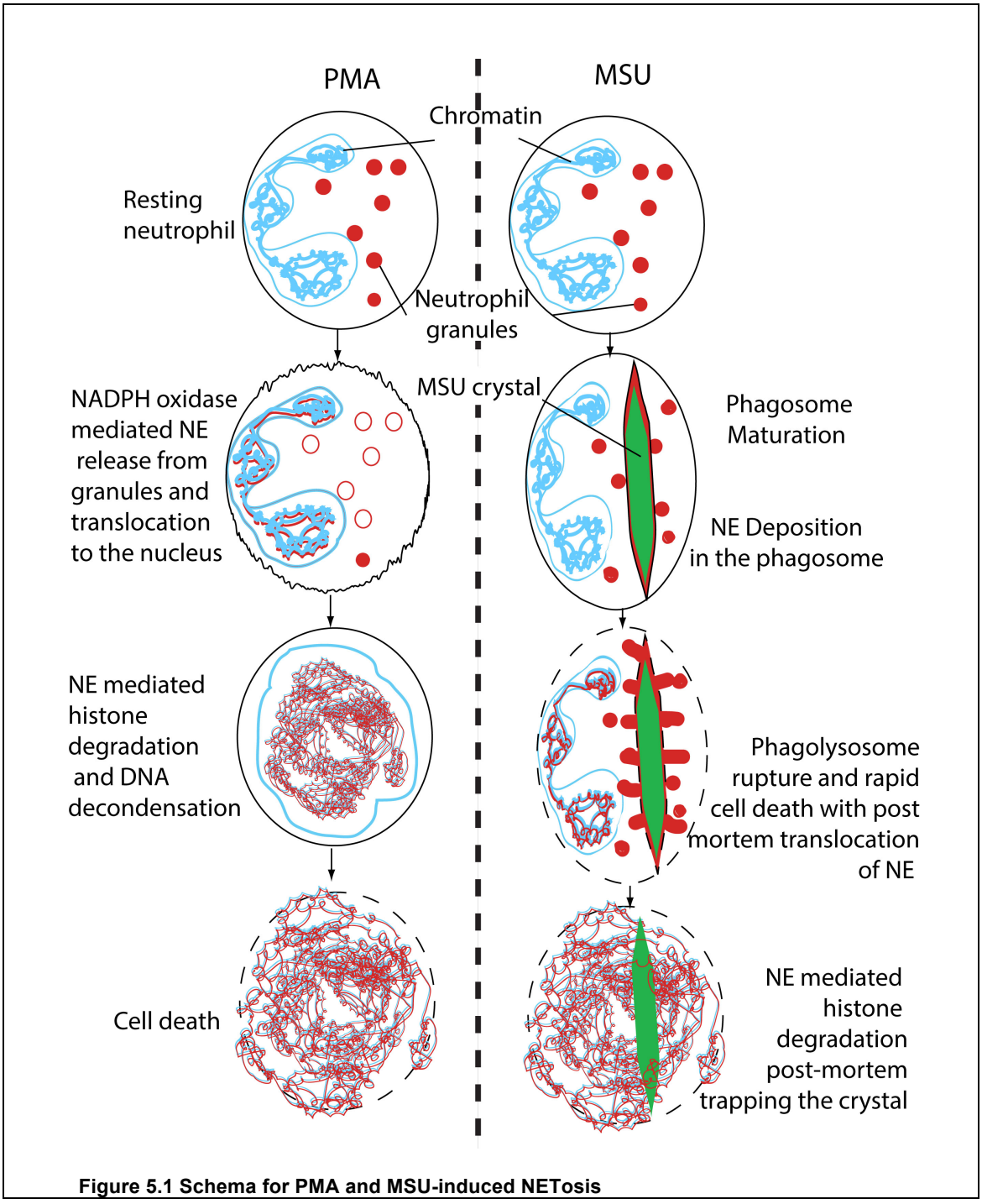


Figure 5.1 Schema for PMA and MSU-induced NETosis

Neutrophils and macrophages are key members of the innate immune response and in gout appear to work in tandem. Resident macrophages seem to provide the initial sensing of danger and then recruit neutrophils to help deal with it (W. J. Martin et al., 2009). The two cell types share phagocytosis as a key function, and they release of mediators critical to dealing with pathogens and amplifying the inflammatory response. There are substantial differences, however, not least being the phagosome dynamics of the two cell types (Nordenfelt & Tapper, 2011). Studies into pathogen-induced inflammasome activation demonstrate important differences in susceptibility to cell death between macrophages and neutrophils (K. W. Chen et al., 2014) and provide insight into the complementary activities of the two. These differences may go some way to explaining differences in responses of the two cell types to crystals. NETosis could serve as a counterpoint to macrophage inflammasome activation, working together to deal with pathogens capable of subverting a single cell type or pathway.

The role of the neutrophil phagosome and its compromise clearly needs to be further studied. The nature of neutrophil lysosome biology also limits the usefulness of current reagents used in assessing lysosomes in other cell types. Advances in microscopy such as super-resolution and high magnification live cell imaging may reveal new aspects of neutrophil cell biology.

This thesis has identified a number of inhibitors that reduce crystal-induced NETosis and some pharmacologically-relevant ineffective compounds, including the three most commonly used anti-gout medications. The latter finding suggests that anti-gout efficacy of these drugs is unlikely to be due to reducing NETosis. In the light of the study's findings relating to a potential inflammation dampening effect of NETs, it may actually be clinically important that these drugs do not interfere with NETosis.

5.3 Different stimuli, different NETs

The NETs released during MSU-induced NETosis differed from PMA-NETs in regard to protein content and susceptibility to DNase degradation. The presence of actin and actin-binding proteins on MSU-NETs raises the possibility that successful phagocytosis allows formation of actin-containing complexes that are at least partially retained during the cell death process. Alternatively, the action of neutrophil elastase during PMA NETosis involves active degradation of cellular actin prior to cell death – a process that is perhaps less complete during more rapid MSU-NETosis (Metzler et al., 2014).

Whilst other studies have found differences between the NET proteomes arising from treatment with different stimuli (Khandpur et al., 2013), no functional relevance of the differing protein content was proposed. I suggest that the actin content of MSU-NETs relative to PMA-NETs provides some resistance against DNase degradation. The physiologic relevance of this difference needs to be established *in vivo* but it does potentially explain the presence of NETs in tophi from patients with gout. Actin may prolong the half-life of MSU-NETs compared to the susceptibility of PMA-NETs to serum degradation *in vitro.*

5.4 NETs in gout – pro- or anti-inflammatory?

The weight of NET literature has proposed NETs as pro-inflammatory mediators contributing to the pathogenesis of non-infectious disease (Grayson et al., 2016). This thesis adds to recent studies demonstrating an unexpected anti-inflammatory role for NETs, at least in the context of gout (Schauer et al., 2014). From the clinical perspective gout is remarkable in that the inflammation induced by crystals is self-limited, despite the inability to clear the crystals in hyperuricemic patients. Secondly, patients with chronic gout develop tophi that are filled with MSU crystals but uninflamed. Whether NETosis can explain all of these phenomena remains to be explored. The data presented in this thesis argue that NETs occur in both acute and chronic gout. *In vivo* evidence for an anti-inflammatory effect of neutrophils in murine MSU-induced inflammation has been reported (Reber et al., 2016; Schauer et al., 2014). The postulated mechanism of neutrophil granule protease-mediated cytokine degradation is not without precedent (Gresnigt et al., 2012) and would potentially have important ramifications in diseases where NETs aggregate in particularly large numbers. In my studies, the effect of neutrophil protease activity was not directly tested, but it is unlikely that inhibiting proteases would prevent neutrophil mediated inhibition of THP-1 cell death. Crystal sequestration may be another factor. Comparing gout to other crystal-driven diseases including pseudogout (where crystal aggregation is less common) and silicosis will be important to determine whether this is a more generalizable phenomenon.

5.5 NETosis, apoptosis and necroptosis

NETosis has been clearly separated from apoptosis both in my studies and others (Remijsen, Vanden Berghe, et al., 2011), but the relationship between NETosis and other forms of cell death remains controversial (Amini et al., 2016; Desai et al., 2016). I

found no evidence for direct involvement of the necroptosis pathway in NETosis. With respect to apoptosis, it became clear that apoptosis and NETosis were mutually exclusive and neutrophils committed to apoptosis were no longer able to generate PMA-induced NETs in a caspase-dependent manner. Surprisingly, several necroptosis inhibitors targeting MLKL were identified as inhibitors of NETosis, but indirectly, via their ability to induce neutrophil apoptosis. The mechanism of action of these compounds remains unclear but is clearly important to examine in future studies. There is active interest in inhibiting necroptosis as a therapy in inflammatory disorders (Kopalli et al., 2016) and appreciating the full range of potential effects is crucial. In some circumstances, induction of neutrophil apoptosis may be attractive as a therapeutic strategy in its own right, given the importance of neutrophils in a number of inflammatory disorders (Hampson et al., 2013).

5.6 Conclusions

This thesis demonstrates that -

(i) the kinetics of NETosis can be quantified using time-lapse imaging. This technique facilitates the understanding of neutrophil cell death biology.

(ii) tophi from gout patients contain structures consistent with NETs. *In vitro*, MSU crystals induce neutrophil cell death and NET release via a pathway distinct from those previously described for “lytic” NETosis. The NETs released are relatively enriched with actin that reduces susceptibility to DNase degradation.

(iii) NETosis induced by PMA and MSU is distinct from necroptosis. Apoptotic caspase-activation reduces the capacity of neutrophil to undergo PMA-induced NETosis. Several necroptosis inhibitors were identified as novel activators of neutrophil apoptosis.

APPENDIX

Mass Spectrometry (LC-MSMS) analysis of MSU- or PMA-induced NETs

Accession: Accession Numbers retrieved from www.uniprot.org;
Identified Proteins: Names of confidently identified proteins (FDR<1%);
Mr: theoretical molecular weight of protein;
Gene Name: Gene identification retrieved from www.uniprot.org;
MSU: Spectrum Count of MSU-stimulated NETs (>95% Conf);
PMA: Spectrum Count of MSU-stimulated NETs (>95% Conf);
MSU/PMA: Fold Change of MSU vs PMA spectrum count > 2 (missing values = 1).
Pink: Ratio of MSU/ PMA spectrum counts > 2 (ie. 2-fold higher in MSU)
Green: Ratio of MSU/ PMA spectrum counts <0.5 (i.e. 2-fold higher in PMA)

Accession	Identified Proteins	Mr	Gene Name	MSU	PMA	MSU /PMA
E7ER44	Lactotransferrin	78 kDa	LTF	167	208	
P05164	Myeloperoxidase	84 kDa	MPO	133	210	
P60709	Actin, cytoplasmic 1	42 kDa	ACTB	100	17	
P62805	Histone H4	11 kDa	HIST1H4A	67	74	
Q2TUW9	Lactoferrin	78 kDa	LTF	67	54	
P35579	Myosin-9	227 kDa	MYH9	47	2	
Q99879	Histone H2B type 1-M	14 kDa	HIST1H2BM	41	26	
P06733	Alpha-enolase	47 kDa	ENO1	36	15	
P30740	Leukocyte elastase inhibitor	43 kDa	SERPINB1	33	20	
P04083	Annexin A1	39 kDa	ANXA1	33	12	
P08311	Cathepsin G	29 kDa	CTSG	30	26	
P41218	Myeloid cell nuclear differentiation antigen	46 kDa	MNDA	28	38	
B7Z565	Highly similar to Alpha-actinin-1	95 kDa	ACTN1	25	5	
P04406	Glyceraldehyde-3-phosphate dehydrogenase	36 kDa	GAPDH	24	11	
P12429	Annexin A3	36 kDa	ANXA3	22	6	
P13796	Plastin-2	70 kDa	LCP1	22	3	
P21333	Filamin-A	281 kDa	FLNA	22	0	
P12724	Eosinophil cationic protein	15 kDa	RNASE3	19	0	

P68871	Hemoglobin subunit beta	16 kDa	HBB	17	55	
P29401	Transketolase	68 kDa	TKT	17	12	
P06744	Glucose-6-phosphate isomerase	63 kDa	GPI	17	0	
P08246	Neutrophil elastase	29 kDa	ELANE	16	3	
B2R4M6	Protein S100	13 kDa	S100CABP	14	9	
P52209	6-phosphogluconate dehydrogenase	53 kDa	PGD	14	0	
P00558	Phosphoglycerate kinase 1	45 kDa	PGK1	14	0	
F1MDH3	Highly similar to Talin-1	271 kDa	TLN1	14	0	
B2RDY9	Adenylyl cyclase-associated protein	52 kDa	CAP	12	8	
P08133	Annexin A6	76 kDa	ANXA6	12	7	
P26038	Moesin	68 kDa	MSN	12	0	
O43707	Alpha-actinin-4	105 kDa	ACTN4	12	0	
P23528	Cofilin-1	19 kDa	CFL1	11	5	
P05109	Protein S100-A8	11 kDa	S100A8	11	5	
P02768	Serum albumin	69 kDa	ALB	11	2	
B7Z992	Highly similar to Gelsolin	79 kDa	GSN	11	0	
P61160	Actin-related protein 2	45 kDa	ACTR2	11	0	
P31946	14-3-3 protein beta/alpha	28 kDa	YWHAB	11	0	
P84228	Histone H3.2	20 kDa	HIS1H3B	10	6	
P0DMV8	Heat shock 70 kDa protein 1A	70 kDa	HSPA1A	10	0	
P80188	Neutrophil gelatinase-associated lipocalin	23 kDa	LCN2	9	2	
P20160	Azurocidin	27 kDa	AZU1	9	0	
P04040	Catalase	60 kDa	CAT	8	5	
P11142	Heat shock cognate 71 kDa protein	71 kDa	HSPA8	8	4	
P11413	Glucose-6-phosphate 1-dehydrogenase	59 kDa	G6PD	8	0	
P37837	Transaldolase	38 kDa	TALDO1	8	0	

P24158	Myeloblastin	28 kDa	PRTN3	8	0	
P59998	Actin-related protein 2/3 complex subunit 4	20 kDa	ARPC4	8	0	
P00338	L-lactate dehydrogenase A chain	37 kDa	LDHA	7	0	
P04908	Histone H2A	14 kDa	HIST1H2AB	7	0	
P07737	Profilin-1	15 kDa	PFN1	6	21	
P60174	Triosephosphate isomerase	27 kDa	TPI1	6	14	
P12724	Eosinophil cationic protein	18 kDa	RNASE3	6	12	
O15511	Actin-related protein 2/3 complex subunit 5	16 kDa	ARPC5	6	7	
P27105	Erythrocyte band 7 integral membrane protein	32 kDa	STOM	6	6	
P50995	Annexin A11	54 kDa	ANXA11	6	0	
P52566	Rho GDP-dissociation inhibitor 2	23 kDa	ARHGDIB	6	0	
P02042	Hemoglobin subunit delta	16 kDa	HBD	6	0	
P61626	Lysozyme C	17 kDa	LYZ	5	7	
P09525	Annexin A4	36 kDa	ANXA4	5	2	
P14618	Pyruvate kinase PKM	58 kDa	PKM	5	0	
B2RDE1	Highly similar to Tropomyosin 3	29 kDa	TPM3	5	0	
P60660	Myosin light polypeptide 6	17 kDa	MYL6	5	0	
P69905	Hemoglobin subunit alpha	16 kDa	HBA1	5	0	
P25815	Protein S100-P	10 kDa	S100P	5	0	
P31997	Carcinoembryonic antigen-related cell adhesion molecule 8	38 kDa	CEACAM8	4	6	

P68104	Elongation factor 1-alpha 1	50 kDa	EEF1A1	4	3	
P07195	L-lactate dehydrogenase B chain	37 kDa	LDHB	4	3	
P04899	Guanine nucleotide-binding protein G(i) subunit alpha-2	40 kDa	GNAI2	4	2	
P06737	Glycogen phosphorylase	97 kDa	PYGL	4	0	
O75083	WD repeat-containing protein 1	66 kDa	WDR1	4	0	
P48616	Vimentin	54 kDa	VIM	4	0	
P04075	Fructose-bisphosphate aldolase A	39 kDa	ALDOA	4	0	
P47756	F-actin-capping protein subunit beta	31 kDa	CAPZB	4	0	
P30040	Endoplasmic reticulum resident protein 29	29 kDa	ERP29	4	0	
P62937	Peptidyl-prolyl cis-trans isomerase A	18 kDa	PPIA	4	0	
P63104	14-3-3 protein zeta/delta	28 kDa	YWHAZ	3	2	
P13807	Glycogen	84 kDa	GYS1	3	0	
P09960	Leukotriene A-4 hydrolase	69 kDa	LTA4H	3	0	
B7Z747	Highly similar to Matrix metalloproteinase-9	66 kDa	MMP9	3	0	
P40121	Macrophage-capping protein	39 kDa	CAPG	3	0	
O00299	Chloride intracellular channel protein 1	27 kDa	CLIC1	3	0	
P09211	Glutathione S-transferase P	23 kDa	GSTP1	3	0	
P51149	Ras-related protein Rab-7a	23 kDa	RAB7A	3	0	
P46940	Ras GTPase-activating-	189 kDa	IQGAP1	3	0	

	like protein IQGAP1					
H7C2Z6	Grancalcin (Fragment)	17 kDa	GCA	3	0	
E7ERL0	Nucleoside diphosphate kinase A	15 kDa	NME1	3	0	
P32119	Peroxiredoxin-2	22 kDa	PRDX2	2	13	
P17213	Bactericidal permeability-increasing protein	54 kDa	BPI	2	4	
P10153	Non-secretory ribonuclease	18 kDa	RNASE2	2	4	
P08238	Heat shock protein HSP 90-beta	83 kDa	HSP90AB1	2	3	
P62258	14-3-3 protein epsilon	29 kDa	YWHAE	2	2	
O60234	Glia maturation factor gamma	17 kDa	GMFG	2	2	
P33778	Histone H2B type 1-B	14 kDa	HIST1H2BB	2	2	
P52790	Hexokinase-3	99 kDa	HK3	2	0	
P17858	ATP-dependent 6-phosphofructokinase	85 kDa	PFKL	2	0	
B4E0R1	Integrin beta	77 kDa	INB	2	0	
O75131	Copine-3	60 kDa	CPNE3	2	0	
P56480	ATP synthase subunit beta	56 kDa	Atp5b	2	0	
Q13231	Chitotriosidase-1	52 kDa	CHIT1	2	0	
Q9WV32	Actin-related protein 2/3 complex subunit 1B	41 kDa	Arpc1b	2	0	
Q15365	Heterogeneous nuclear ribonucleoprotein E1	37 kDa	PCBP1	2	0	
P40925	Malate dehydrogenase	36 kDa	MDH1	2	0	
O15144	Actin-related protein 2/3 complex subunit 2	34 kDa	ARPC2	2	0	
P52907	F-actin-capping protein subunit alpha-1	33 kDa	CAPZA1	2	0	
P00491	Purine nucleoside phosphorylase	32 kDa	PNP	2	0	

G3V5Z7	Proteasome subunit alpha type	28 kDa	PSMA6	2	0	
Q5D862	Filaggrin-2	248 kDa	FLG2	2	0	
P28065	Proteasome subunit beta type-9	23 kDa	PSMB9	2	0	
Q6P5D8	Structural maintenance of chromosomes flexible hinge domain-containing protein 1	226 kDa	Smchd1	2	0	
P30044	Peroxiredoxin-5	22 kDa	PRDX5	2	0	
P19105	Myosin regulatory light chain 12A	20 kDa	MYL12A	2	0	
Q99497	Protein deglycase DJ-1	20 kDa	PARK7	2	0	
Q00610	Clathrin heavy chain 1	192 kDa	CLTC	2	0	
Q9H4G4	Golgi-associated plant pathogenesis-related protein 1	17 kDa	GLIPR2	2	0	
A3KMV5	Ubiquitin-like modifier-activating enzyme 1	118 kDa	UBA1	2	0	
P11678	Eosinophil peroxidase	81 kDa	EPX	0	17	
P02730	Band 3 anion transport protein	102 kDa	SLC4A1	0	5	
P13688	Carcinoembryonic antigen-related cell adhesion molecule 1	58 kDa	CEACAM1	0	4	
P11021	78 kDa glucose-regulated protein	72 kDa	HSPA5	0	3	
P07237	Protein disulfide-isomerase	57 kDa	P4HB	0	3	
P00390	Glutathione reductase	56 kDa	GSR	0	3	
P16157	Ankyrin-1	206 kDa	ANK1	0	3	
P61978	Heterogeneous nuclear ribonucleoprotein K	51 kDa	HNRNPK	0	2	
P07437	Tubulin beta chain	50 kDa	TUBB	0	2	

Q71U36	Tubulin alpha-1A chain	50 kDa	TUBA1A	0	2	
O75367	Core histone macro-H2A.1	40 kDa	H2AFY	0	2	
P00918	Carbonic anhydrase 2	29 kDa	CA2	0	2	
P11277	Spectrin beta chain	243 kDa	SPTB	0	2	
P80311	Peptidyl-prolyl cis-trans isomerase B	24 kDa	PPIB	0	2	
P04792	Heat shock protein beta-1	23 kDa	HSPB1	0	2	

SUPPLEMENTARY MOVIES

Supplementary Movie S1

Time-lapse video from which the montages of PMA- and MSU-stimulated neutrophils in Figure 2A are derived. Neutrophils were pre-incubated with Cell Tracker Green (CTG) and propidium iodide (PI) was added to the media. Stimuli were added and images were taken 15 minutely. Images are merges of phase contrast, CTG (green) and PI (red) images. PI signal is enhanced in the upper panels and reduced in the lower panels of the same images, demonstrating the cells that have died and not undergone nuclear decondensation. Time points as indicated. Scale bar represents 100 μm.

Supplementary Movie S2

An example of time-lapse video from which the montages in Figure 2D are derived. Neutrophils were pre-incubated with CTG and PI and Hoechst 33342 was added to the media. Stimuli were added and images were taken 5 minutely. Hoechst 33342 DNA dye (red), CTG (blue) and PI (green). Scale bar represents 10 μm. Times as indicated hh:mm.

Supplementary Movie S3 (PMA) and S4 (MSU)

Time-lapse video from which the montages of PMA- and MSU-stimulated neutrophils in Figure 4E are derived. DQ ovalbumin signal becomes diffuse prior to cell death in PMA but not MSU treated neutrophils. Time-lapse images taken every two minutes with confocal resonance scanner. DQ ovalbumin (green), PI (red) and phase contrast. Time points as indicated leading up to and after cell death.

Supplementary Movie S5

MSU-induced NETs are degraded in a dose- and time-dependent manner.

PI- stained MSU NETs were transferred to a 96 well microscope plate and imaged every 15 minutes after addition of DNase at the indicated concentrations. Time points as indicated. Scale bar represents 100 μm. Representative of five experiments.

Bibliography

Abbink, J. J., Kamp, A. M., Nieuwenhuys, E. J., Nuijens, J. H., Swaak, A. J., & Hack, C. E. (1991). Predominant role of neutrophils in the inactivation of alpha 2-macroglobulin in arthritic joints. *Arthritis Rheum, 34*(9), 1139-1150.

Abramson, S., Hoffstein, S. T., & Weissmann, G. (1982). Superoxide anion generation by human neutrophils exposed to monosodium urate. *Arthritis Rheum, 25*(2), 174-180.

Akahoshi, T., Namai, R., Sekiyama, N., Tanaka, S., Hosaka, S., & Kondo, H. (1997). Rapid induction of neutrophil apoptosis by sulfasalazine: implications of reactive oxygen species in the apoptotic process. *J Leukoc Biol, 62*(6), 817-826.

Akgul, C., & Edwards, S. W. (2003). Regulation of neutrophil apoptosis via death receptors. *Cell Mol Life Sci, 60*(11), 2402-2408. doi:10.1007/s00018-003-3110-z

Altznauer, F., Conus, S., Cavalli, A., Folkers, G., & Simon, H. U. (2004). Calpain-1 regulates Bax and subsequent Smac-dependent caspase-3 activation in neutrophil apoptosis. *J Biol Chem, 279*(7), 5947-5957. doi:10.1074/jbc.M308576200

Alvarado-Kristensson, M., Melander, F., Leandersson, K., Ronnstrand, L., Wernstedt, C., & Andersson, T. (2004). p38-MAPK signals survival by phosphorylation of caspase-8 and caspase-3 in human neutrophils. *J Exp Med, 199*(4), 449-458. doi:10.1084/jem.20031771

Amini, P., Stojkov, D., Wang, X., Wicki, S., Kaufmann, T., Wong, W. W., . . . Yousefi, S. (2016). NET formation can occur independently of RIPK3 and MLKL signaling. *Eur J Immunol, 46*(1), 178-184. doi:10.1002/eji.201545615

Amulic, B., Cazalet, C., Hayes, G. L., Metzler, K. D., & Zychlinsky, A. (2012). Neutrophil function: from mechanisms to disease. *Annu Rev Immunol, 30*, 459-489. doi:10.1146/annurev-immunol-020711-074942

An, L. L., Mehta, P., Xu, L., Turman, S., Reimer, T., Naiman, B., . . . Fung, M. (2014). Complement C5a potentiates uric acid crystal-induced IL-1beta production. *Eur J Immunol, 44*(12), 3669-3679. doi:10.1002/eji.201444560

Andina, N., Conus, S., Schneider, E. M., Fey, M. F., & Simon, H. U. (2009). Induction of Bim limits cytokine-mediated prolonged survival of neutrophils. *Cell Death Differ, 16*(9), 1248-1255. doi:10.1038/cdd.2009.50

Arnez, K. H., Kindlova, M., Bokil, N. J., Murphy, J. M., Sweet, M. J., & Guncar, G. (2015). Analysis of the N-terminal region of human MLKL, as well as two distinct MLKL isoforms, reveals new insights into necroptotic cell death. *Biosci Rep, 36*(1), e00291. doi:10.1042/BSR20150246

Ayub, K., Laffafian, I., Dewitt, S., & Hallett, M. B. (2004). Ca influx shutdown in neutrophils induced by Fas (CD95) cross-linking. *Immunology, 112*(3), 454-460. doi:10.1111/j.1365-2567.2004.01899.x

Azevedo, E. P., Guimaraes-Costa, A. B., Torezani, G. S., Braga, C. A., Palhano, F. L., Kelly, J. W., . . . Foguel, D. (2012). Amyloid fibrils trigger the release of neutrophil extracellular traps (NETs), causing fibril fragmentation by NET-associated elastase. *J Biol Chem, 287*(44), 37206-37218. doi:10.1074/jbc.M112.369942

Baird, S. K., Kurz, T., & Brunk, U. T. (2006). Metallothionein protects against oxidative stress-induced lysosomal destabilization. *Biochem J, 394*(Pt 1), 275-283. doi:10.1042/BJ20051143

Barabe, F., Gilbert, C., Liao, N., Bourgoin, S. G., & Naccache, P. H. (1998). Crystal-induced neutrophil activation VI. Involvment of FcgammaRIIIB (CD16) and CD11b in response to inflammatory microcrystals. *FASEB J, 12*(2), 209-220.

Barrientos, L., Bignon, A., Gueguen, C., de Chaisemartin, L., Gorges, R., Sandre, C., . . . Chollet-Martin, S. (2014). Neutrophil extracellular traps downregulate lipopolysaccharide-induced activation of monocyte-derived dendritic cells. *J Immunol, 193*(11), 5689-5698. doi:10.4049/jimmunol.1400586

Batinica, M., Stephan, A., Steiger, J., Tantcheva-Poomicronr, I., Eming, S. A., & Fabri, M. (2016). Stimulus-dependent NETosis by neutrophils from a Papillon-Lefevre Syndrome patient. *J Eur Acad Dermatol Venereol*, 1-7. doi:10.1111/jdv.14004

Bauernfeind, F., Bartok, E., Rieger, A., Franchi, L., Nunez, G., & Hornung, V. (2011). Cutting edge: reactive oxygen species inhibitors block priming, but not activation, of the NLRP3 inflammasome. *J Immunol, 187*(2), 613-617. doi:10.4049/jimmunol.1100613

Baumann, M., Pham, C. T., & Benarafa, C. (2013). SerpinB1 is critical for neutrophil survival through cell-autonomous inhibition of cathepsin G. *Blood, 121*(19), 3900-3907, S3901-3906. doi:10.1182/blood-2012-09-455022

Beiter, K., Wartha, F., Albiger, B., Normark, S., Zychlinsky, A., & Henriques-Normark, B. (2006). An endonuclease allows Streptococcus pneumoniae to escape from neutrophil extracellular traps. *Curr Biol, 16*(4), 401-407. doi:10.1016/j.cub.2006.01.056

Beura, L. K., Hamilton, S. E., Bi, K., Schenkel, J. M., Odumade, O. A., Casey, K. A., . . . Masopust, D. (2016). Normalizing the environment recapitulates adult human immune traits in laboratory mice. *Nature, 532*(7600), 512-516. doi:10.1038/nature17655

Bianchi, M., Hakkim, A., Brinkmann, V., Siler, U., Seger, R. A., Zychlinsky, A., & Reichenbach, J. (2009). Restoration of NET formation by gene therapy in CGD controls aspergillosis. *Blood, 114*(13), 2619-2622. doi:10.1182/blood-2009-05-221606

Blomgran, R., Zheng, L., & Stendahl, O. (2004). Uropathogenic Escherichia coli triggers oxygen-dependent apoptosis in human neutrophils through the cooperative effect of type 1 fimbriae and lipopolysaccharide. *Infect Immun, 72*(8), 4570-4578. doi:10.1128/IAI.72.8.4570-4578.2004

Boumpas, D. T., Chrousos, G. P., Wilder, R. L., Cupps, T. R., & Balow, J. E. (1993). Glucocorticoid therapy for immune-mediated diseases: basic and clinical correlates. *Ann Intern Med, 119*(12), 1198-1208.

Brancolini, C., Lazarevic, D., Rodriguez, J., & Schneider, C. (1997). Dismantling cell-cell contacts during apoptosis is coupled to a caspase-dependent proteolytic cleavage of beta-catenin. *J Cell Biol, 139*(3), 759-771.

Branzk, N., Lubojemska, A., Hardison, S. E., Wang, Q., Gutierrez, M. G., Brown, G. D., & Papayannopoulos, V. (2014). Neutrophils sense microbe size and selectively release neutrophil extracellular traps in response to large pathogens. *Nat Immunol, 15*(11), 1017-1025. doi:10.1038/ni.2987

Brinkmann, V., Goosmann, C., Kuhn, L. I., & Zychlinsky, A. (2012). Automatic quantification of in vitro NET formation. *Front Immunol, 3*, 413. doi:10.3389/fimmu.2012.00413

Brinkmann, V., Laube, B., Abu Abed, U., Goosmann, C., & Zychlinsky, A. (2010). Neutrophil extracellular traps: how to generate and visualize them. *J Vis Exp, 36*(36). doi:10.3791/1724

Brinkmann, V., Reichard, U., Goosmann, C., Fauler, B., Uhlemann, Y., Weiss, D. S., . . . Zychlinsky, A. (2004). Neutrophil extracellular traps kill bacteria. *Science, 303*(5663), 1532-1535. doi:10.1126/science.1092385

Brinkmann, V., & Zychlinsky, A. (2012). Neutrophil extracellular traps: is immunity the second function of chromatin? *J Cell Biol, 198*(5), 773-783. doi:10.1083/jcb.201203170

Brojatsch, J., Lima, H., Kar, A. K., Jacobson, L. S., Muehlbauer, S. M., Chandran, K., & Diaz-Griffero, F. (2014). A proteolytic cascade controls lysosome rupture and necrotic cell death mediated by lysosome-destabilizing adjuvants. *PLoS ONE, 9*(6), e95032. doi:10.1371/journal.pone.0095032

Brown, R. A., Lever, R., Jones, N. A., & Page, C. P. (2003). Effects of heparin and related molecules upon neutrophil aggregation and elastase release in vitro. *Br J Pharmacol, 139*(4), 845-853. doi:10.1038/sj.bjp.0705291

Brown, S. B., Bailey, K., & Savill, J. (1997). Actin is cleaved during constitutive apoptosis. *Biochem J, 323 (Pt 1)*, 233-237.

Brumatti, G., & Ekert, P. G. (2013). Seeking a MCL-1 inhibitor. *Cell Death Differ, 20*(11), 1440-1441. doi:10.1038/cdd.2013.114

Brumatti, G., Ma, C., Lalaoui, N., Nguyen, N. Y., Navarro, M., Tanzer, M. C., . . . Silke, J. (2016). The caspase-8 inhibitor emricasan combines with the SMAC mimetic birinapant to induce necroptosis and treat acute myeloid leukemia. *Sci Transl Med, 8*(339), 339ra369. doi:10.1126/scitranslmed.aad3099

Buchanan, J. T., Simpson, A. J., Aziz, R. K., Liu, G. Y., Kristian, S. A., Kotb, M., . . . Nizet, V. (2006). DNase expression allows the pathogen group A Streptococcus to escape killing in neutrophil extracellular traps. *Curr Biol, 16*(4), 396-400. doi:10.1016/j.cub.2005.12.039

Cai, Z., Jitkaew, S., Zhao, J., Chiang, H. C., Choksi, S., Liu, J., . . . Liu, Z. G. (2014). Plasma membrane translocation of trimerized MLKL protein is required for TNF-induced necroptosis. *Nat Cell Biol, 16*(1), 55-65. doi:10.1038/ncb2883

Callus, B. A., & Vaux, D. L. (2007). Caspase inhibitors: viral, cellular and chemical. *Cell Death Differ, 14*(1), 73-78. doi:10.1038/sj.cdd.4402034

Cantin, A. M. (1998). DNase I acutely increases cystic fibrosis sputum elastase activity and its potential to induce lung hemorrhage in mice. *Am J Respir Crit Care Med, 157*(2), 464-469. doi:10.1164/ajrccm.157.2.9608033

Cao, S., Liu, P., Zhu, H., Gong, H., Yao, J., Sun, Y., . . . Xu, Y. (2015). Extracellular Acidification Acts as a Key Modulator of Neutrophil Apoptosis and Functions. *PLoS ONE, 10*(9), e0137221. doi:10.1371/journal.pone.0137221

Cartwright, G. E., Athens, J. W., & Wintrobe, M. M. (1964). The Kinetics of Granulopoiesis in Normal Man. *Blood, 24*, 780-803.

Chauvier, D., Ankri, S., Charriaut-Marlangue, C., Casimir, R., & Jacotot, E. (2007). Broad-spectrum caspase inhibitors: from myth to reality? *Cell Death Differ, 14*(2), 387-391. doi:10.1038/sj.cdd.4402044

Chen, C. J., Shi, Y., Hearn, A., Fitzgerald, K., Golenbock, D., Reed, G., . . . Rock, K. L. (2006). MyD88-dependent IL-1 receptor signaling is essential for gouty inflammation stimulated by monosodium urate crystals. *J Clin Invest, 116*(8), 2262-2271. doi:10.1172/JCI28075

Chen, K. W., Bezbradica, J. S., Gross, C. J., Wall, A. A., Sweet, M. J., Stow, J. L., & Schroder, K. (2016). The murine neutrophil NLRP3 inflammasome is activated by soluble but not particulate or crystalline agonists. *Eur J Immunol, 46*(4), 1004-1010. doi:10.1002/eji.201545943

Chen, K. W., Gross, C. J., Sotomayor, F. V., Stacey, K. J., Tschopp, J., Sweet, M. J., & Schroder, K. (2014). The neutrophil NLRC4 inflammasome selectively promotes IL-1beta maturation without pyroptosis during acute Salmonella challenge. *Cell Rep, 8*(2), 570-582. doi:10.1016/j.celrep.2014.06.028

Chen, X., Li, W., Ren, J., Huang, D., He, W. T., Song, Y., . . . Han, J. (2014). Translocation of mixed lineage kinase domain-like protein to plasma membrane leads to necrotic cell death. *Cell Res, 24*(1), 105-121. doi:10.1038/cr.2013.171

Chhana, A., & Dalbeth, N. (2015). The gouty tophus: a review. *Curr Rheumatol Rep, 17*(3), 19. doi:10.1007/s11926-014-0492-x

Chia, E. W., Grainger, R., & Harper, J. L. (2008). Colchicine suppresses neutrophil superoxide production in a murine model of gouty arthritis: a rationale for use of low-dose colchicine. *Br J Pharmacol, 153*(6), 1288-1295. doi:10.1038/bjp.2008.20

Choi, H. K., Mount, D. B., & Reginato, A. M. (2005). Pathogenesis of gout. *Ann Intern Med, 143*(7), 499-516.

Chow, O. A., von Kockritz-Blickwede, M., Bright, A. T., Hensler, M. E., Zinkernagel, A. S., Cogen, A. L., . . . Nizet, V. (2010). Statins enhance formation of phagocyte extracellular traps. *Cell Host Microbe, 8*(5), 445-454. doi:10.1016/j.chom.2010.10.005

Christofferson, D. E., Li, Y., Hitomi, J., Zhou, W., Upperman, C., Zhu, H., . . . Yuan, J. (2012). A novel role for RIP1 kinase in mediating TNFalpha production. *Cell Death Dis, 3*(6), e320. doi:10.1038/cddis.2012.64

Chun, H. J., Zheng, L., Ahmad, M., Wang, J., Speirs, C. K., Siegel, R. M., . . . Lenardo, M. J. (2002). Pleiotropic defects in lymphocyte activation caused by caspase-8 mutations lead to human immunodeficiency. *Nature, 419*(6905), 395-399. doi:10.1038/nature01063

Chung, Y. H., Kim, D. H., & Lee, W. W. (2016). Monosodium urate crystal-induced pro-interleukin-1beta production is post-transcriptionally regulated via the p38 signaling pathway in human monocytes. *Sci Rep, 6*, 34533. doi:10.1038/srep34533

Cieutat, A. M., Lobel, P., August, J. T., Kjeldsen, L., Sengelov, H., Borregaard, N., & Bainton, D. F. (1998). Azurophilic granules of human neutrophilic leukocytes are deficient in lysosome-associated membrane proteins but retain the mannose 6-phosphate recognition marker. *Blood, 91*(3), 1044-1058.

Clark, R. A., & Nauseef, W. M. (1996). Preparation and Functional Analysis of Human Nonlymphoid Cells *Current Protocols in Immunology* (pp. 1-17). Hoboken, NJ: W. John Wiley & Sons.

Colamussi, M. L., White, M. R., Crouch, E., & Hartshorn, K. L. (1999). Influenza A virus accelerates neutrophil apoptosis and markedly potentiates apoptotic effects of bacteria. *Blood, 93*(7), 2395-2403.

Conrad, M., Angeli, J. P., Vandenabeele, P., & Stockwell, B. R. (2016). Regulated necrosis: disease relevance and therapeutic opportunities. *Nat Rev Drug Discov, 15*(5), 348-366. doi:10.1038/nrd.2015.6

Conus, S., Perozzo, R., Reinheckel, T., Peters, C., Scapozza, L., Yousefi, S., & Simon, H. U. (2008). Caspase-8 is activated by cathepsin D initiating neutrophil apoptosis during the resolution of inflammation. *J Exp Med, 205*(3), 685-698. doi:10.1084/jem.20072152

Cornish, A. L., Campbell, I. K., McKenzie, B. S., Chatfield, S., & Wicks, I. P. (2009). G-CSF and GM-CSF as therapeutic targets in rheumatoid arthritis. *Nat Rev Rheumatol, 5*(10), 554-559. doi:10.1038/nrrheum.2009.178

Cowburn, A. S., Summers, C., Dunmore, B. J., Farahi, N., Hayhoe, R. P., Print, C. G., . . . Chilvers, E. R. (2011). Granulocyte/macrophage colony-stimulating factor causes a paradoxical increase in the BH3-only pro-apoptotic protein Bim in human neutrophils. *Am J Respir Cell Mol Biol, 44*(6), 879-887. doi:10.1165/rcmb.2010-0101OC

Cowburn, A. S., White, J. F., Deighton, J., Walmsley, S. R., & Chilvers, E. R. (2005). z-VAD-fmk augmentation of TNF alpha-stimulated neutrophil apoptosis is compound specific and does not involve the generation of reactive oxygen species. *Blood, 105*(7), 2970-2972. doi:10.1182/blood-2004-07-2870

Cox, G. (1995). Glucocorticoid treatment inhibits apoptosis in human neutrophils. Separation of survival and activation outcomes. *J Immunol, 154*(9), 4719-4725.

Croker, B. A., O'Donnell, J. A., Nowell, C. J., Metcalf, D., Dewson, G., Campbell, K. J., . . . Roberts, A. W. (2011). Fas-mediated neutrophil apoptosis is accelerated by Bid, Bak, and Bax and inhibited by Bcl-2 and Mcl-1. *Proc Natl Acad Sci U S A, 108*(32), 13135-13140. doi:10.1073/pnas.1110358108

Cronstein, B. N., Molad, Y., Reibman, J., Balakhane, E., Levin, R. I., & Weissmann, G. (1995). Colchicine alters the quantitative and qualitative display of selectins on endothelial cells and neutrophils. *J Clin Invest, 96*(2), 994-1002. doi:10.1172/JCI118147

Cronstein, B. N., & Terkeltaub, R. (2006). The inflammatory process of gout and its treatment. *Arthritis Res Ther, 8 Suppl 1*, S3. doi:10.1186/ar1908

Cross, A., Barnes, T., Bucknall, R. C., Edwards, S. W., & Moots, R. J. (2006). Neutrophil apoptosis in rheumatoid arthritis is regulated by local oxygen tensions within joints. *J Leukoc Biol, 80*(3), 521-528. doi:10.1189/jlb.0306178

Cullen, S. P., Kearney, C. J., Clancy, D. M., & Martin, S. J. (2015). Diverse Activators of the NLRP3 Inflammasome Promote IL-1beta Secretion by Triggering Necrosis. *Cell Rep, 11*(10), 1535-1548. doi:10.1016/j.celrep.2015.05.003

Dalbeth, N., Pool, B., Gamble, G. D., Smith, T., Callon, K. E., McQueen, F. M., & Cornish, J. (2010). Cellular characterization of the gouty tophus: a quantitative analysis. *Arthritis Rheum, 62*(5), 1549-1556. doi:10.1002/art.27356

Danial, N. N., & Korsmeyer, S. J. (2004). Cell death: critical control points. *Cell, 116*(2), 205-219. doi:10.1016/S0092-8674(04)00046-7

Davoodian, K., Ritchings, B. W., Ramphal, R., & Bubb, M. R. (1997). Gelsolin activates DNase I in vitro and cystic fibrosis sputum. *Biochemistry, 36*(32), 9637-9641. doi:10.1021/bi9711487

de Buhr, N., & von Kockritz-Blickwede, M. (2016). How Neutrophil Extracellular Traps Become Visible. *J Immunol Res, 2016*(3), 4604713. doi:10.1155/2016/4604713

DeChatelet, L. R., Shirley, P. S., & Johnston, R. B., Jr. (1976). Effect of phorbol myristate acetate on the oxidative metabolism of human polymorphonuclear leukocytes. *Blood, 47*(4), 545-554.

Demers, M., Krause, D. S., Schatzberg, D., Martinod, K., Voorhees, J. R., Fuchs, T. A., . . . Wagner, D. D. (2012). Cancers predispose neutrophils to release extracellular DNA traps that contribute to cancer-associated thrombosis. *Proc Natl Acad Sci U S A, 109*(32), 13076-13081. doi:10.1073/pnas.1200419109

Derouet, M., Thomas, L., Cross, A., Moots, R. J., & Edwards, S. W. (2004). Granulocyte macrophage colony-stimulating factor signaling and proteasome inhibition delay neutrophil apoptosis by increasing the stability of Mcl-1. *J Biol Chem, 279*(26), 26915-26921. doi:10.1074/jbc.M313875200

Derouet, M., Thomas, L., Moulding, D. A., Akgul, C., Cross, A., Moots, R. J., & Edwards, S. W. (2006). Sodium salicylate promotes neutrophil apoptosis by stimulating caspase-dependent turnover of Mcl-1. *J Immunol, 176*(2), 957-965.

Desai, J., Kumar, S. V., Mulay, S. R., Konrad, L., Romoli, S., Schauer, C., . . . Anders, H. J. (2016). PMA and crystal-induced neutrophil extracellular trap formation involves RIPK1-RIPK3-MLKL signaling. *Eur J Immunol, 46*(1), 223-229. doi:10.1002/eji.201545605

Desaulniers, P., Fernandes, M., Gilbert, C., Bourgoin, S. G., & Naccache, P. H. (2001). Crystal-induced neutrophil activation. VII. Involvement of Syk in the responses to monosodium urate crystals. *J Leukoc Biol, 70*(4), 659-668.

Desaulniers, P., Marois, S., Pare, G., Popa-Nita, O., Gilbert, C., & Naccache, P. H. (2006). Characterization of an activation factor released from human neutrophils after stimulation by triclinic monosodium urate crystals. *J Rheumatol, 33*(5), 928-938.

Dibbert, B., Weber, M., Nikolaizik, W. H., Vogt, P., Schoni, M. H., Blaser, K., & Simon, H. U. (1999). Cytokine-mediated Bax deficiency and consequent delayed

neutrophil apoptosis: a general mechanism to accumulate effector cells in inflammation. *Proc Natl Acad Sci U S A, 96*(23), 13330-13335.
Dinarello, C. A. (2009). Immunological and inflammatory functions of the interleukin-1 family. *Annu Rev Immunol, 27*, 519-550. doi:10.1146/annurev.immunol.021908.132612
Dinarello, C. A. (2011). Blocking interleukin-1beta in acute and chronic autoinflammatory diseases. *J Intern Med, 269*(1), 16-28. doi:10.1111/j.1365-2796.2010.02313.x
Ding, J., Wang, K., Liu, W., She, Y., Sun, Q., Shi, J., . . . Shao, F. (2016). Pore-forming activity and structural autoinhibition of the gasdermin family. *Nature, 535*(7610), 111-116. doi:10.1038/nature18590
Dondelinger, Y., Declercq, W., Montessuit, S., Roelandt, R., Goncalves, A., Bruggeman, I., . . . Vandenabeele, P. (2014). MLKL compromises plasma membrane integrity by binding to phosphatidylinositol phosphates. *Cell Rep, 7*(4), 971-981. doi:10.1016/j.celrep.2014.04.026
Douda, D. N., Khan, M. A., Grasemann, H., & Palaniyar, N. (2015). SK3 channel and mitochondrial ROS mediate NADPH oxidase-independent NETosis induced by calcium influx. *Proc Natl Acad Sci U S A, 112*(9), 2817-2822. doi:10.1073/pnas.1414055112
Douda, D. N., Yip, L., Khan, M. A., Grasemann, H., & Palaniyar, N. (2014). Akt is essential to induce NADPH-dependent NETosis and to switch the neutrophil death to apoptosis. *Blood, 123*(4), 597-600. doi:10.1182/blood-2013-09-526707
Duffin, R., Leitch, A. E., Fox, S., Haslett, C., & Rossi, A. G. (2010). Targeting granulocyte apoptosis: mechanisms, models, and therapies. *Immunol Rev, 236*, 28-40. doi:10.1111/j.1600-065X.2010.00922.x
Dzhagalov, I., St John, A., & He, Y. W. (2007). The antiapoptotic protein Mcl-1 is essential for the survival of neutrophils but not macrophages. *Blood, 109*(4), 1620-1626. doi:10.1182/blood-2006-03-013771
El Chemaly, A., Nunes, P., Jimaja, W., Castelbou, C., & Demaurex, N. (2014). Hv1 proton channels differentially regulate the pH of neutrophil and macrophage phagosomes by sustaining the production of phagosomal ROS that inhibit the delivery of vacuolar ATPases. *J Leukoc Biol, 95*(5), 827-839. doi:10.1189/jlb.0513251
El Kebir, D., Jozsef, L., Pan, W., & Filep, J. G. (2008). Myeloperoxidase delays neutrophil apoptosis through CD11b/CD18 integrins and prolongs inflammation. *Circ Res, 103*(4), 352-359. doi:10.1161/01.RES.0000326772.76822.7a
Ermert, D., Urban, C. F., Laube, B., Goosmann, C., Zychlinsky, A., & Brinkmann, V. (2009). Mouse neutrophil extracellular traps in microbial infections. *J Innate Immun, 1*(3), 181-193. doi:10.1159/000205281
Ertel, W., Keel, M., Infanger, M., Ungethüm, U., Steckholzer, U., & Trentz, O. (1998). Circulating mediators in serum of injured patients with septic complications inhibit neutrophil apoptosis through up-regulation of protein-tyrosine phosphorylation. *J Trauma, 44*(5), 767-775.
Ettinger, A., & Wittmann, T. (2014). Fluorescence live cell imaging. *Methods Cell Biol, 123*, 77-94. doi:10.1016/B978-0-12-420138-5.00005-7
Fadeel, B., Ahlin, A., Henter, J. I., Orrenius, S., & Hampton, M. B. (1998). Involvement of caspases in neutrophil apoptosis: regulation by reactive oxygen species. *Blood, 92*(12), 4808-4818.
Faires, J. S., & McCarty, D. J. (1962). Acute arthritis in man and dog after intrasynovial injection of sodium urate crystals. *Lancet, 280*(7258), 682-684.
Farrera, C., & Fadeel, B. (2013). Macrophage clearance of neutrophil extracellular traps is a silent process. *J Immunol, 191*(5), 2647-2656. doi:10.4049/jimmunol.1300436

Fecho, K., & Cohen, P. L. (1998). Fas ligand (gld)- and Fas (lpr)-deficient mice do not show alterations in the extravasation or apoptosis of inflammatory neutrophils. *J Leukoc Biol, 64*(3), 373-383.
Fotouhi-Ardakani, N., Kebir, D. E., Pierre-Charles, N., Wang, L., Ahern, S. P., Filep, J. G., & Milot, E. (2010). Role for myeloid nuclear differentiation antigen in the regulation of neutrophil apoptosis during sepsis. *Am J Respir Crit Care Med, 182*(3), 341-350. doi:10.1164/rccm.201001-0075OC
Francois, S., El Benna, J., Dang, P. M. C., Pedruzzi, E., Gougerot-Pocidalo, M. A., & Elbim, C. (2005). Inhibition of Neutrophil Apoptosis by TLR Agonists in Whole Blood: Involvement of the Phosphoinositide 3-Kinase/Akt and NF- B Signaling Pathways, Leading to Increased Levels of Mcl-1, A1, and Phosphorylated Bad. *J Immunol, 174*(6), 3633-3642. doi:10.4049/jimmunol.174.6.3633
Franklin, B. S., Mangan, M. S., & Latz, E. (2016). Crystal Formation in Inflammation. *Annu Rev Immunol, 34*(1), 173-202. doi:10.1146/annurev-immunol-041015-055539
Franz, S., Munoz, L. E., Heyder, P., Herrmann, M., & Schiller, M. (2015). Unconventional apoptosis of polymorphonuclear neutrophils (PMN): staurosporine delays exposure of phosphatidylserine and prevents phagocytosis by MPhi-2 macrophages of PMN. *Clin Exp Immunol, 179*(1), 75-84. doi:10.1111/cei.12412
Freitas, M., Porto, G., Lima, J. L., & Fernandes, E. (2008). Isolation and activation of human neutrophils in vitro. The importance of the anticoagulant used during blood collection. *Clin Biochem, 41*(7-8), 570-575. doi:10.1016/j.clinbiochem.2007.12.021
Fuchs, T. A., Abed, U., Goosmann, C., Hurwitz, R., Schulze, I., Wahn, V., . . . Zychlinsky, A. (2007). Novel cell death program leads to neutrophil extracellular traps. *J Cell Biol, 176*(2), 231-241. doi:10.1083/jcb.200606027
Gabay, C., Lamacchia, C., & Palmer, G. (2010). IL-1 pathways in inflammation and human diseases. *Nat Rev Rheumatol, 6*(4), 232-241. doi:10.1038/nrrheum.2010.4
Gaidt, M. M., Ebert, T. S., Chauhan, D., Schmidt, T., Schmid-Burgk, J. L., Rapino, F., . . . Hornung, V. (2016). Human Monocytes Engage an Alternative Inflammasome Pathway. *Immunity, 44*(4), 833-846. doi:10.1016/j.immuni.2016.01.012
Galluzzi, L., Vitale, I., Abrams, J. M., Alnemri, E. S., Baehrecke, E. H., Blagosklonny, M. V., . . . Kroemer, G. (2012). Molecular definitions of cell death subroutines: recommendations of the Nomenclature Committee on Cell Death 2012. *Cell Death Differ, 19*(1), 107-120. doi:10.1038/cdd.2011.96
Garcia-Romo, G. S., Caielli, S., Vega, B., Connolly, J., Allantaz, F., Xu, Z., . . . Pascual, V. (2011). Netting neutrophils are major inducers of type I IFN production in pediatric systemic lupus erythematosus. *Sci Transl Med, 3*(73), 73ra20. doi:10.1126/scitranslmed.3001201
Gaudry, M., Gilbert, C., Barabe, F., Poubelle, P. E., & Naccache, P. H. (1995). Activation of Lyn is a common element of the stimulation of human neutrophils by soluble and particulate agonists. *Blood, 86*(9), 3567-3574.
Gaudry, M., Roberge, C. J., de Medicis, R., Lussier, A., Poubelle, P. E., & Naccache, P. H. (1993). Crystal-induced neutrophil activation. III. Inflammatory microcrystals induce a distinct pattern of tyrosine phosphorylation in human neutrophils. *J Clin Invest, 91*(4), 1649-1655. doi:10.1172/JCI116373
Gavillet, M., Martinod, K., Renella, R., Harris, C., Shapiro, N. I., Wagner, D. D., & Williams, D. A. (2015). Flow cytometric assay for direct quantification of neutrophil extracellular traps in blood samples. *Am J Hematol, 90*(12), 1155-1158. doi:10.1002/ajh.24185

Geering, B., Gurzeler, U., Federzoni, E., Kaufmann, T., & Simon, H. U. (2011). A novel TNFR1-triggered apoptosis pathway mediated by class IA PI3Ks in neutrophils. *Blood, 117*(22), 5953-5962. doi:10.1182/blood-2010-11-322206

Geering, B., & Simon, H. U. (2011). Peculiarities of cell death mechanisms in neutrophils. *Cell Death Differ, 18*(9), 1457-1469. doi:10.1038/cdd.2011.75

Gilbert, C., Poubelle, P. E., Borgeat, P., Pouliot, M., & Naccache, P. H. (2003). Crystal-induced neutrophil activation: VIII. Immediate production of prostaglandin E2 mediated by constitutive cyclooxygenase 2 in human neutrophils stimulated by urate crystals. *Arthritis Rheum, 48*(4), 1137-1148. doi:10.1002/art.10851

Ginsberg, M. H., Kozin, F., Chow, D., May, J., & Skosey, J. L. (1977). Adsorption of polymorphonuclear leukocyte lysosomal enzymes to monosodium urate crystals. *Arthritis Rheum, 20*(8), 1538-1542.

Goepel, F., Weinmann, P., Schymeinsky, J., & Walzog, B. (2004). Identification of caspase-10 in human neutrophils and its role in spontaneous apoptosis. *J Leukoc Biol, 75*(5), 836-843. doi:10.1189/jlb.0703317

Gordon, T. P., Clifton, P., James, M. J., & Roberts-Thomson, P. J. (1986). Lack of correlation between in vitro and in vivo effects of low density lipoprotein on the inflammatory activity of monosodium urate crystals. *Ann Rheum Dis, 45*(8), 673-676.

Gottlieb, R. A., Giesing, H. A., Zhu, J. Y., Engler, R. L., & Babior, B. M. (1995). Cell acidification in apoptosis: granulocyte colony-stimulating factor delays programmed cell death in neutrophils by up-regulating the vacuolar H(+)-ATPase. *Proc Natl Acad Sci U S A, 92*(13), 5965-5968.

Goulding, N. J., Euzger, H. S., Butt, S. K., & Perretti, M. (1998). Novel pathways for glucocorticoid effects on neutrophils in chronic inflammation. *Inflamm Res, 47 Suppl 3*, S158-165.

Grayson, P. C., Schauer, C., Herrmann, M., & Kaplan, M. J. (2016). Review: Neutrophils as Invigorated Targets in Rheumatic Diseases. *Arthritis Rheumatol, 68*(9), 2071-2082. doi:10.1002/art.39745

Greenlee-Wacker, M. C., Rigby, K. M., Kobayashi, S. D., Porter, A. R., DeLeo, F. R., & Nauseef, W. M. (2014). Phagocytosis of Staphylococcus aureus by human neutrophils prevents macrophage efferocytosis and induces programmed necrosis. *J Immunol, 192*(10), 4709-4717. doi:10.4049/jimmunol.1302692

Gresnigt, M. S., Joosten, L. A., Verschueren, I., van der Meer, J. W., Netea, M. G., Dinarello, C. A., & van de Veerdonk, F. L. (2012). Neutrophil-mediated inhibition of proinflammatory cytokine responses. *J Immunol, 189*(10), 4806-4815. doi:10.4049/jimmunol.1103551

Gross, O., Yazdi, A. S., Thomas, C. J., Masin, M., Heinz, L. X., Guarda, G., . . . Tschopp, J. (2012). Inflammasome activators induce interleukin-1alpha secretion via distinct pathways with differential requirement for the protease function of caspase-1. *Immunity, 36*(3), 388-400. doi:10.1016/j.immuni.2012.01.018

Guma, M., Ronacher, L., Liu-Bryan, R., Takai, S., Karin, M., & Corr, M. (2009). Caspase 1-independent activation of interleukin-1beta in neutrophil-predominant inflammation. *Arthritis Rheum, 60*(12), 3642-3650. doi:10.1002/art.24959

Gunther, C., He, G. W., Kremer, A. E., Murphy, J. M., Petrie, E. J., Amann, K., . . . Wirtz, S. (2016). The pseudokinase MLKL mediates programmed hepatocellular necrosis independently of RIPK3 during hepatitis. *J Clin Invest, 126*(11), 4346-4360. doi:10.1172/JCI87545

Gupta, A. K., Giaglis, S., Hasler, P., & Hahn, S. (2014). Efficient Neutrophil Extracellular Trap Induction Requires Mobilization of Both Intracellular and

Extracellular Calcium Pools and Is Modulated by Cyclosporine A. *PLoS ONE, 9*(5), e97088. doi:10.1371/journal.pone.0097088

Gupta, A. K., Hasler, P., Holzgreve, W., Gebhardt, S., & Hahn, S. (2005). Induction of neutrophil extracellular DNA lattices by placental microparticles and IL-8 and their presence in preeclampsia. *Hum Immunol, 66*(11), 1146-1154. doi:10.1016/j.humimm.2005.11.003

Hachicha, M., Naccache, P. H., & McColl, S. R. (1995). Inflammatory microcrystals differentially regulate the secretion of macrophage inflammatory protein 1 and interleukin 8 by human neutrophils: a possible mechanism of neutrophil recruitment to sites of inflammation in synovitis. *J Exp Med, 182*(6), 2019-2025.

Hakkim, A., Fuchs, T. A., Martinez, N. E., Hess, S., Prinz, H., Zychlinsky, A., & Waldmann, H. (2011). Activation of the Raf-MEK-ERK pathway is required for neutrophil extracellular trap formation. *Nat Chem Biol, 7*(2), 75-77. doi:10.1038/nchembio.496

Hakkim, A., Furnrohr, B. G., Amann, K., Laube, B., Abed, U. A., Brinkmann, V., . . . Zychlinsky, A. (2010). Impairment of neutrophil extracellular trap degradation is associated with lupus nephritis. *Proc Natl Acad Sci U S A, 107*(21), 9813-9818. doi:10.1073/pnas.0909927107

Halle, M., Liu, Y. C., Hardy, S., Theberge, J. F., Blanchetot, C., Bourdeau, A., . . . Tremblay, M. L. (2007). Caspase-3 regulates catalytic activity and scaffolding functions of the protein tyrosine phosphatase PEST, a novel modulator of the apoptotic response. *Mol Cell Biol, 27*(3), 1172-1190. doi:10.1128/MCB.02462-05

Hamasaki, A., Sendo, F., Nakayama, K., Ishida, N., Negishi, I., Nakayama, K., & Hatakeyama, S. (1998). Accelerated neutrophil apoptosis in mice lacking A1-a, a subtype of the bcl-2-related A1 gene. *J Exp Med, 188*(11), 1985-1992.

Hampson, P., Hazeldine, J., & Lord, J. M. (2013). Neutrophil apoptosis and its induction as a potential treatment for chronic inflammatory disease. *Curr Opin Hematol, 20*(1), 10-15. doi:10.1097/MOH.0b013e32835b06be

Hannah, S., Nadra, I., Dransfield, I., Pryde, J. G., Rossi, A. G., & Haslett, C. (1998). Constitutive neutrophil apoptosis in culture is modulated by cell density independently of beta2 integrin-mediated adhesion. *FEBS Lett, 421*(2), 141-146.

Harbort, C. J., Soeiro-Pereira, P. V., von Bernuth, H., Kaindl, A. M., Costa-Carvalho, B. T., Condino-Neto, A., . . . Amulic, B. (2015). Neutrophil oxidative burst activates ATM to regulate cytokine production and apoptosis. *Blood, 126*(26), 2842-2851. doi:10.1182/blood-2015-05-645424

Hart, S. P., Ross, J. A., Ross, K., Haslett, C., & Dransfield, I. (2000). Molecular characterization of the surface of apoptotic neutrophils: implications for functional downregulation and recognition by phagocytes. *Cell Death Differ, 7*(5), 493-503. doi:10.1038/sj.cdd.4400680

Harter, L., Keel, M., Hentze, H., Steckholzer, U., Ungethum, U., Trentz, O., & Ertel, W. (2001). Spontaneous in contrast to CD95-induced neutrophil apoptosis is independent of caspase activity. *J Trauma, 50*(6), 982-988.

Hasegawa, T., Suzuki, K., Sakamoto, C., Ohta, K., Nishiki, S., Hino, M., . . . Kitagawa, S. (2003). Expression of the inhibitor of apoptosis (IAP) family members in human neutrophils: up-regulation of cIAP2 by granulocyte colony-stimulating factor and overexpression of cIAP2 in chronic neutrophilic leukemia. *Blood, 101*(3), 1164-1171. doi:10.1182/blood-2002-05-1505

Haslett, C., Guthrie, L. A., Kopaniak, M. M., Johnston, R. B., Jr., & Henson, P. M. (1985). Modulation of multiple neutrophil functions by preparative methods or trace concentrations of bacterial lipopolysaccharide. *Am J Pathol, 119*(1), 101-110.

Hawes, M., Allen, C., Turgeon, B. G., Curlango-Rivera, G., Minh Tran, T., Huskey, D. A., & Xiong, Z. (2016). Root Border Cells and Their Role in Plant Defense. *Annu Rev Phytopathol, 54*(1), 143-161. doi:10.1146/annurev-phyto-080615-100140

Healy, L. D., Puy, C., Itakura, A., Chu, T., Robinson, D. K., Bylund, A., . . . McCarty, O. J. (2016). Colocalization of neutrophils, extracellular DNA and coagulation factors during NETosis: Development and utility of an immunofluorescence-based microscopy platform. *J Immunol Methods, 435*, 77-84. doi:10.1016/j.jim.2016.06.002

Hemmers, S., Teijaro, J. R., Arandjelovic, S., & Mowen, K. A. (2011). PAD4-mediated neutrophil extracellular trap formation is not required for immunity against influenza infection. *PLoS ONE, 6*(7), e22043. doi:10.1371/journal.pone.0022043

Hildebrand, J. M., Tanzer, M. C., Lucet, I. S., Young, S. N., Spall, S. K., Sharma, P., . . . Silke, J. (2014). Activation of the pseudokinase MLKL unleashes the four-helix bundle domain to induce membrane localization and necroptotic cell death. *Proc Natl Acad Sci U S A, 111*(42), 15072-15077. doi:10.1073/pnas.1408987111

Hirsch, G., Lavoie-Lamoureux, A., Beauchamp, G., & Lavoie, J. P. (2012). Neutrophils are not less sensitive than other blood leukocytes to the genomic effects of glucocorticoids. *PLoS ONE, 7*(9), e44606. doi:10.1371/journal.pone.0044606

Homburg, C. H., de Haas, M., von dem Borne, A. E., Verhoeven, A. J., Reutelingsperger, C. P., & Roos, D. (1995). Human neutrophils lose their surface Fc gamma RIII and acquire Annexin V binding sites during apoptosis in vitro. *Blood, 85*(2), 532-540.

Hornung, V., Bauernfeind, F., Halle, A., Samstad, E. O., Kono, H., Rock, K. L., . . . Latz, E. (2008). Silica crystals and aluminum salts activate the NALP3 inflammasome through phagosomal destabilization. *Nat Immunol, 9*(8), 847-856. doi:10.1038/ni.1631

Hotchkiss, R. S., Strasser, A., McDunn, J. E., & Swanson, P. E. (2009). Cell death. *N Engl J Med, 361*(16), 1570-1583. doi:10.1056/NEJMra0901217

Iwai, K., Miyawaki, T., Takizawa, T., Konno, A., Ohta, K., Yachie, A., . . . Taniguchi, N. (1994). Differential expression of bcl-2 and susceptibility to anti-Fas-mediated cell death in peripheral blood lymphocytes, monocytes, and neutrophils. *Blood, 84*(4), 1201-1208.

Janicke, R. U., Sprengart, M. L., Wati, M. R., & Porter, A. G. (1998). Caspase-3 is required for DNA fragmentation and morphological changes associated with apoptosis. *J Biol Chem, 273*(16), 9357-9360.

Jankowski, A., Scott, C. C., & Grinstein, S. (2002). Determinants of the phagosomal pH in neutrophils. *J Biol Chem, 277*(8), 6059-6066. doi:10.1074/jbc.M110059200

Janssens, H. J., Janssen, M., van de Lisdonk, E. H., van Riel, P. L., & van Weel, C. (2008). Use of oral prednisolone or naproxen for the treatment of gout arthritis: a double-blind, randomised equivalence trial. *Lancet, 371*(9627), 1854-1860. doi:10.1016/S0140-6736(08)60799-0

Jhunjhunwala, S., Aresta-DaSilva, S., Tang, K., Alvarez, D., Webber, M. J., Tang, B. C., . . . Anderson, D. G. (2015). Neutrophil Responses to Sterile Implant Materials. *PLoS ONE, 10*(9), e0137550. doi:10.1371/journal.pone.0137550

Jiang, C. L., Liu, L., & Tasker, J. G. (2014). Why do we need nongenomic glucocorticoid mechanisms? *Front Neuroendocrinol, 35*(1), 72-75. doi:10.1016/j.yfrne.2013.09.005

Jie, H., He, Y., Huang, X., Zhou, Q., Han, Y., Li, X., . . . Sun, E. (2016). Necrostatin-1 enhances the resolution of inflammation by specifically inducing neutrophil apoptosis. *Oncotarget, 7*(15), 19367-19381. doi:10.18632/oncotarget.8346

Jones, C. J., Morris, K. J., & Jayson, M. I. (1983). Prednisolone inhibits phagocytosis by polymorphonuclear leucocytes via steroid receptor mediated events. *Ann Rheum Dis, 42*(1), 56-62.
Joosten, L. A., Crisan, T. O., Azam, T., Cleophas, M. C., Koenders, M. I., van de Veerdonk, F. L., . . . Dinarello, C. A. (2016). Alpha-1-anti-trypsin-Fc fusion protein ameliorates gouty arthritis by reducing release and extracellular processing of IL-1beta and by the induction of endogenous IL-1Ra. *Ann Rheum Dis, 75*(6), 1219-1227. doi:10.1136/annrheumdis-2014-206966
Joosten, L. A., Netea, M. G., Mylona, E., Koenders, M. I., Malireddi, R. K., Oosting, M., . . . van der Meer, J. W. (2010). Engagement of fatty acids with Toll-like receptor 2 drives interleukin-1beta production via the ASC/caspase 1 pathway in monosodium urate monohydrate crystal-induced gouty arthritis. *Arthritis Rheum, 62*(11), 3237-3248. doi:10.1002/art.27667
Jorch, S. K., & Kubes, P. (2017). An emerging role for neutrophil extracellular traps in noninfectious disease. *Nat Med, 23*(3), 279-287. doi:10.1038/nm.4294
Kahlenberg, J. M., Carmona-Rivera, C., Smith, C. K., & Kaplan, M. J. (2013). Neutrophil extracellular trap-associated protein activation of the NLRP3 inflammasome is enhanced in lupus macrophages. *J Immunol, 190*(3), 1217-1226. doi:10.4049/jimmunol.1202388
Kaiser, W. J., Sridharan, H., Huang, C., Mandal, P., Upton, J. W., Gough, P. J., . . . Mocarski, E. S. (2013). Toll-like receptor 3-mediated necrosis via TRIF, RIP3, and MLKL. *J Biol Chem, 288*(43), 31268-31279. doi:10.1074/jbc.M113.462341
Kaneko, K., Iwamoto, H., Yasuda, M., Inazawa, K., Yamaoka, N., Fukuuchi, T., . . . Fujimori, S. (2014). Proteomic analysis to examine the role of matrix proteins in a gouty tophus from a patient with recurrent gout. *Nucleosides Nucleotides Nucleic Acids, 33*(4-6), 199-207. doi:10.1080/15257770.2014.880476
Kasahara, Y., Iwai, K., Yachie, A., Ohta, K., Konno, A., Seki, H., . . . Taniguchi, N. (1997). Involvement of reactive oxygen intermediates in spontaneous and CD95 (Fas/APO-1)-mediated apoptosis of neutrophils. *Blood, 89*(5), 1748-1753.
Kayagaki, N., Stowe, I. B., Lee, B. L., O'Rourke, K., Anderson, K., Warming, S., . . . Dixit, V. M. (2015). Caspase-11 cleaves gasdermin D for non-canonical inflammasome signalling. *Nature, 526*(7575), 666-671. doi:10.1038/nature15541
Keel, M., Ungethum, U., Steckholzer, U., Niederer, E., Hartung, T., Trentz, O., & Ertel, W. (1997). Interleukin-10 counterregulates proinflammatory cytokine-induced inhibition of neutrophil apoptosis during severe sepsis. *Blood, 90*(9), 3356-3363.
Kenny, E. F., Herzig, A., Krüger, R., Muth, A., Mondal, S., Thompson, P. R., . . . Zychlinsky, A. (2017). Diverse stimuli engage different neutrophil extracellular trap pathways. *eLife, 6*, e24437. doi:10.7554/eLife.24437
Kerr, J. F., Wyllie, A. H., & Currie, A. R. (1972). Apoptosis: a basic biological phenomenon with wide-ranging implications in tissue kinetics. *Br J Cancer, 26*(4), 239-257.
Kessenbrock, K., Frohlich, L., Sixt, M., Lammermann, T., Pfister, H., Bateman, A., . . . Jenne, D. E. (2008). Proteinase 3 and neutrophil elastase enhance inflammation in mice by inactivating antiinflammatory progranulin. *J Clin Invest, 118*(7), 2438-2447. doi:10.1172/JCI34694
Kessenbrock, K., Krumbholz, M., Schonermarck, U., Back, W., Gross, W. L., Werb, Z., . . . Jenne, D. E. (2009). Netting neutrophils in autoimmune small-vessel vasculitis. *Nat Med, 15*(6), 623-625. doi:10.1038/nm.1959
Khandpur, R., Carmona-Rivera, C., Vivekanandan-Giri, A., Gizinski, A., Yalavarthi, S., Knight, J. S., . . . Kaplan, M. J. (2013). NETs are a source of citrullinated

autoantigens and stimulate inflammatory responses in rheumatoid arthritis. *Sci Transl Med, 5*(178), 178ra140. doi:10.1126/scitranslmed.3005580
Khosla, U. M., Zharikov, S., Finch, J. L., Nakagawa, T., Roncal, C., Mu, W., . . . Johnson, R. J. (2005). Hyperuricemia induces endothelial dysfunction. *Kidney Int, 67*(5), 1739-1742. doi:10.1111/j.1523-1755.2005.00273.x
Kienle, K., & Lammermann, T. (2016). Neutrophil swarming: an essential process of the neutrophil tissue response. *Immunol Rev, 273*(1), 76-93. doi:10.1111/imr.12458
Kirkegaard, T., Roth, A. G., Petersen, N. H., Mahalka, A. K., Olsen, O. D., Moilanen, I., . . . Jaattela, M. (2010). Hsp70 stabilizes lysosomes and reverts Niemann-Pick disease-associated lysosomal pathology. *Nature, 463*(7280), 549-553. doi:10.1038/nature08710
Kirschnek, S., Vier, J., Gautam, S., Frankenberg, T., Rangelova, S., Eitz-Ferrer, P., . . . Hacker, G. (2011). Molecular analysis of neutrophil spontaneous apoptosis reveals a strong role for the pro-apoptotic BH3-only protein Noxa. *Cell Death Differ, 18*(11), 1805-1814. doi:10.1038/cdd.2011.69
Kischkel, F. C., Lawrence, D. A., Tinel, A., LeBlanc, H., Virmani, A., Schow, P., . . . Ashkenazi, A. (2001). Death receptor recruitment of endogenous caspase-10 and apoptosis initiation in the absence of caspase-8. *J Biol Chem, 276*(49), 46639-46646. doi:10.1074/jbc.M105102200
Knepper-Nicolai, B., Savill, J., & Brown, S. B. (1998). Constitutive apoptosis in human neutrophils requires synergy between calpains and the proteasome downstream of caspases. *J Biol Chem, 273*(46), 30530-30536. doi:10.1074/jbc.273.46.30530
Kobayashi, S., Yamashita, K., Takeoka, T., Ohtsuki, T., Suzuki, Y., Takahashi, R., . . . Takahashi, A. (2002). Calpain-mediated X-linked inhibitor of apoptosis degradation in neutrophil apoptosis and its impairment in chronic neutrophilic leukemia. *J Biol Chem, 277*(37), 33968-33977. doi:10.1074/jbc.M203350200
Kobayashi, S. D., Braughton, K. R., Whitney, A. R., Voyich, J. M., Schwan, T. G., Musser, J. M., & DeLeo, F. R. (2003). Bacterial pathogens modulate an apoptosis differentiation program in human neutrophils. *Proc Natl Acad Sci U S A, 100*(19), 10948-10953. doi:10.1073/pnas.1833375100
Kobayashi, S. D., Voyich, J. M., Buhl, C. L., Stahl, R. M., & DeLeo, F. R. (2002). Global changes in gene expression by human polymorphonuclear leukocytes during receptor-mediated phagocytosis: cell fate is regulated at the level of gene expression. *Proc Natl Acad Sci U S A, 99*(10), 6901-6906. doi:10.1073/pnas.092148299
Koedel, U., Frankenberg, T., Kirschnek, S., Obermaier, B., Hacker, H., Paul, R., & Hacker, G. (2009). Apoptosis is essential for neutrophil functional shutdown and determines tissue damage in experimental pneumococcal meningitis. *PLoS Pathog, 5*(5), e1000461. doi:10.1371/journal.ppat.1000461.s006
Konig, M. F., & Andrade, F. (2016). A Critical Reappraisal of Neutrophil Extracellular Traps and NETosis Mimics Based on Differential Requirements for Protein Citrullination. *Front Immunol, 7*(9), 461. doi:10.3389/fimmu.2016.00461
Kono, H., Onda, A., & Yanagida, T. (2014). Molecular determinants of sterile inflammation. *Curr Opin Immunol, 26*, 147-156. doi:10.1016/j.coi.2013.12.004
Kopalli, S. R., Kang, T. B., & Koppula, S. (2016). Necroptosis inhibitors as therapeutic targets in inflammation mediated disorders - a review of the current literature and patents. *Expert Opin Ther Pat, 26*(11), 1239-1256. doi:10.1080/13543776.2016.1230201
Korkmaz, B., Horwitz, M. S., Jenne, D. E., & Gauthier, F. (2010). Neutrophil elastase, proteinase 3, and cathepsin G as therapeutic targets in human diseases. *Pharmacol Rev, 62*(4), 726-759. doi:10.1124/pr.110.002733

Kothakota, S., Azuma, T., Reinhard, C., Klippel, A., Tang, J., Chu, K., . . . Williams, L. T. (1997). Caspase-3-generated fragment of gelsolin: effector of morphological change in apoptosis. *Science, 278*(5336), 294-298. doi:10.1126/science.278.5336.294

Kotschy, A., Szlavik, Z., Murray, J., Davidson, J., Maragno, A. L., Le Toumelin-Braizat, G., . . . Geneste, O. (2016). The MCL1 inhibitor S63845 is tolerable and effective in diverse cancer models. *Nature, 538*(7626), 477-482. doi:10.1038/nature19830

Kotzin, J. J., Spencer, S. P., McCright, S. J., Kumar, D. B., Collet, M. A., Mowel, W. K., . . . Henao-Mejia, J. (2016). The long non-coding RNA Morrbid regulates Bim and short-lived myeloid cell lifespan. *Nature, 537*(7619), 239-243. doi:10.1038/nature19346

Krey, P. R., & Bailen, D. A. (1979). Synovial fluid leukocytosis. A study of extremes. *Am J Med, 67*(3), 436-442.

Kuroda, E., Ishii, K. J., Uematsu, S., Ohata, K., Coban, C., Akira, S., . . . Morimoto, Y. (2011). Silica crystals and aluminum salts regulate the production of prostaglandin in macrophages via NALP3 inflammasome-independent mechanisms. *Immunity, 34*(4), 514-526. doi:10.1016/j.immuni.2011.03.019

Lafont, E., Milhas, D., Teissié, J., Therville, N., Andrieu-Abadie, N., Levade, T., . . . Ségui, B. (2010). Caspase-10-Dependent Cell Death in Fas/CD95 Signalling Is Not Abrogated by Caspase Inhibitor zVAD-fmk. *PLoS ONE, 5*(10), e13638. doi:10.1371/journal.pone.0013638.g008

Lande, R., Ganguly, D., Facchinetti, V., Frasca, L., Conrad, C., Gregorio, J., . . . Gilliet, M. (2011). Neutrophils activate plasmacytoid dendritic cells by releasing self-DNA-peptide complexes in systemic lupus erythematosus. *Sci Transl Med, 3*(73), 73ra19. doi:10.1126/scitranslmed.3001180

Latz, E., Xiao, T. S., & Stutz, A. (2013). Activation and regulation of the inflammasomes. *Nat Rev Immunol, 13*(6), 397-411. doi:10.1038/nri3452

Lazarides, E., & Lindberg, U. (1974). Actin is the naturally occurring inhibitor of deoxyribonuclease I. *Proc Natl Acad Sci U S A, 71*(12), 4742-4746.

Leavey, P. J., Sellins, K. S., Thurman, G., Elzi, D., Hiester, A., Silliman, C. C., . . . Ambruso, D. R. (1998). In vivo treatment with granulocyte colony-stimulating factor results in divergent effects on neutrophil functions measured in vitro. *Blood, 92*(11), 4366-4374.

Lee, A., Whyte, M. K., & Haslett, C. (1993). Inhibition of apoptosis and prolongation of neutrophil functional longevity by inflammatory mediators. *J Leukoc Biol, 54*(4), 283-288.

Lee, D., Long, S. A., Adams, J. L., Chan, G., Vaidya, K. S., Francis, T. A., . . . Nuttall, M. E. (2000). Potent and selective nonpeptide inhibitors of caspases 3 and 7 inhibit apoptosis and maintain cell functionality. *J Biol Chem, 275*(21), 16007-16014.

Lee, G. S., Subramanian, N., Kim, A. I., Aksentijevich, I., Goldbach-Mansky, R., Sacks, D. B., . . . Chae, J. J. (2012). The calcium-sensing receptor regulates the NLRP3 inflammasome through Ca2+ and cAMP. *Nature, 492*(7427), 123-127. doi:10.1038/nature11588

Leitch, A. E., Lucas, C. D., Marwick, J. A., Duffin, R., Haslett, C., & Rossi, A. G. (2012). Cyclin-dependent kinases 7 and 9 specifically regulate neutrophil transcription and their inhibition drives apoptosis to promote resolution of inflammation. *Cell Death Differ, 19*(12), 1950-1961. doi:10.1038/cdd.2012.80

Leuenroth, S. J., Grutkoski, P. S., Ayala, A., & Simms, H. H. (2000). The loss of Mcl-1 expression in human polymorphonuclear leukocytes promotes apoptosis. *J Leukoc Biol, 68*(1), 158-166.

Levine, A. P., Duchen, M. R., de Villiers, S., Rich, P. R., & Segal, A. W. (2015). Alkalinity of neutrophil phagocytic vacuoles is modulated by HVCN1 and has consequences for myeloperoxidase activity. *PLoS ONE, 10*(4), e0125906. doi:10.1371/journal.pone.0125906

Levine, B., Mizushima, N., & Virgin, H. W. (2011). Autophagy in immunity and inflammation. *Nature, 469*(7330), 323-335. doi:10.1038/nature09782

Lewis, H. D., Liddle, J., Coote, J. E., Atkinson, S. J., Barker, M. D., Bax, B. D., . . . Wilson, D. M. (2015). Inhibition of PAD4 activity is sufficient to disrupt mouse and human NET formation. *Nat Chem Biol, 11*(3), 189-191. doi:10.1038/nchembio.1735

Li, P., Li, M., Lindberg, M. R., Kennett, M. J., Xiong, N., & Wang, Y. (2010). PAD4 is essential for antibacterial innate immunity mediated by neutrophil extracellular traps. *J Exp Med, 207*(9), 1853-1862. doi:10.1084/jem.20100239

Li, P., Nijhawan, D., Budihardjo, I., Srinivasula, S. M., Ahmad, M., Alnemri, E. S., & Wang, X. (1997). Cytochrome c and dATP-dependent formation of Apaf-1/caspase-9 complex initiates an apoptotic protease cascade. *Cell, 91*(4), 479-489.

Liao, D., Sun, L., Liu, W., He, S., Wang, X., & Lei, X. (2014). Necrosulfonamide inhibits necroptosis by selectively targeting the mixed lineage kinase domain-like protein. *MedChemComm, 5*(3), 333-337. doi:10.1039/c3md00278k

Lieschke, G. J., Grail, D., Hodgson, G., Metcalf, D., Stanley, E., Cheers, C., . . . Dunn, A. R. (1994). Mice lacking granulocyte colony-stimulating factor have chronic neutropenia, granulocyte and macrophage progenitor cell deficiency, and impaired neutrophil mobilization. *Blood, 84*(6), 1737-1746.

Liles, W. C., Dale, D. C., & Klebanoff, S. J. (1995). Glucocorticoids inhibit apoptosis of human neutrophils. *Blood, 86*(8), 3181-3188.

Liles, W. C., Kiener, P. A., Ledbetter, J. A., Aruffo, A., & Klebanoff, S. J. (1996). Differential expression of Fas (CD95) and Fas ligand on normal human phagocytes: implications for the regulation of apoptosis in neutrophils. *J Exp Med, 184*(2), 429-440.

Lindqvist, L. M., Heinlein, M., Huang, D. C., & Vaux, D. L. (2014). Prosurvival Bcl-2 family members affect autophagy only indirectly, by inhibiting Bax and Bak. *Proc Natl Acad Sci U S A, 111*(23), 8512-8517. doi:10.1073/pnas.1406425111

Linkermann, A., Kunzendorf, U., & Krautwald, S. (2014). Phosphorylated MLKL causes plasma membrane rupture. *Mol Cell Oncol, 1*(1), e29915. doi:10.4161/mco.29915

Lippolis, J. D., Reinhardt, T. A., Goff, J. P., & Horst, R. L. (2006). Neutrophil extracellular trap formation by bovine neutrophils is not inhibited by milk. *Vet Immunol Immunopathol, 113*(1-2), 248-255. doi:10.1016/j.vetimm.2006.05.004

Liu, C. Y., Takemasa, A., Liles, W. C., Goodman, R. B., Jonas, M., Rosen, H., . . . Chuang, P. I. (2003). Broad-spectrum caspase inhibition paradoxically augments cell death in TNF-alpha -stimulated neutrophils. *Blood, 101*(1), 295-304. doi:10.1182/blood-2001-12-0266

Liu-Bryan, R., Scott, P., Sydlaske, A., Rose, D. M., & Terkeltaub, R. (2005). Innate immunity conferred by Toll-like receptors 2 and 4 and myeloid differentiation factor 88 expression is pivotal to monosodium urate monohydrate crystal-induced inflammation. *Arthritis Rheum, 52*(9), 2936-2946. doi:10.1002/art.21238

Loison, F., Zhu, H., Karatepe, K., Kasorn, A., Liu, P., Ye, K., . . . Luo, H. R. (2014). Proteinase 3-dependent caspase-3 cleavage modulates neutrophil death and inflammation. *J Clin Invest, 124*(10), 4445-4458. doi:10.1172/JCI76246

Lood, C., Blanco, L. P., Purmalek, M. M., Carmona-Rivera, C., De Ravin, S. S., Smith, C. K., . . . Kaplan, M. J. (2016). Neutrophil extracellular traps enriched in

oxidized mitochondrial DNA are interferogenic and contribute to lupus-like disease. *Nat Med, 22*(2), 146-153. doi:10.1038/nm.4027
Lucas, C. D., Allen, K. C., Dorward, D. A., Hoodless, L. J., Melrose, L. A., Marwick, J. A., . . . Rossi, A. G. (2013). Flavones induce neutrophil apoptosis by down-regulation of Mcl-1 via a proteasomal-dependent pathway. *FASEB J, 27*(3), 1084-1094. doi:10.1096/fj.12-218990
Lum, J. J., Bren, G., McClure, R., & Badley, A. D. (2005). Elimination of senescent neutrophils by TNF-related apoptosis-inducing [corrected] ligand. *J Immunol, 175*(2), 1232-1238. doi:10.4049/jimmunol.175.2.1232
Lundqvist-Gustafsson, H., & Bengtsson, T. (1999). Activation of the granule pool of the NADPH oxidase accelerates apoptosis in human neutrophils. *J Leukoc Biol, 65*(2), 196-204.
Luo, H. R., & Loison, F. (2008). Constitutive neutrophil apoptosis: mechanisms and regulation. *Am J Hematol, 83*(4), 288-295. doi:10.1002/ajh.21078
Lyons, P. A., Koukoulaki, M., Hatton, A., Doggett, K., Woffendin, H. B., Chaudhry, A. N., & Smith, K. G. (2007). Microarray analysis of human leucocyte subsets: the advantages of positive selection and rapid purification. *BMC Genomics, 8*, 64. doi:10.1186/1471-2164-8-64
Ma, B., Marcotte, D., Paramasivam, M., Michelsen, K., Wang, T., Bertolotti-Ciarlet, A., . . . Silvian, L. F. (2016). ATP-Competitive MLKL Binders Have No Functional Impact on Necroptosis. *PLoS ONE, 11*(11), e0165983. doi:10.1371/journal.pone.0165983
Maianski, N. A., Geissler, J., Srinivasula, S. M., Alnemri, E. S., Roos, D., & Kuijpers, T. W. (2004). Functional characterization of mitochondria in neutrophils: a role restricted to apoptosis. *Cell Death Differ, 11*(2), 143-153. doi:10.1038/sj.cdd.4401320
Maianski, N. A., Mul, F. P., van Buul, J. D., Roos, D., & Kuijpers, T. W. (2002). Granulocyte colony-stimulating factor inhibits the mitochondria-dependent activation of caspase-3 in neutrophils. *Blood, 99*(2), 672-679. doi:10.1182/blood.V99.2.672
Maianski, N. A., Roos, D., & Kuijpers, T. W. (2003). Tumor necrosis factor alpha induces a caspase-independent death pathway in human neutrophils. *Blood, 101*(5), 1987-1995. doi:10.1182/blood-2002-02-0522
Maianski, N. A., Roos, D., & Kuijpers, T. W. (2004). Bid truncation, bid/bax targeting to the mitochondria, and caspase activation associated with neutrophil apoptosis are inhibited by granulocyte colony-stimulating factor. *J Immunol, 172*(11), 7024-7030.
Majno, G., & Joris, I. (1995). Apoptosis, oncosis, and necrosis. An overview of cell death. *The American journal of pathology, 146*(1), 3-15.
Mallinson, P. I., Reagan, A. C., Coupal, T., Munk, P. L., Ouellette, H., & Nicolaou, S. (2014). The distribution of urate deposition within the extremities in gout: a review of 148 dual-energy CT cases. *Skeletal Radiol, 43*(3), 277-281. doi:10.1007/s00256-013-1771-8
Mankan, A. K., Dau, T., Jenne, D., & Hornung, V. (2012). The NLRP3/ASC/Caspase-1 axis regulates IL-1beta processing in neutrophils. *Eur J Immunol, 42*(3), 710-715. doi:10.1002/eji.201141921
Marcos, V., Nussbaum, C., Vitkov, L., Hector, A., Wiedenbauer, E. M., Roos, D., . . . Hartl, D. (2009). Delayed but functional neutrophil extracellular trap formation in neonates. *Blood, 114*(23), 4908-4911; author reply 4911-4902. doi:10.1182/blood-2009-09-242388
Marcos, V., Zhou, Z., Yildirim, A. O., Bohla, A., Hector, A., Vitkov, L., . . . Hartl, D. (2010). CXCR2 mediates NADPH oxidase-independent neutrophil extracellular

trap formation in cystic fibrosis airway inflammation. *Nat Med, 16*(9), 1018-1023. doi:10.1038/nm.2209
Martin, C., Ohayon, D., Alkan, M., Mocek, J., Pederzoli-Ribeil, M., Candalh, C., . . . Witko-Sarsat, V. (2016). Neutrophil-Expressed p21/waf1 Favors Inflammation Resolution in Pseudomonas aeruginosa Infection. *Am J Respir Cell Mol Biol, 54*(5), 740-750. doi:10.1165/rcmb.2015-0047OC
Martin, K. R., Ohayon, D., & Witko-Sarsat, V. (2015). Promoting apoptosis of neutrophils and phagocytosis by macrophages: novel strategies in the resolution of inflammation. *Swiss Med Wkly, 145*, w14056. doi:10.4414/smw.2015.14056
Martin, S. J., Reutelingsperger, C. P., McGahon, A. J., Rader, J. A., van Schie, R. C., LaFace, D. M., & Green, D. R. (1995). Early redistribution of plasma membrane phosphatidylserine is a general feature of apoptosis regardless of the initiating stimulus: inhibition by overexpression of Bcl-2 and Abl. *J Exp Med, 182*(5), 1545-1556.
Martin, W. J., Walton, M., & Harper, J. (2009). Resident macrophages initiating and driving inflammation in a monosodium urate monohydrate crystal-induced murine peritoneal model of acute gout. *Arthritis Rheum, 60*(1), 281-289. doi:10.1002/art.24185
Martinelli, S., Urosevic, M., Daryadel, A., Oberholzer, P. A., Baumann, C., Fey, M. F., . . . Yousefi, S. (2004). Induction of genes mediating interferon-dependent extracellular trap formation during neutrophil differentiation. *J Biol Chem, 279*(42), 44123-44132. doi:10.1074/jbc.M405883200
Martinod, K., Fuchs, T. A., Zitomersky, N. L., Wong, S. L., Demers, M., Gallant, M., . . . Wagner, D. D. (2015). PAD4-deficiency does not affect bacteremia in polymicrobial sepsis and ameliorates endotoxemic shock. *Blood, 125*(12), 1948-1956. doi:10.1182/blood-2014-07-587709
Martinod, K., & Wagner, D. D. (2014). Thrombosis: tangled up in NETs. *Blood, 123*(18), 2768-2776. doi:10.1182/blood-2013-10-463646
Martinod, K., Witsch, T., Farley, K., Gallant, M., Remold-O'Donnell, E., & Wagner, D. D. (2016). Neutrophil elastase-deficient mice form neutrophil extracellular traps in an experimental model of deep vein thrombosis. *J Thromb Haemost, 14*(3), 551-558. doi:10.1111/jth.13239
Martinon, F., Petrilli, V., Mayor, A., Tardivel, A., & Tschopp, J. (2006). Gout-associated uric acid crystals activate the NALP3 inflammasome. *Nature, 440*(7081), 237-241. doi:10.1038/nature04516
Marwick, J. A., Dorward, D. A., Lucas, C. D., Jones, K. O., Sheldrake, T. A., Fox, S., . . . Rossi, A. G. (2013). Oxygen levels determine the ability of glucocorticoids to influence neutrophil survival in inflammatory environments. *J Leukoc Biol, 94*(6), 1285-1292. doi:10.1189/jlb.0912462
Matsukawa, A., Yoshimura, T., Maeda, T., Takahashi, T., Ohkawara, S., & Yoshinaga, M. (1998). Analysis of the cytokine network among tumor necrosis factor alpha, interleukin-1beta, interleukin-8, and interleukin-1 receptor antagonist in monosodium urate crystal-induced rabbit arthritis. *Lab Invest, 78*(5), 559-569.
McGill, N. W., & Dieppe, P. A. (1991). The role of serum and synovial fluid components in the promotion of urate crystal formation. *J Rheumatol, 18*(7), 1042-1045.
McGuire, M. J., Lipsky, P. E., & Thiele, D. L. (1993). Generation of active myeloid and lymphoid granule serine proteases requires processing by the granule thiol protease dipeptidyl peptidase I. *J Biol Chem, 268*(4), 2458-2467.
Metzler, K. D., Fuchs, T. A., Nauseef, W. M., Reumaux, D., Roesler, J., Schulze, I., . . . Zychlinsky, A. (2011). Myeloperoxidase is required for neutrophil extracellular trap formation: implications for innate immunity. *Blood, 117*(3), 953-959. doi:10.1182/blood-2010-06-290171

Metzler, K. D., Goosmann, C., Lubojemska, A., Zychlinsky, A., & Papayannopoulos, V. (2014). A myeloperoxidase-containing complex regulates neutrophil elastase release and actin dynamics during NETosis. *Cell Rep, 8*(3), 883-896. doi:10.1016/j.celrep.2014.06.044

Miao, E. A., Leaf, I. A., Treuting, P. M., Mao, D. P., Dors, M., Sarkar, A., . . . Aderem, A. (2010). Caspase-1-induced pyroptosis is an innate immune effector mechanism against intracellular bacteria. *Nat Immunol, 11*(12), 1136-1142. doi:10.1038/ni.1960

Mica, L., Harter, L., Trentz, O., & Keel, M. (2004). Endotoxin reduces CD95-induced neutrophil apoptosis by cIAP-2-mediated caspase-3 degradation. *J Am Coll Surg, 199*(4), 595-602. doi:10.1016/j.jamcollsurg.2004.05.272

Mihalache, C. C., Yousefi, S., Conus, S., Villiger, P. M., Schneider, E. M., & Simon, H. U. (2011). Inflammation-associated autophagy-related programmed necrotic death of human neutrophils characterized by organelle fusion events. *J Immunol, 186*(11), 6532-6542. doi:10.4049/jimmunol.1004055

Misawa, T., Takahama, M., Kozaki, T., Lee, H., Zou, J., Saitoh, T., & Akira, S. (2013). Microtubule-driven spatial arrangement of mitochondria promotes activation of the NLRP3 inflammasome. *Nat Immunol, 14*(5), 454-460. doi:10.1038/ni.2550

Mitroulis, I., Kambas, K., Chrysanthopoulou, A., Skendros, P., Apostolidou, E., Kourtzelis, I., . . . Ritis, K. (2011). Neutrophil extracellular trap formation is associated with IL-1beta and autophagy-related signaling in gout. *PLoS ONE, 6*(12), e29318. doi:10.1371/journal.pone.0029318

Miwa, K., Asano, M., Horai, R., Iwakura, Y., Nagata, S., & Suda, T. (1998). Caspase 1-independent IL-1beta release and inflammation induced by the apoptosis inducer Fas ligand. *Nature Medicine, 4*(11), 1287-1292. doi:10.1038/3276

Mocarski, E. S., Upton, J. W., & Kaiser, W. J. (2011). Viral infection and the evolution of caspase 8-regulated apoptotic and necrotic death pathways. *Nat Rev Immunol, 12*(2), 79-88. doi:10.1038/nri3131

Mocsai, A., Ruland, J., & Tybulewicz, V. L. (2010). The SYK tyrosine kinase: a crucial player in diverse biological functions. *Nat Rev Immunol, 10*(6), 387-402. doi:10.1038/nri2765

Mocsai, A., Zhou, M., Meng, F., Tybulewicz, V. L., & Lowell, C. A. (2002). Syk is required for integrin signaling in neutrophils. *Immunity, 16*(4), 547-558.

Mohanty, T., Sjogren, J., Kahn, F., Abu-Humaidan, A. H., Fisker, N., Assing, K., . . . Sorensen, O. E. (2015). A novel mechanism for NETosis provides antimicrobial defense at the oral mucosa. *Blood, 126*(18), 2128-2137. doi:10.1182/blood-2015-04-641142

Morgan, D. O. (1997). Cyclin-dependent kinases: engines, clocks, and microprocessors. *Annu Rev Cell Dev Biol, 13*(1), 261-291. doi:10.1146/annurev.cellbio.13.1.261

Moulding, D. A., Akgul, C., Derouet, M., White, M. R., & Edwards, S. W. (2001). BCL-2 family expression in human neutrophils during delayed and accelerated apoptosis. *J Leukoc Biol, 70*(5), 783-792.

Moulding, D. A., Quayle, J. A., Hart, C. A., & Edwards, S. W. (1998). Mcl-1 expression in human neutrophils: regulation by cytokines and correlation with cell survival. *Blood, 92*(7), 2495-2502.

Munoz-Planillo, R., Kuffa, P., Martinez-Colon, G., Smith, B. L., Rajendiran, T. M., & Nunez, G. (2013). K(+) efflux is the common trigger of NLRP3 inflammasome activation by bacterial toxins and particulate matter. *Immunity, 38*(6), 1142-1153. doi:10.1016/j.immuni.2013.05.016

Murphy, B. M., O'Neill, A. J., Adrain, C., Watson, R. W., & Martin, S. J. (2003). The apoptosome pathway to caspase activation in primary human neutrophils

exhibits dramatically reduced requirements for cytochrome C. *J Exp Med, 197*(5), 625-632. doi:10.1084/jem.20021862
Murphy, J. M., Czabotar, P. E., Hildebrand, J. M., Lucet, I. S., Zhang, J. G., Alvarez-Diaz, S., . . . Alexander, W. S. (2013). The pseudokinase MLKL mediates necroptosis via a molecular switch mechanism. *Immunity, 39*(3), 443-453. doi:10.1016/j.immuni.2013.06.018
Murphy, J. M., & Silke, J. (2014). Ars Moriendi; the art of dying well - new insights into the molecular pathways of necroptotic cell death. *EMBO reports, 15*(2), 155-164. doi:10.1002/embr.201337970
Murray, J., Barbara, J. A., Dunkley, S. A., Lopez, A. F., Van Ostade, X., Condliffe, A. M., . . . Chilvers, E. R. (1997). Regulation of neutrophil apoptosis by tumor necrosis factor-alpha: requirement for TNFR55 and TNFR75 for induction of apoptosis in vitro. *Blood, 90*(7), 2772-2783.
Naccache, P. H., & Fernandes, M. J. (2016). Challenges in the characterization of neutrophil extracellular traps: The truth is in the details. *Eur J Immunol, 46*(1), 52-55. doi:10.1002/eji.201546022
Naccache, P. H., Grimard, M., Roberge, C. J., Gilbert, C., Lussier, A., de Medicis, R., & Poubelle, P. E. (1991). Crystal-induced neutrophil activation. I. Initiation and modulation of calcium mobilization and superoxide production by microcrystals. *Arthritis Rheum, 34*(3), 333-342.
Nakazawa, D., Shida, H., Kusunoki, Y., Miyoshi, A., Nishio, S., Tomaru, U., . . . Ishizu, A. (2016). The responses of macrophages in interaction with neutrophils that undergo NETosis. *J Autoimmun, 67*, 19-28. doi:10.1016/j.jaut.2015.08.018
Nauseef, W. M., & Kubes, P. (2016). Pondering neutrophil extracellular traps with healthy skepticism. *Cell Microbiol, 18*(10), 1349-1357. doi:10.1111/cmi.12652
Neeli, I., & Radic, M. (2013). Opposition between PKC isoforms regulates histone deimination and neutrophil extracellular chromatin release. *Front Immunol, 4*, 38. doi:10.3389/fimmu.2013.00038
Netea, M. G., Nold-Petry, C. A., Nold, M. F., Joosten, L. A., Opitz, B., van der Meer, J. H., . . . Dinarello, C. A. (2009). Differential requirement for the activation of the inflammasome for processing and release of IL-1beta in monocytes and macrophages. *Blood, 113*(10), 2324-2335. doi:10.1182/blood-2008-03-146720
Neumann, K., Castineiras-Vilarino, M., Hockendorf, U., Hannesschlager, N., Lemeer, S., Kupka, D., . . . Ruland, J. (2014). Clec12a is an inhibitory receptor for uric acid crystals that regulates inflammation in response to cell death. *Immunity, 40*(3), 389-399. doi:10.1016/j.immuni.2013.12.015
Newton, R. (2014). Anti-inflammatory glucocorticoids: changing concepts. *Eur J Pharmacol, 724*(C), 231-236. doi:10.1016/j.ejphar.2013.05.035
Ng, G., Sharma, K., Ward, S. M., Desrosiers, M. D., Stephens, L. A., Schoel, W. M., . . . Shi, Y. (2008). Receptor-independent, direct membrane binding leads to cell-surface lipid sorting and Syk kinase activation in dendritic cells. *Immunity, 29*(5), 807-818. doi:10.1016/j.immuni.2008.09.013
Nguyen-Jackson, H., Panopoulos, A. D., Zhang, H., Li, H. S., & Watowich, S. S. (2010). STAT3 controls the neutrophil migratory response to CXCR2 ligands by direct activation of G-CSF-induced CXCR2 expression and via modulation of CXCR2 signal transduction. *Blood, 115*(16), 3354-3363. doi:10.1182/blood-2009-08-240317
Nicholson, D. W. (1999). Caspase structure, proteolytic substrates, and function during apoptotic cell death. *Cell Death and Differentiation, 6*(11), 1028-1042. doi:10.1038/sj.cdd.4400598
Nordenfelt, P., & Tapper, H. (2011). Phagosome dynamics during phagocytosis by neutrophils. *J Leukoc Biol, 90*(2), 271-284. doi:10.1189/jlb.0810457

Nuki, G. (2008). Colchicine: its mechanism of action and efficacy in crystal-induced inflammation. *Curr Rheumatol Rep, 10*(3), 218-227.
Oda, E., Ohki, R., Murasawa, H., Nemoto, J., Shibue, T., Yamashita, T., . . . Tanaka, N. (2000). Noxa, a BH3-only member of the Bcl-2 family and candidate mediator of p53-induced apoptosis. *Science, 288*(5468), 1053-1058. doi:10.1126/science.288.5468.1053
Ortiz-Bravo, E., & Schumacher Jr, H. R. (1993). Components generated locally as well as serum alter the phlogistic effect of monosodium urate crystals in vivo. *J Rheumatol, 20*(7), 1162-1166.
Palic, D., Ostojic, J., Andreasen, C. B., & Roth, J. A. (2007). Fish cast NETs: neutrophil extracellular traps are released from fish neutrophils. *Dev Comp Immunol, 31*(8), 805-816. doi:10.1016/j.dci.2006.11.010
Palmer, D. G., Hogg, N., Denholm, I., Allen, C. A., Highton, J., & Hessian, P. A. (1987). Comparison of phenotype expression by mononuclear phagocytes within subcutaneous gouty tophi and rheumatoid nodules. *Rheumatol Int, 7*(5), 187-193.
Pang, L., Hayes, C. P., Buac, K., Yoo, D. G., & Rada, B. (2013). Pseudogout-associated inflammatory calcium pyrophosphate dihydrate microcrystals induce formation of neutrophil extracellular traps. *J Immunol, 190*(12), 6488-6500. doi:10.4049/jimmunol.1203215
Panopoulos, A. D., Zhang, L., Snow, J. W., Jones, D. M., Smith, A. M., El Kasmi, K. C., . . . Watowich, S. S. (2006). STAT3 governs distinct pathways in emergency granulopoiesis and mature neutrophils. *Blood, 108*(12), 3682-3690. doi:10.1182/blood-2006-02-003012
Papayannopoulos, V., Metzler, K. D., Hakkim, A., & Zychlinsky, A. (2010). Neutrophil elastase and myeloperoxidase regulate the formation of neutrophil extracellular traps. *J Cell Biol, 191*(3), 677-691. doi:10.1083/jcb.201006052
Parker, H., Dragunow, M., Hampton, M. B., Kettle, A. J., & Winterbourn, C. C. (2012). Requirements for NADPH oxidase and myeloperoxidase in neutrophil extracellular trap formation differ depending on the stimulus. *J Leukoc Biol, 92*(4), 841-849. doi:10.1189/jlb.1211601
Pascual, E. (1991). Persistence of monosodium urate crystals and low-grade inflammation in the synovial fluid of patients with untreated gout. *Arthritis Rheum, 34*(2), 141-145.
Pascual, E., & Sivera, F. (2007). Time required for disappearance of urate crystals from synovial fluid after successful hypouricaemic treatment relates to the duration of gout. *Ann Rheum Dis, 66*(8), 1056-1058. doi:10.1136/ard.2006.060368
Pesanti, E. L., & Axline, S. G. (1975). Phagolysosome formation in normal and colchicine-treated macrophages. *J Exp Med, 142*(4), 903-913. doi:10.1084/jem.142.4.903
Pestonjamasp, K., Amieva, M. R., Strassel, C. P., Nauseef, W. M., Furthmayr, H., & Luna, E. J. (1995). Moesin, ezrin, and p205 are actin-binding proteins associated with neutrophil plasma membranes. *Mol Biol Cell, 6*(3), 247-259.
Pham, C. T. N. (2006). Neutrophil serine proteases: specific regulators of inflammation. *Nature Reviews Immunology, 6*(7), 541-550. doi:10.1038/nri1841
Pham, C. T. N. (2008). Neutrophil serine proteases fine-tune the inflammatory response. *The international journal of biochemistry & cell biology, 40*(6-7), 1317-1333. doi:10.1016/j.biocel.2007.11.008
Phelps, P. (1969). Polymorphonuclear leukocyte motility in vitro. II. Stimulatory effect of monosodium urate crystals and urate in solution; partial inhibition by colchicine and indomethacin. *Arthritis Rheum, 12*(3), 189-196.

Pillay, J., den Braber, I., Vrisekoop, N., Kwast, L. M., de Boer, R. J., Borghans, J. A., . . . Koenderman, L. (2010). In vivo labeling with 2H2O reveals a human neutrophil lifespan of 5.4 days. *Blood, 116*(4), 625-627. doi:10.1182/blood-2010-01-259028

Pilsczek, F. H., Salina, D., Poon, K. K., Fahey, C., Yipp, B. G., Sibley, C. D., . . . Kubes, P. (2010). A novel mechanism of rapid nuclear neutrophil extracellular trap formation in response to Staphylococcus aureus. *J Immunol, 185*(12), 7413-7425. doi:10.4049/jimmunol.1000675

Pongracz, J., Webb, P., Wang, K., Deacon, E., Lunn, O. J., & Lord, J. M. (1999). Spontaneous neutrophil apoptosis involves caspase 3-mediated activation of protein kinase C-delta. *J Biol Chem, 274*(52), 37329-37334. doi:10.1074/jbc.274.52.37329

Poon, I. K., Lucas, C. D., Rossi, A. G., & Ravichandran, K. S. (2014). Apoptotic cell clearance: basic biology and therapeutic potential. *Nat Rev Immunol, 14*(3), 166-180. doi:10.1038/nri3607

Popa-Nita, O., Marois, L., Pare, G., & Naccache, P. H. (2008). Crystal-induced neutrophil activation: X. Proinflammatory role of the tyrosine kinase Tec. *Arthritis Rheum, 58*(6), 1866-1876. doi:10.1002/art.23801

Popa-Nita, O., & Naccache, P. H. (2010). Crystal-induced neutrophil activation. *Immunol Cell Biol, 88*(1), 32-40. doi:10.1038/icb.2009.98

Popa-Nita, O., Proulx, S., Pare, G., Rollet-Labelle, E., & Naccache, P. H. (2009). Crystal-induced neutrophil activation: XI. Implication and novel roles of classical protein kinase C. *J Immunol, 183*(3), 2104-2114. doi:10.4049/jimmunol.0900906

Prince, L. R., Bianchi, S. M., Vaughan, K. M., Bewley, M. A., Marriott, H. M., Walmsley, S. R., . . . Whyte, M. K. (2008). Subversion of a lysosomal pathway regulating neutrophil apoptosis by a major bacterial toxin, pyocyanin. *J Immunol, 180*(5), 3502-3511.

Rada, B., Jendrysik, M. A., Pang, L., Hayes, C. P., Yoo, D. G., Park, J. J., . . . Leto, T. L. (2013). Pyocyanin-enhanced neutrophil extracellular trap formation requires the NADPH oxidase. *PLoS ONE, 8*(1), e54205. doi:10.1371/journal.pone.0054205

Reber, L. L., Gaudenzio, N., Starkl, P., & Galli, S. J. (2016). Neutrophils are not required for resolution of acute gouty arthritis in mice. *Nat Med, 22*(12), 1382-1384. doi:10.1038/nm.4216

Remijsen, Q., Kuijpers, T. W., Wirawan, E., Lippens, S., Vandenabeele, P., & Vanden Berghe, T. (2011). Dying for a cause: NETosis, mechanisms behind an antimicrobial cell death modality. *Cell Death Differ, 18*(4), 581-588. doi:10.1038/cdd.2011.1

Remijsen, Q., Vanden Berghe, T., Wirawan, E., Asselbergh, B., Parthoens, E., De Rycke, R., . . . Vandenabeele, P. (2011). Neutrophil extracellular trap cell death requires both autophagy and superoxide generation. *Cell Res, 21*(2), 290-304. doi:10.1038/cr.2010.150

Renshaw, S. A., Parmar, J. S., Singleton, V., Rowe, S. J., Dockrell, D. H., Dower, S. K., . . . Whyte, M. K. (2003). Acceleration of human neutrophil apoptosis by TRAIL. *J Immunol, 170*(2), 1027-1033.

Renshaw, S. A., Timmons, S. J., Eaton, V., Usher, L. R., Akil, M., Bingle, C. D., & Whyte, M. K. (2000). Inflammatory neutrophils retain susceptibility to apoptosis mediated via the Fas death receptor. *J Leukoc Biol, 67*(5), 662-668.

Repine, J. E., White, J. G., Clawson, C. C., & Holmes, B. M. (1974). Effects of phorbol myristate acetate on the metabolism and ultrastructure of neutrophils in chronic granulomatous disease. *J Clin Invest, 54*(1), 83-90. doi:10.1172/JCI107752

Rickard, J. A., Anderton, H., Etemadi, N., Nachbur, U., Darding, M., Peltzer, N., . . . Silke, J. (2014). TNFR1-dependent cell death drives inflammation in Sharpin-deficient mice. *eLife, 3*. doi:10.7554/eLife.03464

Riddle, J. M., Bluhm, G. B., & Barnhart, M. I. (1967). Ultrastructural study of leucocytes and urates in gouty arthritis. *Ann Rheum Dis, 26*(5), 389-401.

Roberge, C. J., Gaudry, M., de Medicis, R., Lussier, A., Poubelle, P. E., & Naccache, P. H. (1993). Crystal-induced neutrophil activation. IV. Specific inhibition of tyrosine phosphorylation by colchicine. *J Clin Invest, 92*(4), 1722-1729. doi:10.1172/JCI116759

Roberge, C. J., Gaudry, M., Gilbert, C., Malawista, S. E., de Medicis, R., Lussier, A., . . . Naccache, P. H. (1996). Paradoxical effects of colchicine on the activation of human neutrophilis by chemotactic factors and inflammatory microcrystal. *J Leukoc Biol, 59*(6), 864-871.

Roberge, C. J., Grassi, J., De Medicis, R., Frobert, Y., Lussier, A., Naccache, P. H., & Poubelle, P. E. (1991). Crystal-neutrophil interactions lead to interleukin-1 synthesis. *Agents Actions, 34*(1-2), 38-41.

Rohrbach, A. S., Hemmers, S., Arandjelovic, S., Corr, M., & Mowen, K. A. (2012). PAD4 is not essential for disease in the K/BxN murine autoantibody-mediated model of arthritis. *Arthritis Res Ther, 14*(3), R104. doi:10.1186/ar3829

Romero, V., Fert-Bober, J., Nigrovic, P. A., Darrah, E., Haque, U. J., Lee, D. M., . . . Andrade, F. (2013). Immune-mediated pore-forming pathways induce cellular hypercitrullination and generate citrullinated autoantigens in rheumatoid arthritis. *Sci Transl Med, 5*(209), 209ra150. doi:10.1126/scitranslmed.3006869

Rongvaux, A., Jackson, R., Harman, C. C., Li, T., West, A. P., de Zoete, M. R., . . . Flavell, R. A. (2014). Apoptotic caspases prevent the induction of type I interferons by mitochondrial DNA. *Cell, 159*(7), 1563-1577. doi:10.1016/j.cell.2014.11.037

Rosen, H. (2013). Editorial: of mice and men--yet again. *J Leukoc Biol, 94*(2), 210-212. doi:10.1189/jlb.0413187

Rossi, A., & Lord, J. M. (2013). Adiponectin inhibits neutrophil apoptosis via activation of AMP kinase, PKB and ERK 1/2 MAP kinase. *Apoptosis, 18*(12), 1469-1480. doi:10.1007/s10495-013-0893-8

Rossi, A. G., Sawatzky, D. A., Walker, A., Ward, C., Sheldrake, T. A., Riley, N. A., . . . Haslett, C. (2006). Cyclin-dependent kinase inhibitors enhance the resolution of inflammation by promoting inflammatory cell apoptosis. *Nat Med, 12*(9), 1056-1064. doi:10.1038/nm1468

Rowe, S. J., Allen, L., Ridger, V. C., Hellewell, P. G., & Whyte, M. K. B. (2002). Caspase-1-Deficient Mice Have Delayed Neutrophil Apoptosis and a Prolonged Inflammatory Response to Lipopolysaccharide-Induced Acute Lung Injury. *J Immunol, 169*(11), 6401-6407. doi:10.4049/jimmunol.169.11.6401

Sackett, D. L., & Varma, J. K. (1993). Molecular mechanism of colchicine action: induced local unfolding of beta-tubulin. *Biochemistry, 32*(49), 13560-13565.

Saffar, A. S., Ashdown, H., & Gounni, A. S. (2011). The molecular mechanisms of glucocorticoids-mediated neutrophil survival. *Curr Drug Targets, 12*(4), 556-562.

Sanford, A. N., Suriano, A. R., Herche, D., Dietzmann, K., & Sullivan, K. E. (2006). Abnormal apoptosis in chronic granulomatous disease and autoantibody production characteristic of lupus. *Rheumatology (Oxford), 45*(2), 178-181. doi:10.1093/rheumatology/kei135

Sanmun, D., Witasp, E., Jitkaew, S., Tyurina, Y. Y., Kagan, V. E., Ahlin, A., . . . Fadeel, B. (2009). Involvement of a functional NADPH oxidase in neutrophils and macrophages during programmed cell clearance: implications for chronic

granulomatous disease. *Am J Physiol Cell Physiol, 297*(3), C621-631. doi:10.1152/ajpcell.00651.2008
Scatizzi, J. C., Hutcheson, J., Pope, R. M., Firestein, G. S., Koch, A. E., Mavers, M., . . . Perlman, H. (2010). Bim-Bcl-2 homology 3 mimetic therapy is effective at suppressing inflammatory arthritis through the activation of myeloid cell apoptosis. *Arthritis Rheum, 62*(2), 441-451. doi:10.1002/art.27198
Schauer, C., Janko, C., Munoz, L. E., Zhao, Y., Kienhofer, D., Frey, B., . . . Herrmann, M. (2014). Aggregated neutrophil extracellular traps limit inflammation by degrading cytokines and chemokines. *Nat Med, 20*(5), 511-517. doi:10.1038/nm.3547
Scheel-Toellner, D., Wang, K., Craddock, R., Webb, P. R., McGettrick, H. M., Assi, L. K., . . . Lord, J. M. (2004). Reactive oxygen species limit neutrophil life span by activating death receptor signaling. *Blood, 104*(8), 2557-2564. doi:10.1182/blood-2004-01-0191
Scheel-Toellner, D., Wang, K., Singh, R., Majeed, S., Raza, K., Curnow, S. J., . . . Lord, J. M. (2002). The death-inducing signalling complex is recruited to lipid rafts in Fas-induced apoptosis. *Biochem Biophys Res Commun, 297*(4), 876-879.
Schlesinger, N., Alten, R. E., Bardin, T., Schumacher, H. R., Bloch, M., Gimona, A., . . . So, A. K. (2012). Canakinumab for acute gouty arthritis in patients with limited treatment options: results from two randomised, multicentre, active-controlled, double-blind trials and their initial extensions. *Ann Rheum Dis, 71*(11), 1839-1848. doi:10.1136/annrheumdis-2011-200908
Schorn, C., Frey, B., Lauber, K., Janko, C., Strysio, M., Keppeler, H., . . . Herrmann, M. (2011). Sodium overload and water influx activate the NALP3 inflammasome. *J Biol Chem, 286*(1), 35-41. doi:10.1074/jbc.M110.139048
Schorn, C., Janko, C., Krenn, V., Zhao, Y., Munoz, L. E., Schett, G., & Herrmann, M. (2012). Bonding the foe - NETting neutrophils immobilize the pro-inflammatory monosodium urate crystals. *Front Immunol, 3*, 376. doi:10.3389/fimmu.2012.00376
Schumacher, H. R., & Phelps, P. (1971). Sequential changes in human polymorphonuclear leukocytes after urate crystal phagocytosis. An electron microscopic study. *Arthritis Rheum, 14*(4), 513-526.
Scott, P., Ma, H., Viriyakosol, S., Terkeltaub, R., & Liu-Bryan, R. (2006). Engagement of CD14 mediates the inflammatory potential of monosodium urate crystals. *J Immunol, 177*(9), 6370-6378.
Seegmiller, J. E., Howell, R. R., & Malawista, S. E. (1962). The inflammatory reaction to sodium urate. *JAMA, 180*(6), 469-475. doi:10.1001/jama.1962.03050190031006
Serhan, C. N., Lundberg, U., Weissmann, G., & Samuelsson, B. (1984). Formation of leukotrienes and hydroxy acids by human neutrophils and platelets exposed to monosodium urate. *Prostaglandins, 27*(4), 563-581.
Shi, J., Zhao, Y., Wang, K., Shi, X., Wang, Y., Huang, H., . . . Shao, F. (2015). Cleavage of GSDMD by inflammatory caspases determines pyroptotic cell death. *Nature, 526*(7575), 660-665. doi:10.1038/nature15514
Shi, W., Xu, C., Hussain, M., Wu, F., Lu, M., Wu, X., . . . Wu, J. (2017). Inhibition of Myosin Light-Chain Kinase Enhances the Clearance of Lipopolysaccharide-Induced Lung Inflammation Possibly by Accelerating Neutrophil Apoptosis. *Shock*, 1-24. doi:10.1097/SHK.0000000000000863
Shoji, A., Yamanaka, H., & Kamatani, N. (2004). A retrospective study of the relationship between serum urate level and recurrent attacks of gouty arthritis: evidence for reduction of recurrent gouty arthritis with antihyperuricemic therapy. *Arthritis Rheum, 51*(3), 321-325. doi:10.1002/art.20405

Silke, J., Rickard, J. A., & Gerlic, M. (2015). The diverse role of RIP kinases in necroptosis and inflammation. *Nat Immunol, 16*(7), 689-697. doi:10.1038/ni.3206

Smith, W. L., DeWitt, D. L., & Garavito, R. M. (2000). Cyclooxygenases: Structural, Cellular, and Molecular Biology. *Annu Rev Biochem, 69*, 145-182.

So, A., De Smedt, T., Revaz, S., & Tschopp, J. (2007). A pilot study of IL-1 inhibition by anakinra in acute gout. *Arthritis Res Ther, 9*(2), R28. doi:10.1186/ar2143

Sorensen, O. E., Clemmensen, S. N., Dahl, S. L., Ostergaard, O., Heegaard, N. H., Glenthoj, A., . . . Borregaard, N. (2014). Papillon-Lefevre syndrome patient reveals species-dependent requirements for neutrophil defenses. *J Clin Invest, 124*(10), 4539-4548. doi:10.1172/JCI76009

Spilbert, I., Gallacher, A., Mehta, J. M., & Mandell, B. (1976). Urate crystal-induced chemotactic factor: isolation and partial characterization. *J Clin Invest, 58*(4), 815-819. doi:10.1172/JCI108533

Squier, M. K., Sehnert, A. J., Sellins, K. S., Malkinson, A. M., Takano, E., & Cohen, J. J. (1999). Calpain and calpastatin regulate neutrophil apoptosis. *J Cell Physiol, 178*(3), 311-319. doi:10.1002/(SICI)1097-4652(199903)178:3<311::AID-JCP5>3.0.CO;2-T

Su, L., Quade, B., Wang, H., Sun, L., Wang, X., & Rizo, J. (2014). A plug release mechanism for membrane permeation by MLKL. *Structure, 22*(10), 1489-1500. doi:10.1016/j.str.2014.07.014

Sun, L., Wang, H., Wang, Z., He, S., Chen, S., Liao, D., . . . Wang, X. (2012). Mixed lineage kinase domain-like protein mediates necrosis signaling downstream of RIP3 kinase. *Cell, 148*(1-2), 213-227. doi:10.1016/j.cell.2011.11.031

Suzuki, K., Hino, M., Hato, F., Tatsumi, N., & Kitagawa, S. (1999). Cytokine-specific activation of distinct mitogen-activated protein kinase subtype cascades in human neutrophils stimulated by granulocyte colony-stimulating factor, granulocyte-macrophage colony-stimulating factor, and tumor necrosis factor-alpha. *Blood, 93*(1), 341-349.

Sweeney, J. F., Nguyen, P. K., & Hinshaw, D. B. (2001). Caspase-3 inhibition partially protects oxidant production in apoptotic human neutrophils. *J Surg Res, 98*(1), 66-70. doi:10.1006/jsre.2001.6170

Taggart, C., Cervantes-Laurean, D., Kim, G., McElvaney, N. G., Wehr, N., Moss, J., & Levine, R. L. (2000). Oxidation of either methionine 351 or methionine 358 in alpha 1-antitrypsin causes loss of anti-neutrophil elastase activity. *J Biol Chem, 275*(35), 27258-27265. doi:10.1074/jbc.M004850200

Tait, S. W., Ichim, G., & Green, D. R. (2014). Die another way--non-apoptotic mechanisms of cell death. *J Cell Sci, 127*(Pt 10), 2135-2144. doi:10.1242/jcs.093575

Tak, T., Tesselaar, K., Pillay, J., Borghans, J. A., & Koenderman, L. (2013). What's your age again? Determination of human neutrophil half-lives revisited. *J Leukoc Biol, 94*(4), 595-601. doi:10.1189/jlb.1112571

Tanzer, M. C., Khan, N., Rickard, J. A., Etemadi, N., Lalaoui, N., Spall, S. K., . . . Silke, J. (2017). Combination of IAP antagonist and IFNgamma activates novel caspase-10- and RIPK1-dependent cell death pathways. *Cell Death Differ, 24*(3), 481-491. doi:10.1038/cdd.2016.147

Tanzer, M. C., Matti, I., Hildebrand, J. M., Young, S. N., Wardak, A., Tripaydonis, A., . . . Murphy, J. M. (2016). Evolutionary divergence of the necroptosis effector MLKL. *Cell Death Differ, 23*(7), 1185-1197. doi:10.1038/cdd.2015.169

Terkeltaub, R. A. (2010). Update on gout: new therapeutic strategies and options. *Nat Rev Rheumatol, 6*(1), 30-38. doi:10.1038/nrrheum.2009.236

Terkeltaub, R. A., Curtiss, L. K., Tenner, A. J., & Ginsberg, M. H. (1984). Lipoproteins containing apoprotein B are a major regulator of neutrophil responses to

monosodium urate crystals. *J Clin Invest, 73*(6), 1719-1730. doi:10.1172/JCI111380
Terkeltaub, R. A., Dyer, C. A., Martin, J., & Curtiss, L. K. (1991). Apolipoprotein (apo) E inhibits the capacity of monosodium urate crystals to stimulate neutrophils. Characterization of intraarticular apo E and demonstration of apo E binding to urate crystals in vivo. *J Clin Invest, 87*(1), 20-26. doi:10.1172/JCI114971
Terkeltaub, R. A., Tenner, A. J., Kozin, F., & Ginsberg, M. H. (1983). Plasma protein binding by monosodium urate crystals. Analysis by two-dimensional gel electrophoresis. *Arthritis Rheum, 26*(6), 775-783.
Thiele, D. L., & Lipsky, P. E. (1992). Apoptosis is induced in cells with cytolytic potential by L-leucyl-L-leucine methyl ester. *J Immunol, 148*(12), 3950-3957.
Tofts, P. S., Chevassut, T., Cutajar, M., Dowell, N. G., & Peters, A. M. (2011). Doubts concerning the recently reported human neutrophil lifespan of 5.4 days. *Blood, 117*(22), 6050-6052; author reply 6053-6054. doi:10.1182/blood-2010-10-310532
Tsuchida, H., Takeda, Y., Takei, H., Shinzawa, H., Takahashi, T., & Sendo, F. (1995). In vivo regulation of rat neutrophil apoptosis occurring spontaneously or induced with TNF-alpha or cycloheximide. *J Immunol, 154*(5), 2403-2412.
Urban, C. F., Ermert, D., Schmid, M., Abu-Abed, U., Goosmann, C., Nacken, W., . . . Zychlinsky, A. (2009). Neutrophil extracellular traps contain calprotectin, a cytosolic protein complex involved in host defense against Candida albicans. *PLoS Pathog, 5*(10), e1000639. doi:10.1371/journal.ppat.1000639
van Raam, B. J., Drewniak, A., Groenewold, V., van den Berg, T. K., & Kuijpers, T. W. (2008). Granulocyte colony-stimulating factor delays neutrophil apoptosis by inhibition of calpains upstream of caspase-3. *Blood, 112*(5), 2046-2054. doi:10.1182/blood-2008-04-149575
Vandenabeele, P., Grootjans, S., Callewaert, N., & Takahashi, N. (2013). Necrostatin-1 blocks both RIPK1 and IDO: consequences for the study of cell death in experimental disease models. *Cell Death Differ, 20*(2), 185-187. doi:10.1038/cdd.2012.151
Varfolomeev, E. E., Schuchmann, M., Luria, V., Chiannilkulchai, N., Beckmann, J. S., Mett, I. L., . . . Wallach, D. (1998). Targeted disruption of the mouse Caspase 8 gene ablates cell death induction by the TNF receptors, Fas/Apo1, and DR3 and is lethal prenatally. *Immunity, 9*(2), 267-276.
Vier, J., Groth, M., Sochalska, M., & Kirschnek, S. (2016). The anti-apoptotic Bcl-2 family protein A1/Bfl-1 regulates neutrophil survival and homeostasis and is controlled via PI3K and JAK/STAT signaling. *Cell Death Dis, 7*(2), e2103. doi:10.1038/cddis.2016.23
Villanueva, E., Yalavarthi, S., Berthier, C. C., Hodgin, J. B., Khandpur, R., Lin, A. M., . . . Kaplan, M. J. (2011). Netting neutrophils induce endothelial damage, infiltrate tissues, and expose immunostimulatory molecules in systemic lupus erythematosus. *J Immunol, 187*(1), 538-552. doi:10.4049/jimmunol.1100450
Villunger, A., Scott, C., Bouillet, P., & Strasser, A. (2003). Essential role for the BH3-only protein Bim but redundant roles for Bax, Bcl-2, and Bcl-w in the control of granulocyte survival. *Blood, 101*(6), 2393-2400. doi:10.1182/blood-2002-07-2132
von Kockritz-Blickwede, M., Chow, O. A., & Nizet, V. (2009). Fetal calf serum contains heat-stable nucleases that degrade neutrophil extracellular traps. *Blood, 114*(25), 5245-5246. doi:10.1182/blood-2009-08-240713
von Kockritz-Blickwede, M., Goldmann, O., Thulin, P., Heinemann, K., Norrby-Teglund, A., Rohde, M., & Medina, E. (2008). Phagocytosis-independent antimicrobial activity of mast cells by means of extracellular trap formation. *Blood, 111*(6), 3070-3080. doi:10.1182/blood-2007-07-104018

Vossenaar, E. R., Zendman, A. J., van Venrooij, W. J., & Pruijn, G. J. (2003). PAD, a growing family of citrullinating enzymes: genes, features and involvement in disease. *Bioessays, 25*(11), 1106-1118. doi:10.1002/bies.10357
Walker, T. R., Ruchaud-Sparagano, M. H., McMeekin, S. R., & Dransfield, I. (2004). A critical 'threshold' of beta 2-integrin engagement regulates augmentation of cytokine-mediated superoxide anion release. *Br J Pharmacol, 141*(7), 1131-1140. doi:10.1038/sj.bjp.0705715
Wallingford, W. R., & McCarty, D. J. (1971). Differential membranolytic effects of microcrystalline sodium urate and calcium pyrophosphate dihydrate. *J Exp Med, 133*(1), 100-112.
Wang, H., Sun, L., Su, L., Rizo, J., Liu, L., Wang, L. F., . . . Wang, X. (2014). Mixed lineage kinase domain-like protein MLKL causes necrotic membrane disruption upon phosphorylation by RIP3. *Mol Cell, 54*(1), 133-146. doi:10.1016/j.molcel.2014.03.003
Wang, J., Chun, H. J., Wong, W., Spencer, D. M., & Lenardo, M. J. (2001). Caspase-10 is an initiator caspase in death receptor signaling. *Proc Natl Acad Sci U S A, 98*(24), 13884-13888. doi:10.1073/pnas.241358198
Wang, K., Hampson, P., Hazeldine, J., Krystof, V., Strnad, M., Pechan, P., & M, J. (2012). Cyclin-dependent kinase 9 activity regulates neutrophil spontaneous apoptosis. *PLoS ONE, 7*(1), e30128. doi:10.1371/journal.pone.0030128
Wang, X., He, Z., Liu, H., & Yousefi, S. (2016). Neutrophil Necroptosis Is Triggered by Ligation of Adhesion Molecules following GM-CSF Priming. *J Immunol, 197*(10), 4090-4100.
Wang, Y., Li, M., Stadler, S., Correll, S., Li, P., Wang, D., . . . Coonrod, S. A. (2009). Histone hypercitrullination mediates chromatin decondensation and neutrophil extracellular trap formation. *J Cell Biol, 184*(2), 205-213. doi:10.1083/jcb.200806072
Wang, Y., Wysocka, J., Sayegh, J., Lee, Y. H., Perlin, J. R., Leonelli, L., . . . Coonrod, S. A. (2004). Human PAD4 regulates histone arginine methylation levels via demethylimination. *Science, 306*(5694), 279-283. doi:10.1126/science.1101400
Ward, C., Chilvers, E. R., Lawson, M. F., Pryde, J. G., Fujihara, S., Farrow, S. N., . . . Rossi, A. G. (1999). NF-kappa B Activation Is a Critical Regulator of Human Granulocyte Apoptosis in Vitro. *J Biol Chem, 274*(7), 4309-4318. doi:10.1074/jbc.274.7.4309
Wardle, D. J., Burgon, J., Sabroe, I., Bingle, C. D., Whyte, M. K., & Renshaw, S. A. (2011). Effective Caspase Inhibition Blocks Neutrophil Apoptosis and Reveals Mcl-1 as Both a Regulator and a Target of Neutrophil Caspase Activation. *PLoS ONE, 6*(1), e15768. doi:10.1371/journal.pone.0015768.s001
Warnatsch, A., Ioannou, M., Wang, Q., & Papayannopoulos, V. (2015). Inflammation. Neutrophil extracellular traps license macrophages for cytokine production in atherosclerosis. *Science, 349*(6245), 316-320. doi:10.1126/science.aaa8064
Watson, R. W., Rotstein, O. D., Parodo, J., Bitar, R., Hackam, D., & Marshall, J. C. (1997). Granulocytic differentiation of HL-60 cells results in spontaneous apoptosis mediated by increased caspase expression. *FEBS Lett, 412*(3), 603-609. doi:10.1016/S0014-5793(97)00779-5
Webster, S. J., Daigneault, M., Bewley, M. A., Preston, J. A., Marriott, H. M., Walmsley, S. R., . . . Dockrell, D. H. (2010). Distinct cell death programs in monocytes regulate innate responses following challenge with common causes of invasive bacterial disease. *J Immunol, 185*(5), 2968-2979. doi:10.4049/jimmunol.1000805
Wehrli, M., Cortinas-Elizondo, F., Hlushchuk, R., Daudel, F., Villiger, P. M., Miescher, S., . . . von Gunten, S. (2014). Human IgA Fc receptor FcalphaRI (CD89) triggers different forms of neutrophil death depending on the inflammatory

microenvironment. *J Immunol, 193*(11), 5649-5659. doi:10.4049/jimmunol.1400028
Wei, M. C., Zong, W. X., Cheng, E. H., Lindsten, T., Panoutsakopoulou, V., Ross, A. J., . . . Korsmeyer, S. J. (2001). Proapoptotic BAX and BAK: a requisite gateway to mitochondrial dysfunction and death. *Science, 292*(5517), 727-730. doi:10.1126/science.1059108
Wei, S., Liu, J. H., Epling-Burnette, P. K., Gamero, A. M., Ussery, D., Pearson, E. W., . . . Djeu, J. Y. (1996). Critical role of Lyn kinase in inhibition of neutrophil apoptosis by granulocyte-macrophage colony-stimulating factor. *J Immunol, 157*(11), 5155-5162.
Weinrauch, Y., Drujan, D., Shapiro, S. D., Weiss, J., & Zychlinsky, A. (2002). Neutrophil elastase targets virulence factors of enterobacteria. *Nature, 417*(6884), 91-94. doi:10.1038/417091a
Weissmann, G., & Rita, G. A. (1972). Molecular basis of gouty inflammation: interaction of monosodium urate crystals with lysosomes and liposomes. *Nat New Biol, 240*(101), 167-172.
White, M. J., McArthur, K., Metcalf, D., Lane, R. M., Cambier, J. C., Herold, M. J., . . . Kile, B. T. (2014). Apoptotic caspases suppress mtDNA-induced STING-mediated type I IFN production. *Cell, 159*(7), 1549-1562. doi:10.1016/j.cell.2014.11.036
Whyte, M. K., Meagher, L. C., MacDermot, J., & Haslett, C. (1993). Impairment of function in aging neutrophils is associated with apoptosis. *J Immunol, 150*(11), 5124-5134.
Wicki, S., Gurzeler, U., Wei-Lynn Wong, W., Jost, P. J., Bachmann, D., & Kaufmann, T. (2016). Loss of XIAP facilitates switch to TNFalpha-induced necroptosis in mouse neutrophils. *Cell Death Dis, 7*(10), e2422. doi:10.1038/cddis.2016.311
Willis, V. C., Banda, N. K., Cordova, K. N., Chandra, P. E., Robinson, W. H., Cooper, D. C., . . . Holers, V. M. (2017). Protein arginine deiminase 4 inhibition is sufficient for the amelioration of collagen-induced arthritis. *Clin Exp Immunol*, 1-43. doi:10.1111/cei.12932
Willis, V. C., Gizinski, A. M., Banda, N. K., Causey, C. P., Knuckley, B., Cordova, K. N., . . . Holers, V. M. (2011). N-alpha-benzoyl-N5-(2-chloro-1-iminoethyl)-L-ornithine amide, a protein arginine deiminase inhibitor, reduces the severity of murine collagen-induced arthritis. *J Immunol, 186*(7), 4396-4404. doi:10.4049/jimmunol.1001620
Winterbourn, C. C., Kettle, A. J., & Hampton, M. B. (2016). Reactive Oxygen Species and Neutrophil Function. *Annu Rev Biochem, 85*(1), 765-792. doi:10.1146/annurev-biochem-060815-014442
Witko-Sarsat, V., Mocek, J., Bouayad, D., Tamassia, N., Ribeil, J. A., Candalh, C., . . . Cassatella, M. A. (2010). Proliferating cell nuclear antigen acts as a cytoplasmic platform controlling human neutrophil survival. *J Exp Med, 207*(12), 2631-2645. doi:10.1084/jem.20092241
Witko-Sarsat, V., & Ohayon, D. (2016). Proliferating cell nuclear antigen in neutrophil fate. *Immunol Rev, 273*(1), 344-356. doi:10.1111/imr.12449
Wong, S. L., Demers, M., Martinod, K., Gallant, M., Wang, Y., Goldfine, A. B., . . . Wagner, D. D. (2015). Diabetes primes neutrophils to undergo NETosis, which impairs wound healing. *Nat Med, 21*(7), 815-819. doi:10.1038/nm.3887
Wright, H. L., Moots, R. J., & Edwards, S. W. (2014). The multifactorial role of neutrophils in rheumatoid arthritis. *Nat Rev Rheumatol, 10*(10), 593-601. doi:10.1038/nrrheum.2014.80
Wu, J., Huang, Z., Ren, J., Zhang, Z., He, P., Li, Y., . . . Han, J. (2013). Mlkl knockout mice demonstrate the indispensable role of Mlkl in necroptosis. *Cell Res, 23*(8), 994-1006. doi:10.1038/cr.2013.91

Wu, X. W., Lee, C. C., Muzny, D. M., & Caskey, C. T. (1989). Urate oxidase: primary structure and evolutionary implications. *Proc Natl Acad Sci U S A, 86*(23), 9412-9416.

Xu, Y., Loison, F., & Luo, H. R. (2010). Neutrophil spontaneous death is mediated by down-regulation of autocrine signaling through GPCR, PI3Kgamma, ROS, and actin. *Proc Natl Acad Sci U S A, 107*(7), 2950-2955. doi:10.1073/pnas.0912717107

Yagnik, D. R., Evans, B. J., Florey, O., Mason, J. C., Landis, R. C., & Haskard, D. O. (2004). Macrophage release of transforming growth factor beta1 during resolution of monosodium urate monohydrate crystal-induced inflammation. *Arthritis Rheum, 50*(7), 2273-2280. doi:10.1002/art.20317

Yamamoto, A., Taniuchi, S., Tsuji, S., Hasui, M., & Kobayashi, Y. (2002). Role of reactive oxygen species in neutrophil apoptosis following ingestion of heat-killed Staphylococcus aureus. *Clin Exp Immunol, 129*(3), 479-484. doi:10.1046/j.1365-2249.2002.01930.x

Yan, B., Liu, L., Huang, S., Ren, Y., Wang, H., Yao, Z., . . . Zhang, Z. (2017). Discovery of a new class of highly potent necroptosis inhibitors targeting the mixed lineage kinase domain-like protein. *Chem Commun (Camb)*, 1-4. doi:10.1039/c7cc00667e

Yaseen, R., Blodkamp, S., Luthje, P., Reuner, F., Vollger, L., Naim, H. Y., & von Kockritz-Blickwede, M. (2017). Antimicrobial activity of HL-60 cells compared to primary blood-derived neutrophils against Staphylococcus aureus. *J Negat Results Biomed, 16*(1), 2. doi:10.1186/s12952-017-0067-2

Yipp, B. G., & Kubes, P. (2013). NETosis: how vital is it? *Blood, 122*(16), 2784-2794. doi:10.1182/blood-2013-04-457671

Yipp, B. G., Petri, B., Salina, D., Jenne, C. N., Scott, B. N., Zbytnuik, L. D., . . . Kubes, P. (2012). Infection-induced NETosis is a dynamic process involving neutrophil multitasking in vivo. *Nat Med, 18*(9), 1386-1393. doi:10.1038/nm.2847

Yoon, S., Bogdanov, K., Kovalenko, A., & Wallach, D. (2016). Necroptosis is preceded by nuclear translocation of the signaling proteins that induce it. *Cell Death Differ, 23*(2), 253-260. doi:10.1038/cdd.2015.92

Yost, C. C., Schwertz, H., Cody, M. J., Wallace, J. A., Campbell, R. A., Vieira-de-Abreu, A., . . . Zimmerman, G. A. (2016). Neonatal NET-inhibitory factor and related peptides inhibit neutrophil extracellular trap formation. *J Clin Invest, 126*(10), 3783-3798. doi:10.1172/JCI83873

Yousefi, S., Gold, J. A., Andina, N., Lee, J. J., Kelly, A. M., Kozlowski, E., . . . Simon, H. U. (2008). Catapult-like release of mitochondrial DNA by eosinophils contributes to antibacterial defense. *Nat Med, 14*(9), 949-953. doi:10.1038/nm.1855

Yousefi, S., Mihalache, C., Kozlowski, E., Schmid, I., & Simon, H. U. (2009). Viable neutrophils release mitochondrial DNA to form neutrophil extracellular traps. *Cell Death Differ, 16*(11), 1438-1444. doi:10.1038/cdd.2009.96

Zhou, L., Somasundaram, R., Nederhof, R. F., Dijkstra, G., Faber, K. N., Peppelenbosch, M. P., & Fuhler, G. M. (2012). Impact of human granulocyte and monocyte isolation procedures on functional studies. *Clin Vaccine Immunol, 19*(7), 1065-1074. doi:10.1128/CVI.05715-11

Zhu, D., Hattori, H., Jo, H., Jia, Y., Subramanian, K. K., Loison, F., . . . Luo, H. R. (2006). Deactivation of phosphatidylinositol 3,4,5-trisphosphate/Akt signaling mediates neutrophil spontaneous death. *Proc Natl Acad Sci U S A, 103*(40), 14836-14841. doi:10.1073/pnas.0605722103